

482282

AFAPL-TR-65-53
Part I

ENCL TO LMSC A813650

2

22

PROGRAM ASTEC (ADVANCED SOLAR TURBO ELECTRIC CONCEPT)

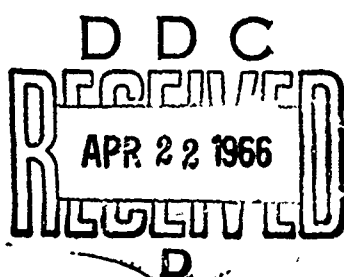
Part I. Candidate Materials Laboratory Tests

Lockheed Missiles & Space Company

TECHNICAL REPORT AFAPL-TR-65-53, PART 1

March 1966

Air Force Aero Propulsion Laboratory
Research and Technology Division
Air Force Systems Command
Wright-Patterson Air Force Base, Ohio



NOTICES

When Government drawings, specifications, or other data are used for any purpose other than in connection with a definitely related Government procurement operation, the United States Government thereby incurs no responsibility nor any obligation whatsoever; and the fact that the Government may have formulated, furnished, or in any way supplied the said drawings, specifications, or other data, is not to be regarded by implication or otherwise as in any manner licensing the holder or any other person or corporation, or conveying any rights or permission to manufacture, use, or sell any patented invention that may in any way be related thereto.

Copies of this report should not be returned to the Research and Technology Division unless return is required by security considerations, contractual obligations, or notice on a specific document.

PROGRAM ASTEC

(ADVANCED SOLAR TURBO ELECTRIC CONCEPT)

Part I. Candidate Materials Laboratory Tests

FOREWORD

This document is one of a series pertaining to the Advanced Solar Turbo Electric Concept (ASTEC) Program conducted for the Air Force Aero Propulsion Laboratory by the Lockheed Missiles & Space Company (LMSC), Sunnyvale, California, under Air Force Project 678A, Contract AF 33(615)-1577.

The Air Force Program Manager is Buryl L. McFadden, Jr., the Project Engineer Lt. P. W. Lauderback, who directs the program for G. E. Thompson, Technical Manager, Dynamic Energy Conversion (APIP-1), Energy Conversion Branch, Aerospace Power Division.

At LMSC, responsibility is assigned to the ASTEC Program Office of the Booster Programs organization. W. W. Hurtt is Program Manager. The authors of this report and principal investigators were T. L. Blakney, W. Bradshaw, G. R. Cunningham, H. E. Pollard, J. B. Rittenhouse, W. F. Schmidt, and D. A. Vance. Technical direction and coordination of the work effort was supplied by D. F. Farwell.

This report (Part I) covers work performed by LMSC from contract date, 1 July 1964, to 1 October 1965. This report was submitted March 1966.

The Lockheed number for this report (Part I) is LMSC D-03-65-4.

This series comprises the following documents:

- Part I Candidate Materials Laboratory Tests
- Part II High Temperature Materials Laboratory Tests
- Part III Candidate Materials Orbital Evaluation
- Part IV Solar Collector Development Support Tasks

This technical report has been reviewed and is approved.

Glenn M. Kevern, Chief
Energy Conversion Branch
Aerospace Power Division

ABSTRACT

A space power system of the type envisioned by the ASTEC program requires the development of a lightweight solar collector of high reflectance which is capable of withstanding the space environment for an extended period of time. A survey of the environment of interest for ASTEC purposes revealed four potential sources of damage to collector materials: solar ultraviolet radiation, low-energy electrons encountered in the auroral zones, vacuum, and combined temperature levels and thermal cycling. A laboratory test program was conducted to determine the basic thermophysical, optical, and mechanical properties of materials developed by the solar-collector industry for use in the ASTEC program, and to test the degrading effects of various segregated and combined elements of the space environment on these materials. Of six material systems selected by AFAPL for testing, four were epoxy-bonded metal systems, one was phenolic foam with a metal surface, and one was polyurethane-rigidized nylon with an aluminized mylar surface. Three of the four metal systems were honeycomb configurations; these proved to be far superior from a structural standpoint to the nonhoneycomb types. All the reflective surfaces degraded to some extent in the simulated ASTEC environment, but material systems with bare metal surfaces were significantly more stable than systems with silicon oxide overcoatings. In addition, these systems had a higher initial reflectance. No material proved to be ideally suited in all respects for use in the ASTEC solar collector. Recommendations are made for additional testing to determine more exactly the mechanical properties of the most promising material or materials and to establish with greater certainty the degree of optical stability of these materials in the ASTEC environment.

PREVIOUS PAGE WAS BLANK, THEREFORE NOT FILMED.

CONTENTS

Section		Page
I	INTRODUCTION	1
	1. Purpose of Testing	1
	2. Description of Candidate Materials	2
	3. Scope of Testing	7
	4. Organization of This Report	9
II	THERMOPHYSICAL PROPERTIES	11
	1. Introduction	11
	2. Thermal Conductance	11
	a. Description of Apparatus	11
	b. Test Procedure	14
	c. Test Results	15
	d. Comments and Interpretation of Results	23
	3. Linear Thermal Expansion	24
	a. Description of Apparatus	24
	b. Test Procedure	29
	c. Test Results	31
	d. Comments and Interpretation of Results	41
	4. Heat Capacity	44
	a. Description of Apparatus	44
	b. Test Procedure	44
	c. Test Results	46
	5. Weight Loss	49
	a. Description of Apparatus	49
	b. Test Procedure	49
	c. Test Results	52
	d. Comments and Interpretation of Results	60
	6. Thermal/Vacuum Environmental Stability	74
	a. Description of Apparatus	75
	b. Test Procedure	75
	c. Test Results	75
	d. Comments and Interpretation of Results	75
	7. Thermal Cycling	83
	a. Description of Apparatus	84
	b. Test Procedure	84
	c. Test Results	86
	d. Comments and Interpretation of Results	86

Section	Page
III OPTICAL PROPERTIES	114
1. Introduction	114
2. Initial Optical Property Measurements	114
a. Solar Absorptance and Infrared Emittance Values	115
b. Comments and Interpretation of Results	116
3. Ultraviolet Irradiation	116
a. Description of Apparatus	116
b. Test Procedure	126
c. Test Results	126
d. Comments and Interpretation of Results	130
4. Electron Bombardment	130
a. Description of Apparatus	130
b. Test Procedure	131
c. Test Results	131
d. Comments and Interpretation of Results	132
5. Combined Environment	132
a. Description of Apparatus	132
b. Test Procedure	132
c. Test Results	132
d. Comments and Interpretation of Results	137
IV MECHANICAL PROPERTIES	140
1. Introduction	140
2. Panel Shear	140
a. Description of Apparatus	142
b. Test Procedure	145
c. Test Results	145
d. Comments and Interpretation of Results	149
3. Panel Bend	164
a. Description of Apparatus	164
b. Test Procedure	167
c. Test Results	167
d. Comments and Interpretation of Results	167
4. Facing Tension	180
a. Description of Apparatus	180
b. Test Procedure	184
c. Test Results	184
d. Comments and Interpretation of Results	184
5. Facing Separation	196
a. Description of Apparatus	196
b. Test Procedure	199
c. Test Results	199
d. Comments and Interpretation of Results	199
6. Core Compression	215
a. Description of Apparatus	215
b. Test Procedure	215
c. Test Results	217
d. Comments and Interpretation of Results	217

Section		Page
V	CONCLUSIONS	233
VI	RECOMMENDATIONS	238
VII	REFERENCES	239
Appendix		
I	TEST RESULTS - CANDIDATE MATERIAL A	241
II	TEST RESULTS - CANDIDATE MATERIAL B	253
III	TEST RESULTS - CANDIDATE MATERIAL C	273
IV	TEST RESULTS - CANDIDATE MATERIALS D-F	284
V	TEST RESULTS - CANDIDATE MATERIALS G-K	304

ILLUSTRATIONS

Figure	Page
1 Candidate Material A	4
2 Candidate Material B	4
3 Candidate Material C	5
4 Candidate Materials D-F	5
5 Candidate Materials G-K	6
6 Material L	6
7 Thermal Conductance Apparatus - 7-in. -Diameter Guarded Hot Plate	12
8 Thermal Conductance Apparatus - 12-in. -Square Hot Plate	13
9 Thermal Conductance of Material A	17
10 Thermal Conductance of Material B	19
11 Thermal Conductance of Material C	20
12 Thermal Conductance of Materials D-F	21
13 Thermal Conductance of Materials G-K, 1-in. -Thick Specimen	22
14 Temperature Distribution Along Wall of One Cylinder of Materials G-K	22
15 Thermal Expansion Apparatus for Measurements From -320° to +150° F	25
16 Expansion Specimen and Dilatometer With Heater	26
17 Linear Thermal Expansion of Reference Materials in Quartz Tube Dilatometer Apparatus	27
18 Horizontal Tube Linear Thermal Expansion Apparatus	28
19 Percent Thermal Expansion of Quartz Dilatometer Tubes	30
20 Linear Thermal Expansion of Material B, Reflective Surface	32
21 Linear Thermal Expansion of Material B, Foam Structure, in X-X Direction	33
22 Linear Thermal Expansion of Material B, Foam Structure, in Y-Y Direction	34

Figure		Page
23	Linear Thermal Expansion of Material B, Foam Structure, in Z-Z Direction	35
24	Linear Thermal Expansion of Material B, Epoxy Backing Surface	36
25	Comparison of Linear Thermal Expansion of Material B, Reflective Surface, Before and After 6,000-Cycle Thermal-Cycling Test	37
26	Linear Thermal Expansion of Materials G-K, Reflective Surface	38
27	Linear Thermal Expansion of Materials G-K, Back Surface	39
28	Comparison of Linear Thermal Expansion of Materials G-K, Before and After 6,000-Cycle Thermal-Cycling Test	40
29	Linear Thermal Expansion of Material L, Rigidized Facing of Structure	42
30	Linear Thermal Expansion of Material L, Flexible Epoxy Sublayer	43
31	Flooded Ice-Mantle Calorimeter for Measurement of Enthalpy Between -250° and +250° F	45
32	Enthalpy of Material B, Foam Structure, Referenced to 32° F	47
33	Heat Capacity of Material B, Foam Structure	47
34	Enthalpy of Material B, Epoxy Backing Surface	48
35	Heat Capacity of Material B, Epoxy Backing Surface	48
36	Weight-Loss Apparatus	50
37	Detail of Heating Chamber, Weight-Loss Apparatus	51
38	Typical Weight-Loss Curves	53
39	Weight Loss Versus Time at Temperature, Material A, Epoxy Adhesive	54
40	Equilibrium Weight Loss as a Function of Temperature, Material A, Epoxy Adhesive	55
41	Appearance of Material L, Composite Structure, Before Test	57
42	Equilibrium Weight Loss Versus Temperature, Material B, Phenolic Foam	59
43	Equilibrium Weight Loss Versus Temperature, Material C, Epoxy Adhesive	61
44	Equilibrium Weight Loss Versus Temperature, Material C, Epoxy Sublayer	62

Figure		Page
45	Equilibrium Weight Loss Versus Temperature, Materials D-F, Epoxy Facing Adhesive	63
46	Equilibrium Weight Loss Versus Temperature, Materials D-F, Epoxy Backing Adhesive	64
47	Equilibrium Weight Loss Versus Temperature, Material D, Epoxy Sublayer	65
48	Equilibrium Weight Loss Versus Temperature, Materials E-F, Epoxy Sublayer	66
49	Equilibrium Weight Loss Versus Temperature, Materials G-K, Epoxy Adhesive	67
50	Equilibrium Weight Loss Versus Temperature, Material L, Epoxy Sublayer	68
51	Equilibrium Weight Loss Versus Temperature, Material L, Entire Composite Except Aluminized-Mylar Film	69
52	Appearance of Material L, Composite Structure, After Test at 500° F	70
53	Equilibrium Weight Loss Versus Temperature, Material L, Aluminized-Mylar Film	71
54	Degradation of Material B, Phenolic Foam	73
55	Thermal/Vacuum Stability Apparatus	76
56	Thermal/Vacuum Environmental Stability Test Specimens	77
57	Iron-Constantan Thermocouple Attached to Specimen Group	78
58	Radiant-Heating Assemblies for Thermal/Vacuum Environmental Stability Tests	79
59	Thermal Cycling Apparatus	85
60	Temperature Histories of Front and Back Faces (One Cycle), Material A	96
61	Thermal Cycling Samples, Material A	97
62	Temperature Histories of Front and Back Faces (One Cycle), Material B	98
63	Thermal Cycling Samples, Material B	99
64	Temperature Histories of Front and Back Faces (One Cycle), Material C	100
65	Thermal Cycling Samples, Material C	101
66	Temperature Histories of Front and Back Faces (One Cycle), Material D	102

Figure		Page
67	Thermal Cycling Samples, Material D	103
68	Temperature Histories of Front and Back Faces (One Cycle), Material E	104
69	Thermal Cycling Samples, Material E	105
70	Temperature Histories of Front and Back Faces (One Cycle), Material F	106
71	Thermal Cycling Samples, Material F	107
72	Temperature Histories of Front and Back Faces (One Cycle), Material J	108
73	Thermal Cycling Samples, Material J	109
74	Temperature Histories of Front and Back Faces (One Cycle), Material K	110
75	Thermal Cycling Samples, Material K	111
76	Temperature Histories of Front and Back Faces (One Cycle), Material L	112
77	Thermal Cycling Samples, Material L	113
78	Spectral-Reflectance Measurements of Unexposed Surfaces, Materials A-E; 1-20 μ Region	117
79	Spectral-Reflectance Measurements of Unexposed Surfaces, Materials F-K; 1-20 μ Region	118
80	Spectral-Reflectance Measurements of Unexposed Surfaces, Material B; 0.27-1.8 μ Region	119
81	Spectral-Reflectance Measurements of Unexposed Surfaces, Materials A, C, and D; 0.27-1.8 μ Region	120
82	Spectral-Reflectance Measurements of Unexposed Surfaces, Materials E and F; 0.27-1.8 μ Region	121
83	Spectral-Reflectance Measurements of Unexposed Surfaces, Material G; 0.27-1.8 μ Region	122
84	Spectral-Reflectance Measurements of Unexposed Surfaces, Material H; 0.27-1.8 μ Region	123
85	Spectral-Reflectance Measurements of Unexposed Surfaces, Materials J and K; 0.27-1.8 μ Region	124
86	Spectral-Reflectance Measurements of Unexposed Surfaces, Material L; 0.27-1.8 μ Region	125
87	Ultraviolet-Radiation Damage to Reflective Surfaces, Materials A-E	127

Figure	Page
88 Ultraviolet-Radiation Damage to Reflective Surfaces, Materials F-H	128
89 Ultraviolet-Radiation Damage to Reflective Surfaces, Materials J-L	129
90 Damage to Reflective Surfaces Caused by 5-keV Electrons, Materials A-F	133
91 Damage to Reflective Surfaces Caused by 5-keV Electrons, Materials G-K	134
92 Combined Environment Chamber	135
93 Combined Environment Apparatus	136
94 Damage to Reflective Surfaces Caused Simultaneously by 5-keV Electrons and Ultraviolet Radiation, Materials A-E	138
95 Damage to Reflective Surfaces Caused Simultaneously by 5-keV Electrons and Ultraviolet Radiation, Materials F-K	139
96 Panel Shear Apparatus Diagram	143
97 Panel Shear Apparatus	144
98 Elevated Temperature Oven	146
99 Cryogenic Refrigerator	147
100 Cryogenic Refrigerator - Internal View	148
101 Material A (AJ-8) - Panel Shear	150
102 Material A (AJ-9) - Panel Shear	151
103 Material B (BJ-2) - Panel Shear	153
104 Material B (BJ-6) - Panel Shear	154
105 Material B (BJ-9) - Panel Shear	155
106 Material C (CJ-3) - Panel Shear	157
107 Material C (CJ-4) - Panel Shear	158
108 Material D (DJ-4) - Panel Shear	160
109 Material D (DJ-6) - Panel Shear	161
110 Panel Bend Apparatus Diagram	165
111 Panel Bend Apparatus	166
112 Material A (AK-1, 2) - Panel Bend	168
113 Material A (AK-5, 6) - Panel Bend	169
114 Material B (BK-1, 3, 4) - Panel Bend	171

Figure		Page
115	Material B (BK-6, 7, 8) – Panel Bend	172
116	Material C (CK-1, 2, 3, 4) – Panel Bend	174
117	Material D (DK-1, 4) – Panel Bend	176
118	Material G (GK-1) – Panel Bend	177
119	Material L (LK-6) – Panel Bend	179
120	Facing Tension – Specimen Detail	181
121	Facing Tension Test – Specimen Grips	182
122	Facing Tension Apparatus Diagram	183
123	Material A (AL-3) – Facing Tension	185
124	Material B (BL-12) – Facing Tension	188
125	Material C (CL-4) – Facing Tension	190
126	Material D (DL-2, 14) – Facing Tension	192
127	Material G (GL-7) – Facing Tension	194
128	Facing Separation Apparatus Diagram	197
129	Facing Separation Apparatus	198
130	Material A (AM-2) – Facing Separation	201
131	Material B (BM-6) – Facing Separation	203
132	Material B (BM-10) – Facing Separation	204
133	Material B (BM-8) – Facing Separation	205
134	Material C (CM-7) – Facing Separation	207
135	Material C (CM-11) – Facing Separation	208
136	Material E (EM-3) – Facing Separation	211
137	Material E (EM-5) – Facing Separation	212
138	Core Compression Apparatus Diagram	216
139	Material A (AN-1, 5) – Core Compression	221
140	Material A (AN-13) – Core Compression	222
141	Material C (CN-2) – Core Compression	226
142	Material D (DN-5, 6) – Core Compression	228
143	Material G (GN-5) – Core Compression	231
Appendix I: TEST RESULTS – CANDIDATE MATERIAL A		
144	Weight Loss Versus Time at Temperature, Epoxy Adhesive	242

Figure		Page
145	Equilibrium Weight Loss as a Function of Temperature, Epoxy Adhesive	243
146	Thermal Conductance of Composite Structures	245
147	Temperature Histories of Front and Back Faces During Thermal Cycling	246
Appendix II: TEST RESULTS – CANDIDATE MATERIAL B		
148	Equilibrium Weight Loss Versus Temperature, Foam Structure	254
149	Thermal Conductance of Foam Structure (With Hard Facing)	256
150	Linear Thermal Expansion of Reflective Surface	257
151	Linear Thermal Expansion of Foam Structure in X-X Direction	258
152	Linear Thermal Expansion of Foam Structure in Y-Y Direction	259
153	Linear Thermal Expansion of Foam Structure in Z-Z Direction	260
154	Linear Thermal Expansion of Epoxy Backing Surface	261
155	Comparison of Linear Thermal Expansion of Reflective Surface Before and After 6,000-Cycle Thermal Cycling Test	262
156	Enthalpy of Foam Structure Referenced to 32° F	263
157	Heat Capacity of Foam Structure	263
158	Enthalpy of Epoxy Backing Surface	264
159	Heat Capacity of Epoxy Backing Surface	264
160	Temperature Histories of Front and Back Faces During Thermal Cycling	265
Appendix III: TEST RESULTS – CANDIDATE MATERIAL C		
161	Equilibrium Weight Loss Versus Temperature, Epoxy Adhesive	274
162	Equilibrium Weight Loss Versus Temperature, Epoxy Sublayer	275
163	Thermal Conductance of Composite Structure	277
164	Temperature Histories of Front and Back Faces During Thermal Cycling	278
Appendix IV: TEST RESULTS – CANDIDATE MATERIALS D–F		
165	Equilibrium Weight Loss Versus Temperature, Epoxy Facing Adhesive	285
166	Equilibrium Weight Loss Versus Temperature, Epoxy Backing Adhesive	286
167	Equilibrium Weight Loss Versus Temperature, Epoxy Sublayer, Material D	287

Figure		Page
168	Equilibrium Weight Loss Versus Temperature, Epoxy Sublayer, Materials E-F	288
169	Thermal Conductance of Composite Structure	290
170	Temperature Histories of Front and Back Faces During Thermal Cycling, Material D	292
171	Temperature Histories of Front and Back Faces During Thermal Cycling, Material E	294
172	Temperature Histories of Front and Back Faces During Thermal Cycling, Material F	296
Appendix V: TEST RESULTS - CANDIDATE MATERIALS G-K		
173	Equilibrium Weight Loss Versus Temperature, Epoxy Adhesive	305
174	Thermal Conductance of Composite Structure, 1-in.-Thick Specimen	307
175	Temperature Distribution Along Wall of One Cylinder of Composite Structure	307
176	Linear Thermal Expansion of Reflective Surface	308
177	Linear Thermal Expansion of Back Surface	309
178	Comparison of Linear Thermal Expansion Before and After 6,000-Cycle Thermal Cycling Test	310
179	Temperature Histories of Front and Back Faces During Thermal Cycling, Material J	311
180	Temperature Histories of Front and Back Faces During Thermal Cycling, Material K	312

TABLES

Table	Page
I Candidate Material Identification	3
II Test Identification	7
III Representative Sample Configurations	9
IV Candidate Materials Laboratory Evaluations	10
V Description of Thermal Conductance Specimens	16
VI Mean Coefficient of Linear Thermal Expansion of Materials G-K	41
VII Description of Materials for Weight-Loss Behavior to 500° F	56
VIII Short-Term Weight Loss of Polymeric Reflector Components	58
IX Thermal/Vacuum 100-Hour Test	80
X Thermal/Vacuum 1,000-Hour Test	81
XI Thermal/Vacuum 6,000-Hour Test	82
XII Thermal Cycling Results - Material A	87
XIII Thermal Cycling Results - Material B	88
XIV Thermal Cycling Results - Material C	89
XV Thermal Cycling Results - Material D	90
XVI Thermal Cycling Results - Material E	91
XVII Thermal Cycling Results - Material F	92
XVIII Thermal Cycling Results - Material J	94
XIX Thermal Cycling Results - Material K	94
XX Thermal Cycling Results - Material L	95
XXI Solar Absorptance and Infrared Emissittance	115
XXII Ultraviolet Exposure Results	130
XXIII 5-keV Electron Exposure Results	131
XXIV Solar Reflectance After Combined-Environmental Exposure	137
XXV Mechanical Properties Tests on Candidate Materials - Unexposed Specimens	141

Table		Page
XXVI	Material A - Panel-Shear Test	149
XXVII	Material B - Panel-Shear Test	152
XXVIII	Material C - Panel-Shear Test	156
XXIX	Material D - Panel-Shear Test	159
XXX	Material G - Panel-Shear Test	162
XXXI	Panel-Shear-Test Summary	163
XXXII	Material A - Panel-Bend Test	170
XXXIII	Material B - Panel-Bend Test	170
XXXIV	Material C - Panel-Bend Test	173
XXXV	Material D - Panel-Bend Test	175
XXXVI	Material G - Panel-Bend Test	175
XXXVII	Material L - Panel-Bend Test	178
XXXVIII	Panel-Bend-Test Summary	178
XXXIX	Material A - Facing-Tension Test	186
XL	Material B - Facing-Tension Test	187
XLI	Material C - Facing-Tension Test	189
XLII	Material D - Facing-Tension Test	191
XLIII	Material G - Facing-Tension Test	193
XLIV	Facing-Tension-Test Summary	195
XLV	Material A - Facing-Separation Test	200
XLVI	Material B - Facing-Separation Test	202
XLVII	Material C - Facing-Separation Test	206
XLVIII	Materials D-F - Facing-Separation Test	210
XLIX	Materials G-K - Facing-Separation Test	213
L	Facing-Separation-Test Summary - Unexposed Specimens	214
LI	Material A - Core-Compression Test	219
LII	Material B - Core-Compression Test	223
LIII	Material C - Core-Compression Test	225
LIV	Materials D-F - Core-Compression Test	227
LV	Material G - Core-Compression Test	229

Table		Page
LVI	Core-Compression-Test Summary – Unexposed Specimens	232
LVII	Summary of Candidate Materials Test Results	235
Appendix I: TEST RESULTS – CANDIDATE MATERIAL A		
LVIII	Short-Term Weight Loss in Vacuum, Epoxy Adhesive	244
LIX	Long-Term Thermal/Vacuum Exposure, Composite Structure	244
LX	Behavior Under Thermal Cycling, Composite Structure	247
LXI	Summary of Optical-Properties Test Results	247
LXII	Panel-Shear Test, Composite Structure	248
LXIII	Panel-Bend Test, Composite Structure	248
LXIV	Facing-Tension Test, Facing Material	249
LXV	Facing-Separation Test, Composite Structure	250
LXVI	Core-Compression Test, Composite Structure	251
Appendix II: TEST RESULTS – CANDIDATE MATERIAL B		
LXVII	Short-Term Weight Loss in Vacuum, Foam Structure	255
LXVIII	Long-Term Thermal/Vacuum Exposure, Composite Structure	255
LXIX	Behavior Under Thermal Cycling, Composite Structure	266
LXX	Summary of Optical-Properties Test Results	267
LXXI	Panel-Shear Test, Composite Structure	267
LXXII	Panel-Bend Test, Composite Structure	268
LXXIII	Facing-Tension Test, Facing and Backing Materials	269
LXXIV	Facing-Separation Test, Composite Structure	270
LXXV	Core-Compression Test, Composite Structure	271
Appendix III: TEST RESULTS – CANDIDATE MATERIAL C		
LXXVI	Short-Term Weight Loss in Vacuum	276
LXXVII	Long-Term Thermal/Vacuum Exposure, Composite Structure	276
LXXVIII	Behavior Under Thermal Cycling, Composite Structure	279
LXXIX	Summary of Optical-Properties Test Results	280
LXXX	Panel-Shear Test, Composite Structure	280
LXXXI	Panel-Bend Test, Composite Structure	281
LXXXII	Facing-Tension Test, Facing Material	281

Table		Page
LXXXIII	Facing-Separation Test, Composite Structure	282
LXXXIV	Core-Compression Test, Composite Structure	283
Appendix IV:	TEST RESULTS – CANDIDATE MATERIALS D–F	
LXXXV	Short-Term Weight Loss in Vacuum	289
LXXXVI	Long-Term Thermal/Vacuum Exposure, Composite Structure	291
LXXXVII	Behavior Under Thermal Cycling, Composite Structure, Material D	293
LXXXVIII	Behavior Under Thermal Cycling, Composite Structure, Material E	295
LXXXIX	Behavior Under Thermal Cycling, Composite Structure, Material F	297
XC	Summary of Optical-Properties Test Results	299
XCI	Panel-Shear Test, Composite Structure	300
XCII	Panel-Bend Test, Composite Structure	300
XCIII	Facing-Tension Test, Facing and Backing Materials	301
XCIV	Facing-Separation Test, Composite Structure	302
XCV	Core-Compression Test, Composite Structure	303
Appendix V:	TEST RESULTS – CANDIDATE MATERIALS G–K	
XCVI	Short-Term Weight Loss in Vacuum, Epoxy Adhesive	306
XCVII	Long-Term Thermal/Vacuum Exposure, Composite Structure	306
XCVIII	Behavior Under Thermal Cycling, Composite Structure	313
XCIX	Summary of Optical-Properties Test Results	314
C	Panel-Shear Test, Composite Structure	314
CI	Panel-Bend Test, Composite Structure	315
CII	Facing-Tension Test, Facing Material	315
CIII	Facing-Separation Test, Composite Structure	316
CIV	Core-Compression Test, Composite Structure	317

NOMENCLATURE

C	thermal conductance
C_p	specific heat
E	modulus of elasticity
EI/b	bending stiffness per unit width
G	shear modulus of elasticity
k	thermal conductivity
M_e	maximum elastic moment
M_u	ultimate moment
t	temperature
α	absorptance
α_t	total hemispherical absorptance
$\alpha_{\lambda n}$	near-normal spectral absorptance
ϵ	emittance
ϵ_t	total hemispherical emittance
ρ	solar reflectance
$\rho_{\lambda n}$	near-normal spectral reflectance

Section I INTRODUCTION

This report summarizes the technical effort on the Lockheed Missiles & Space Company (LMSC) Candidate Materials Laboratory Study Program, a portion of the ASTEC program at LMSC. This work effort is in direct support of the Air Force Solar Turbo Electric Concept (ASTEC)-Program 678A.

1. PURPOSE OF TESTING

The objectives of this work effort were as follows:

- Determine the basic thermophysical, optical, and mechanical properties of materials developed by the solar-collector industry for use in the ASTEC program.
- Test the degrading effects of various segregated and combined elements of the space environment on these materials.

Selection of the tests to be performed on a given material was based on the properties and environmental data required for subsequent thermal, structural, and performance analyses. Where possible, test methods were selected to make use of existing test apparatus.

Several points should be emphasized regarding the conditions of testing:

- The test activity represents the accumulation of basic material-properties data for materials that have been proposed in solar-collector designs to the Air Force under Sundstrand Contract AF 33(615)-2141. There were no specific design criteria against which the candidate materials were to be measured in the LMSC laboratory program.
- The LMSC task was solely to make findings regarding the nature and characteristics of the candidate materials. Evaluation of these findings was to be made by the Air Force without specific recommendations from LMSC as to the best product.
- The LMSC technical effort did not include additional testing to determine the causes of failures (when they occurred) of the candidate materials in any phase of the test program.

The space environment of interest for purposes of the ASTEC program is that of a circular polar orbit ranging in altitude from 200 to 500 nm. In this environment, the potential sources of damage to candidate materials under consideration were believed (at time of test selection) to be the following:

- Solar ultraviolet radiation
- Low-energy electrons encountered in the auroral zones
- Vacuum
- Temperature levels and thermal cycling

The test program, accordingly, was designed to determine the effects of these environmental elements on the candidate materials during a simulated orbit life of up to 14 months. Dose levels were established on the basis of the known characteristics of the ASTEC environment. The temperature range to be investigated (from -200 to +250° F) was determined by ASTEC system considerations and by the thermal constraints imposed by the organic constituents of the candidate collector systems.

2. DESCRIPTION OF CANDIDATE MATERIALS

Six material systems were selected and approved for testing by AFAPL; five were developed for use in a petaline solar collector, while the sixth was intended for use in a rigidized-in-place configuration. Only the first five were involved in the orbital collector competition; the rigidized-in-place material was included in the test program by direction of AFAPL as representative of a material that might be used in a second- or third-generation solar collector.

Companies supplying material systems were the following: Electro Optical Systems, General Electric Company, Viron Division of Geophysics Corporation of America, Goodyear Aerospace Corporation, Ryan Aeronautical Company, and Thompson-Ramo-Wooldridge, Inc.

The candidate materials were obtained by LMSC from the respective vendors in quantities and sizes specified by LMSC. In the case of the petaline systems, each vendor certified that the material or materials supplied were representative of those being proposed to the Air Force under the Sundstrand program. Such certification was not required in the case of the rigidized-in-place material. Specimens, for the most part, were tested without further processing by LMSC; it was necessary for certain tests, however, to cut the materials to the required size and/or shape.

Of the six types of materials tested, four were epoxy-bonded metal systems, one was phenolic foam with a metal surface, and one was a polyurethane rigidized-in-place system. The reflective surfaces included vacuum-deposited aluminum with or without various undercoatings and overcoatings, vacuum-deposited silver with or without overcoating, and aluminized mylar. A more detailed description of the candidate materials is given in Table I. Photographs showing back-face, front-face, and cross-section views of each material are presented in Figures 1 through 6.

It can be seen in Table I that the candidate materials were identified only by letter. This system of identification, making no reference to the manufacturer, was established to preclude the possibility of bias on the part of those conducting the tests; the

Table I. Candidate Material Identification

Letter designation	Structure	Reflective surface
A	Aluminum honeycomb, epoxy bonded to aluminum front and back sheets	Aluminum substrate, vacuum-deposited aluminum
B	Electroformed nickel sheet backed with phenolic foam with epoxy-bonded aluminized-mylar back surface	Nickel substrate, vacuum-deposited aluminum, silicon-oxide overcoating
C	Aluminum honeycomb, epoxy bonded to aluminum front and back sheets	Aluminum substrate, epoxy, silicon oxide, vacuum-deposited aluminum, silicon oxide
D	(Same as C)	Aluminum substrate, epoxy, silicon oxide, vacuum-deposited aluminum
E	(Same as C)	Aluminum substrate, epoxy, silicon oxide, vacuum-deposited aluminum
F	(Same as C)	Aluminum substrate, epoxy, silicon oxide, vacuum-deposited aluminum, silicon oxide
G	Electroformed nickel front and back sheets separated by 1-1/2-in. diameter nickel cylinders, joined with epoxy	Nickel substrate, vacuum-deposited silver
H	(Same as G)	Nickel substrate, silver, silicon oxide
J	(Same as G)	Nickel substrate, chrome, silicon oxide, aluminum
K	(Same as G)	Nickel substrate, chrome, silicon oxide, aluminum, silicon oxide
L	Polyurethane-rigidized nylon	Aluminized mylar with epoxy sublayer

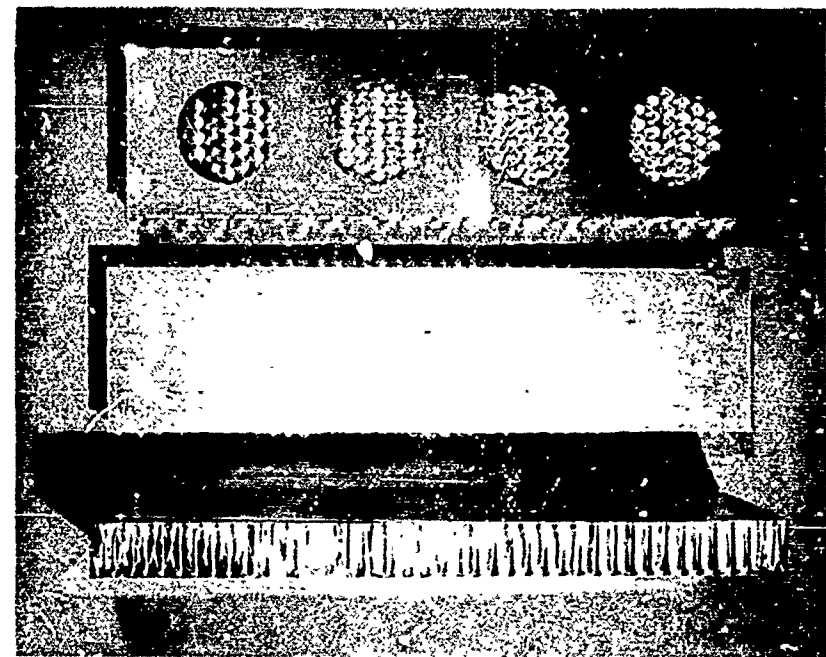


Figure 1 Candidate Material A

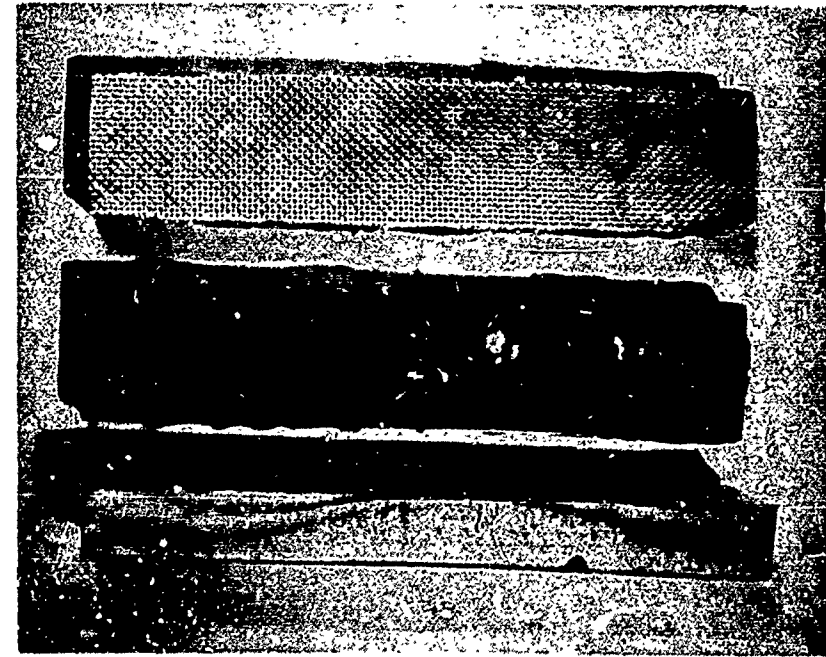


Figure 2 Candidate Material B

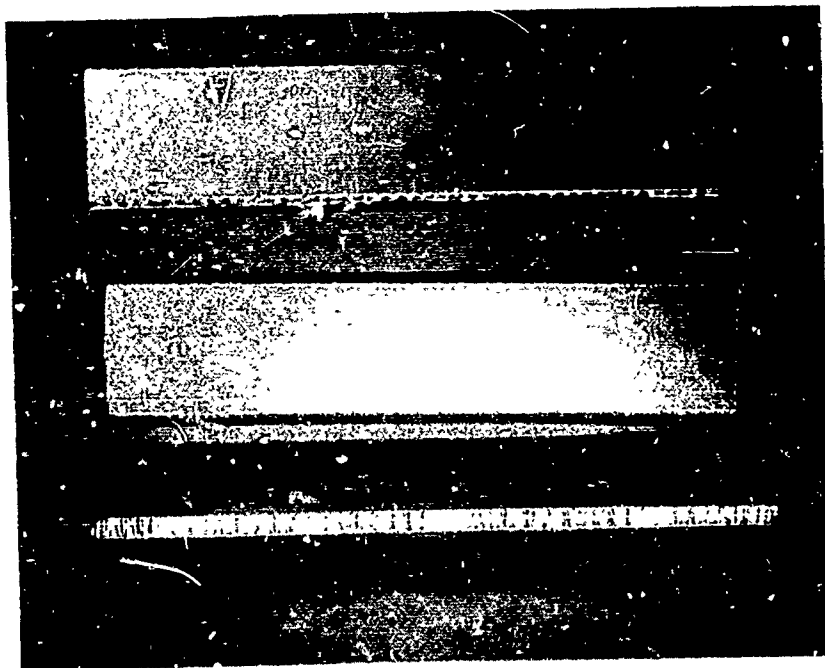


Figure 3 Candidate Material C

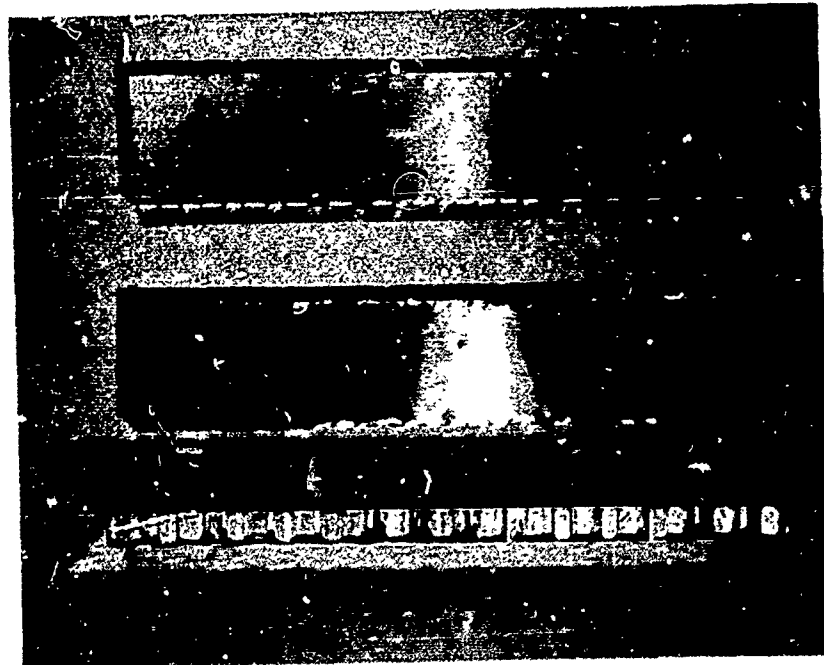


Figure 4 Candidate Materials D-F

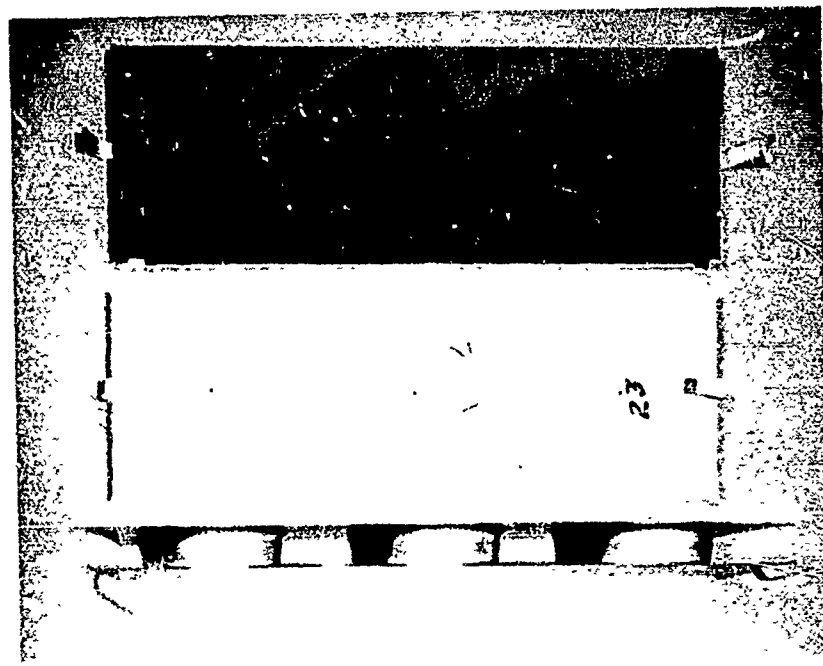


Figure 5 Candidate Materials G-K

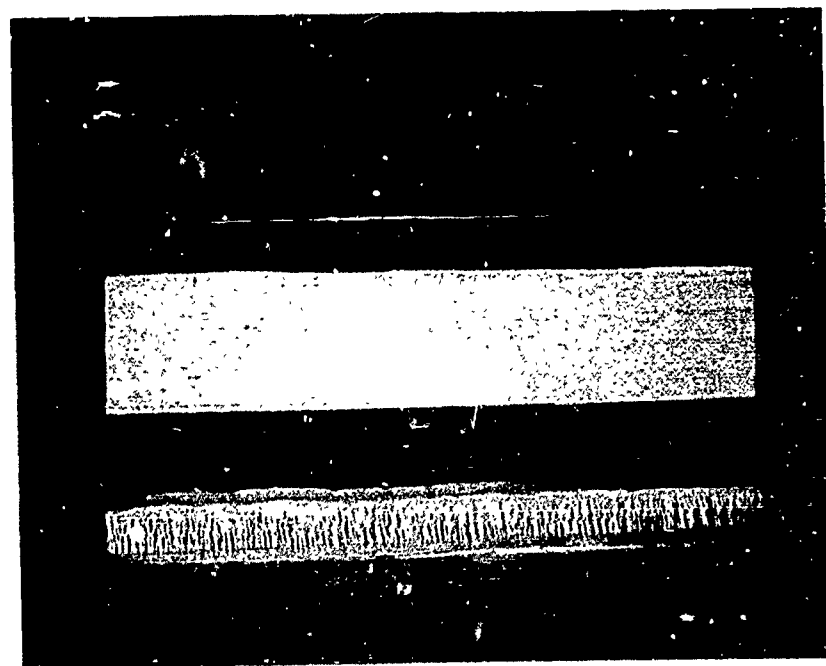


Figure 6 Material L

system is used throughout this report. The tests performed on the specimen were also identified by letter; the letter test code is presented in Table II. Each sample was thus identified by two or more letters. The first letter designated the candidate material, and the following letter(s) designated the test(s) performed on that sample. If more than two letters were used, the order of the letters was the order in which the tests were to be performed. Completing the identification system was a hyphen followed by an arabic numeral, indicating that the sample in question was the first, second, etc., such sample.

Table II. Test Identification

Letter designation	Test
A	Thermal conductance
B	Thermal expansion
C	Heat capacity
D	Thermal diffusivity
E	Weight loss
F	Thermal and vacuum environment
G	Thermal cycling
H	Solar absorptance and infrared emittance
J	Panel shear
K	Panel bend
L	Facing tension
M	Facing separation
N	Core compression
P	Ultraviolet irradiation, room temperature
Q	Ultraviolet irradiation, high temperature
R	Electron irradiation, room temperature
S	Electron irradiation, high temperature
T	Electron plus ultraviolet irradiation, room temperature
U	Electron plus ultraviolet irradiation, high temperature

For example, sample CGM-2 designated the second sample of material C on which a thermal cycling followed by a facing-separation test was performed.

3. SCOPE OF TESTING

The total test effort was grouped into three major categories:

- Thermophysical Properties
 - Thermal conductance
 - Thermal expansion
 - Heat capacity
 - Weight loss in vacuum
 - Thermal/vacuum environmental stability
 - Thermal cycling

- Optical Properties
 - Solar absorptance and infrared emittance
 - Ultraviolet irradiation (uv)
 - Electron bombardment (e^-)
 - Combined environment (uv + e^-)
- Mechanical Properties
 - Panel shear
 - Panel bend
 - Facing tension
 - Facing separation
 - Core compression

In certain cases, to determine the impact of environmental testing on structural or reflective properties, samples were subjected to sequential testing. Thus, thermal cycling and thermal/vacuum stability tests were followed by facing-separation or core-compression tests. Ultraviolet irradiation, electron bombardment, combined environment, and thermal cycling tests were followed by measurements of solar absorptance and infrared emittance.

The original test plan included one additional test, thermal diffusivity, in the thermophysical-properties category. Thermal diffusivity is expressed by the ratio of thermal conductivity to the product of density and specific heat. It was believed that the thermal conductivity of electroformed nickel, used in two of the candidate material systems, might be different from that of commercial nickel. It was, therefore, planned to determine the thermal conductivity, k , by measurement of thermal diffusivity and prior knowledge of ρ and C_p .

It was subsequently concluded, however, that the difference in thermal conductivity between electroformed nickel and commercial nickel was not appreciable. The basis for this conclusion was the finding that the coefficient of thermal expansion of electroformed nickel was not significantly different from that of commercial nickel, and that, accordingly, the electroforming process had not significantly altered the structure of the nickel. With AFAPL approval, therefore, thermal diffusivity tests were eliminated from the test program.

Configuration of specimens was determined by the nature of the particular test. Thus, for the optical-properties measurements, it was necessary to use only the reflective surfaces, whereas composite structures were required for most of the mechanical-properties testing. Representative sample configurations for the different tests are shown in Table III.

Although test conditions were identical for all candidate materials, it was not necessary to perform all listed evaluations on each material. Certain of the thermophysical-property measurements were not made on the metallic structures, for example, because the properties in question have been well established for metals. The evaluations planned for each of the candidate materials are shown in Table IV.

Table III. Representative Sample Configurations

Test	Sample configuration (in.)
Thermal conductance	7 diam. by 1/4 to 3/4 thick
Thermal expansion	Various
Heat capacity	Various(a)
Weight loss in vacuum	Various
Thermal/vacuum environmental stability	3 diam. by 1/4 to 3/4 thick
Thermal cycling	3 diam. by 1/4 to 3/4 thick
Solar absorptance and infrared emittance	1 diam.(b)
Ultraviolet irradiation	5/8 by 1(b)
Electron bombardment	5/8 by 1(b)
Combined environment	5/8 by 1(b)
Panel shear	2 by 3 by 1/4 to 1 thick
Panel bend	2 by 10 by 1/4 to 1 thick
Facing tension	3/4 by 6(b)
Facing separation	3 diam. by 1/4 to 1 thick
Core compression	3 diam. by 1/4 to 1 thick

(a) 20-g mass required.

(b) Thickness of reflective surface.

In the early stages of the test program, severe degradation was noted in Material L during both the thermal cycling and the thermal/vacuum stability tests. In both cases, samples of this material exhibited blistering and warping of the aluminized-mylar reflective surface, to the point where the bond between the structure and reflective surface had been largely destroyed. (See Figure 75.) It was accordingly judged that continued inclusion of this material in the testing program would be purposeless. This conclusion was brought to the attention of AFAPL, which directed that no further testing be performed on Material L. Results of tests on this material which were then available, however, are included in this report.

4. ORGANIZATION OF THIS REPORT

This report is organized into seven sections and five appendixes. Section II presents a discussion of thermophysical-properties testing; Section III, a discussion of optical-properties testing; and Section IV, a discussion of mechanical-properties testing. Conclusions of the study are presented in Section V, and a tabular compilation is also presented for those tests results that it was believed would be of particular significance in determining which materials most nearly meet the requirements of the ASTEC program. Recommendations appear in Section VI. Each of the five appendixes, I through V, presents all test results for one of the five candidate material systems.

Table IV. Candidate Materials Laboratory Evaluations

Candidate material system	Thermophysical properties				Optical properties				Mechanical properties			
	Thermal conductivity	Thermal expansion (a)	Heat capacity	Weight loss	Thermal & vacuum environment	Solar absorptance & infrared emittance (b)	Ultraviolet irradiation bombardment	Combined environment	Panel shear	Panel bend	Facing separation (c)	Core compression (d)
A Composite structure	Epoxy bonding adhesive	Composite structure	Composite structure	Reflective surface	Reflective surface	Reflective surface	Reflective surface	Reflective surface	Composite structure	Composite structure	Facing material	Composite structure
B Composite structure; phenolic foam	Phenolic foam	Composite structure	Composite structure	Reflective surface	Reflective surface	Reflective surface	Reflective surface	Reflective surface	Composite structure	Composite structure	Facing material; facing material	Composite structure
C Composite structure	Epoxy bonding adhesive	Composite structure	Composite structure	Reflective surface	Reflective surface	Reflective surface	Reflective surface	Reflective surface	Composite structure	Composite structure	Facing material	Composite structure
D-F Composite structure	Bonding adhesive (2 types); epoxy sublayer (2 types)	Composite structure	Composite structure	Reflective surface	Reflective surface	Reflective surface	Reflective surface	Reflective surface	Composite structure	Composite structure	Facing material; facing material	Composite structure
G-K Composite structure	Facing and backing material	Epoxy bonding adhesive	Composite structure	Reflective surface	Reflective surface	Reflective surface	Reflective surface	Reflective surface	Composite structure	Composite structure	Facing material	Composite structure
L Composite structure	Epoxy sublayer; composite structure	Epoxy sublayer; composite structure	Composite structure	Reflective surface	Reflective surface	Reflective surface	Reflective surface	Reflective surface	Composite structure	Composite structure	Facing material; epoxy sublayer	Composite structure

(a) This test was performed also on Materials B and G-K after thermal/vacuum exposure and thermal cycling.

(b) These measurements were made also on samples exposed to ultraviolet irradiation, electrons, and combined environment, and to thermal cycling.

(c) This test was performed also after thermal/vacuum exposure and thermal cycling.

(d) This test was performed also after thermal/vacuum exposure and thermal cycling.

Section II

THERMOPHYSICAL PROPERTIES

1. INTRODUCTION

Six types of tests were used to determine the thermophysical properties of candidate materials:

- Thermal conductance
- Thermal expansion
- Heat capacity
- Weight loss in vacuum
- Thermal/vacuum environmental stability
- Thermal cycling

It was not necessary to perform all these tests on all of the materials being evaluated. Thus, thermal expansion measurements were omitted in the case of the honeycomb structures, since the expansion characteristics of such structures are well known. Similarly, heat capacity, and weight loss tests were performed only on the organic constituents of the candidate materials. Where appropriate, properties were evaluated as a function of time as well as temperature. Specimens were exposed to the thermal/vacuum environment for periods of 100, 1,000, and 6,000 hr and to thermal cycling for 100, 1,000, and 6,000 cycles (each cycle lasted ~ 40 min).

Specimens exposed to the thermal/vacuum environment and to thermal cycling were then subjected to additional testing to determine the effects of these exposures upon structural and optical properties. Thermal/vacuum exposure was followed by either facing-separation or core-compression tests. Specimens which had been thermally cycled also were subjected to these tests; in addition, reflectance measurements were made. The results of these subsequent evaluations are presented in appropriate sections of this report.

2. THERMAL CONDUCTANCE

Thermal conductances of the composite structures were measured using 7-in. diameter and 12-in. square guarded hot-plate apparatus in accordance with the procedures of ASTM C177-63, "Standard Method of Test for Thermal Conductivity of Materials by Means of the Guarded Hot Plate."

a. Description of Apparatus

The guarded hot-plate apparatus was selected to provide data of sufficient accuracy to enable reliable thermal analysis of the proposed structures. The equipment (Figures 7

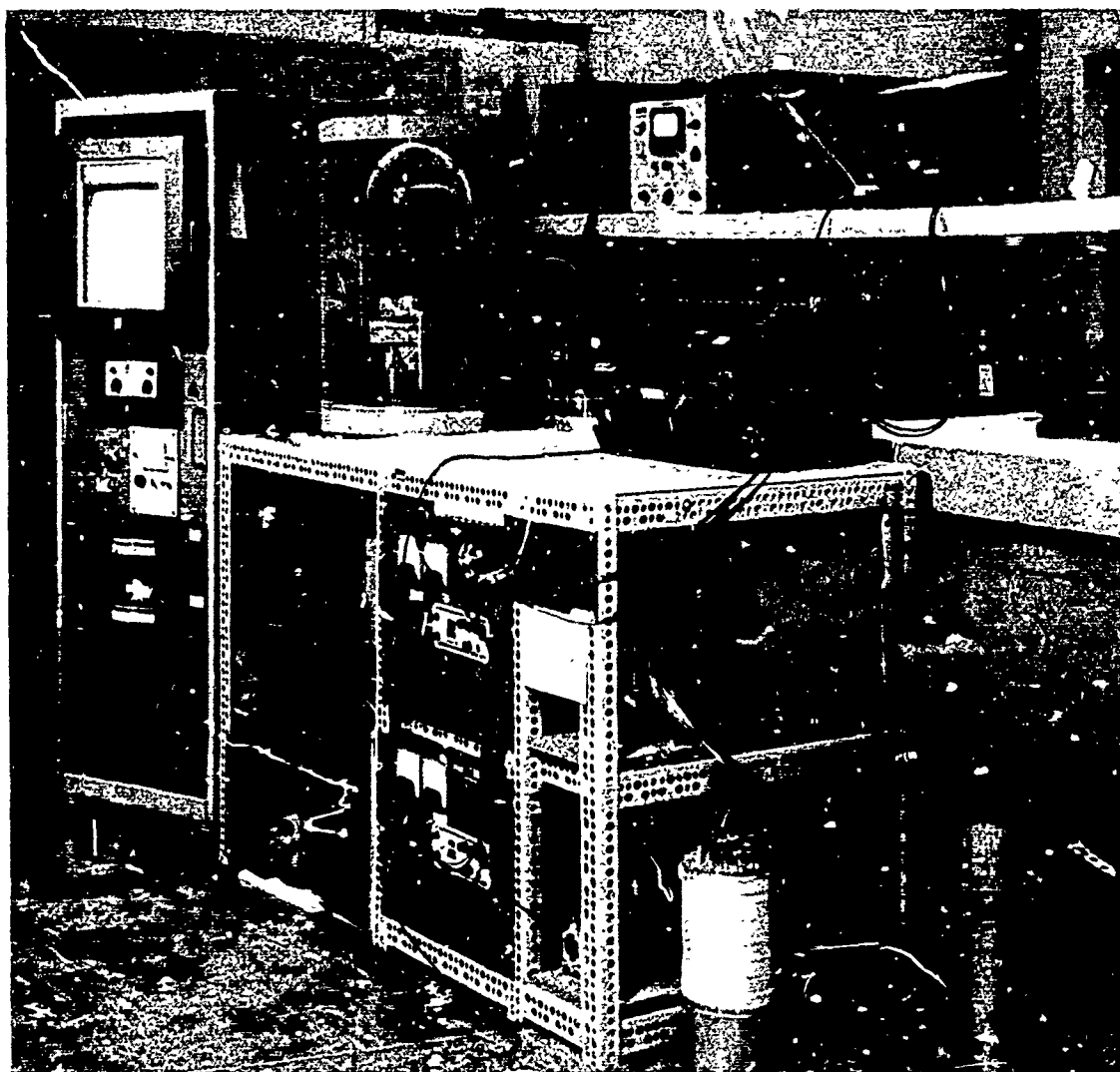


Figure 7 Thermal Conductance Apparatus - 7-in.-Diameter Guarded Hot Plate

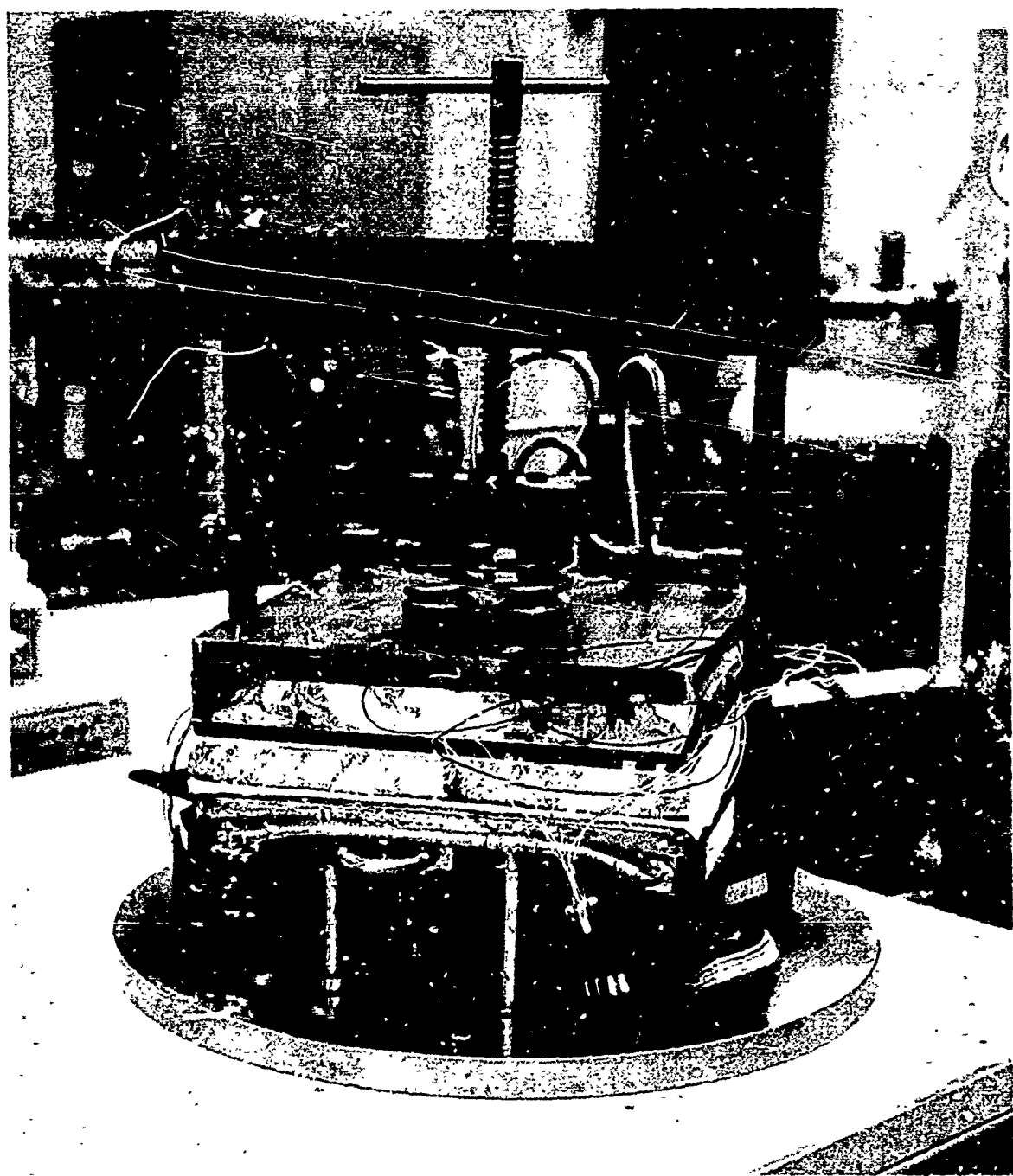


Figure 8 Thermal Conductance Apparatus - 12 in. -Square Hot Plate

and 8) was constructed in accordance with the recommendations of ASTM C177-63 for the "Metal Surfaced Hot Plate." A 7-in.-diameter hot plate apparatus was used for all structures with the exception of materials G-K. This structure was tested in a 12-in.-square hot plate. The 7-in.-diameter apparatus has a 4-in.-diameter main heater with a 7-in. o.d. by 4-1/8 in. i.d. guard heater. The 12-in.-square unit has a 6-in.-square main heater with a 12-in.-square guard heater having a 1/16 in. separation from the main heater. With the exception of size, both units are of the same construction and employ identical control systems.

All surfaces of guard heater, main heater, and cooling units in contact with the specimens are 1/4 in. annealed copper. Heating units are made from 1-mil stainless steel foil separated from the surface plates by 5-mil mica. Chromel-alumel thermocouples are located in each surface plate of the main heater, guard heater, and cooling units. Three thermocouples are in each main surface plate, two in each guard plate, and four in each cooling unit. Their junctions are peened into the copper approximately 1/16 in. below the specimen surfaces. Four differential thermocouples, electrically insulated from the plates, are installed between the edges of the main and guard surface plates for control of the guard to main heater temperature.

A regulated dc power supply is used to provide power to the main heater. Guard heater power is supplied by a silicon-controlled rectifier which is controlled by a Leeds and Northrop CAT unit. The differential thermocouples are connected in series and the output fed into a Leeds and Northrop null detector having a sensitivity of $10 \mu\text{V}$ full scale. This detector controls the CAT unit. The maximum imbalance of temperature between main and guard surfaces with this control system is 0.1°F .

Each apparatus is installed in a vacuum chamber which has an oil diffusion pump and mechanical fore pump with a LN_2 trap located between the diffusion pump and chamber. A vacuum of 10^{-5} Torr is maintained in the chamber for all tests. The cooling units are connected to a circulating system with heat exchanges and temperature controllers for varying cooling unit surface plate temperature between -300 and $+350^\circ\text{F}$. Each assembly is mounted in a frame which is capable of exerting a force of 2,000 lb on the 7-in.-diameter unit and 4,000 lb on the 12-in.-square unit.

All thermocouple outputs are read, referenced to the ice point, with a Leeds and Northrop Model K-3 precision potentiometer. Main heater current and voltage drop are measured using calibrated precision shunts and voltage dividers. The outputs from these devices are measured with the K-3 instrument.

b. Test Procedure

The honeycomb and electroformed structure samples were instrumented with five thermocouples cemented to each surface, three in the area of the main heater and two in the area of the guard heater. A conductive epoxy cement was used to attach the junctions to the surfaces. Three-mil diameter chromel-alumel thermocouples were used for all specimens. In addition to the surfaces, three thermocouples were attached to a central

cylinder support of the electroformed structure. All leads were thermally grounded to the surface for 1/2-in. with cement. Surface temperatures of organic structures were measured with thermocouples formed by spot welding 3-mil wire to 1-mil pure copper foil, 1/4-in. square. The junction was formed through the foil by a 1/16-in. separation between wires. The foil was cemented to the surfaces of the structures. Leads were insulated from metal surfaces with 1-mil tape. Fiberfrax (R) paper 1/16-in. thick was placed between the surface plates and specimen surfaces to achieve a uniform thermal resistance at each interface. Sufficient pressure was applied to the assembly to assure uniform contact with each structure.

The total resistance method of ASTM C177-63 was not used for these tests, since only very light forces could be applied to the structure and the surfaces were not uniform. Consequently, the temperature differences measured between surfaces were used to calculate conductance.

The edges of the stack were covered with a 2-in. thickness of fiber glass to reduce edge losses. The system was then evacuated to a pressure of at least 10^{-5} Torr. The cooling units were adjusted to maintain the desired cold face temperatures before power was applied to the heater unit. The temperature drop across each specimen was adjusted to 25° to 100° F for each test. Temperatures and power were recorded at 30-min intervals, until thermal equilibrium was established. This was achieved when the conductance calculated for four successive sets of readings did not vary by more than 1 percent.

Thermal conductance was calculated by use of the following expression:

$$C = \left(\frac{1.707EI}{A\Delta t} \right) - Q'$$

where E is voltage drop across main heater, v; I is main heater current, amps; A is area of main heater, FE^2 ; Δt is temperature difference across the specimen, °F; and Q' is summation of losses from specimen and heater due to imbalance in guarding.

c. Test Results

Thermal conductance measurements were performed on the system materials listed in Table V. During all tests, the ambient pressure was maintained at 10^{-4} Torr or less. For all metal structures, the temperature difference between hot and cold faces did not exceed 100° F to minimize radiative energy transfer. The data for each material are given in the following subsections.

Material A. The conductance, in vacuum, for the 1/4 in. and 3/4 in. nominal thickness structures are shown by Figure 9. For these measurements the 1-1/2 in.-diameter opening in the rear face was covered with a plate of 5-mil aluminum. This was to eliminate the effect on conductance of the hot-plate boundary surface emittance due to radiant exchange through this opening. The measured conductance values are for a structure having solid faces, and they do not include energy transfer by radiation through the opening.

Table V. Description of Thermal Conductance Specimens

Material	Specimen			
	Dimensions	Facing	Core	Bulk density
A	7 in. diam. by 0.757 in. thick	0.004-0.005 in. aluminum	1/4 in. hexagonal cells, 0.001 in. aluminum wall	4.1
A	7 in. diam. by 0.257 in. thick	0.004-0.005 in. aluminum	3/4 in. hexagonal cells, 0.001 in. aluminum wall	8.4
B	7 in. diam. by 0.505-0.520 in. thick 7 in. diam. by 1/2 in. nominal thickness	0.010-0.020 hard epoxy-phenolic type material	0.475 in. thick	6-8
B	7 in. diam. by 1/2 in. nominal thickness	none	0.475 in. thick	1.8-1.9
C	7 in. diam. by 0.296 in. thick	~ 0.003 in. aluminum	1/8 in. hexagonal cell, 0.001 in. aluminum wall	9.7
D-F	7 in. diam. by 0.525 in. thick	0.004 and 0.008 in. aluminum faces	3/8 in. hexagonal cell, 0.001 in. aluminum wall	5.8
G-K	12 in. square by 1 in. thick	0.002 in. nickel	1 in. high by 1-1/2 in. nominal diam. cylinders, 0.002 in. wall, nickel, ~ 3 in. on centers	-

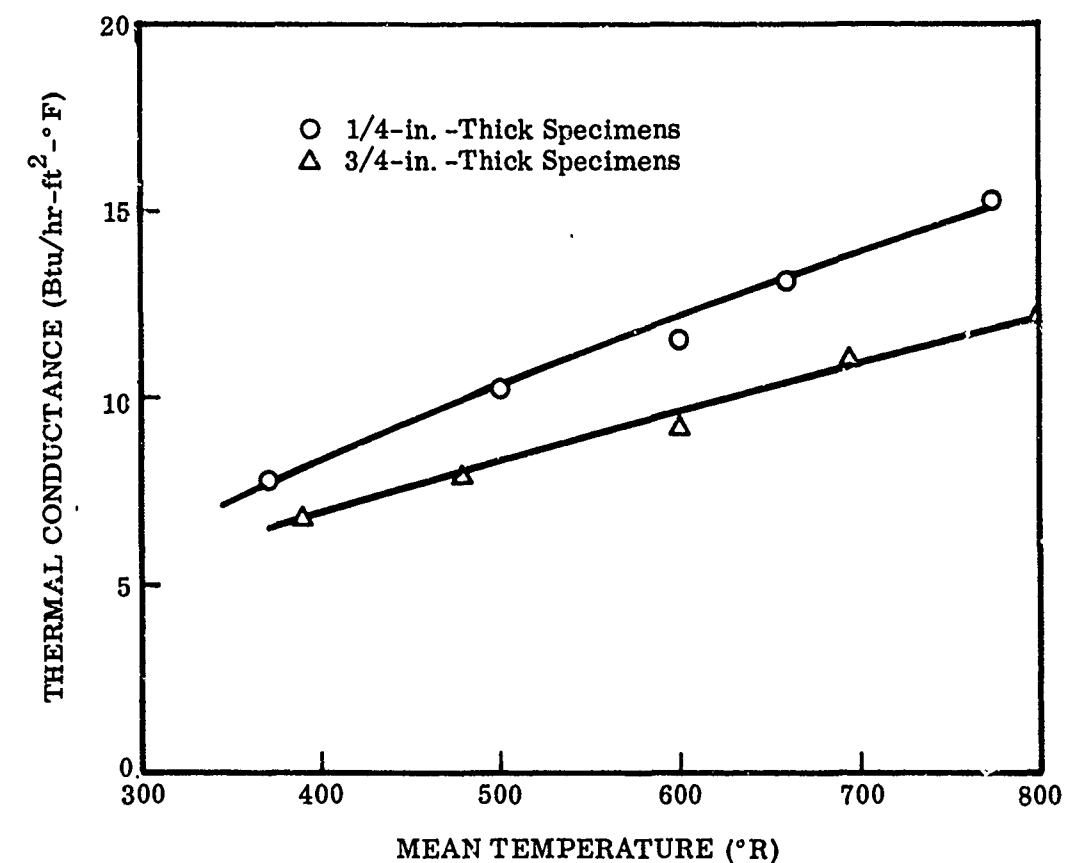


Figure 9 Thermal Conductance of Material A

The data indicate that a major portion of the total thermal resistance of the structure is at the joint or bonds between the core and structure. This is demonstrated by the increase in conductance of only approximately 25 percent with a 300 percent decrease in core thickness. During the tests the temperature gradient between faces was kept small to reduce to a minimum any radiant energy exchange contribution to the overall conductance. Thus, these data represent the energy transfer through the solid portion of the structure. The estimated maximum uncertainty in these data is 10 percent.

Material B. The thermal conductance values for the composite structure of Material B are shown by Figure 10. The structure consisted of a plastic foam core, with hard plastic faces bonded to the surfaces of the core. The nominal thickness of the test specimen was 1/2 in.

The points plotted in Figure 10 represent the average conductance from each set of two specimens measured in the guarded-hot-plate apparatus. As the individual specimens were not uniform in surface condition, the variation in conductance based on each individual sample cannot be estimated. All four samples had a very poor surface or facing. They contained cracks and numerous voids or depressions. This poor surface condition prevented the achievement of a uniform thermal resistance at the interfaces between the heating and cooling units and the specimens. This is presumed to be the major cause for the wide spread in data for the two sets of specimens (~ 25 percent). The point with the symbol \square is felt to be high by reason of a compression of the specimen at the higher temperature caused by the weight of the heater units.

Material C. Figure 11 shows the experimental value of thermal conductance of the honeycomb structure of this system as a function of mean temperature. In all cases, the temperature difference between faces did not exceed 50°F so as to minimize heat transfer by radiation. Thus, these conductance values represent the heat transfer by conduction through the solid portions of the structure, that is, the cell walls. Based on core geometry and material, it is estimated that the major thermal resistance to heat transfer by conduction between faces is the glue or bond joint between the core and faces. The maximum uncertainty for these data is estimated to be 15 percent.

Materials D-F. Figure 12 shows the experimentally determined values of thermal conductance as a function of mean temperature for the D-F structure. The ambient pressure during these tests was 10^{-5} Torr or less. The temperature difference between hot and cold faces did not exceed 25°F at any mean temperature (taken as average of hot and cold face temperature). Therefore, the reported conductances are for the energy transport through the solid portions of the structure. The estimated maximum uncertainty for these data is 10 percent.

Materials G-K. Figure 13 illustrates the experimentally determined values of conductance for this structure at an ambient pressure of 10^{-5} Torr or less. Over the entire temperature range the maximum temperature differences between faces did not exceed 80°F to minimize radiant-energy transfer. The decreasing conductance with increasing temperature is due almost entirely to the solid connecting link between faces, the cylinder section. The thermal conductivity of nickel follows the same trend.

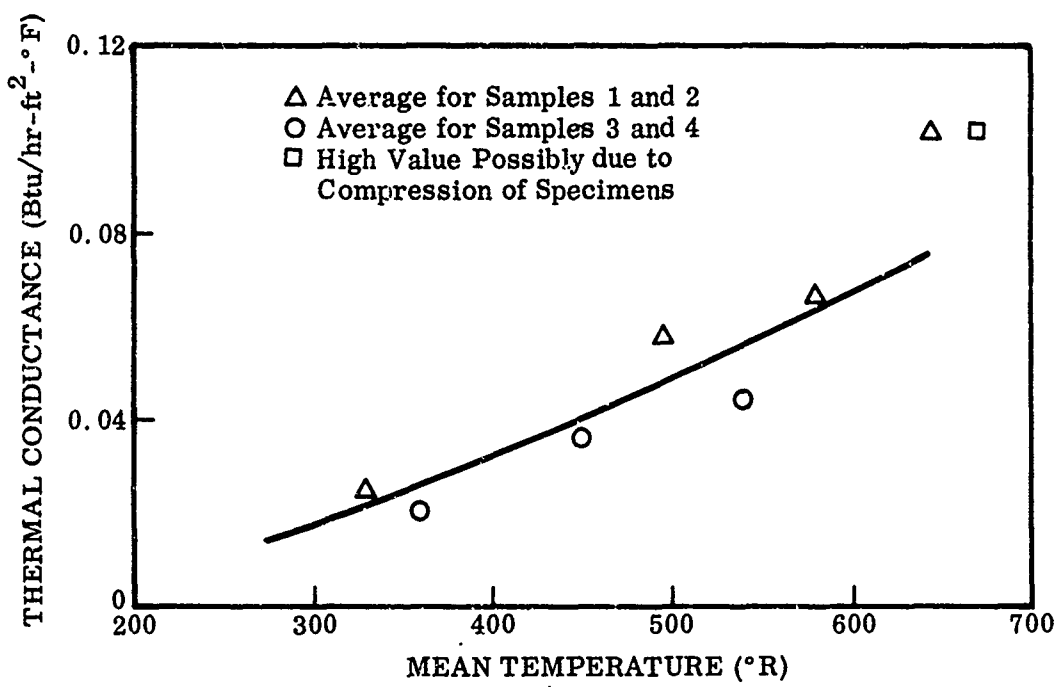


Figure 10 Thermal Conductance of Material B

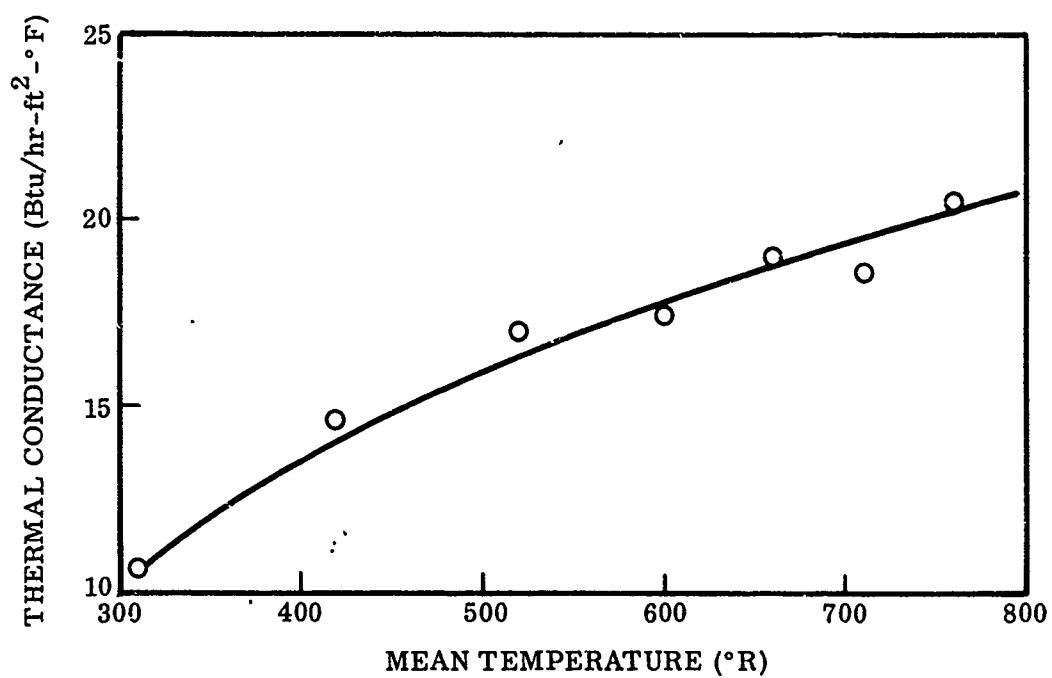


Figure 11 Thermal Conductance of Material C

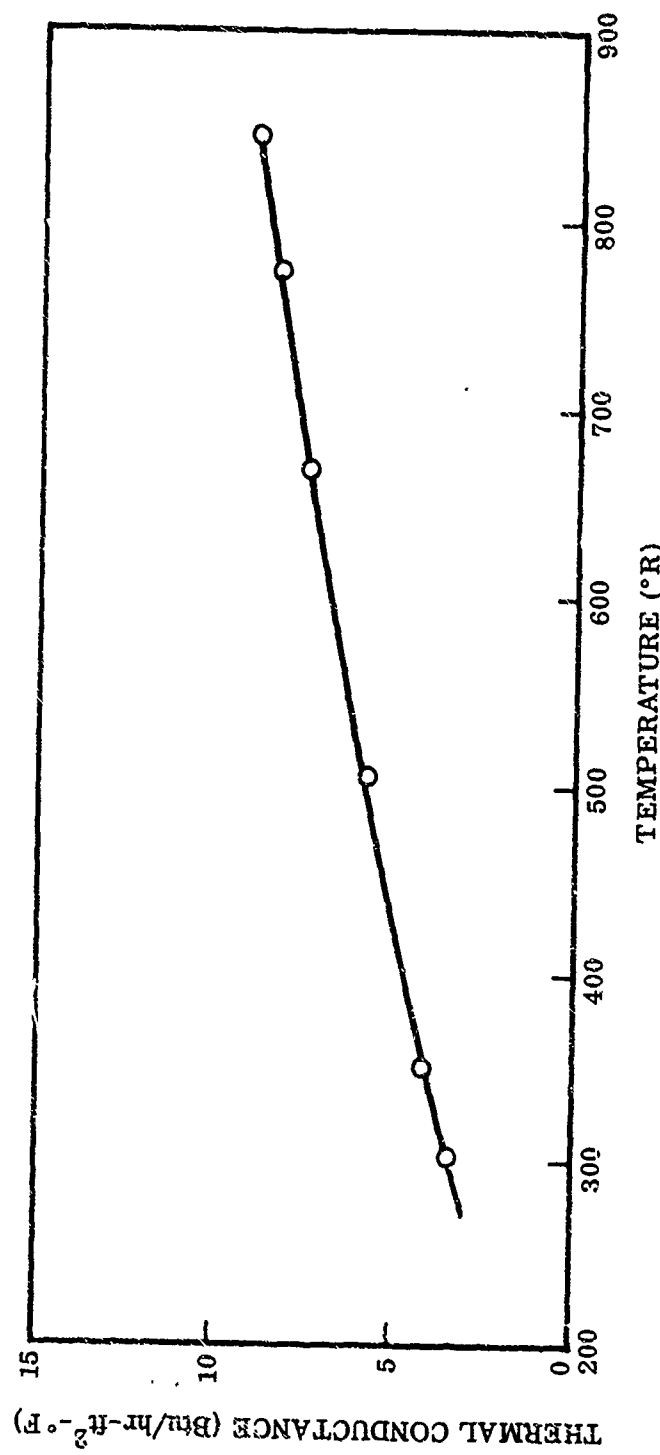


Figure 112 Thermal Conductance of Materials D - F

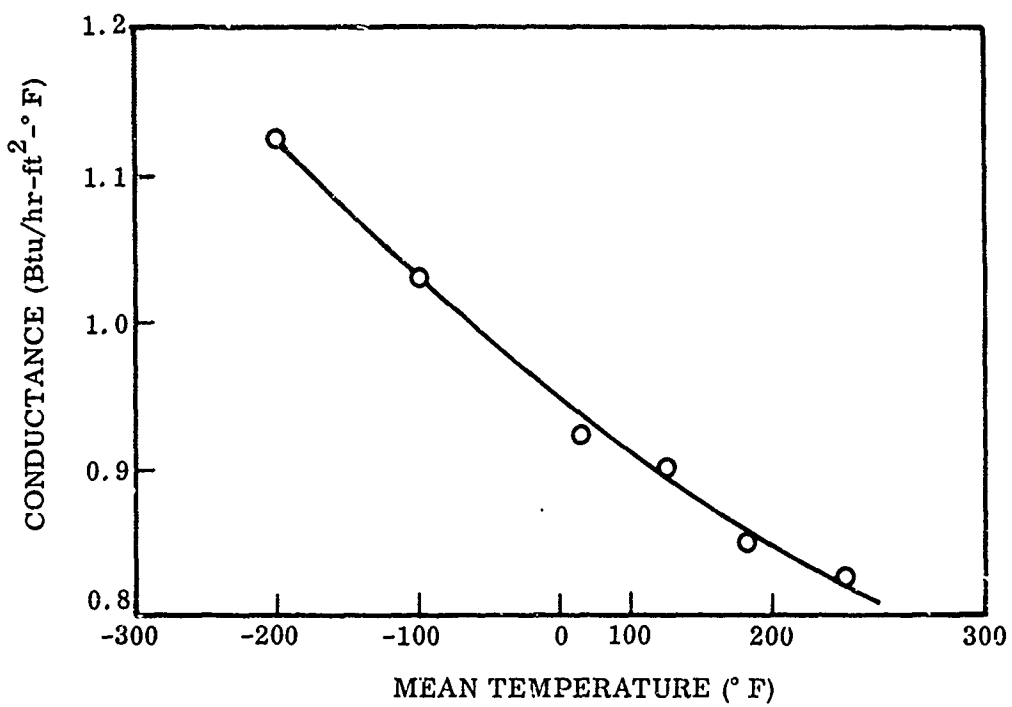


Figure 13 Thermal Conductance of Materials G-K, 1-in.-Thick Specimen

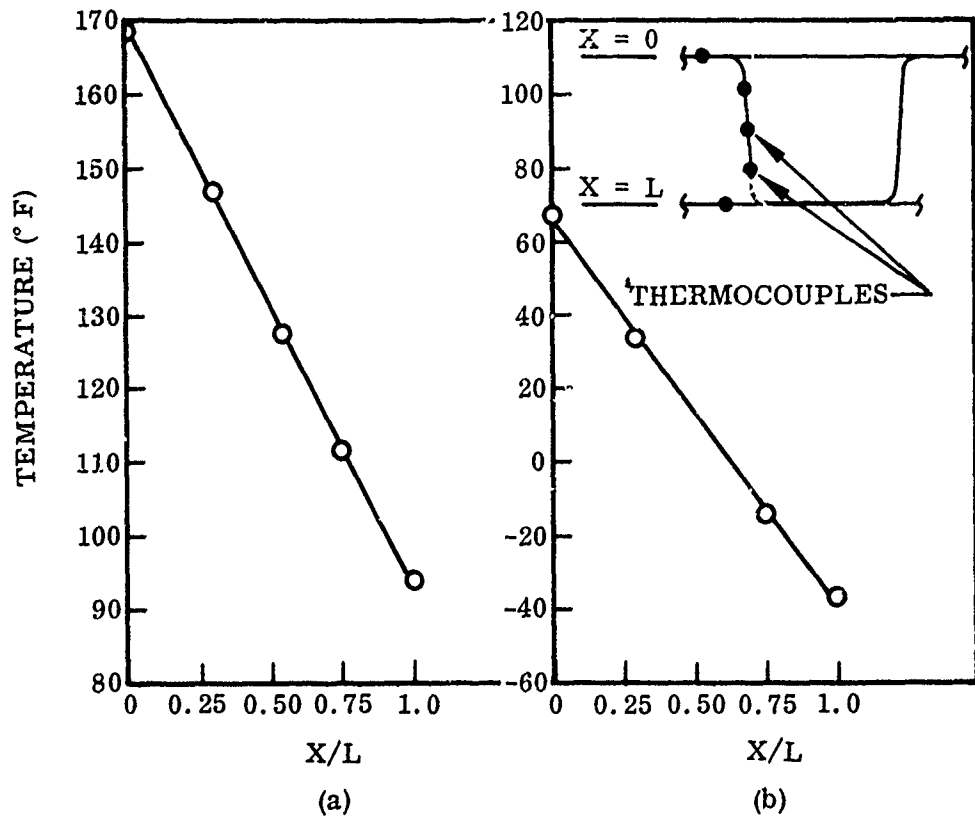


Figure 14 Temperature Distribution Along Wall of One Cylinder of Materials G-K ($X/L = 0$ and 1.0 Are on Faces of Structure)

Figure 14 shows several temperature gradients measured along one cylinder in the central test area. The data indicate that the thermal resistance of the glue or bond joint between cylinder ends and face is very small. Examination of the specimen showed very large bond areas compared to the conduction area through the cylinder. The ratio of the resistance of the cylinder to the joint is estimated to be of the order of 10 to 100.

The maximum uncertainty in those conductance data is estimated to be 15 percent. This is due principally to the temperature variation across the surface which resulted in a maximum uncertainty in Δt of 9 percent. A uniform thermal resistance between the faces and the heating and cooling units could not be achieved due to the lack of rigidity of the face structure.

d. Comments and Interpretation of Results

The thermal conductance, in vacuum, of composites such as honeycombs depends upon the energy transport through the solid connecting portion of the composite and the radiant energy transfer between faces. Since this latter mechanism for a given configuration depends upon the absolute temperatures of the faces as well as the temperature gradient along the cell walls, the experimental determinations of conductances of such geometries would have to cover a wide range of hot and cold face temperature levels. To minimize testing, it is common practice to measure the conductance of the solid portion as a function of a mean temperature and then calculate the total conductance for given temperature boundaries using the measured solid phase conductance and the calculated radiant exchange between faces for the temperatures of interest with consideration of the cell geometry. Radiant exchange may be handled as described in the literature (1 through 5).

All tests of the metal structure were carried out with the Δt across the faces less than 100°F. For all test conditions, this procedure reduced radiant exchange to less than 10 percent. All of the composites except material C had relatively low emittance surfaces for facing materials, ϵ_t range of 0.04 to 0.10 (effective emittance increased to 0.3 to 0.4 with glue at bond areas). Consequently, it is felt that calculation of a radiant term is not necessary for these structures for the temperature ranges of interest in this program (-250 to +250°F with $\Delta t < 100^\circ\text{F}$), and neglecting this term would not influence the conductance values by more than 10 percent. Material C employs a high-emittance organic layer covering the inner surfaces of each facing or skin, and some estimation of radiant transfer should be included for large temperature excursions. Room temperature total emittance measurements were made on facing materials using the Lion Emissometer to obtain approximate emittance values for comparative purposes:

<u>Material</u>	<u>ϵ_t (Lion) for Inner Surfaces of Faces or Skin</u>
A	0.03-0.05; with glue, effective emittance for area within cell walls ≈ 0.3
C	plastic facing ≈ 0.8
D-F	same as A except ≈ 0.4 with glue
G-K	0.03 for polished surface, 0.10 for dull surface

3. LINEAR THERMAL EXPANSION

Of the many methods available for determining the linear thermal expansion of materials, the fused quartz tube and dial indicator method, ASTM D696-44, was chosen for its mechanical simplicity and adaptability to measurement over a wide temperature range with reasonable accuracy. A special horizontal quartz-tube dilatometer was required for measurement of the organic materials above room temperature as the vertical apparatus places sufficient force on the specimens to cause distortion or collapse of the low density and thin sheet materials at elevated temperatures.

a. Description of Apparatus

The quartz-tube, dial-indicator apparatus is shown diagrammatically in Figure 15. A schematic of the heater and specimen is shown in Figure 16. The dial indicator is a Starrett 25-209 with a total range of 0.015-in. and a least count of 5×10^{-5} in. The system provides for a helium atmosphere surrounding the sample as well as for a helium heat exchange gas. The helium atmosphere surrounding the dial indicator is contained in a pyrex chamber, thus allowing visual observation of the gage. Dimensional changes in specimen length are transmitted to the dial indicator by a quartz rider. To eliminate temperature gradients within the sample, thin copper cylinders are placed inside and outside of the quartz sample tube. Nichrome wire is wrapped around the exterior cylinder to provide precise temperature control. Radiation energy exchange is reduced by several layers of aluminum foil in the annular space between the pyrex and sample tubes. Specimen temperature is measured with a 3-mil chromel-alumel thermocouple cemented to the specimen at its midpoint. Continuous temperature readout is accomplished with an Electro-Instruments 4010 Digital Voltmeter.

The overall accuracy of the quartz dilatometer units with dial indicator was verified using Armco iron, graphite, and synthetic sapphire reference standards. These data are shown by Figure 17. A comparative run also was made with a fused silica specimen. The percent expansion with reference to the dilatometer was less than ± 0.001 percent to 800° F.

The horizontal dilatometer unit is a Leitz Model HTV unit, equipped for photographic recording, with a vacuum furnace assembly. This apparatus (Figure 18) measures dimensional changes with reference to a standard specimen. The unknown and standard are located side by side in the furnace. Each is held in a quartz tube with a central quartz rod to transmit dimensional changes to an optical system. The movement of the specimen rod with regard to the standard moves a prism which traces a temperature-length plot with a light beam on a ground glass or a photographic plate. This apparatus places a load of less than 10 g on the specimen.

Specimen and standard lengths were 5/8 in. for this program. The standard was 99.9 percent pure aluminum furnished by the manufacturer with calibration data. Temperature of the specimen and standard was measured with a chromel-alumel thermocouple placed between the two in the furnace.

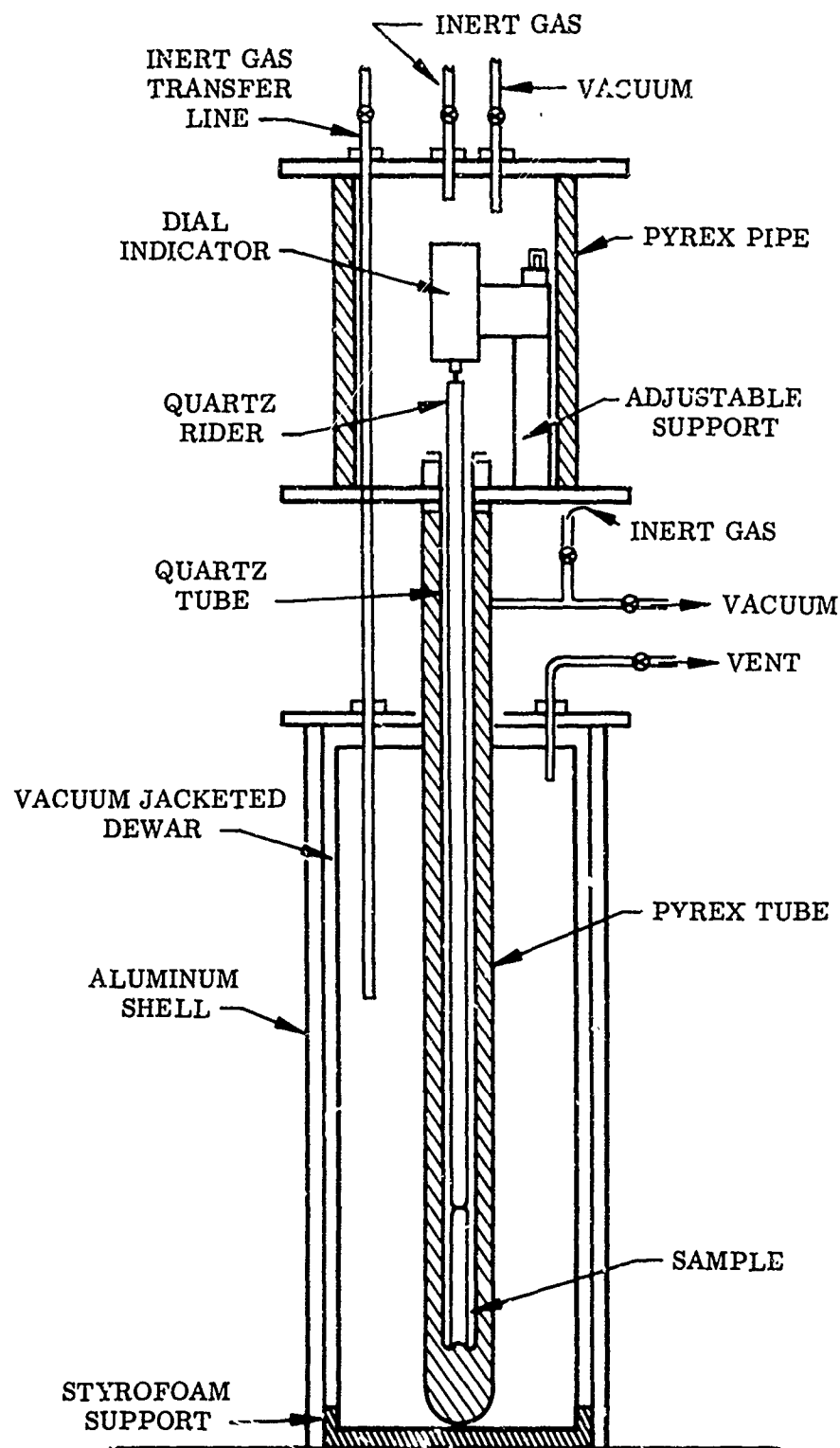


Figure 15 Thermal Expansion Apparatus for Measurements From -320 to +150° F

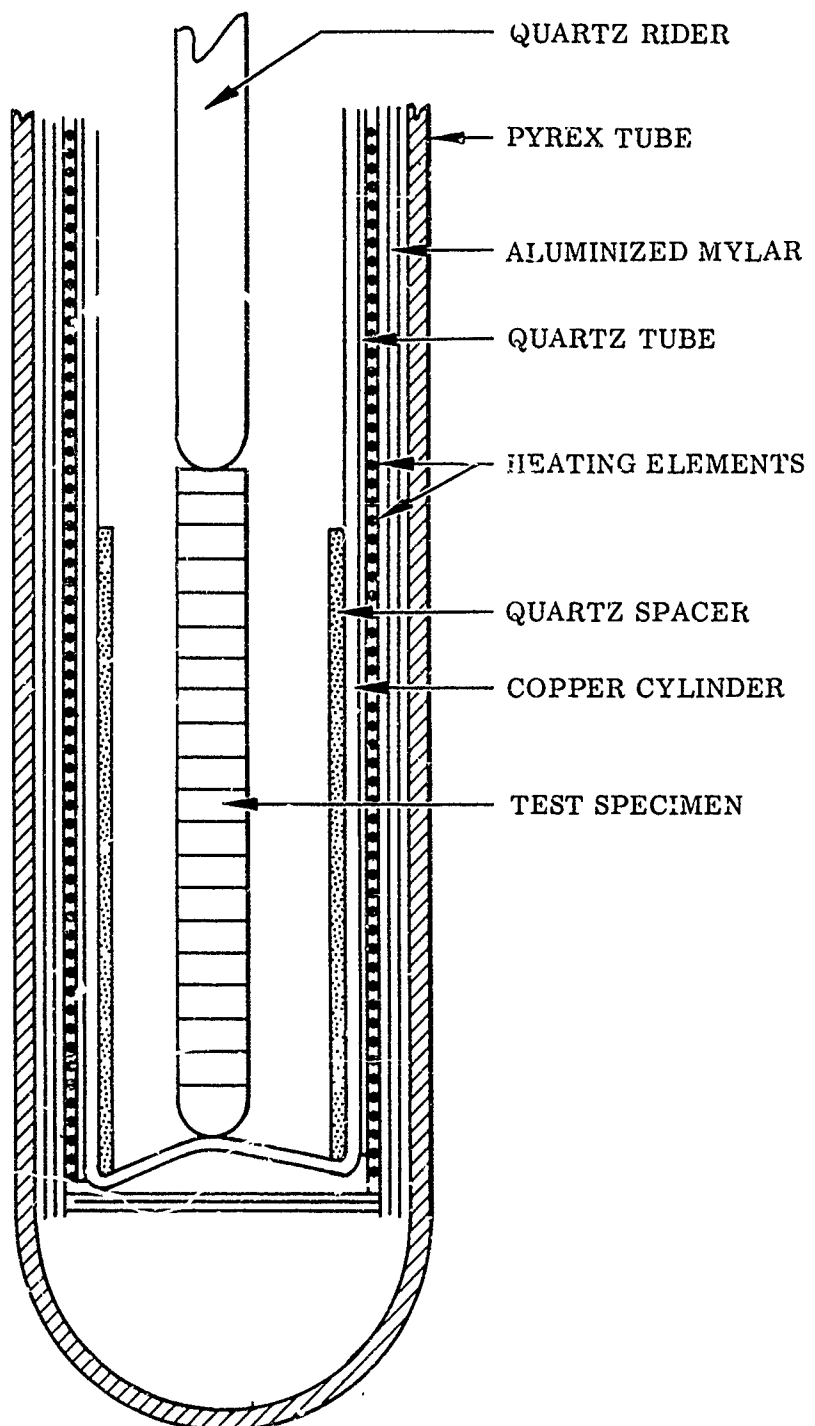


Figure 16 Expansion Specimen and Dilatometer With Heater

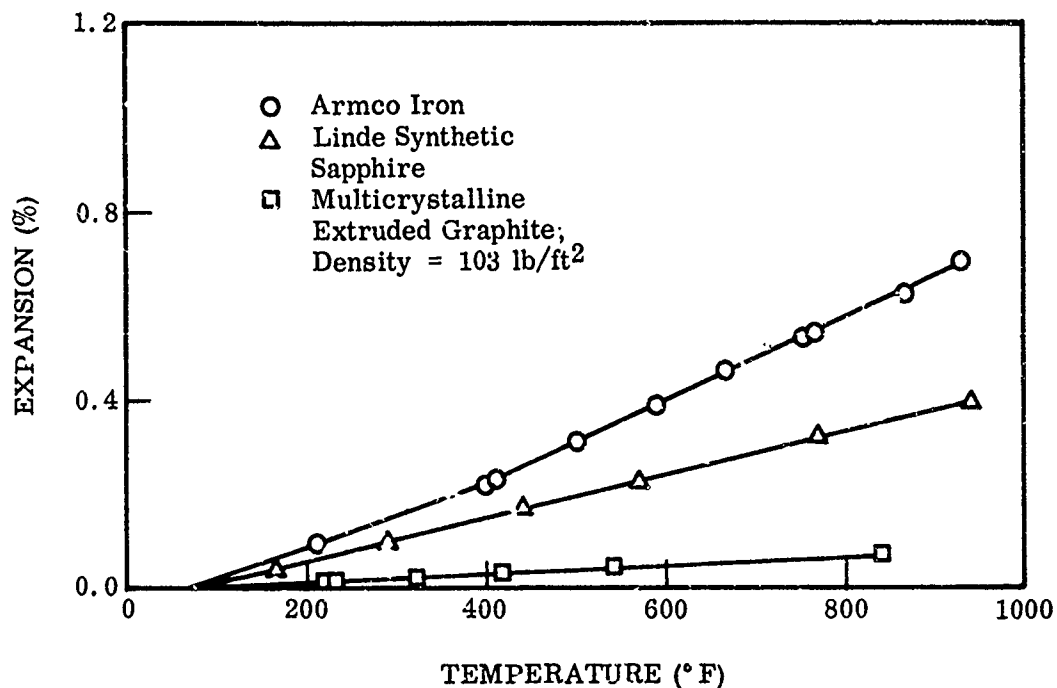
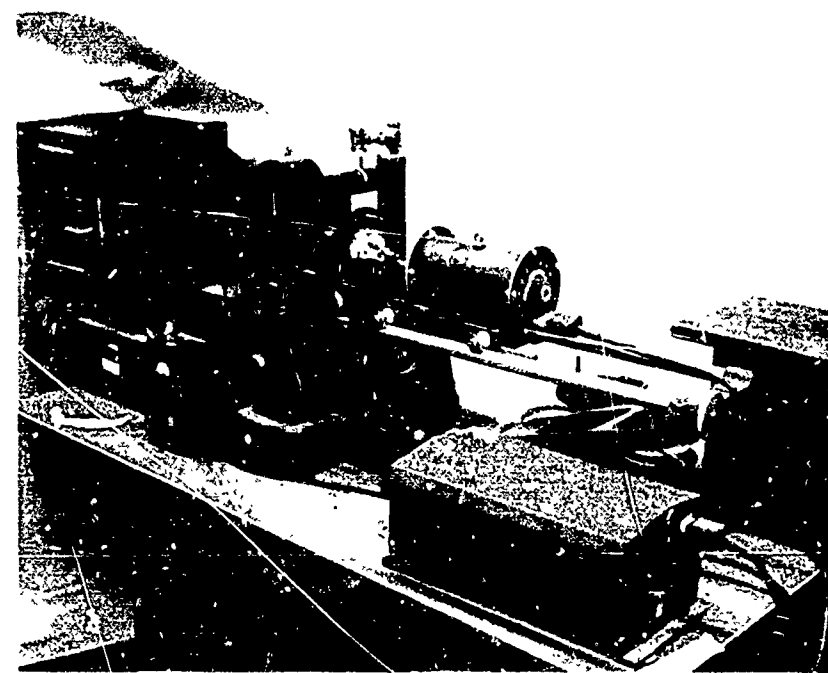
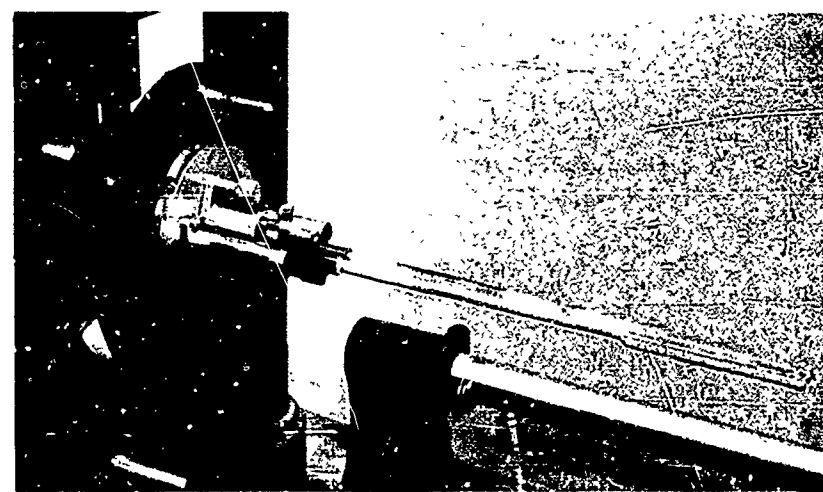


Figure 17 Linear Thermal Expansion of Reference Materials in Quartz Tube Dilatometer Apparatus



(a) Overall Assembly



(b) Sample and Standard Holder

Figure 18 Horizontal Tube Linear Thermal Expansion Apparatus

b. Test Procedure

For the dial indicator apparatus, the specimens were prepared in cylindrical or rectangular form, 3-in. long by 3/8-in. diameter or square. Thin material was tightly wrapped to form a cylinder, the ends and midpoint being secured with 5-mil copper wire. Quartz discs were placed at each end of the specimens to provide a uniformly distributed contact force from the hemispherical ends of the quartz tube and rider. A thermocouple is cemented to the specimen, and it is then placed in the quartz tube. The rider is inserted into the tube, and the dial indicator set so that the dial reads close to full-scale deflection. With the enclosure sealed, the apparatus is evacuated and subsequently pressurized with helium and maintained at approximately 2 psig. The helium in the annular region is used as a noncondensable heat exchange medium. Cryogen is then transferred to the Dewar and the sample is allowed to cool until the desired equilibrium temperature is achieved with the heater on. Heat exchange gas is then removed and electrical power adjusted to the heater to allow a heating rate of 4°F/min. Data are recorded at approximately 50°F intervals.

Specimens for the Leitz apparatus were 5/8-in.-long by 3/16-in.-diameter cylinders. Ends of cylinders wrapped from thin materials were secured with copper wire. After placing the standard and specimen in the quartz tube the furnace is placed over the dilatometer unit. The zero reading is recorded at room temperature. Furnace temperature is then increased in approximately 50°F intervals. Change in dimension with reference to the standard is recorded when equilibrium temperature is achieved.

Data from the dial indicator apparatus are reduced to linear thermal expansion by the following expression:

$$\text{Percent Expansion} = \left(\frac{\Delta L + A}{L} \right) \times 10^2$$

where

ΔL = change in dimension of specimen from dial indicator reading
 A = correction for change in length of quartz tube over specimen length (from Figure 19)
 L = length of specimen

Percent thermal expansion is calculated from the data from the Leitz dilatometer apparatus in the following manner:¹

$$\text{Percent Expansion} = \left(\frac{Y}{X} \right) (K) \times 10^2$$

where

Y = distance from center of coordinate axis to point on relative length change plot (from light beam on grid plate) along ordinate
 X = distance from center of coordinate axis along abscissa
 K = expansion of reference standard (in./in.) at test temperature

¹No corrections for quartz tube expansion (or contraction) are required as both reference and specimen are of the same length and are held in quartz tubes.

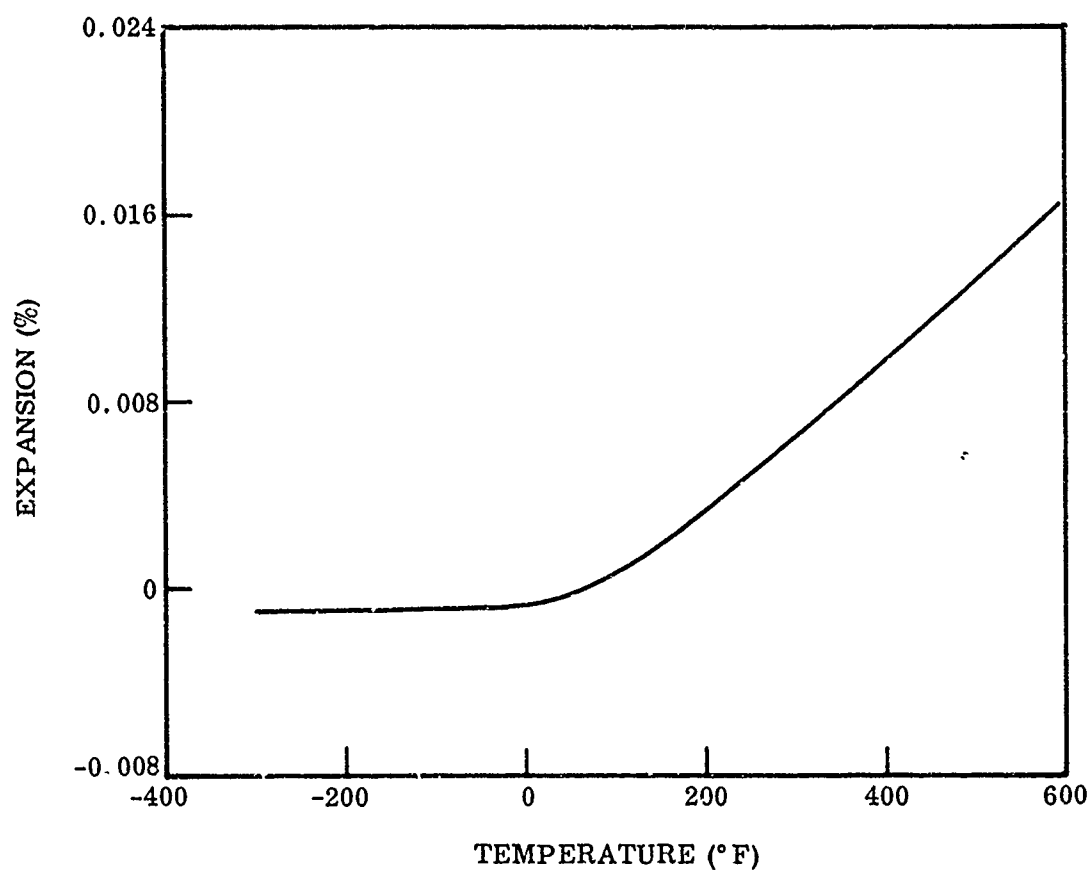


Figure 19 Percent Thermal Expansion of Quartz Dilatometer Tubes

c. Test Results

Linear thermal expansion measurements were performed on components of three candidate material systems, B, G-K, and L. No data were obtained for Materials A, C, and D-F as these all employed materials having well-documented thermal expansion properties. Materials G-K were composed of a metallic structure, but, as they were fabricated by an electroforming process, expansion measurements were made to assess the effects of the formation process on the general thermal properties of the metal. An electroformed metal was also used for a portion of Material B, and, similarly, expansion data were obtained for this component. All other expansion measurements were performed on structural organic materials.

The quartz-tube, dial-indicator apparatus was used for all measurements below 70° F and for all metals. The Leitz apparatus was used for all organic materials above 70° F as it imposed a very light load on the specimen, and any effects such as constraint with internal yielding of the structure were minimized.

Material B. The results of the expansion measurements for the components of this system are shown graphically by Figures 20 through 25. Data on the electroformed face material are contained in Figure 20. No significant hysteresis effect was noted upon cooling. The coefficient of linear thermal expansion over the temperature range of 80° to 300° F is 7.8×10^{-6} in./in.° F, which compares well with the value of 7.8×10^{-6} recommended in the literature (6). The coefficients of expansion between -100° and +30° F and between -250° and +80° F are 5.3×10^{-6} and 4.5×10^{-6} in./in.° F.

The data on the foam structural material are shown in Figures 21 through 23, and for the x-x, y-y, and z-z directions. The data from -300° F to room temperature were the same for all three directions. Also the contraction or negative coefficient of expansion from room temperature to ~ 150° F was similar in all three directions. The principal difference with specimen direction occurred above 150° F, where the data in the z-z direction showed less contraction with increasing temperature to 250° F. This variation might be due to the nonuniformity of density in the very low-density structure (1.4 lb/ft³ for expansion sample).

To determine whether cycling stresses had any significant effect on the electroformed material, thermal expansion measurements were performed on a sample of reflector surface material at the end of the 6,000-cycle thermal-cycling test (subsection II. 7). These results are shown in Figure 25. A 10-percent increase was observed in the coefficient of linear thermal expansion from -250° to +80° F for the post-test specimen. However, it is felt that the variation in expansion is due to a combination of experimental uncertainties and nonuniformity of material from specimen to specimen rather than a significant change in structure.

In the case of Material B, the large differences in thermal expansion of the facing and foam material should result in large stresses of the interface between the materials which might result in mechanical failure at this interface with subsequent separation of the materials during the temperature excursions of a day-night orbit.

Materials G-K. Linear thermal expansion data for the electroformed faces of the structure of the G-K system are shown in Figures 26 through 28. No significant differences

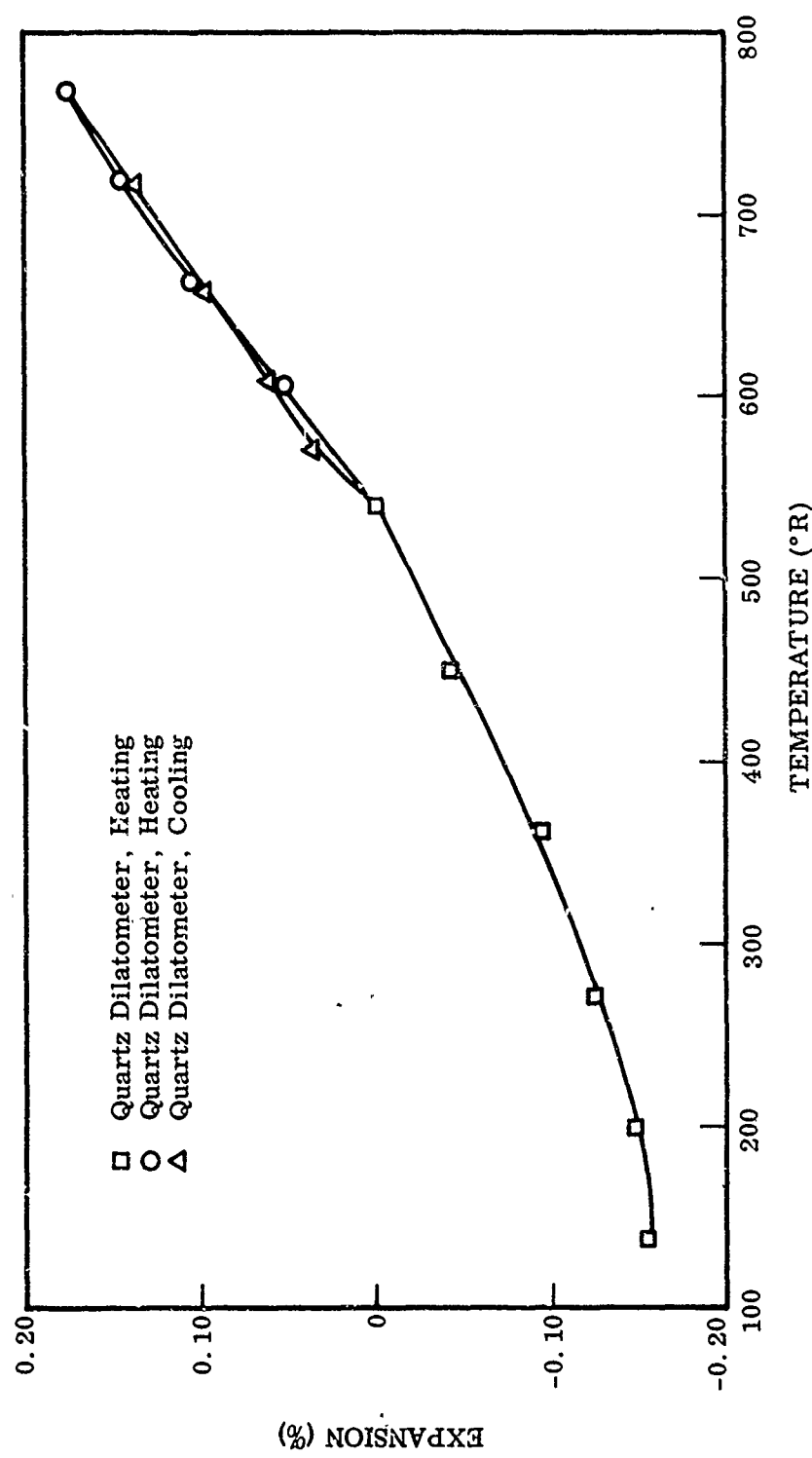


Figure 20 Linear Thermal Expansion of Material B, Reflective Surface

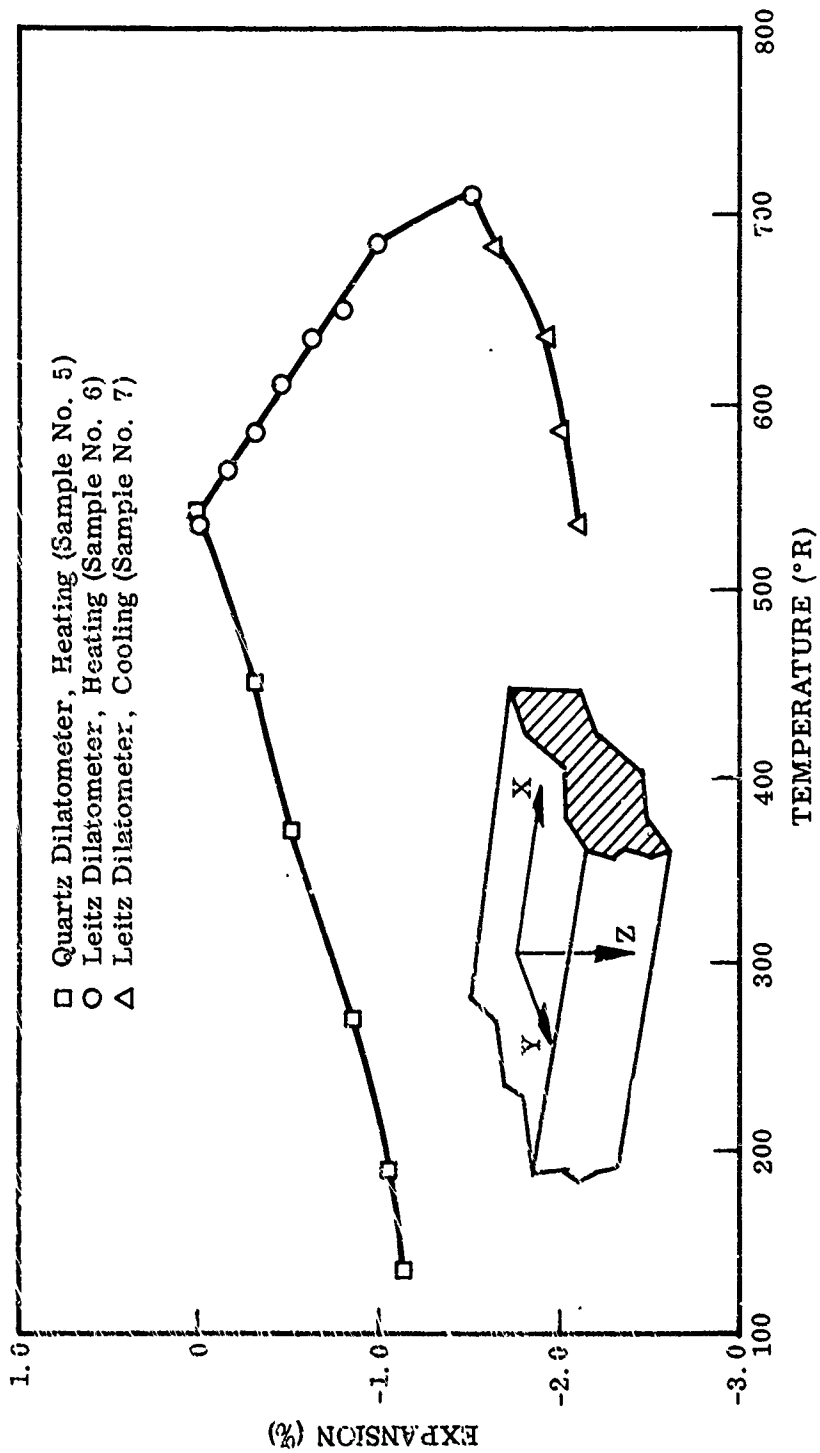


Figure 21 Linear Thermal Expansion of Material B, Foam Structure, in X-X Direction

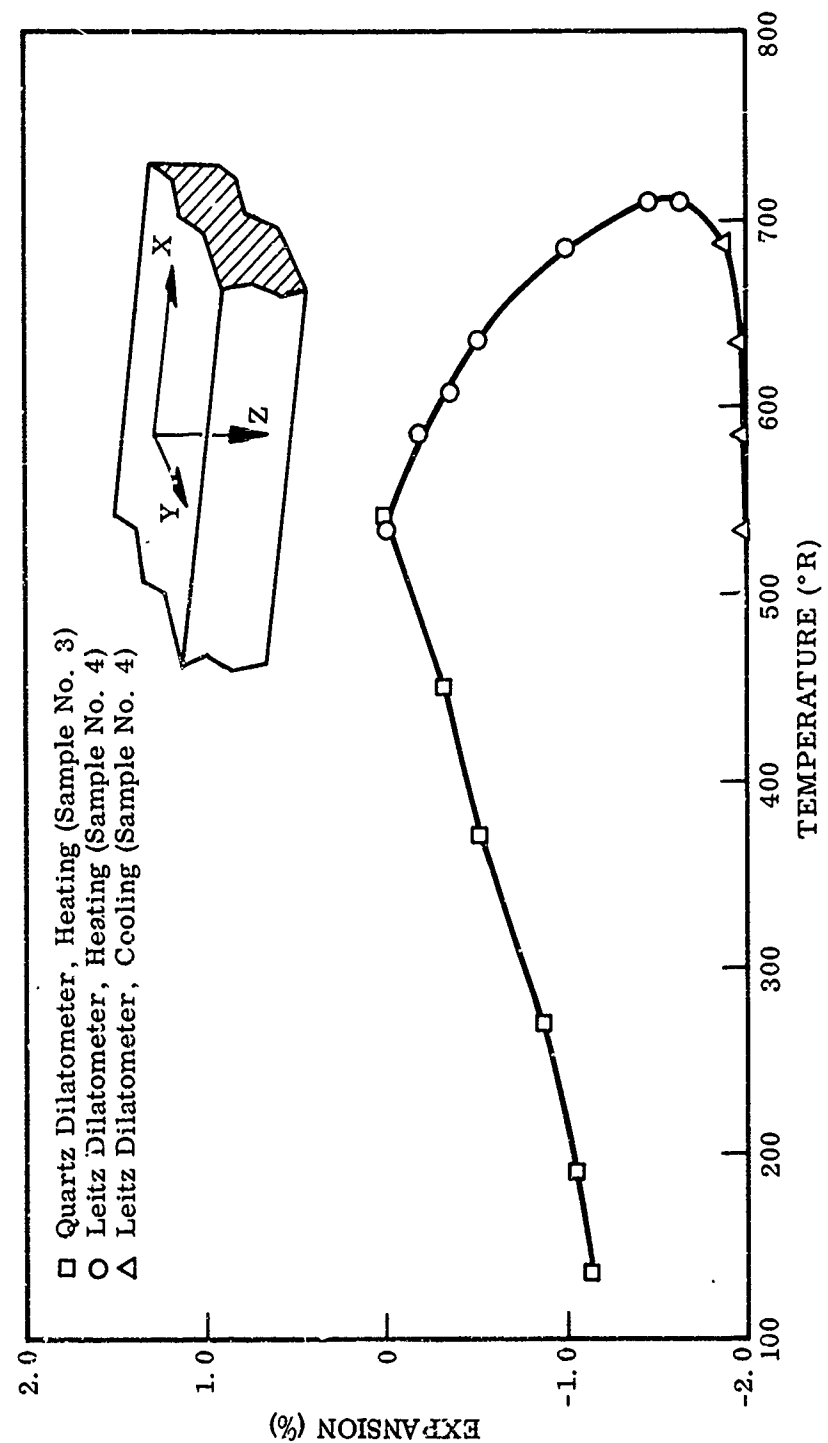


Figure 22 Linear Thermal Expansion of Material B, Foam Structure, in Y-Z Direction

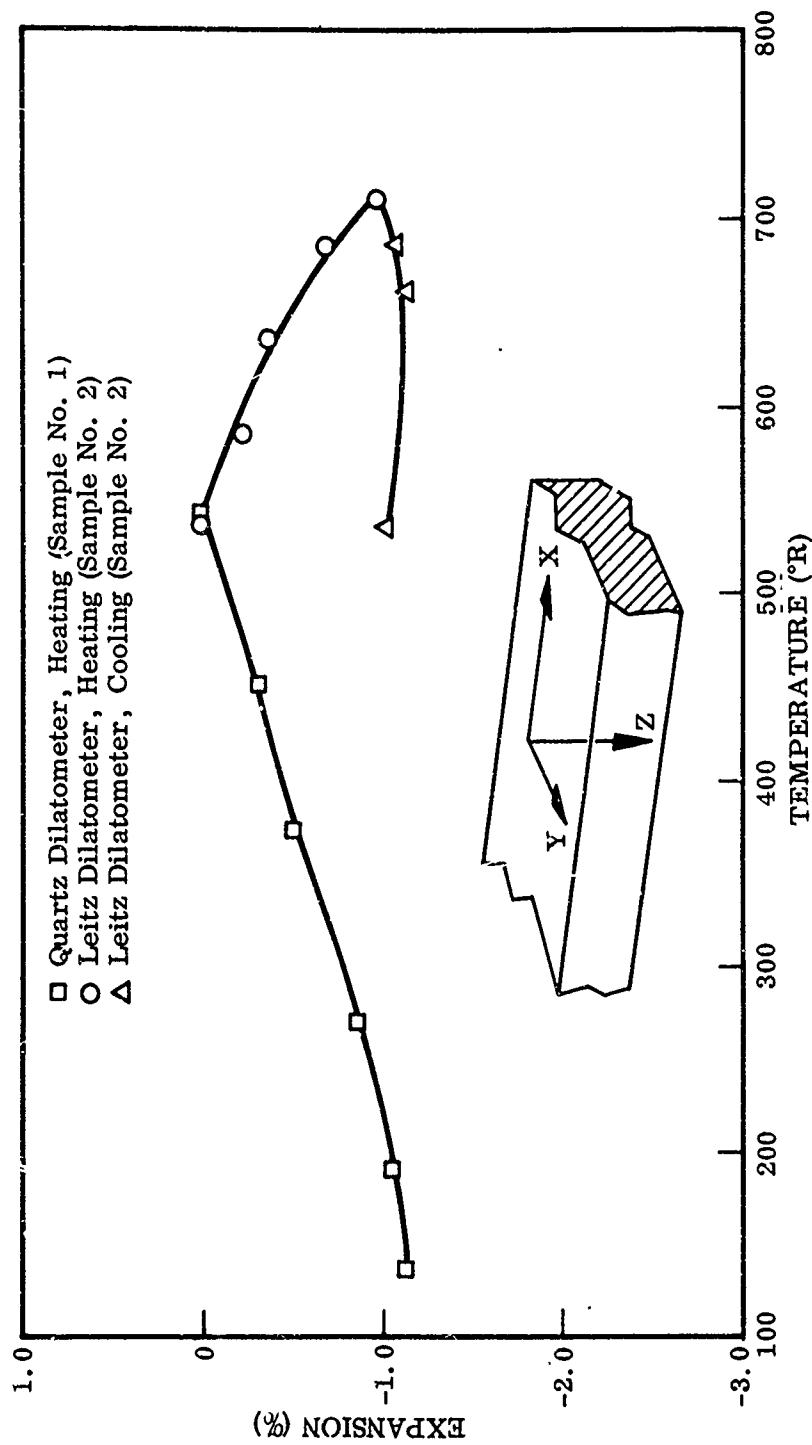


Figure 23 Linear Thermal Expansion of Material B, Foam Structure, in Z-Z Direction

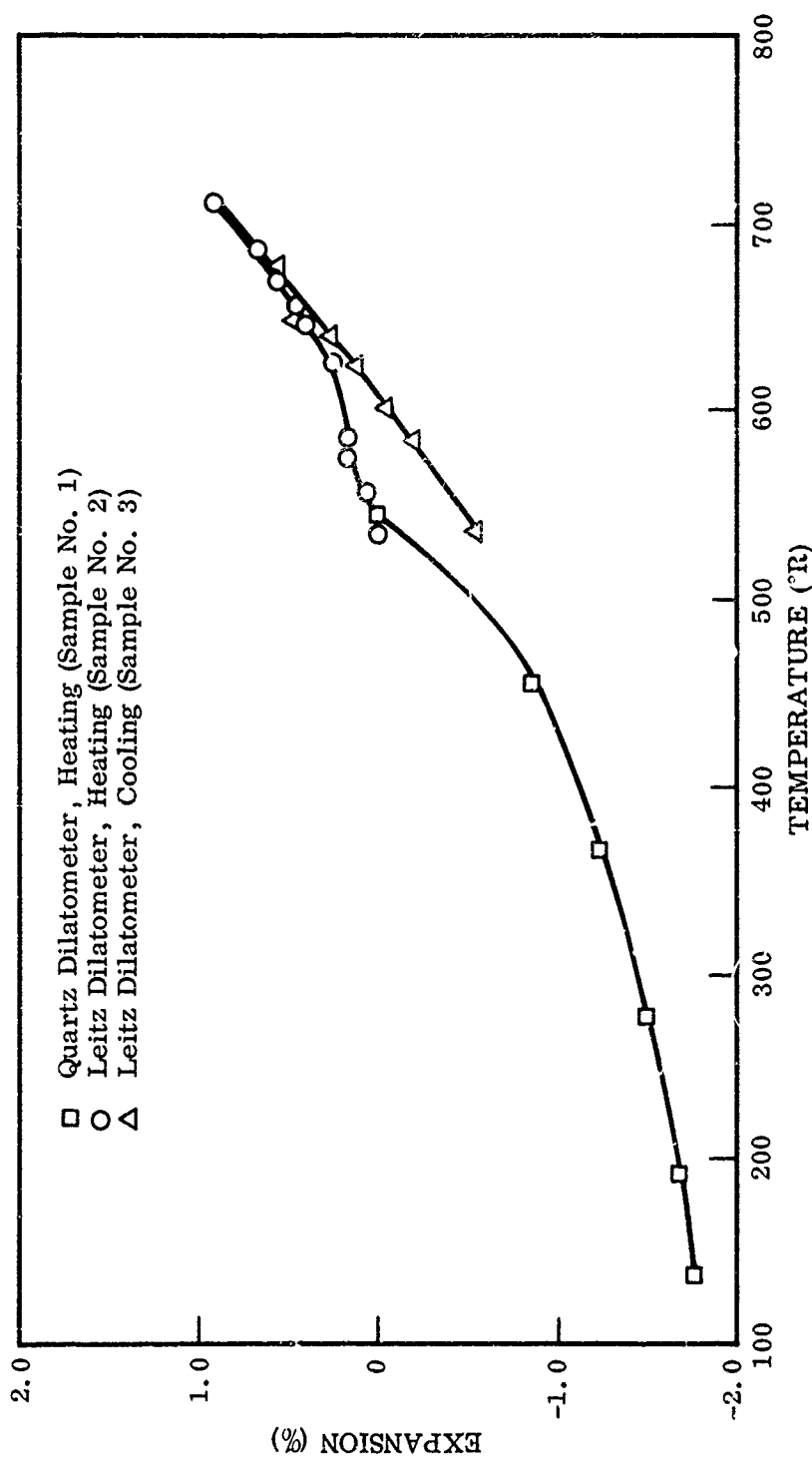


Figure 24 Linear Thermal Expansion of Material B, Epoxy Backing Surface

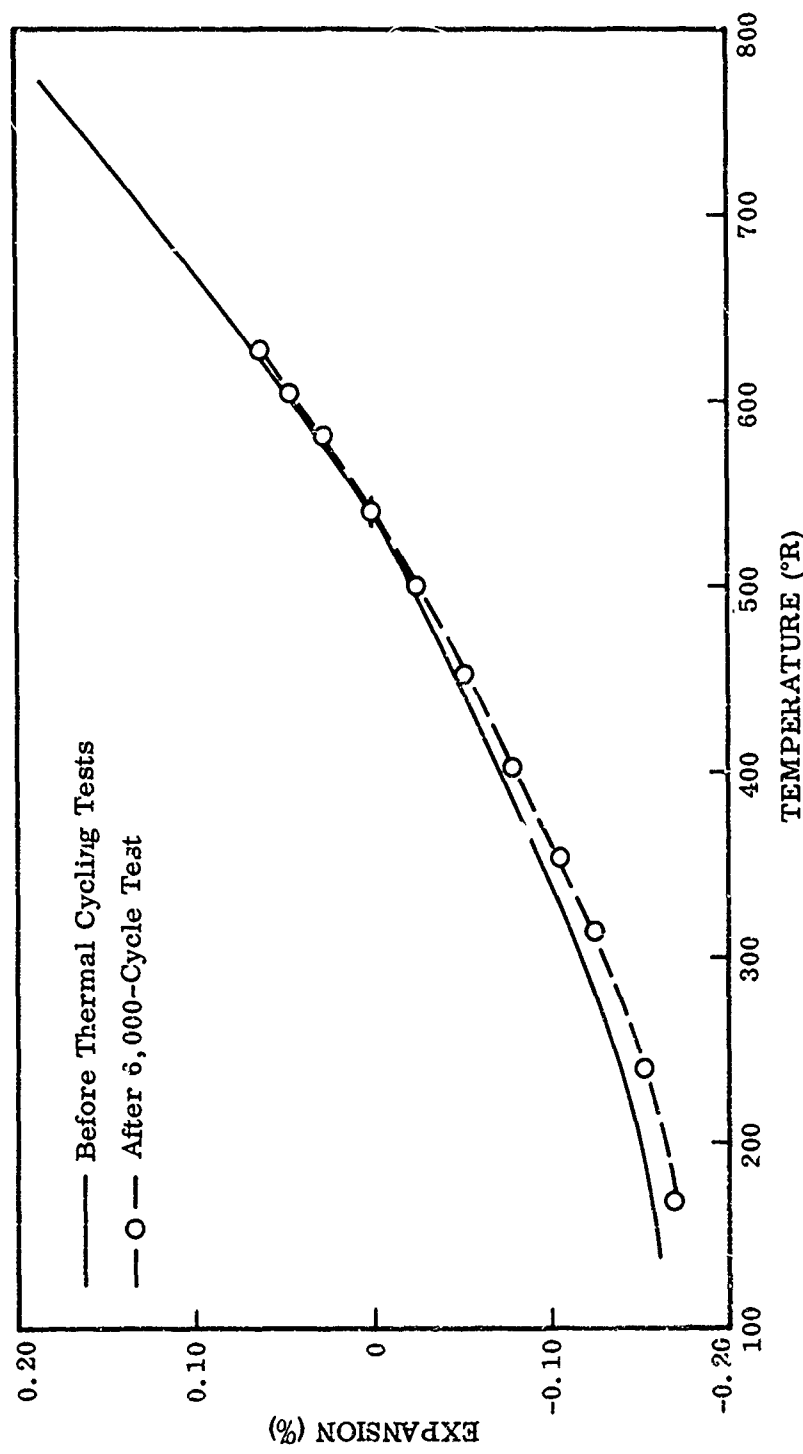


Figure 25 Comparison of Linear Thermal Expansion of Material B, Reflective Surface, Before and After 6,000-Cycle Thermal-Cycling Test

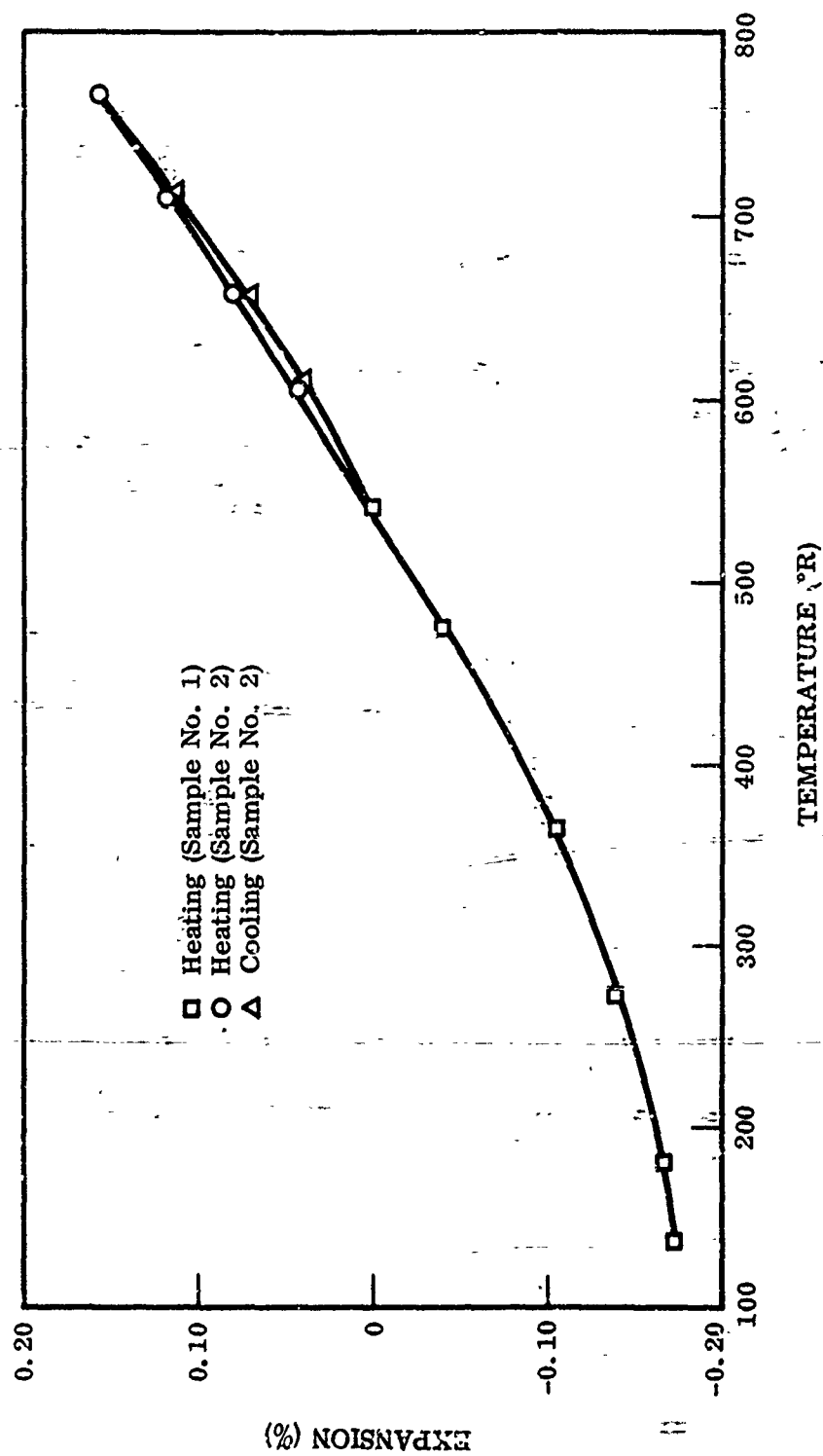


Figure 26 Linear Thermal Expansion of Materials G-K, Reflective Surface

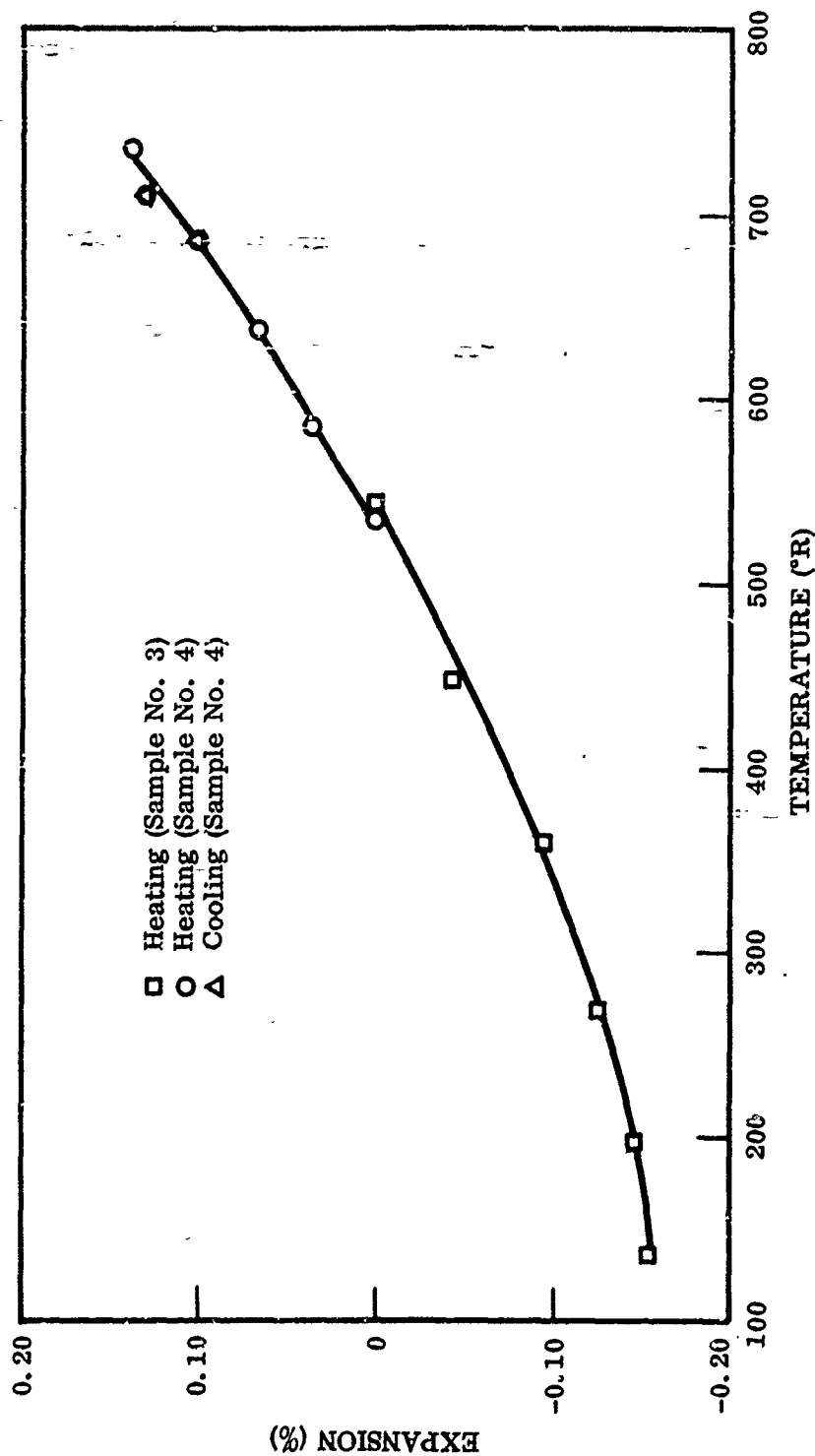


Figure 27 Linear Thermal Expansion of Materials G-K, Back Surface

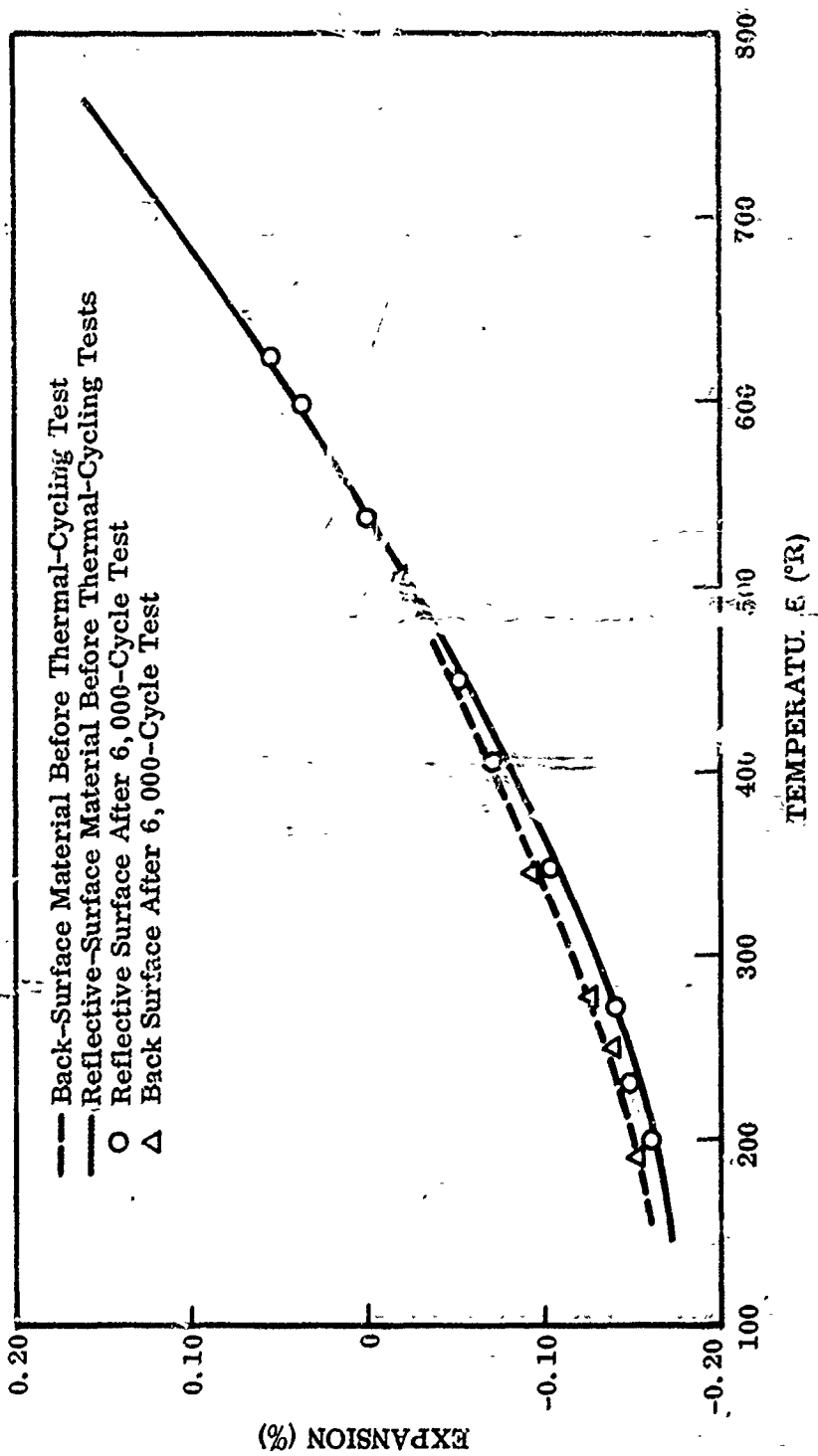


Figure 28 Comparison of Linear Thermal Expansion of Materials G-K, Before and After 6,000-Cycle Thermal-Cycling Test

were observed in the behavior of the two specimens from room temperature to 300° F. The data from -320° to +80° F showed a larger coefficient for the sample cut from the reflective surface specimen. The room temperature to 250° F expansion coefficient is less than that reported for pure nickel. This may be due to the structure resulting from the electroforming process. However, no analysis was made of the structures of either specimen. The calculated coefficients of linear expansion for several temperature ranges are shown in Table VI.

Table VI. Mean Coefficient of Linear Thermal Expansion of Materials G-K

Material	Mean Coefficient of Expansion (in./in.° F)		
	70° to 250° F	-100° to 70° F	-250° to 70° F
Reflective Surface Substrate	7.0×10^{-6}	5.9×10^{-6}	4.8×10^{-3}
Rear Surface	7.0×10^{-6}	5.3×10^{-6}	4.3×10^{-6}

cycle thermal-cycling test to determine whether the cycling stresses resulted in a significant alteration of structure which would be evidenced by a major change in coefficient of linear thermal expansion. The results of these tests are shown in Figure 28. No change in properties was noted which could be ascribed to the thermal cycling.

Material L. Thermal expansion measurements were completed on the samples of Material L before it was deleted from the program. These data are shown in Figures 29 and 30. The rigidized faces of the structural material exhibited peculiar expansion above room temperature. The change in slope during the heating cycle may be due to a change in composition or cure of the rigidizing compound as the change is not as pronounced during the subsequent cooling cycle.

Expansion data for the flexible epoxy sublayer (Figure 30) show a large change in coefficient of expansion between -60 and -100° F. This may be due either to a transformation or a change in properties due to the effects of a plasticizer in this temperature range. A permanent change in dimension was observed upon cooling from +250° F.

d. Comments and Interpretation of Results

The organic materials exhibited a permanent change in dimension after the initial heating cycle and showed a very pronounced hysteresis on cooling with a large permanent deformation at room temperature.

No change in structure of the electroformed materials (B and G-K) was noted during the thermal-cycling tests. This is evidenced by a comparison of pre- and post-test expansion measurements.

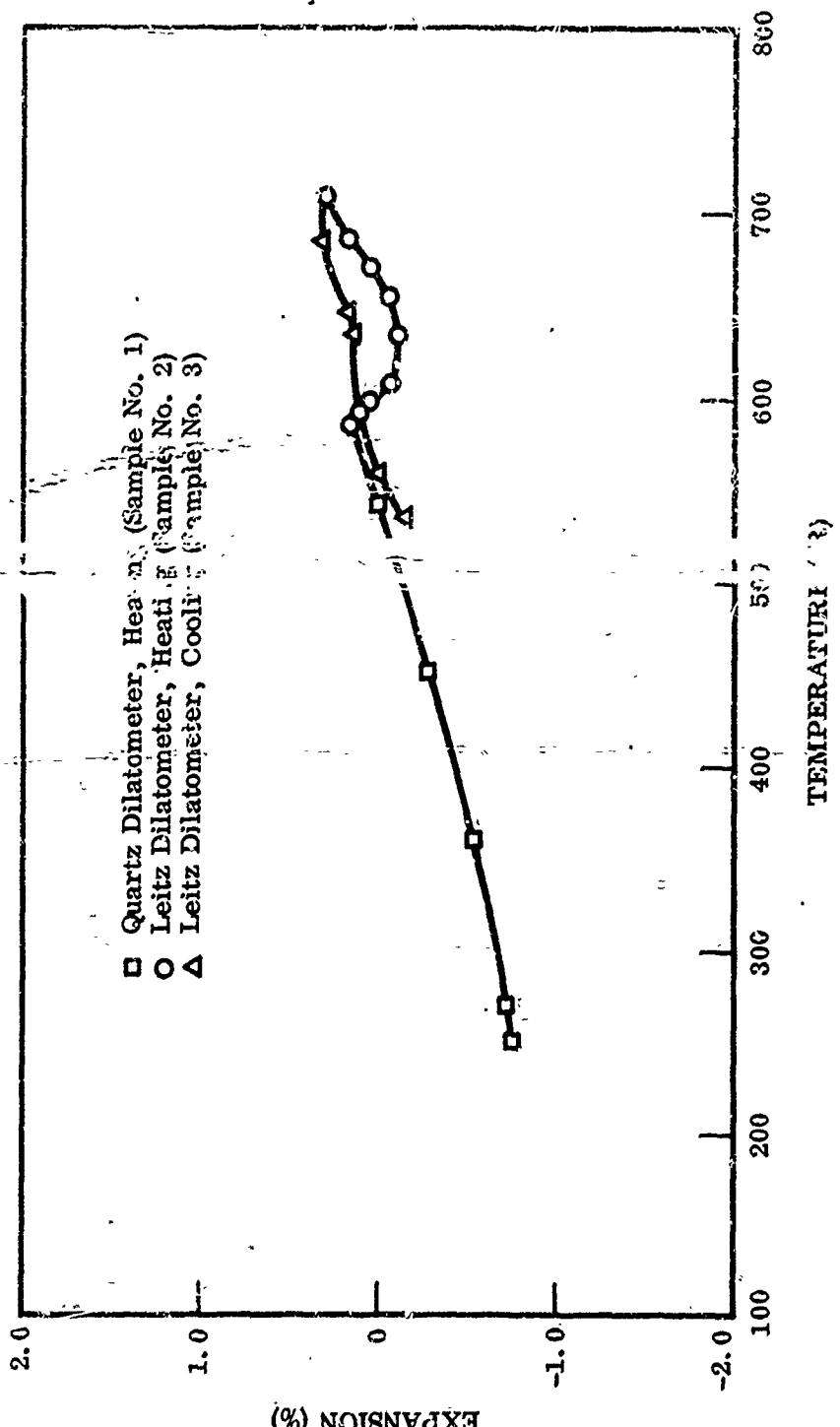


Figure 29 Linear Thermal Expansion of Materia I. Rigidized Facing of Structure

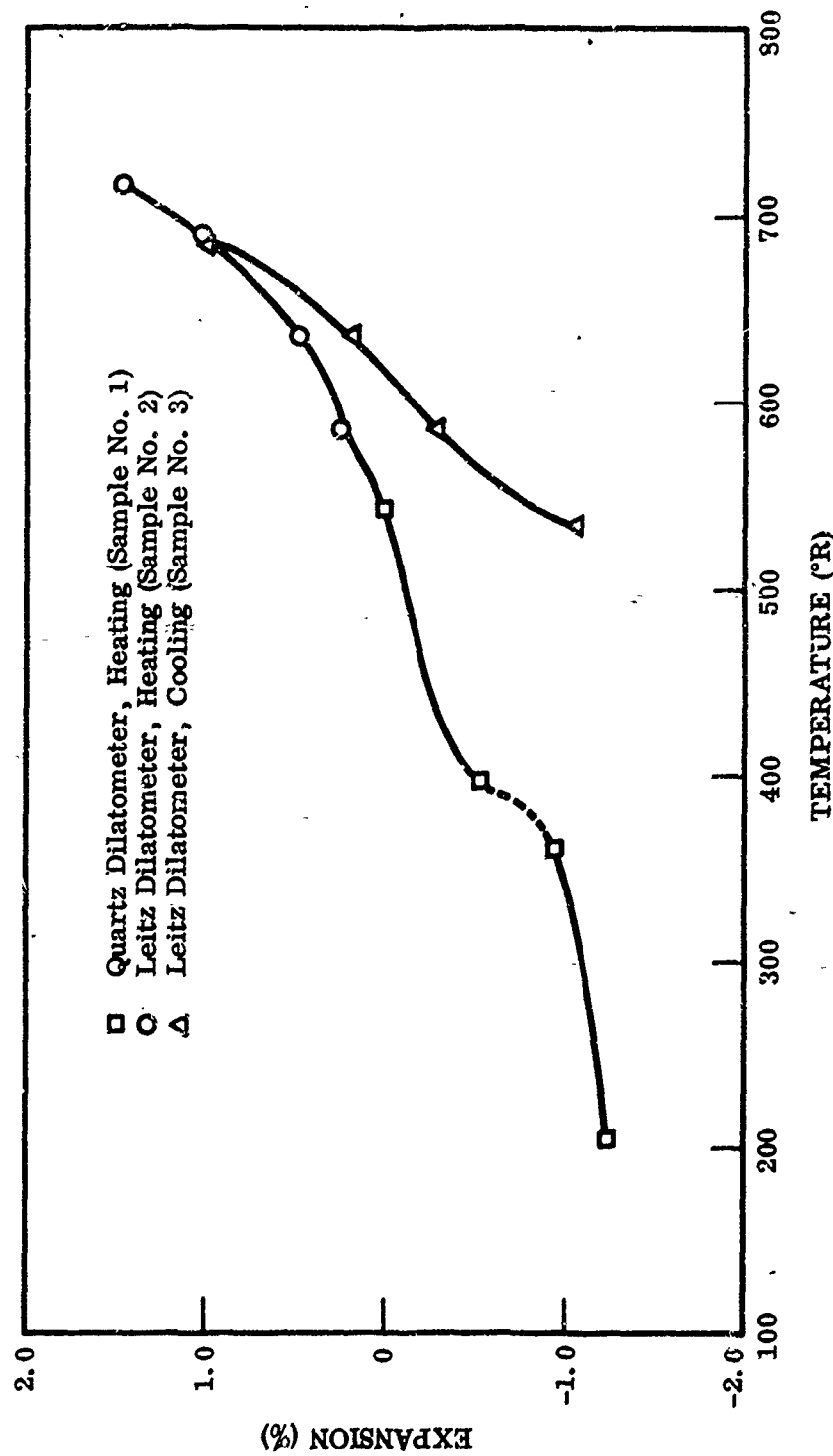


Figure 30 Linear Thermal Expansion of Material L, Flexible Epoxy Sublayer

4. HEAT CAPACITY

Heat capacities of the organic constituents of the composite material B were measured using a flooded ice-mantle calorimeter. The values of heat capacity as a function of temperature were calculated from the measured specimen enthalpy, referenced to 32° F.

a. Description of Apparatus

A flooded ice-mantle calorimeter, similar to that described in (7), was chosen for measurement of enthalpy of the specimens, as referenced to 32° F, from -250° to +250° F. The apparatus, shown by Figure 31, consists of a finned copper heat receiver which is sealed into a silvered dewar. The dewar is immersed in an ice-water bath that is contained within a insulated vessel. The volume between the receiver and dewar, which is filled with oxygen-free distilled water and mercury, is connected to a precision-bore capillary-tube manometer.

Specimens are contained in oxidized stainless-steel capsules. Capsule and specimen are filled with nitrogen and brought to an equilibrium temperature in a wire-wound alumina tube furnace or a nitrogen gas cooled chamber. All parts of the apparatus are purged with nitrogen gas during a run. The capsule is supported within the furnace or cooling chamber by a drop mechanism which is operated to allow the capsule containing the specimen to fall into the heat receiver. Shutters in the receiver minimize radiative exchange between the container, receiver, and the furnace or cooling chamber. Specimen temperature is measured by a 3-mil chromel-alumel thermocouple probe which is located in a hole drilled to the center of the specimen.

b. Test Procedure

Initially, the capsule is calibrated for heat content over the desired measurement temperature range. This calibration accounts for the heat content of the capsule as well as heat losses which occur during the finite drop time. The specimen is cut or formed to a cylindrical shape 3/4-in. diameter by 1-1/2-in. long. A minimum of 5 g of material is used (low-density materials are pressed into a pellet shape of the proper weight). After weighing of capsule and specimen to the nearest milligram, the capsule, with sample, is suspended in the cooling chamber or furnace. After temperature equilibrium is attained, capsule and specimen are dropped into the calorimeter. The heat given up by the capsule and specimen is measured by the change in volume of water within the manometer due to melting or freezing of a portion of the ice mantle on the heat receiver.



Figure 31 Flooded Ice-Mantle Calorimeter for Measurement of Enthalpy Between
-250° and + 250°F

The enthalpy of the specimen is calculated as follows:

$$\Delta V_{\text{sample}} = \Delta V_{\text{total}} - \Delta V_{\text{capsule}}$$

$$\Delta H_{32, \text{sample}} = \frac{\Delta V_{\text{sample}} \times 3.5}{m}$$

where

ΔV = the volume change due to the melting or freezing of a portion of the ice mantle (ΔV capsule obtained from calibration data for a specific capsule at the drop temperature).

3.5 = volume conversion constant

ΔH_{32} = enthalpy reference to 32° F

m = mass of specimen

The maximum uncertainty for these measurements is 2 percent, based on periodic apparatus calibration with an alpha alumina standard. Agreement of enthalpy values to within 1 percent of NBS data is achieved with the apparatus.

Heat capacity is calculated from the derivative of the equation for a smooth curve passed through the enthalpy data. A computer routine is used to fit the data of enthalpy versus temperature to a polynomial expression of the form $\Delta H_{32} = at + bt^2 + 6/t + C$ (8). The maximum uncertainty for heat capacity values is 5 percent.

c. Test Results

Heat capacity data were calculated for the two organic constituents of Material B. The measured enthalpy data and calculated heat capacity for the foam material are shown by Figures 32 and 33, respectively. The bulk density of the specimen used for this testing phase was 1.4 g/ft³.

The data for the facing material are shown by Figures 34 and 35.

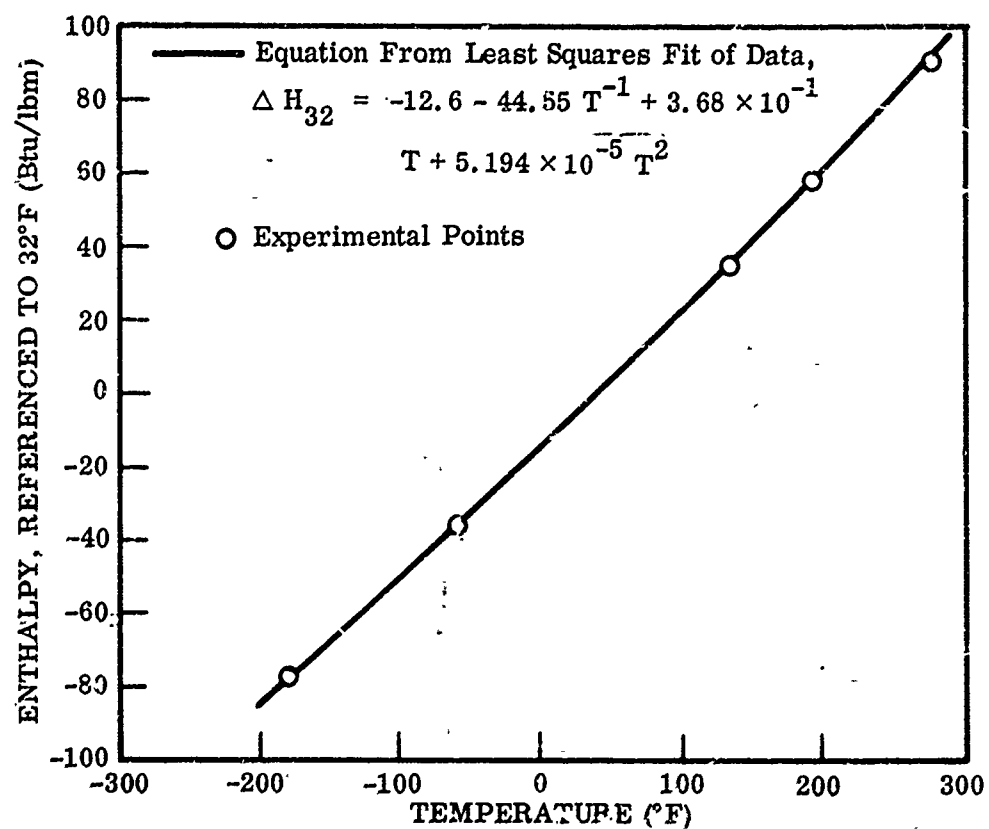


Figure 32. Enthalpy of Material B, Foam Structure, Referenced to 32° F
(Bulb Density $\approx 1.4 \text{ lb/ft}^3$)

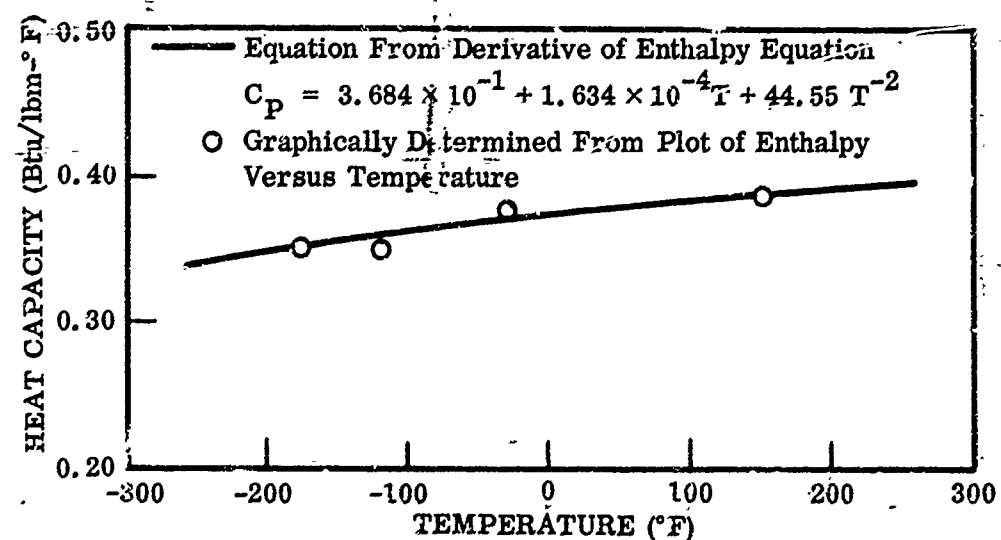


Figure 33 Heat Capacity of Material B, Foam Structure

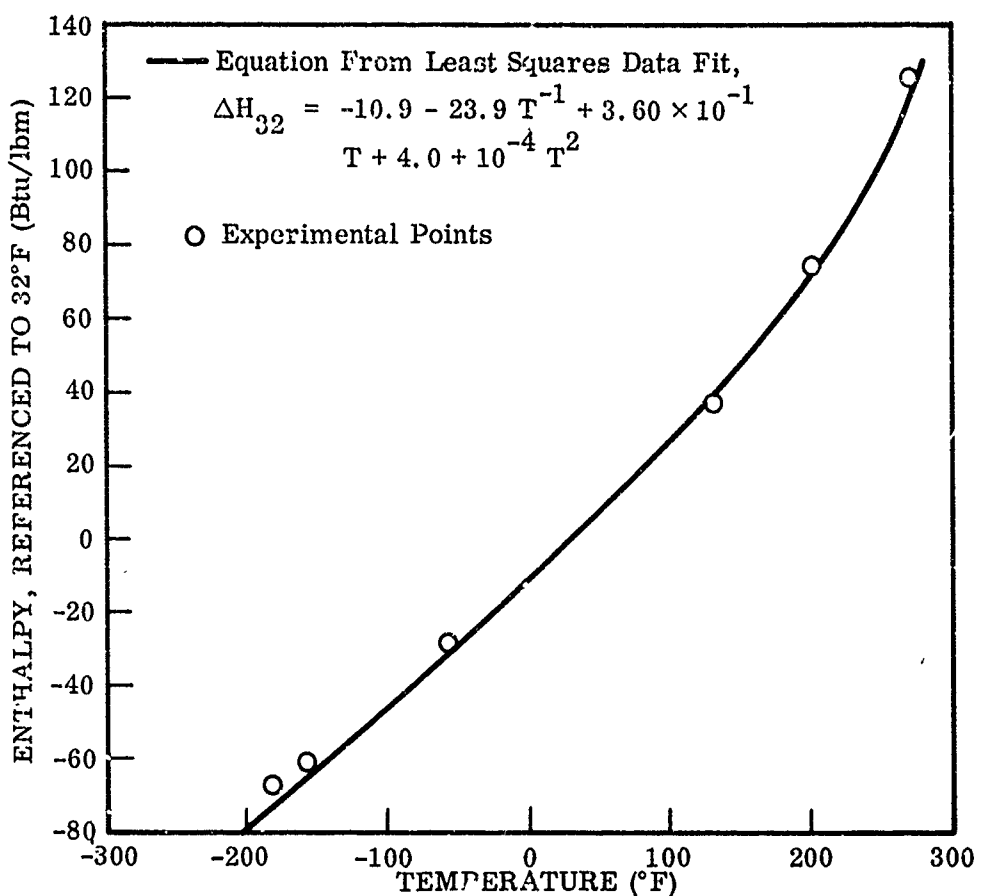


Figure 34 Enthalpy of Material B, Epoxy Backing Surface

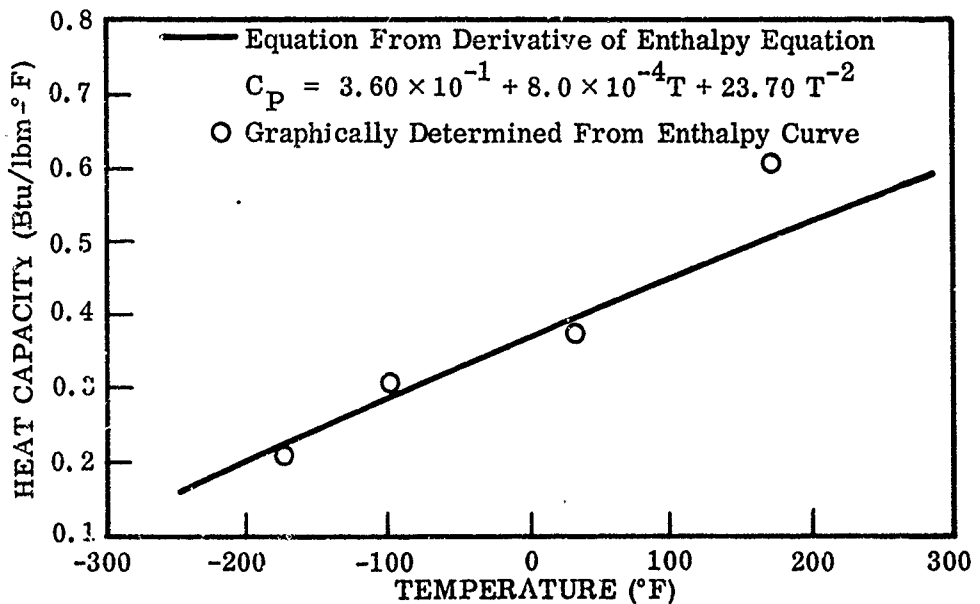


Figure 35 Heat Capacity of Material B, Epoxy Backing Surface

5. WEIGHT LOSS

The study of short-time weight-loss behavior of polymeric reflector components was carried out to see at what temperature the performance of these materials might become marginal.

Weight-loss behavior in vacuum from 100° to 500° F was used as the primary criterion. Short-time weight loss can result from any or all of the following factors: (1) loss of adsorbed water, (2) loss of volatiles entrapped in the polymer, and (3) loss of weight resulting from degradation and depolymerization of the material itself. The first factor, loss of adsorbed water, has no deleterious effect. The second factor could be deleterious if the volatile constituents caused a pressure buildup, which could warp the structure or affect the strength of the bond. Extensive material degradation would be associated with complete weakening and loss of structural strength of any bonding agent.

Effects of degradation on sample structure and appearance were noted. No extensive investigation of the effects of degradation was made, since all materials were to be subjected to long-term vacuum stability tests, together with evaluation of the effect on optical and mechanical properties.

a. Description of Apparatus

The weight-loss apparatus, shown in Figure 36, consists of an automatic recording balance housed in a vacuum pressure shell evacuated by a diffusion and fore pump. The vacuum attainable when a sample is not outgassing heavily is 10^{-8} Torr. A balance motor that raises and lowers weights is housed outside the vacuum shell.

Test samples were suspended by Nichrome wire in a small glass heating unit. The sample itself was contained in a small quartz bucket. A record of weight and temperature was kept by a two-pen recorder. The sample was suspended in a glass heating unit shown in Figure 37. A 1,000-ml cold trap was located above the sample to condense volatiles and keep them from contaminating the balance. The trap had a baffle on the bottom to keep the condensables from running back down into the hot zone. The sample was heated by glass heating tape wrapped around a Vycor tube. Electrical power input was controlled by means of a Variac. A chromel-alumel thermocouple was mounted just underneath the sample to record temperature.

b. Test Procedure

For test purposes, a section of each solid sample was cut to fit into the quartz sample bucket of the balance. Thin sheet samples were rolled up to form a bundle of suitable size and weight. The rigidized composite, Material L, was crushed together and suspended on a Nichrome hook for weighing.

The preweighed sample was then placed in a quartz bucket and suspended in the balance, and the system was evacuated to 10^{-8} Torr. The sample was brought to 100° F and held there until no appreciable further weight loss was noted. The exposure temperature

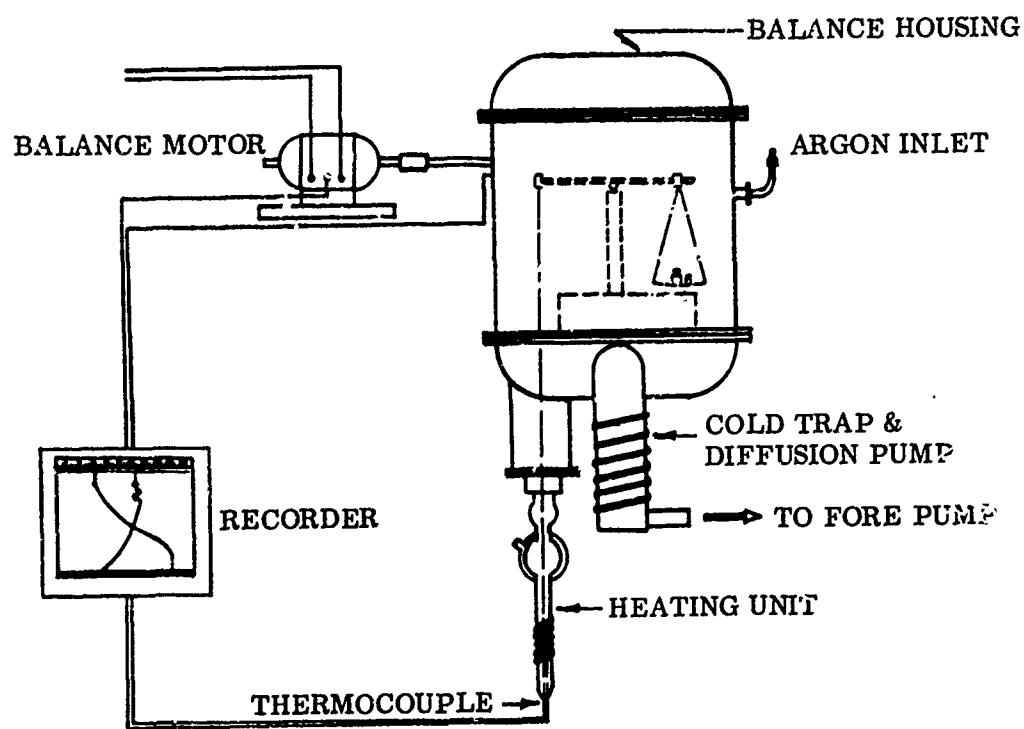


Figure 36 Weight-Loss Apparatus

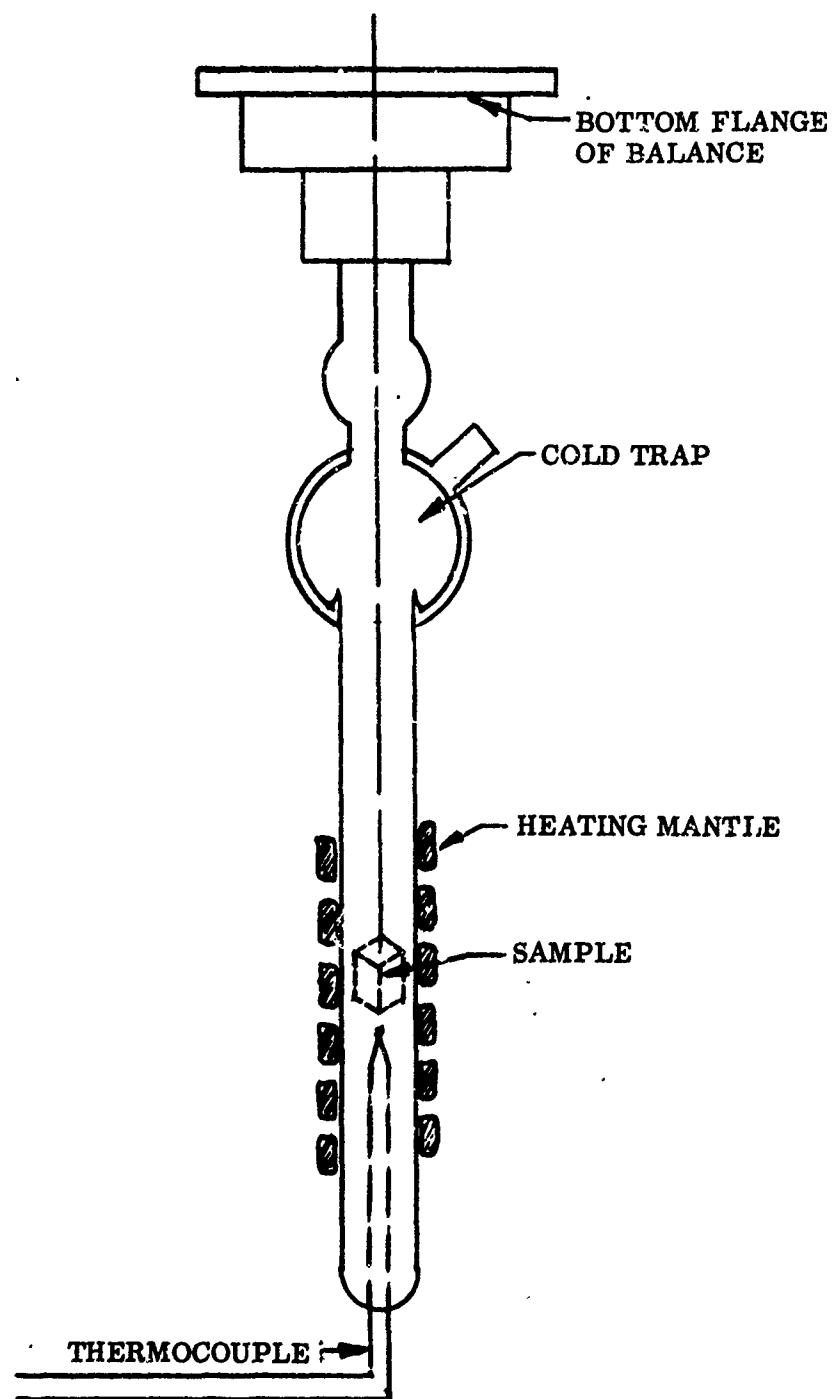


Figure 37 Detail of Heating Chamber, Weight-Loss Apparatus

was increased in 100° F increments to 500° F, holding at each temperature until near-equilibrium was attained. A typical weight-loss and heating-cycle curve, A, is shown in Figure 38. In general, a sample was held at temperature 50 min to achieve weight-loss characteristic for that temperature. In the final step, the sample was usually held at 500° F for 2.5 hr to make sure the observed weight loss was complete. Samples were weighed at the end of the test as a check on balance accuracy.

The precision of the balance was ± 0.1 mg. Its accuracy was of the same order. Samples were 0.5 g in size, so that the accuracy of weight-loss measurement was ± 0.02 percent. The thermocouple was checked at 212° F using boiling water as a reference standard. The accuracy was ± 0.2 percent. The estimated repeatability in weight-loss behavior was ± 5 percent and can be attributed primarily to variation in material formulation.

To test the effect of heat cycle, a sample was brought to 500° F as rapidly as possible (curves B, Figure 38). The total observed weight loss was of the same magnitude. The amount of weight loss appears to be relatively independent of rate of heating.

If weight-loss behavior is plotted versus time at temperature, a series of curves like those in Figure 39 is obtained. For any temperature, there is an initial rapid weight loss followed by a period in which the rate of weight loss is very slow and apparently reaches equilibrium conditions.

Except for the initial period, the weight loss at a given temperature will be approximately the same, irrespective of time (Figure 39). It is, therefore, reasonable to plot total weight loss versus temperature as shown in Figure 40. Data for all samples were plotted in this way.

c. Test Results

Eleven samples grouped into six lots (Table VII) were evaluated for short-time weight-loss effects to 500° F. All of these were organic in nature. They included bonding agents, sublayer materials, or foams to be used in portions of the reflector surfaces supplied by five vendors. Material L was received as the complete composite (Figure 41). It consisted of a polyurethane-rigidized nylon structure with a reflective surface of aluminized mylar bonded to the structure with flexible epoxy. Data are presented in summary form in Table VIII.

Material A. The plot of total weight loss versus temperature (Figure 40) illustrates that the loss of weight by this epoxy adhesive did not become significant (greater than 10 percent) below 400° F. The residue at 500° F was a bloated, porous brown char.

Material B. In this material (foamed polymeric) the greatest weight loss was below 200° F (Figure 42), which probably resulted from loss of adsorbed water. Once the water vapor was lost, the increase in weight loss was directly proportional to temperature, but small (2.0 percent by weight per 100° F). The total weight loss attributed to volatiles other than water was 6.0 percent by weight. The residue at 500° F was slightly discolored, had retained its original shape, but had lost considerable structural strength.

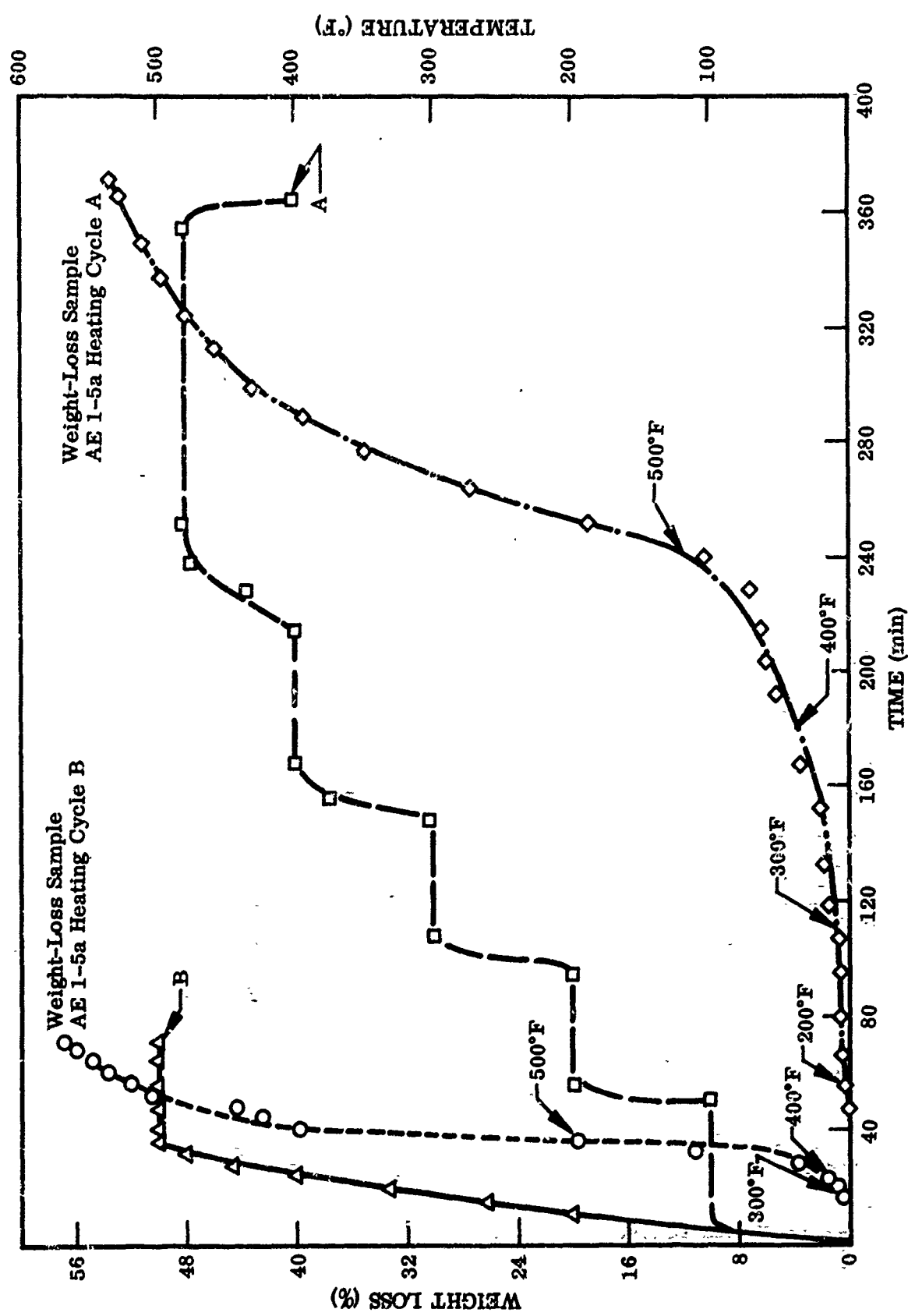


Figure 38 . Typical Weight-Loss Curves

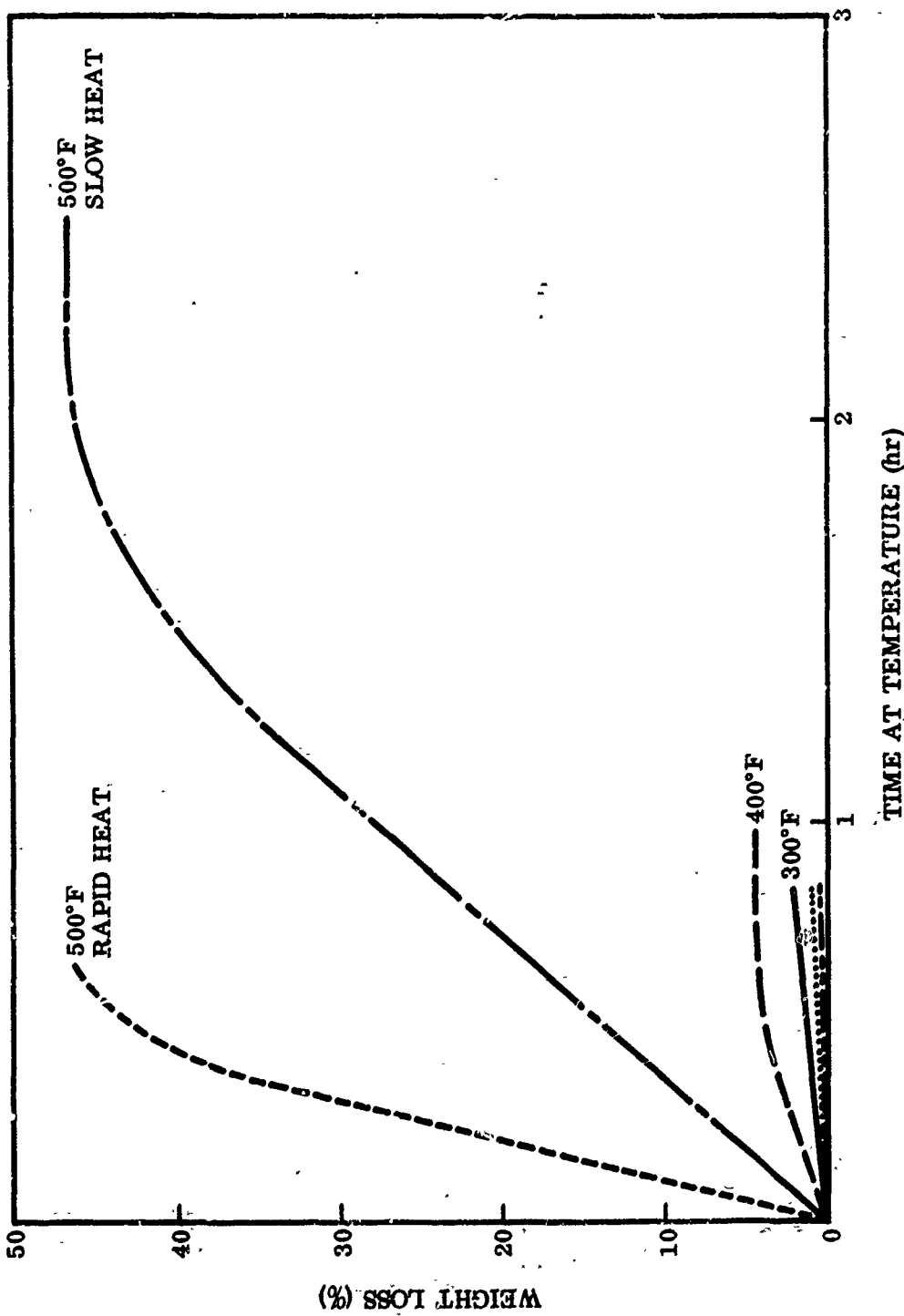


Figure 39 Weight Loss Versus Time at Temperature, Material A, Epoxy Adhesive

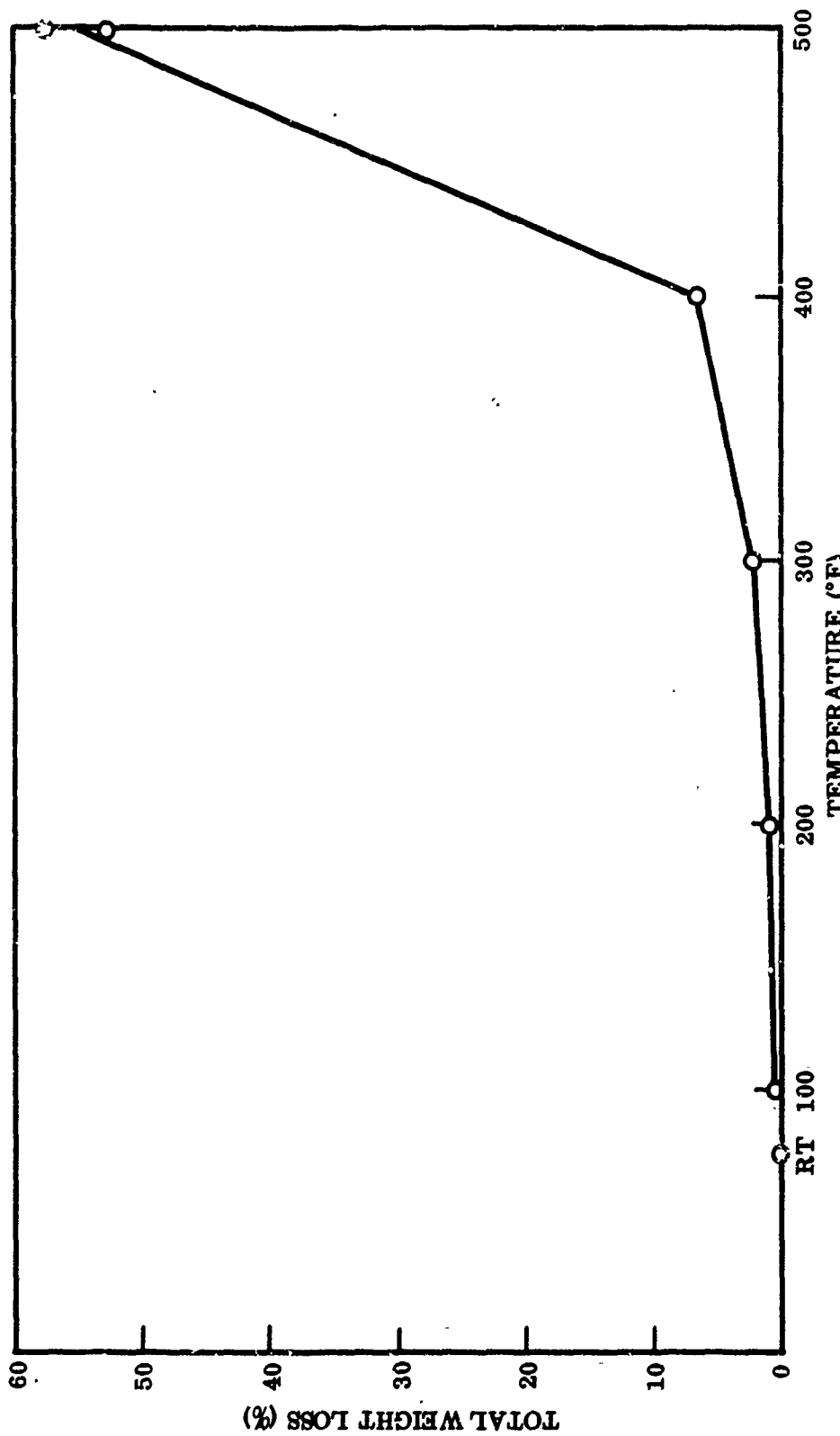
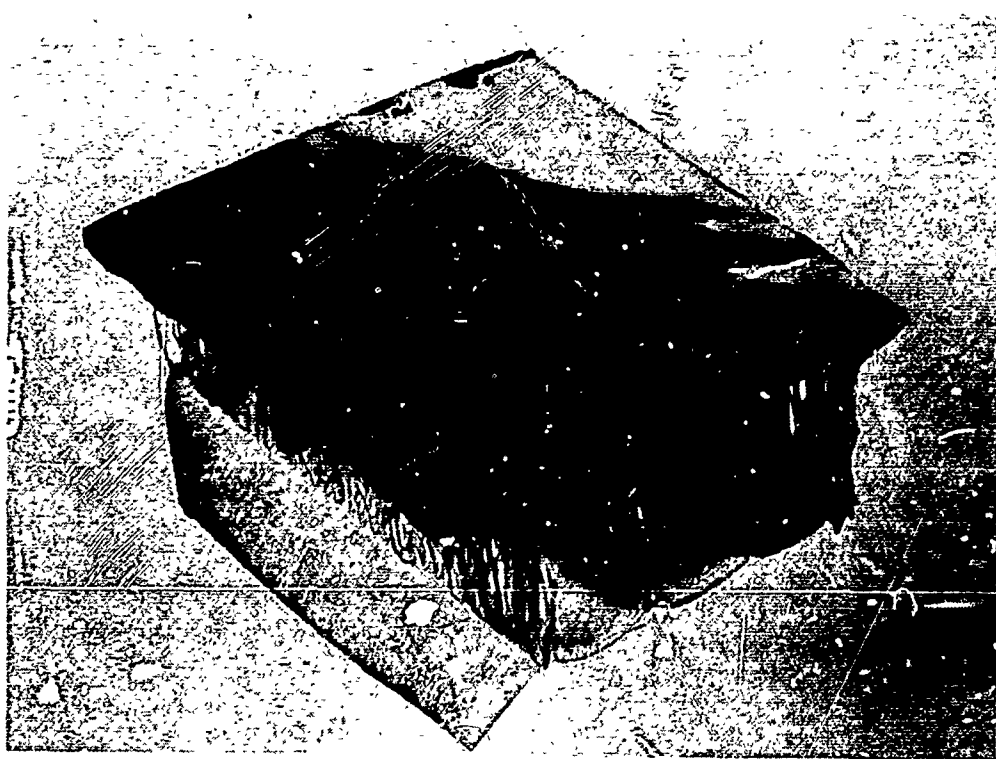


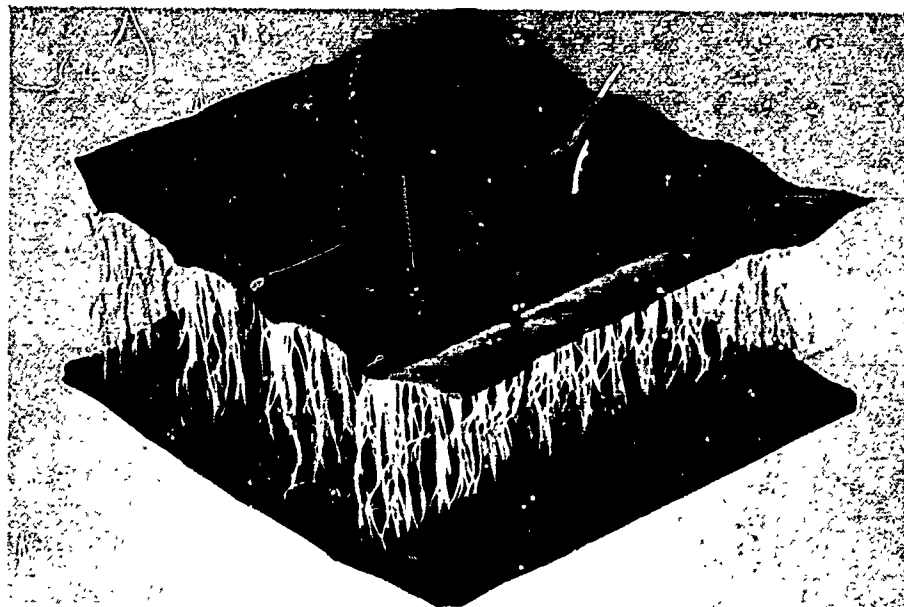
Figure 40 Equilibrium Weight Loss as a Function of Temperature, Material A, Epoxy Adhesive

Table VII. Description of Materials for Weight-Loss Behavior to 500° F

Material	Physical description	Vendor chemical description
Material A epoxy adhesive	Greenish yellow, 1-in.-diam. by 1-in.-long cylindrical plug	RACO 803 epoxy bonding adhesive
Material B phenolic foam	Red-colored foam, ~ 1 in. thick	Phenolic foam
Material C epoxy adhesive	Creamy white, 1-in.-diam. by 1-1/8-in.-long cylindrical plugs	Epoxy bonding adhesive
Material C epoxy sublayer	Amber colored, some cracks, 1-in.-diam. by 11/16-in.-long cylinder	Epoxy sublayer material
Materials D-F epoxy facing adhesive	Black, 1-in.-diam. by 1-in.-long cylindrical plugs	Eccobond 45 with catalyst no. 15 adhesive
Materials D-F epoxy backing adhesive	Black, 1-in.-diam. by 1-in.-long cylindrical plugs	Eccobond 45 with catalyst no. 15 and 2% Emerson and Cuming SC filler
Material D epoxy sublayer	Yellowish, transparent, 1-in.-wide thin sheet	Epoxy sublayer, Emerson and Cuming EP 3A and B
Materials E-F epoxy sublayer	Amber, transparent, 1-in.-wide thin sheet	Bee Chemical, D5H-30004 Coating with ET 438 catalyst
Materials G-K epoxy adhesive	Greenish yellow plastic in a shallow metal dish; plastic apparently contains some bubbles of entrapped gas	Epoxy bonding adhesive
Material L epoxy sublayer	Amber, translucent, 1-in.-diam. by 1-in.-long, cylindrical plug; fine bubbles dispersed throughout	Epoxy sublayer
Material L composite structure	White fibrous stringy material, rigidized surfaces; one surface has an upper layer of aluminized mylar (see Figure 39)	Polyurethane-rigidized nylon composite



(a) Reflector Surface



(b) Back Surface

Figure 41 Appearance of Material L, Composite Structure, Before Test

Table VIII. Short-Term Weight Loss of Polymeric Reflector Components

Material identification	Test conditions		Cumulative weight loss (%)	Maximum short-term temp. stability	Comments
	Temp. (°F)	Total time (min)			
Material A epoxy adhesive	100	48	0.29	400°F	Bloated, porous brown residue at 500°F
	200	96	0.71		
	300	141	1.72		
	400	214	6.2		
	500	362	52.4		
Material B phenolic foam	100	48	3.7	500°F; sample slightly discolored at 500°F; considerable structural strength lost	Most of weight loss is of adsorbed water evolved below 200°F
	200	97	7.8		
	300	151	9.6		
	400	205	11.4		
	500	322	14.2		
Material C epoxy adhesive	100	48	0.34	Good to 350°F	Bloated, porous black residue at 500°F
	200	96	2.47		
	300	152	4.59		
	400	212	14.93		
	500	362	62.0		
Material C epoxy sublayer	100	48	1.0	Marginal at 300°F; weight loss = 14.5%	Porous glassy black carbon formed at 500°F
	200	96	8.15		
	300	152	14.5		
	400	212	27.5		
	500	362	82.0		
Materials D-F epoxy facing adhesive	100	48	0.4	Good to 300°F; marginal at 40°F	Bloated, porous black residue at 500°F
	200	94	2.23		
	300	150	4.92		
	400	185	9.9		
	500	297	51.0		
Materials D-F epoxy backing adhesive	100	27	0.875	Good to 300°F	Bloated, porous black residue at 500°F
	200	75	2.63		
	300	128	6.05		
	400	188	22.3		
	500	308	58.0		
Material D epoxy sublayer	100	48	0.53	Good to 300°F	Black glassy residue at 500°F
	200	100	2.83		
	300	156	4.6		
	400	212	13.8		
	500	362	82.7		
Materials E-F epoxy sublayer	100	48	1.39	Probably to 300°F	Glossy brown film at 500°F
	200	96	7.45		
	300	152	12.8		
	400	208	33.35		
	500	358	64.5		
Materials G-K epoxy adhesive	100	48	0.27	Good to 300°F	Porous black residue at 500°F
	200	96	1.1		
	300	152	2.8		
	400	212	15.6		
	500	362	59.62		
Material L epoxy sublayer	100	48	0.91	Marginal at 300°F	Bloated, black residue at 500°F
	200	96	7.2		
	300	152	13.7		
	400	212	28.8		
	500	362	70.0		
Material L polyurethane-rigidized nylon composite	100	48	0.91	Probably good to 275°F	Sublayer coating badly bloated at 300°F; see Figure 52
	200	96	4.37		
	300	152	12.6		
	400	212	19.4		
	500	232(a)	50.4		
Material L aluminized-mylar reflecting film	100	45	0.53	400°F	No visible damage at 200°F; sample degraded into a golden yellow ball at 500°F
	200	65	0.73		
	300	—	1.45		
	400	180	2.91		
	500	240	31.9		

(a) Sample stuck to side of enclosure.

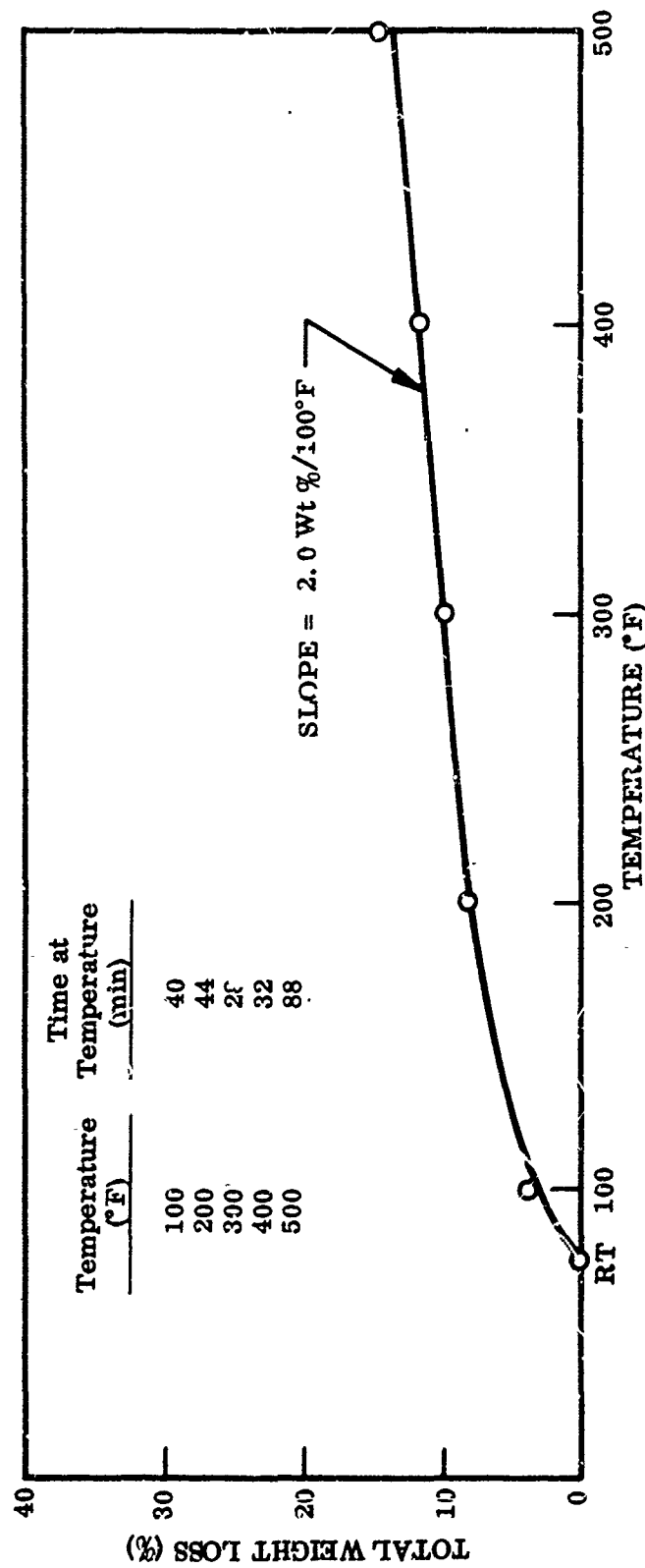


Figure 42 Equilibrium Weight Loss Versus Temperature, Material B, Phenolic Foam

Material C. The short-time weight loss of samples CE 1-5 (epoxy adhesive) remained slight below 350°F (Figure 43). The residue at 500°F was a bloated, porous black char. For samples CE 6-10 (epoxy sublayer material), the weight loss increased 5%/100°F to 300°F (Figure 44). At higher temperatures, the $\Delta\omega/\Delta t^2$ became much greater. The residue remaining at the end of the test (less than 20 percent) was a porous black glassy carbon.

Materials D-F. The weight loss with temperature, $\Delta\omega/\Delta t$, of samples DE 1-5 (epoxy adhesive) remained slight to 350°F but increased rapidly above that temperature (Figure 45). The residue at 500°F (45 percent by weight) was a bloated, porous black char.

For samples DE 6-10 (epoxy adhesive), $\Delta\omega/\Delta t$ was slight to 300°F (Figure 46) and thereafter increased with temperature. The char residue (42.5 percent by weight) was bloated, porous, and black.

In samples DE 11-15 (epoxy sublayer material), $\Delta\omega/\Delta t$ was small to 350°F but increased rapidly with further increase in temperature (Figure 47). The residue at 500°F (17.5 percent by weight) was a black glassy carbon.

In samples DE 16-20 (epoxy sublayer material), $\Delta\omega/\Delta t = 5\%/100°F$ to 300°F and increased to about 20 percent for each 100°F increase from 300 to 500°F (Figure 48). The residue at 500°F was a glossy brown film.

Materials G-K. These samples (epoxy bonding adhesive) were quite stable to 300°F ($\Delta\omega/\Delta t = 1\%/100°F$) but degraded markedly at temperatures above 300°F (Figure 49). The residue at 500°F (40 percent by weight) was a porous black char.

Material L. Samples LE 1-5 (epoxy adhesive) lost weight at a moderate rate below 300°F ($\Delta\omega/\Delta t < 5\%/100°F$) but degraded more rapidly at higher temperature (Figure 50).

The samples of LE 6-10 (polyurethane-rigidized nylon) acted in a manner similar to the epoxies. They were fairly stable below 300°F, but extensive material degradation set in above 400°F (Figure 51). When a sample was taken to 500°F, the reflecting sublayer was badly bloated and deformed (Figure 52). The mylar surface film was stable to 400°F (Figure 53) and $\Delta\omega/\Delta t = 0.6\%/100°F$. Above 400°F extensive weight loss was observed and the material lost all form and structure.

d. Comments and Interpretation of Results

The type of weight-loss behavior exhibited by the epoxy adhesive or sublayers was similar in all cases. Below 300°F, the weight loss was fairly small (from 1.7 to 15 percent, Table VIII). Between 300 and 400°F, the weight loss increased sharply to as much as 33 percent. At 500°F, the materials were badly degraded, and the weight loss rose to 50 to 80 percent. The low-temperature weight loss is probably

²Change in weight with temperature change.

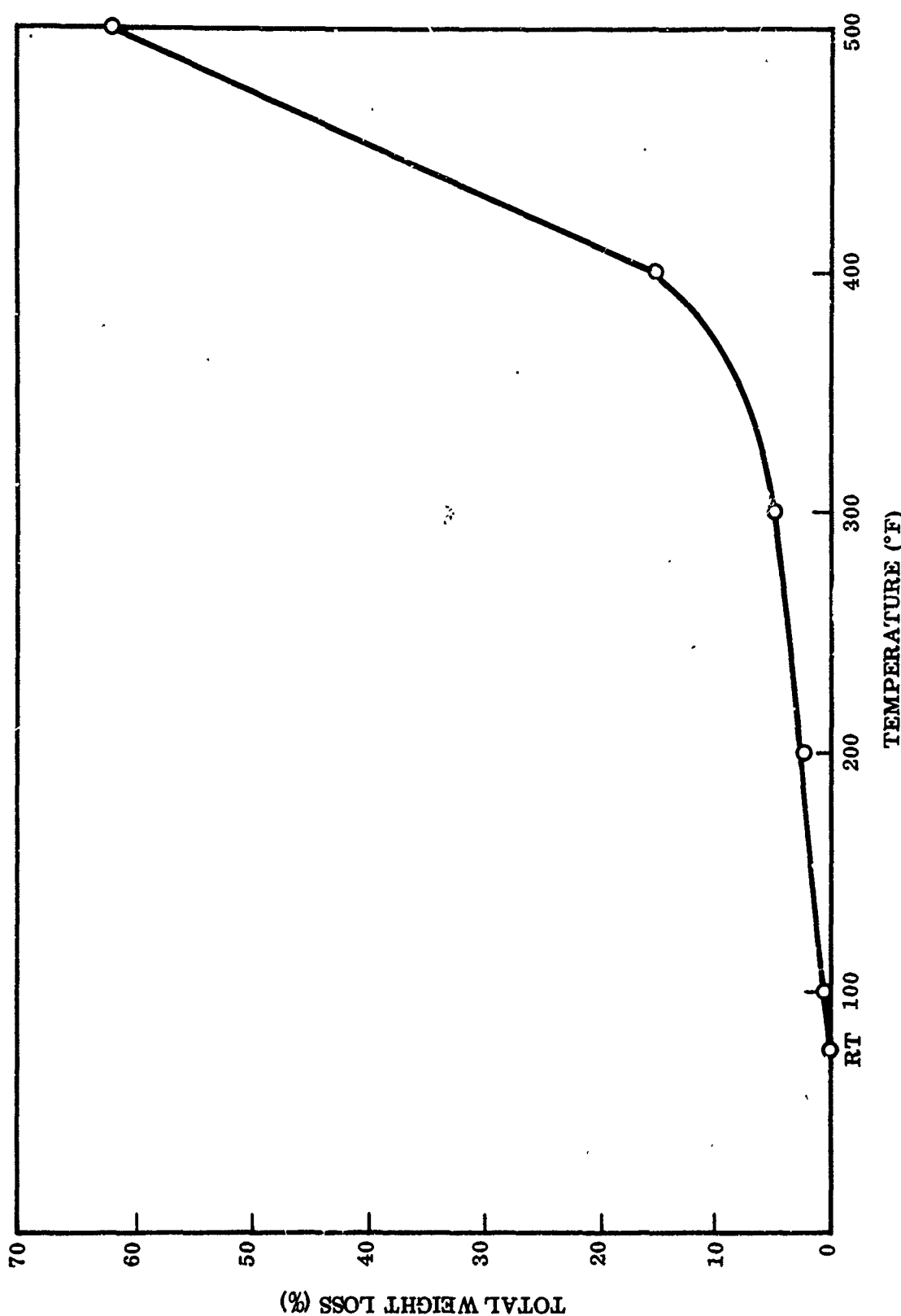


Figure 43 Equilibrium Weight Loss Versus Temperature, Material C, Epoxy Adhesive

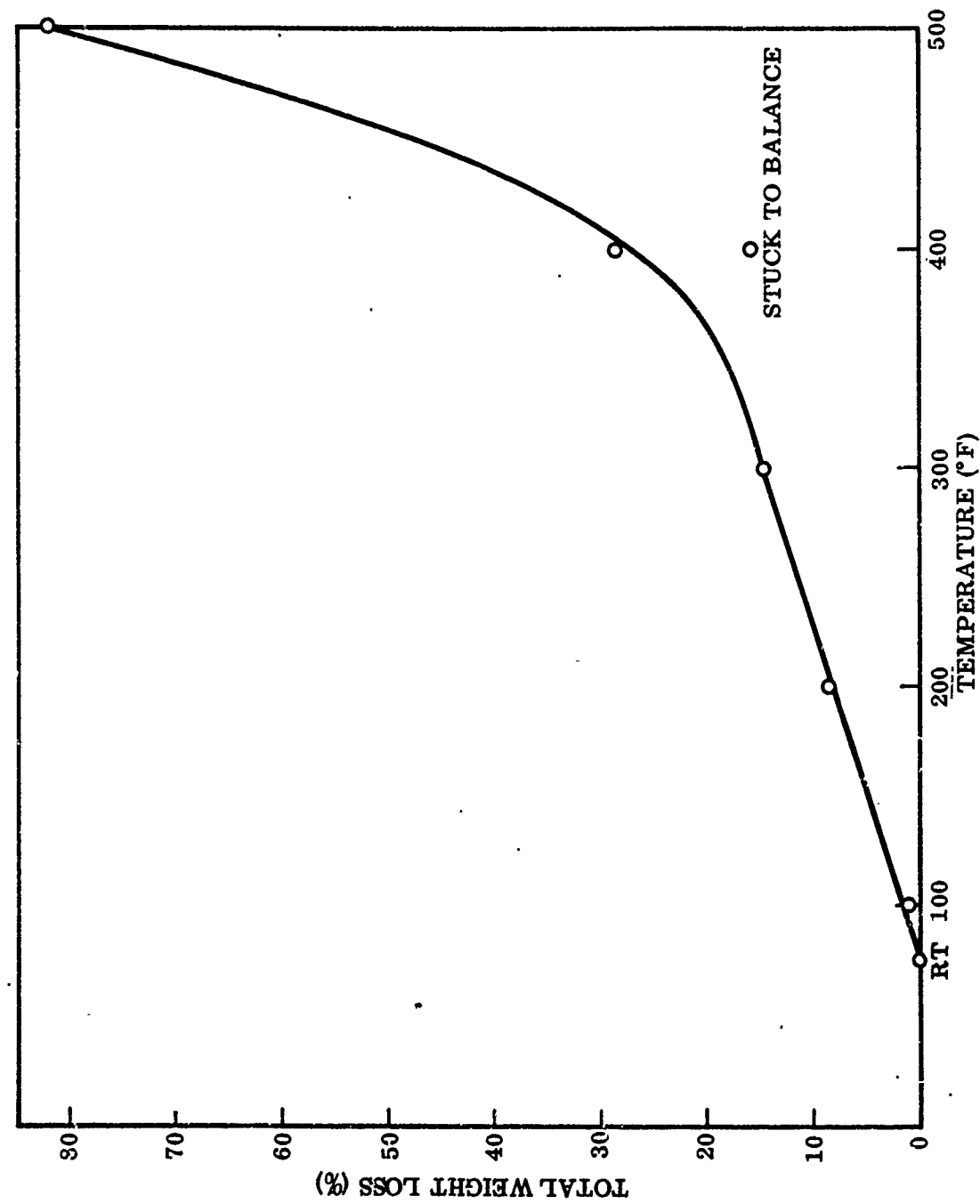


Figure 44 Equilibrium Weight Loss Versus Temperature, Material C, Epoxy Sublayer

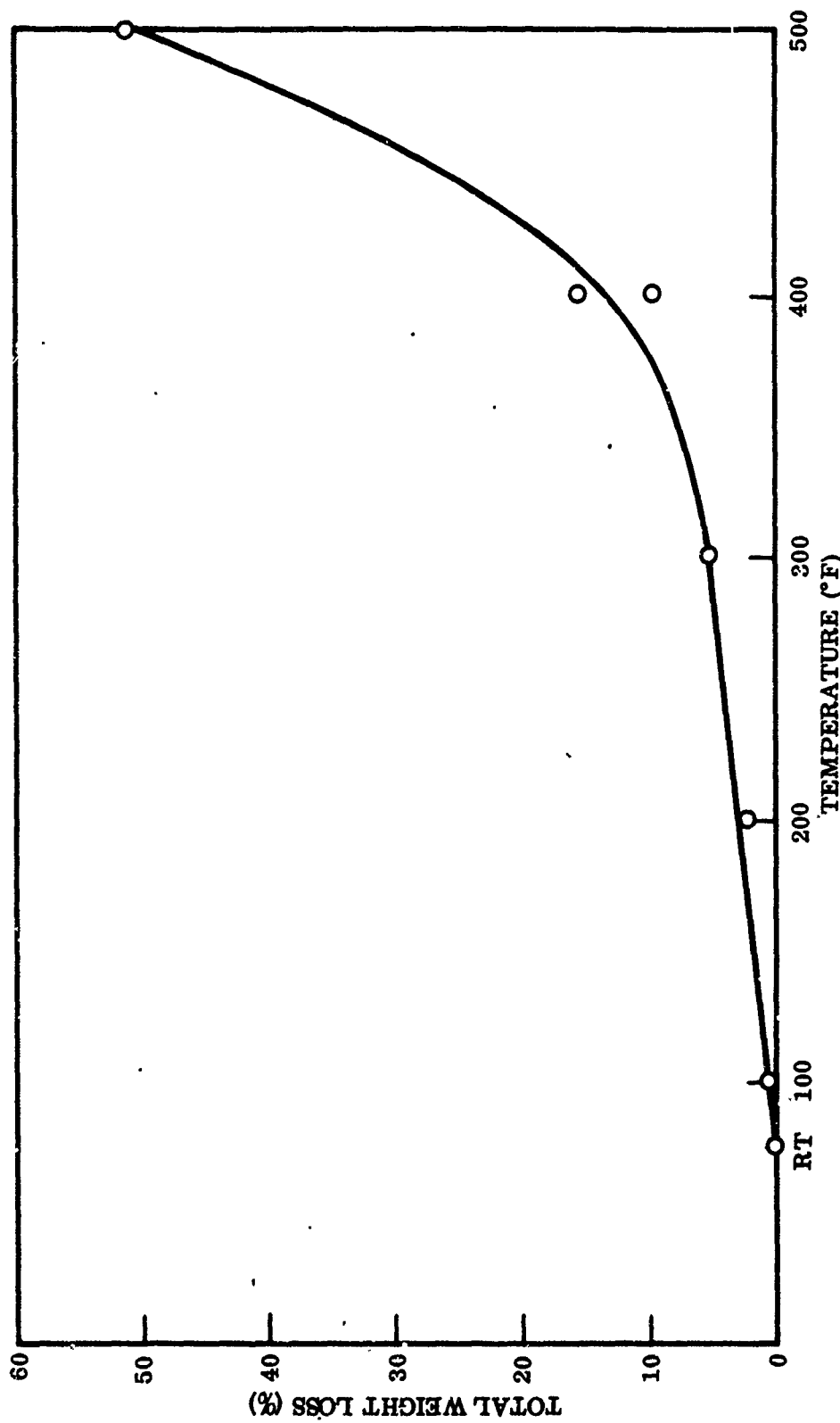


Figure 45 Equilibrium Weight Loss Versus Temperature, Materials D-F, Epoxy Facing Adhesive

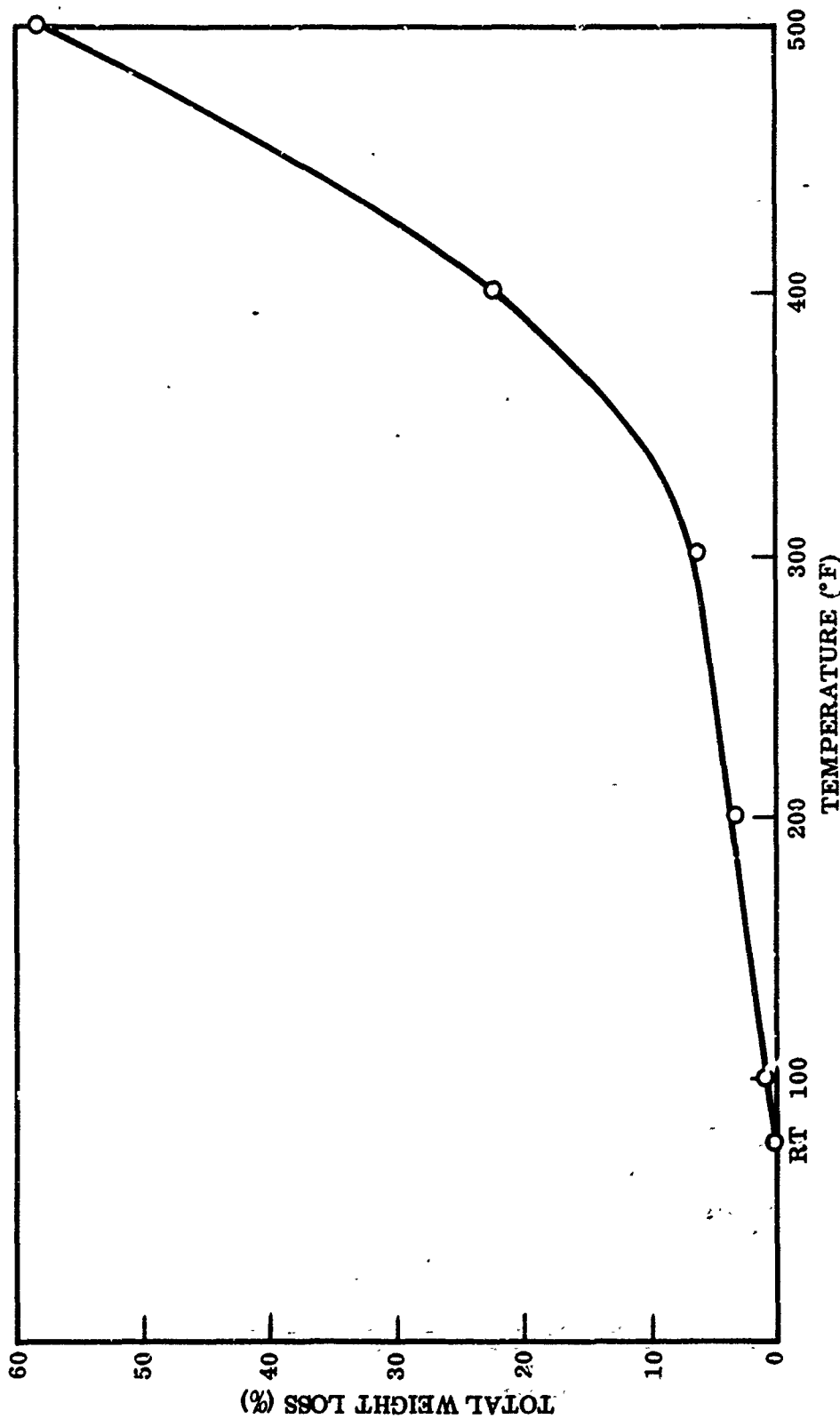


Figure 46 Equilibrium Weight Loss Versus Temperature, Materials D-F, Epoxy Backing Adhesive

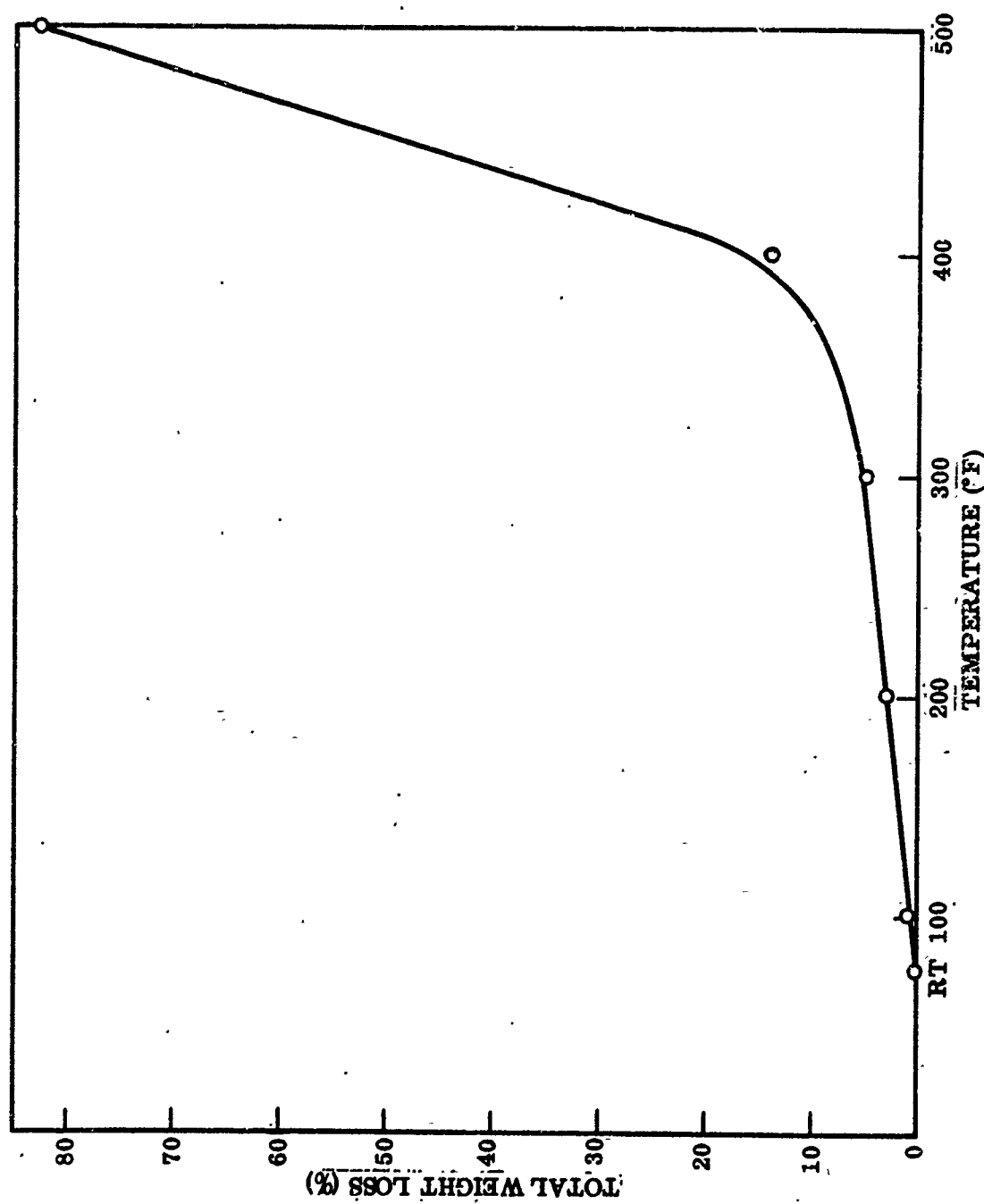


Figure 47. Equilibrium Weight Loss Versus Temperature, Material D, Epoxy Sublayer

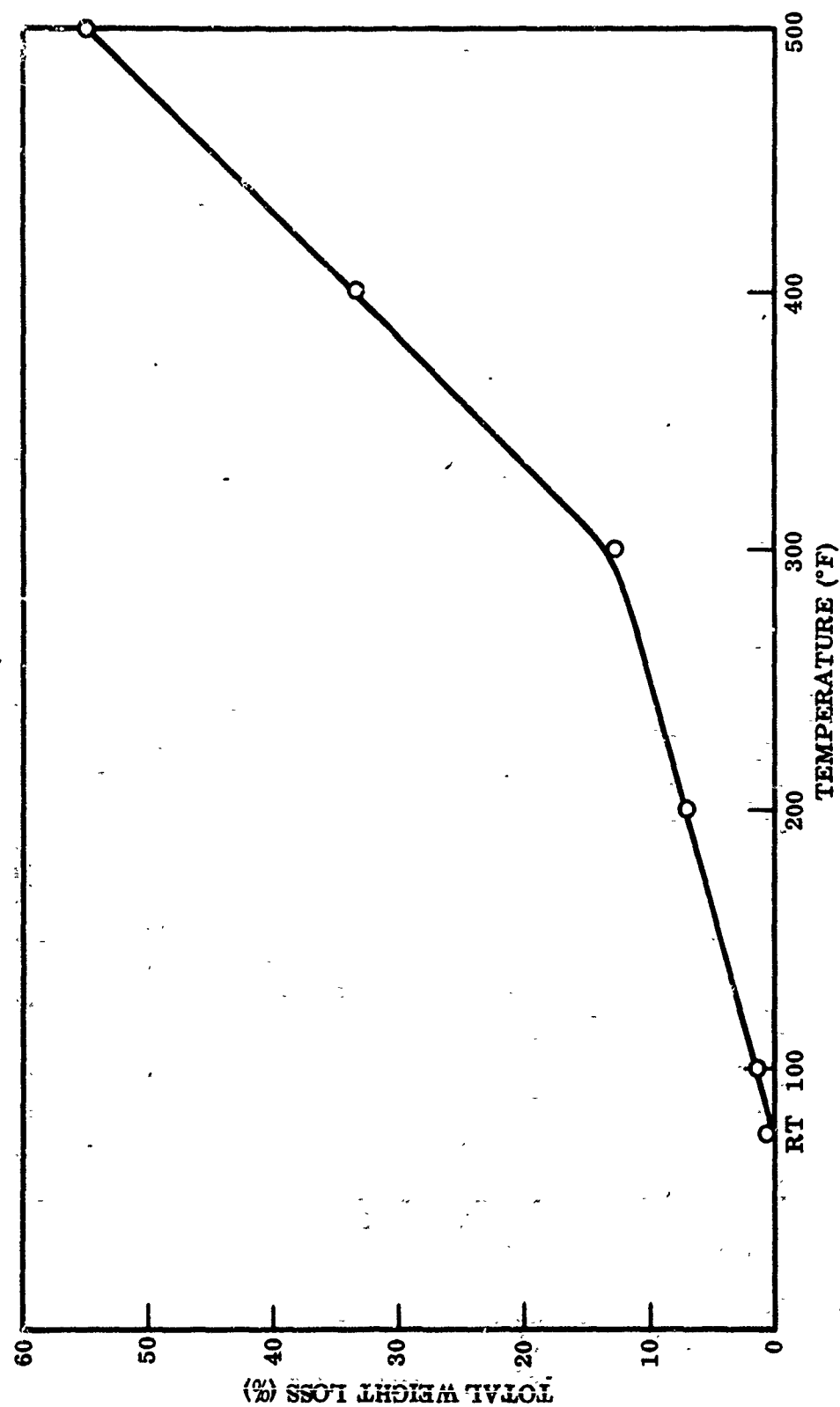


Figure 48 Equilibrium Weight Loss Versus Temperature, Materials E-F, Epoxy Sublayer

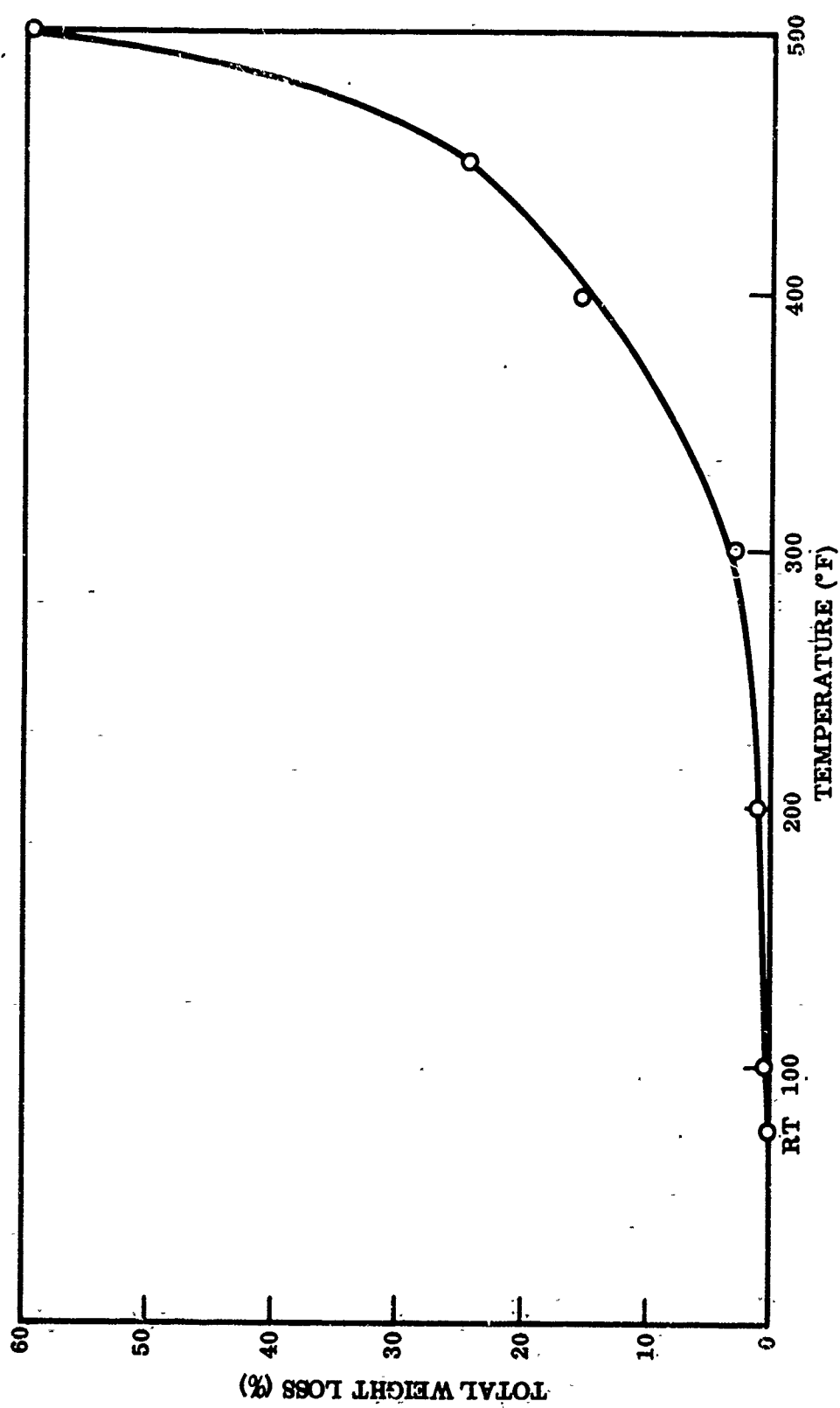


Figure 49 Equilibrium Weight Loss Versus Temperature, Materials G-K, Epoxy Adhesive

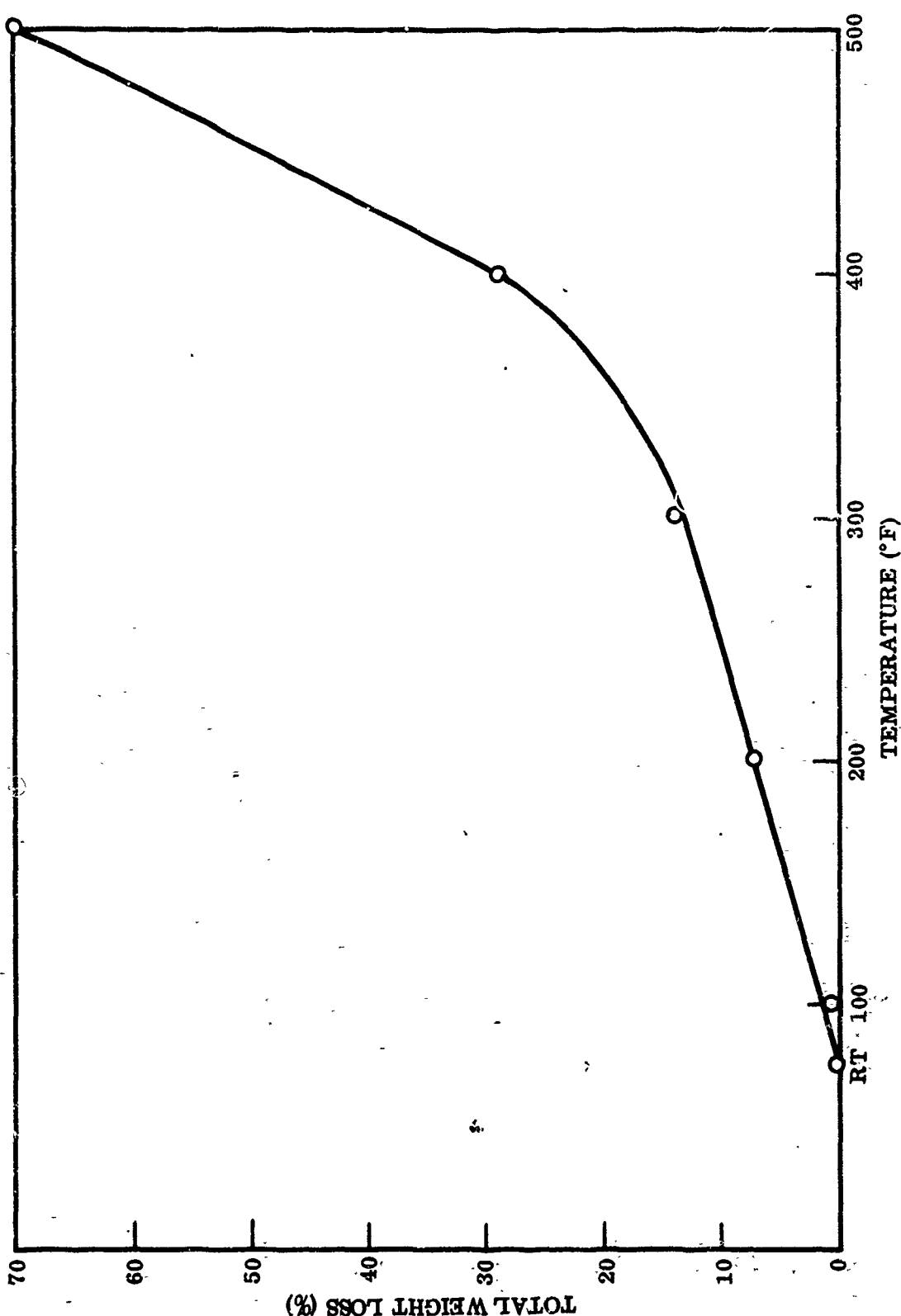


Figure 50 Equilibrium Weight Loss Versus Temperature, Material L, Epoxy Sublayer

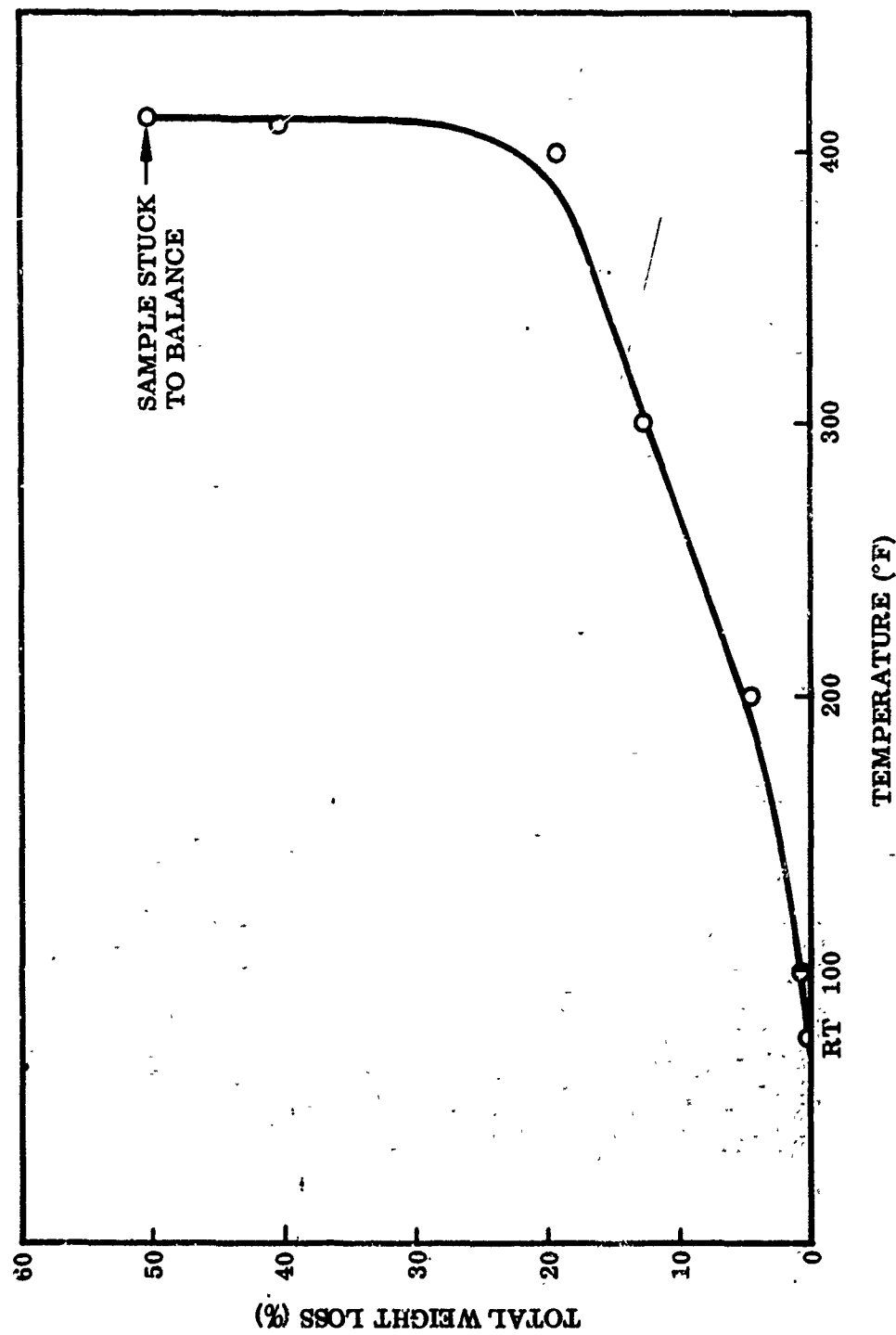
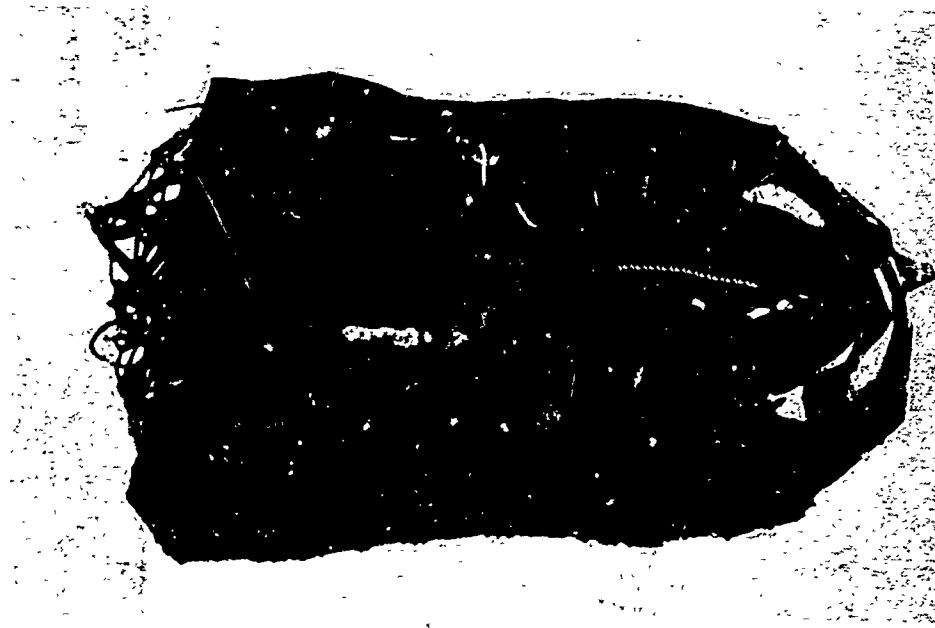


Figure 51 Equilibrium Weight Loss Versus Temperature, Material I, Entire Composite Except Aluminized-Mylar Film



(a) Back Face



(b) Reflector Surface Sublayer

**Figure 52. Appearance of Material L, Composite Structure,
After Test at 500°F**

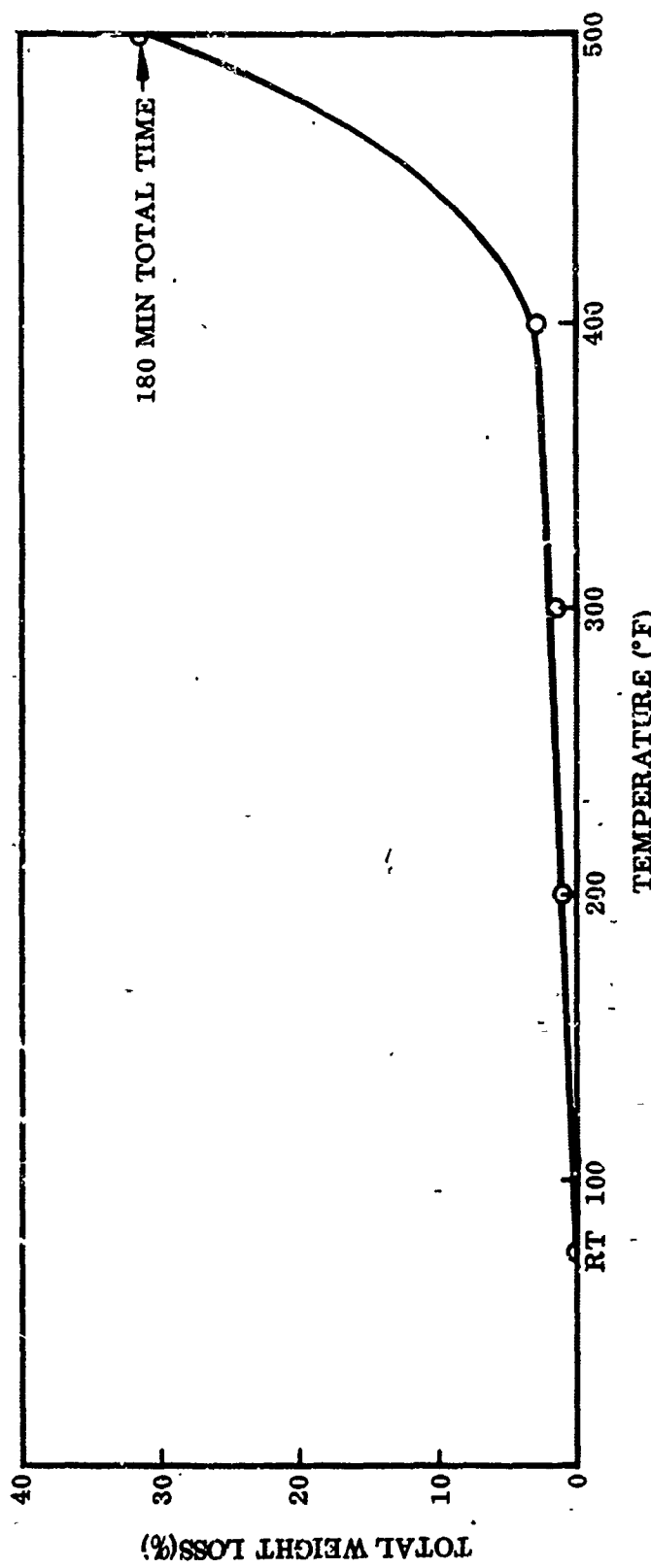


Figure 53 Equilibrium Weight Loss Versus Temperature, Material L, Aluminized-Mylar Film

due to loss of adsorbed water or similar low-temperature volatiles. Higher boiling-point volatiles are given off between 200° and 300°F. These may amount to as little as 6.2 percent for the Material A adhesive or as much as 14.5 percent for the Material C sublayer material.

Volatilization of less than 15 percent probably does not deleteriously affect the structure of the organic component. When the amount of volatile material given off is greater than 15 percent, some material degradation may be taking place; i.e., in an adhesive the bond may be weakening. If the amount of gases given off becomes great enough, the pressure buildup could become sufficient to warp the structure or cause the reflector surface to bloat.

For purposes of comparison, a volatile loss of 10 percent was considered fairly safe. Greater losses were considered marginal. Unless the composite structure is vented, the generated gas pressures could cause warping or bloating of a portion of the structure. Such effects have been noted in a study of the failure of an epoxy-bonded honeycomb structure (9). Losses greater than 30 percent are probably indicative of material degradation with associated weakening of any bond and loss of structural integrity.

Based on the foregoing criteria, all the epoxy adhesive and sublayer materials have short-term thermal stability to approximately 300°F (Table VIII). Some may be stable to 400°F. All are extensively degraded at 500°F.

In the epoxies, the rate of weight loss does not exhibit Arrhenius-type behavior; i.e., it is not a direct function of the absolute temperature. The data suggest that these materials act as a mixture of volatile components rather than as a compound. The rate of weight loss is a function of individual vapor pressures and the concentration of these volatiles.

In the Material B phenolic foam, the weight loss is directly proportional to temperature with an activation energy of 5.76 kcal/g-mole (Figure 54). This indicates that the process observed is one of material degradation rather than loss of entrapped volatiles. However, the increase in weight loss with temperature ($\Delta\omega/\Delta t$) is quite low. This material has short-time stability to 500°F, so any short-time excursion to such temperature should be relatively harmless.

The composite sample of polyurethane-rigidized nylon acts in a manner analogous to the epoxies. The weight loss is a function of individual vapor pressures or degradation rates and their concentration. The epoxy sublayer material is the least stable component of the composite. It bloats badly and causes the structure to warp. The most stable component is the aluminized-mylar surface layer, which remains stable to 400°F.

Short-time weight-loss behavior is indicative of the possible effect of temperature excursions above the planned operating temperature of 250°F. Long-time vacuum

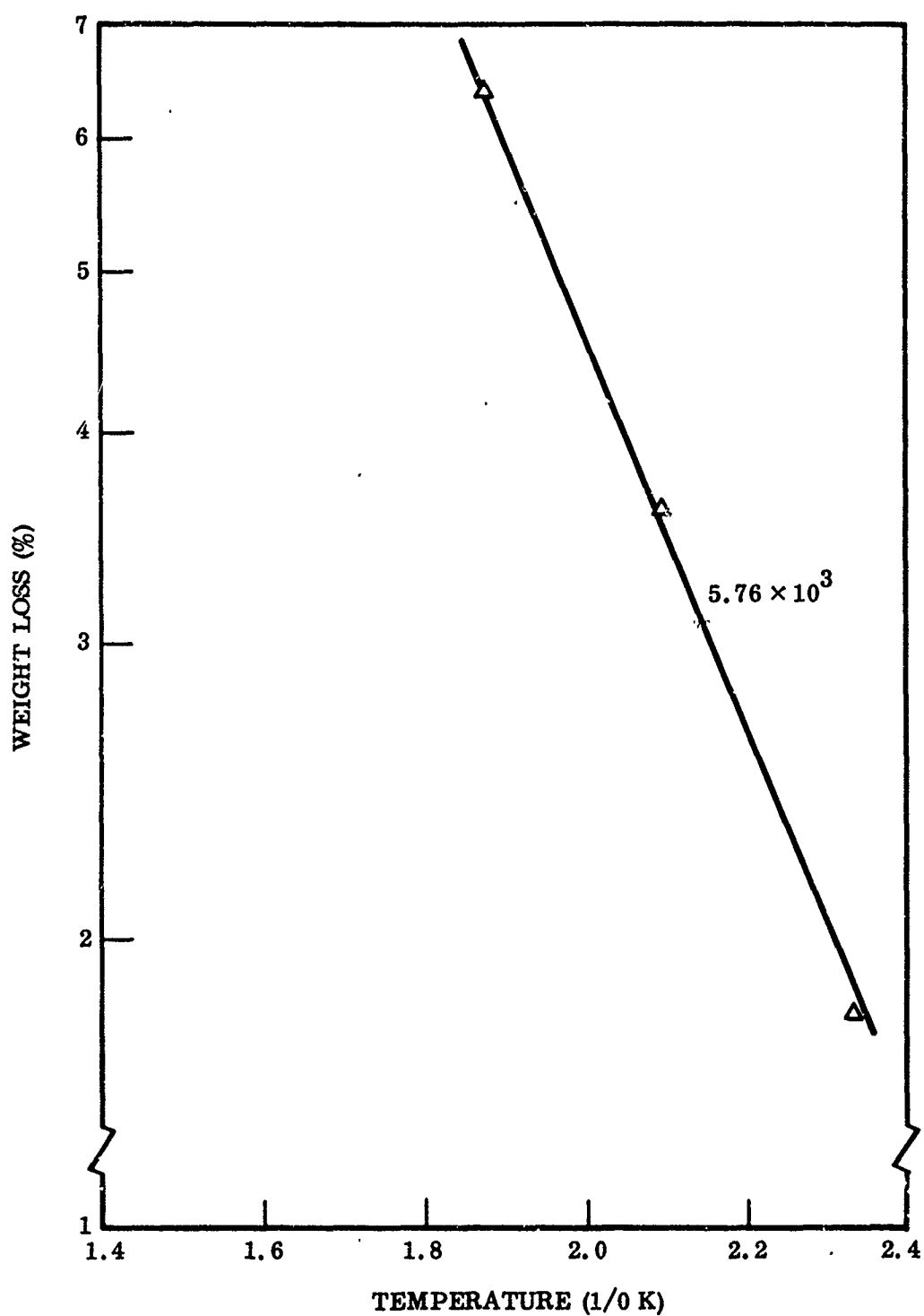


Figure 54 Degradation of Material B, Phenolic Foam

stability tests at $t = 250^{\circ}\text{F}$, together with measurement of changes in optical and mechanical properties described in other sections of this report, should indicate their long-term behavior.

Since the processes of degradation are time- as well as temperature-dependent, short-term high-temperature stability cannot be equated with long-time stability at lower temperature. Thus, phenolic foam, which has short-time stability, could degrade extensively over a long period of time. On the other hand, the epoxies that degrade badly above 300°F may perform quite adequately for long periods provided the temperature is maintained below 300°F .

To summarize, all of the polymeric materials tested have reasonable thermal stability to 300°F as indicated by short-time weight-loss measurements.

Degradation of epoxy adhesive and sublayer materials becomes deleterious at temperatures above 300°F . The extent of degradation depends upon the specific formulation. Some samples are reasonably stable to 400°F . These epoxies act as a mixture of volatile components, with the amount of material given off as a function of individual vapor pressures. At 500°F all of these samples are thoroughly charred and many are badly bloated as a result of gaseous entrapment during degradation.

The Material L rigidized-polyurethane structure is stable to 300°F . The reflecting sublayer is badly bloated and deformed at 500°F . The reflecting aluminized-mylar surface is stable to 400°F but decomposes rapidly and destructively at higher temperatures.

Material B phenolic foam is relatively stable to 500°F from the standpoint of both weight loss and structural integrity.

6. THERMAL/VACUUM ENVIRONMENTAL STABILITY

A study of thermal/vacuum environmental stability was conducted to determine the long-term effect of temperature in the range of $250^{\circ} \pm 5^{\circ}\text{F}$ in vacuum at 5×10^{-6} Torr or less on the performance of candidate materials. Changes in structural properties during exposure were the primary criteria. Thermal/vacuum environmental stability of composite materials can be influenced by (1) loss of adsorbed water, (2) loss of volatiles in the polymeric materials making up the composite, or (3) degradation and depolymerization of the adhesives, bonding agents, or facing sheets making up the composite material. Loss of adsorbed water occurs in the early stages of thermal/vacuum exposure and should have no deleterious effects on the structural properties of the composite materials. The loss of volatile constituents could cause an increase in pressure in the structure that, if not properly vented, could affect the strength of adhesive bonds or warp the structure. Degradation and depolymerization could change the properties of the bonding agents or adhesives and cause loss of structural strength.

No quantitative investigation of the effects of degradation was made, because all materials were to be evaluated in subsequent mechanical-properties tests after exposure to the thermal/vacuum environment.

a. Description of Apparatus

The equipment used in the long-term thermal/vacuum stability tests is shown in Figure 55. Two vacuum systems were used, one for the 100- and the 6,000-hr test and the other for the 1,000-hr test. With the exception of the size of the pumping system, 4-in. diffusion pump for the 1,000-hr test and 6-in. for the 100- and 6,000-hr test, the equipment was the same in all three tests. An 18-in. bell jar on a 20-in. base plate containing electrical, thermocouple, and vacuum gage feed-throughs was connected to a liquid-nitrogen-trap oil-diffusion-pump vacuum system. The liquid-nitrogen trap was designed to minimize migration or creep of pump fluids into the test chamber. With the specimens at the 250°F test temperature, a vacuum of less than 5×10^{-6} Torr was achieved 16 hr after start of test and maintained thereafter.

The specimens, 3-in. diameter by 0.25-in. thick, were supported as shown in Figure 56 on stainless-steel rods and strip-fastened with stainless-steel bolts. An iron-constantan thermocouple was attached to one specimen of each group of three specimens as shown in Figure 57. The specimens were supported in stainless-steel radiant-heater assemblies as shown in Figure 58. Electrical power to the radiant heaters was indicated and controlled to $250 \pm 5^\circ\text{F}$; thermocouples used with the indicator-controller equipment were calibrated in boiling water at 212°F.

b. Test Procedure

The specimens were weighed before and after exposure. The temperature, vacuum, and liquid-nitrogen level were monitored twice daily during the tests. At the conclusion of each test, the specimens were removed from the vacuum and from the radiant heaters, and their condition noted. The specimens, exposure data, and observations were used for further evaluation.

The temperature was controlled at 250°F throughout the tests. Temperatures did not rise above 250°F and did not fall below 244°F at any time during the test periods. The temperature reached an equilibrium value for each group of three specimens after 1.5 hr of exposure and remained at that value throughout the test period.

The vacuum pressure reached 5×10^{-6} Torr in less than 16 hr of exposure. With continued exposure, the vacuum pressure decreased until at the end of the 100-hr period the pressure was 7×10^{-7} Torr. At the end of the 1,000 hr period, the pressure was 2×10^{-6} Torr. After 5,550 hr, the pressure in the 6,000-hr test was 7×10^{-8} Torr.

c. Test Results

Weight loss and appearance of specimens after 100 hr of exposure are shown in Table IX. Similar data at the termination of 1,000- and 6,000-hr tests are shown in Tables X and XI, respectively.

Results of the mechanical-properties tests carried out after each exposure will be found in subsections IV.5 and IV.6.

d. Comments and Interpretation of Results

Short-term weight-loss determinations of adhesive bonding agents and other components of the composite materials that were performed in detail and at higher temperatures

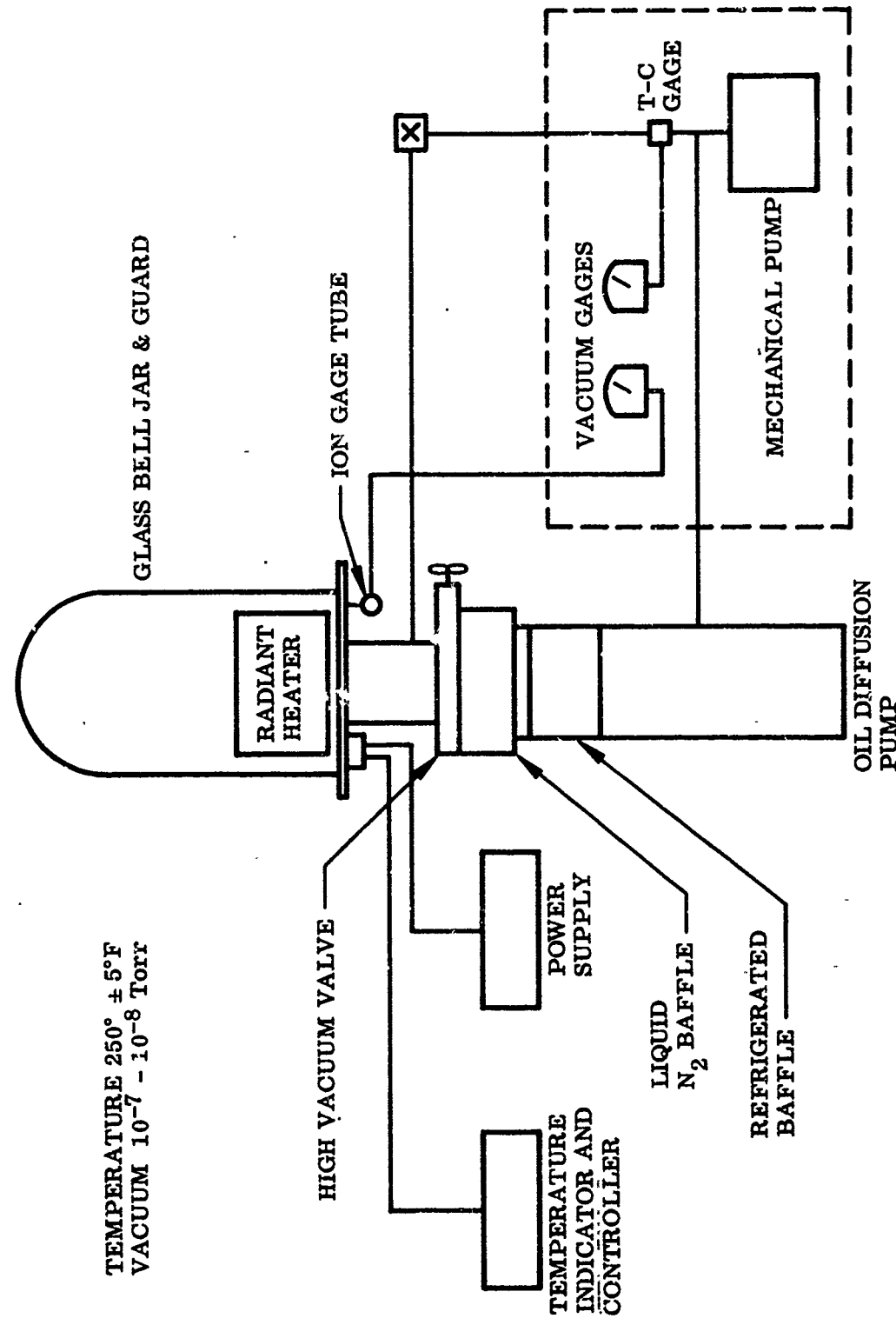


Figure 55 Thermal/ Vacuum Stability Apparatus



Figure 56 Thermal/Vacuum Environmental Stability Test Specimens



Figure 57 Iron-Constantan Thermocouple Attached to Specimen Group

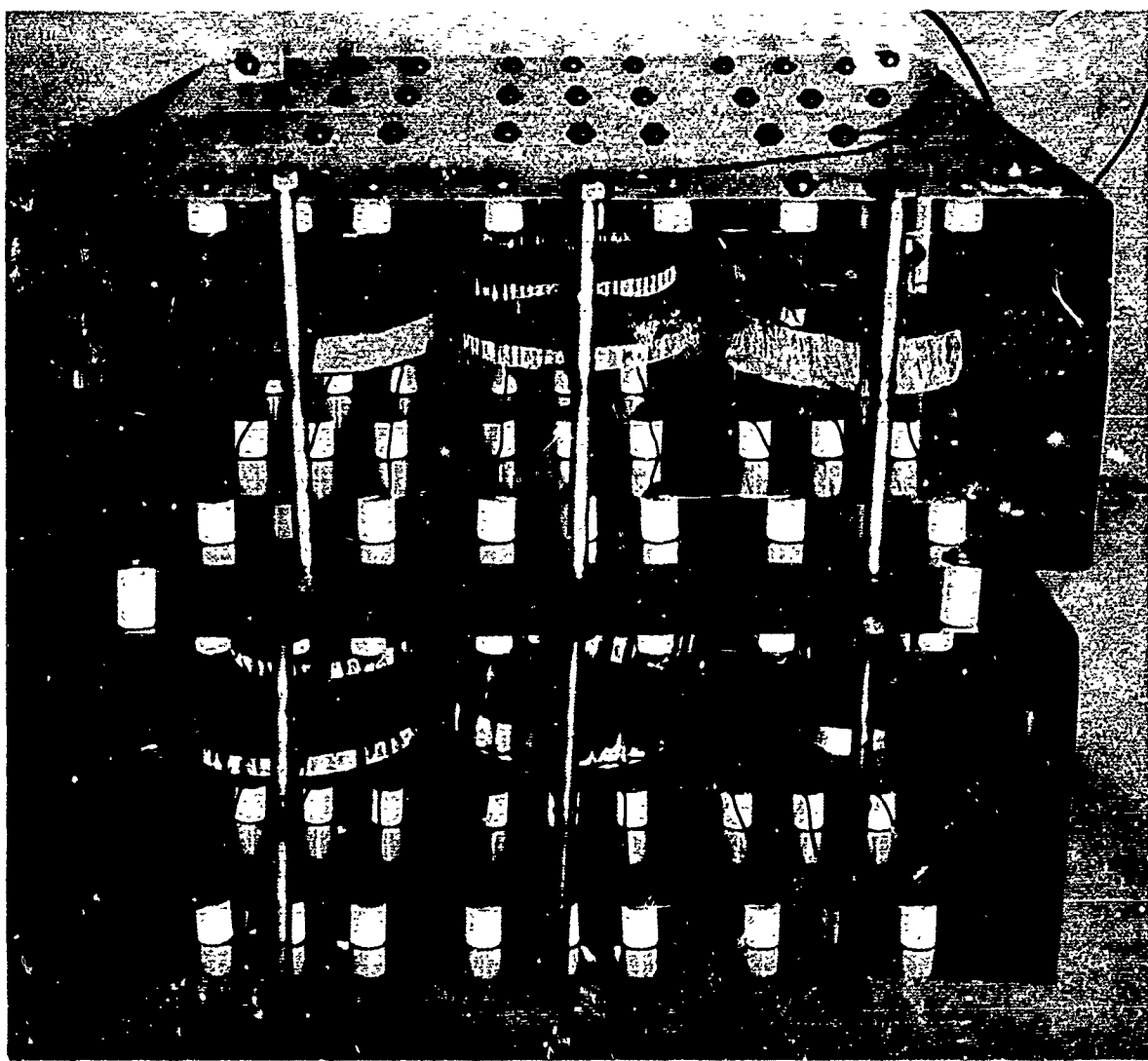


Figure 58 Radiant-Heating Assemblies for Thermal/Vacuum Environmental Stability Tests

Table IX . Thermal/Vacuum 100-Hour Test

Specimen designation	Weight before (g)	Weight after (g)	Weight loss (g)	Change (%)	Post-test appearance
AF-1	3.8228	3.7942	0.0286	0.75	Slight flow of bonding agent
AFN-1	3.7890	3.7582	0.0308	0.81	Same as AF-1
AFM-1	3.7475	3.7162	0.0313	0.835	Same as AF-1
BFN-1	7.6182	7.3710	0.2472	3.24	No change
BFM-1	9.6278	9.3366	0.2912	3.01	No change
BFB-1	7.7580	7.5024	0.2556	3.30	No change
CF-1	4.5874	4.5173	0.0701	1.53	One face turned brown
CFN-1	4.5562	4.4876	0.0686	1.51	Same as CF-1
CFM-1	4.5704	4.5005	0.0699	1.53	Same as CF-1
EF-1	8.6000	8.5450	0.0550	0.64	White spots on one face
EFN-1	8.9963	8.9388	0.0575	0.64	No change
EFM-1	8.6462	8.5914	0.0548	0.635	No change
GF-1	4.3653	4.3638	0.0015	0.03	Bonding between sheet and top of conical section
GFM-1	4.8585	4.8565	0.0020	0.04	75% separated before start of test; specimen fell apart from handling after test
GFN-1	4.2269	4.2250	0.0019	0.045	Same as GF-1 before test; no change during test
LF-1	10.6769	9.6375	1.0394	9.75	Bonding between sheet and top of conical section 100% separated before test; no change during test
LFM-1	7.4785	6.9818	0.4967	6.65	Aluminized mylar face blistered and specimen warped
LFN-1	9.6240	8.6783	0.9457	9.83	Aluminized mylar face blistered slightly
					Same as LF-1

Table X . Thermal/vacuum 1,000-Hour Test

Specimen designation	Weight before (g)	Weight after (g)	Weight loss (g)	Weight Change (%)	Post-test appearance
AF-3	3.7940	3.7451	0.0489	1.29	Slight flow of bonding agent
AFM-3	4.000	3.9261	0.0739	1.84	Same as AF-3
AFN-3	3.9278	3.8703	0.0575	1.46	Same as AF-3
BFN-3	8.1627	7.8823	0.2804	3.43	Smooth face pulled away from main body in one spot; slight discoloration
BFM-3	9.0251	8.7235	0.2916	3.23	Smooth face slightly discolored
BFB-3	8.6695	8.3245	0.3450	3.98	Same as BFM-3
CF-3	4.4452	4.3825	0.0627	1.41	Honeycomb impression visible on one face
CFM-3	4.4872	4.4154	0.0718	1.60	Same as CF-3
CFN-3	4.5307	4.4551	0.0756	1.67	Same as CF-3
EF-3	8.7416	8.6651	0.0765	0.875	Small dents on one face; hairline cracks and minor discoloration other face; bonding agent shows slight flow and evaporation causing discolored deposits on interior of honeycomb
EFM-3	9.730	9.5966	0.1334	1.37	
EFN-3	8.9018	8.8244	0.0774	0.87	
GF-3	4.4500	4.4472	0.0028	0.06	Bonding between sheet and top of conical section completely separated before test; polished face shows minor discoloration
GFM-3	4.7786	4.7750	0.0036	0.07	Same as GF-3 except 25% separation before test
GFN-3	4.0036	3.9993	0.0043	0.107	Same as GF-3 except 50% separation before test

Table XI. Thermal/Vacuum 6,000-Hour Test

Specimen designation	Weight before (g)	Weight after (g)	Weight loss (g)	Change (%)	Post-test appearance
AF-2	3.7978	3.7302	0.0676	1.78	Slight flow of bonding agent
AFM-2	3.8238	3.7457	0.0781	2.04	Same as AF-2
AFN-2	3.9290	3.8482	0.0808	2.06	Same as AF-2
BFB-2	10.1970	9.8276	0.3694	3.62	No change
BFM-2	8.5144	8.1630	0.3514	4.13	No change
BFN-2	8.4190	8.1031	0.3159	3.75	No change
CF-2	4.6602	4.5835	0.0767	1.65	No change
CFM-2	4.5631	4.4926	0.0705	1.55	No change
CFN-2	4.6365	4.5540	0.0825	1.78	No change
EF-2	8.8536	8.7724	0.0812	0.91	No change
EFM-2	9.0063	8.9008	0.1055	1.17	No change
EFN-2	8.7538	8.6678	0.0960	1.10	No change
GF-2	4.1453	4.1395	0.0058	0.14	Bonding between sheet and top of conical section 50% separated before test; no change during test
GFM-2	4.3648	4.3592	0.0056	0.13	No change
GFN-2	4.2477	4.2435	0.0042	0.10	Same as GF-2
LF-2	16.1561	14.1473	2.0088	12.4	Aluminized mylar face blistered; specimen badly warped
LFM-2	8.8530	7.8731	0.9799	11.1	Aluminized mylar face blistered
LFN-2	8.2303	7.3482	0.8821	10.7	Same as LFM-2

were discussed in the previous subsection. These results are more meaningful than the weight losses determined in the thermal/vacuum environmental stability tests.

Most samples of Material G had separation of one face from the spacer upon delivery to the laboratory. These separations were complete or partial and resulted from handling in specimen marking and preparation.

The average weight loss of the Material A specimens was comparatively small in the 100-hr exposure (0.30 percent). However, weight loss increased sharply with exposure time; it was 91 percent greater in the 1,000-hr exposure than in the 100-hr exposure and 145 percent greater in the 6,000-hr exposure than in the 100-hr exposure. Moreover, a slight flow of the bonding agent was noted in the specimens after termination of all tests.

Samples of Material B lost a significant fraction of their total weight in each of the tests. Weight loss was 12 percent greater in the 1,000-hr exposure and 20 percent greater in the 1,000-hr exposure than in the 100-hr exposure. In the 1,000-hr test, the smooth face of each of the three specimens separated from the rest of the structure in one spot and was slightly discolored. No observable change occurred in any of the specimens in either the 100-hr or the 1,000-hr test.

Although the Material C samples lost more weight in the 100-hr exposure than any of the other honeycomb structures, this material was quite stable in the longer exposures. The increase in weight loss from the 100-hr to the 1,000-hr test was only 3 percent and from the 100-hr to the 6,000-hr test, only 9 percent. In the 100-hr test, one face of the samples was discolored brown. In the 1,000-hr test, an impression of the honeycomb structure was visible on one face. No observable change occurred, however, during the 6,000-hr exposure.

Material E lost less weight in all three exposures than any of the other honeycomb structures. The increase in weight loss from the 100-hr to the 1,000-hr test was quite large (62 percent), but the weight change in the 1,000-hr and 6,000-hr exposures was practically the same (1.04 and 1.06 percent, respectively). Although in the 1,000-hr exposure small dents on one face and hairline cracks were observed on all three samples, no observable change occurred during the 6,000-hr exposure.

Material G proved to be quite stable in the thermal/vacuum environment if weight loss is taken as the criterion. The average loss after the 6,000-hr exposure was only 0.12 percent. This, however, was three times the average loss in the 100-hr test and 50 percent greater than the loss in the 1,000-hr test.

Material L lost a greater fraction of its weight than did any other material tested. The average weight loss was 8.77 percent after the 100-hr test and 11.4 percent after the 6,000-hr exposure. Because it was decided to eliminate Material L from the testing program prior to the start of the 1,000-hr test, no data from this test are available for this material.

7. THERMAL CYCLING

Temperature-cycling tests were performed on the candidate materials evaluated in this program. The principal objective of these tests was to determine the effects of multiple thermal cycling over a predetermined temperature range on the mechanical, optical, and structural properties of the materials, and also to determine the effects of thermal cycling on the candidate material surfaces.

Each candidate material, with the exception of Materials G and H, was scheduled to be thermally cycled 100, 1,000, and 6,000 times (6,000 cycles being equivalent to 14 months in orbit). For the reasons stated in subsection II. 7. b, however, the 6,000-cycle test was not performed on Material E, and the same test was terminated after 3,000 cycles in the case of Material F.

The reason for omitting Materials G and H from this phase of the test program was that their behavior under thermal cycling would not be expected to differ significantly from that of Materials J and K, respectively. Material G has a reflective surface of bare silver, whereas Material J has a surface of bare aluminum with sublayers of chrome and silicon oxide; Material H has a reflective surface of silver with a silicon oxide coating, whereas Material K has a surface of similarly coated aluminum with sublayers of chrome and silicon oxide. All four materials have the same basic structure and were produced by the same vendor. It was therefore concluded that Material G would survive thermal cycling as well as Material J, and that Material H would behave as well as Material K.

a. Description of Apparatus

Nine separate vacuum chambers were used for the thermal-cycling tests. Each chamber consisted of the following:

- Liquid-nitrogen temperature cold wall
- 500-W tungsten lamp radiant energy source
- View window
- Instrumentation for control, thermometry, and measurement of reflector surface distortion

The apparatus is shown in Figure 59. Each specimen was instrumented to record front- and back-surface temperatures. The radiant energy source was controlled by the front- and back-surface temperatures. The reflective surface distortions were monitored by viewing the mirror image of a diffusely illuminated grid.

b. Test Procedure

Each thermal cycle consisted of a short heating period and a longer cooling period. During the heating period the tungsten energy source was on until a maximum reflector-surface temperature of 250° F was reached (approximately 4 min). The specimen was then allowed to cool for 36 min, the maximum time in the shadow of the earth for a noon-orbit, 90-min period. The cycle was then repeated. Photographs were made periodically of the specimen image during heating and cooling. Vacuum pressure varied from chamber to chamber, the extremes being 10^{-6} and 5×10^{-5} .

The test plan provided for three exposures of each candidate material, the first for 100, the second for 1,000, and the third for 6,000 cycles. Upon completion of each test, the specimen was examined visually for permanent structural and reflective surface damage, and reflectance was measured by means of a Cary Model 14 spectrophotometer. (See subsection III. 2.) Core compression, thermal expansion, or facing separation tests were then conducted, as appropriate, on the exposed specimens.

Figure 59 Thermal Cycling Apparatus



Test failures occurred on several occasions because of either controller malfunctions or loss of vacuum. As a rule, such tests were rerun with new samples, but this procedure was not followed in the case of the 6,000-cycle exposure of Material E. The initial 6,000-cycle test was terminated after 4,292 cycles when overheating occurred by reason of a controller malfunction. To have initiated a replacement test would have delayed the completion of the test program by several months; therefore, because Material E differs from Material D only in the epoxy used for the leveling layer, the 6,000-cycle test was omitted for Material E. A departure from the test plan occurred also in the case of Material F. Failures were experienced in both the initial 6,000-cycle test and the replacement test. A third 6,000-cycle test was commenced, but it was terminated after 3,000 cycles. This was in the interest of expeditious completion of the test program, and it appeared justified because (1) none of the materials that had completed the full 6,000 cycles had shown appreciable degradation during the final 3,000 cycles and (2) the reflective surface of Material F had proved to be much inferior in the ASTEC environment to those of Materials D and E, which were supplied by the same vendor. (See Section III.)

c. Test Results

Results of thermal cycling tests on the subject materials, accompanied by photographs, are presented in Tables XII through XX. Graphs showing a typical temperature cycle for each sample and photos of selected samples are shown in Figures 60 through 77.

Results of the mechanical-properties tests carried out after each exposure will be found in subsections IV.5 and IV.6. See subsection II.3 for the thermal expansion measurements made on several of the materials (B and J-K).

d. Comments and Interpretation of Results

The reflective surfaces of Materials L and B were seriously distorted early in the tests. Material L was deleted from further tests by direction of AFAPL because of the separation of the aluminized mylar from the flexible epoxy layer.

In view of the thermal expansion data for Material B, which showed that the pink phenolic foam contracted while the electroformed nickel expanded at elevated temperature, the separation of the surface from the structure was not unexpected.

At the other extreme, Materials J and K showed no distortion with thermal cycling. The aluminum honeycomb samples all displayed distortion or show-through at the low temperatures and returned to approximately the original condition at elevated temperatures.

Reflectance of specimens after exposure was the same for all materials except B and L. No reflectance measurements were made on these materials, the surfaces being judged not suitable for further testing.

Table XII. Thermal Cycling Results - Material A

Specimen	Duration of test (cycles)	Pre-test condition	In situ condition		Post-test condition	Reflectance after exposure
			Cycle	Condition		
AGN-1	100	Surfaces flat (see Figure 61a)	0-125	No change noted (see Figure 61b)	No change noted	No change
AGM-1	1,000	Front surface flat; no honey-comb structure shows through (see Figure 61c)	0-4	No change noted	No change noted	No change
			67	Surface appears wavy when cool		
			68-1,007	No further change noted (see Figure 61d)		
AGM-2	6,000	Front surface flat; no honey-comb structure shows through	0-6,002	Surface appears wavy when cool, flat when heated (see Figure 61e)	No change noted	No change

Table XIII. Thermal Cycling Results - Material B

Specimen	Duration of test (cycles)	Pre-test condition	In situ condition		Post-test condition	Reflectance after exposure
			Cycle	Condition		
BGM-1	100	Sample flat and smooth (see Figure 63a)	1	Large blisters appeared on cooling cycle at 30°F and below (see Figure 63b)	Blister remained on surface of sample	Judged not suitable for testing
			2-35	Blister increased in size		
			36-106	No further changes noted (see Figures 63c and 63d)		
BGM-2	1,000	Sample flat and smooth	1	Large blister appeared upon cooling (see Figure 63e)	After test, two large and one small blister were noted on back surface; front surfaced warped in many places	Judged not suitable for testing
			2-327	No further changes, except sample appears to be more distorted		
			328-1,042	No further changes noted (see Figure 63f)		
BGM-3	6,000	Sample flat and smooth	0-6,004	Surface extremely wavy in appearance when cold, relatively flat when hot (see Figures 63g and 63h)	Front surface very wavy	Judged not suitable for testing

Table XIV . Thermal Cycling Results - Material C

Specimen	Duration of test (cycles)	Pre-test condition	In situ condition		Post-test condition	Reflectance after exposure
			Cycle	Condition		
CG-2	100	See Fig- ure 65a	0-104	No change noted (see Figures 65b and 65c)	No change noted	No change
CGN-1	1,000	Front sur- face some- what wavy; reflecting surface has striations & tiny blisters over about 50% of the surface	0-1,008	No change noted (see Figure 65d)	Visible blis- ters (3/16-in. diam.) on front surface	No change
CGM-3	6,000	Front sur- face some- what wavy with many tiny dimples	0-6,000	No change noted (see Figures 65e and 65f)	No change noted	No change

Table XV. Thermal Cycling Results - Material D

Specimen	Duration of test (cycles)	Pre-test condition	In situ condition		Post-test condition	Reflectance after exposure
			Cycle	Condition		
DGM-1	100	Very good reflecting surface on front face; no apparent imperfections on either face (see Figure 67a)	0-100	No change noted (see Figure 67b)	Very fine cracks noted over entire front face of sample	No change
DGN-1	1,000	Very good surface	0-138	Craze marks noted over entire surface	Very fine cracks noted over entire surface; aluminum reflective coating peeled at several points	No change (where surface intact)
			166	Peeling at several points on front surface, max. 1/4-in. dia.		
			1,000	No further change noted		
DGN-3	6,000	Surface smooth	0-6,000	Craze marks noted over entire surface (not evident in Figures 67c and 67d)	Very fine cracks noted over entire surface	No change

Table XVI. Thermal Cycling Results - Material E

Specimen	Duration of test (cycles)	Pre-test condition	In situ condition		Post-test condition	Reflectance after exposure
			Cycle	Condition		
EGM-1	100	Front surface smooth except for slight convexity at edges (see Figure 69a)	0-100	No changes noted (see Figure 69b)	Front surface unchanged	No change
EGN-1	1,000	Front surface smooth	0-885	No change noted	-	Not tested
			895	Test failure - sample overheated		
EGN-3	1,000	Front surface smooth	0-1,000	Hairline defects covered front surface	Hairline cracks in coating; larger but less frequent than those in Material D	No change
EGM-2	6,000	Front surface smooth except for 1/8-in. dimple near center of surface and 1/16-in. dimple off center	0-111	No change noted	(Test not rerun)	Not tested
			147	Three small-hairline defects appeared on front surface		
			148-356	Hairline defects covered entire front surface		
			357-4, 292	No change noted (see Figure 69c)		
			4, 292	Test failure - sample overheated		

Table XVII. Thermal Cycling Results - Material F

Specimen	Duration of test (cycles)	Pre-test condition	In situ condition		Post-test Condition	Reflectance after exposure
			Cycle	Condition		
FGM-1	100	Front face slightly concave on one side; surface has frosty appearance (see Figure 71a)	0-8	No change noted	Frosty appearance of front surface more pronounced. Craze marks clearly visible. Honeycomb pattern clearly shows through on reverse side.	No change
			43	Network of craze marks noted on front surface (see Figure 71b)		
			96-100	Craze marks more distinct		
FGN-2	6,000	Front surface has frosty appearance (see Figure 71c)	22	Hairline craze defects show on front surface; surface appears frosty	See Figure 71e	Not tested
			23-882	No further change noted (see Figure 71d)		
			883	Edge raised slightly at three spots		
			1,137	Noticeable blue tinge to front surface noted; hairline craze defects appear green		
			1,246	Test failure (vacuum lost)		

Table XVII --- Continued

Specimen	Scheduled duration of test (cycles)	Pre-test condition	In situ condition		Post-test condition	Reflectance after exposure
			Cycle	Condition		
FG-1	1,000	Front surface frosty blue in appearance	0-64	Hairline craze marks noted	Hairline crazes in reflective coating	No change
			65-1,000	No further change noted		
FG-2	6,000	Front surface frosty blue in appearance; one small dimple noted in upper left corner of surface	0-27	Sample appears badly clouded	—	Not tested
			28-63	Several hairline craze marks appeared on sample		
			64-2,086	No further change noted		
			2,087	Test failure — sample remained at test temperature for 9 hr as result of controller malfunction		
FGN-1	6,000 (test terminated at 3,000 cycles)	Front surface frosty blue in appearance	0-76	Craze marks noted	Hairline crazes in reflective coating	No change
			77-3,000	No further change noted (see Figure 71f)		

Table XVIII. Thermal Cycling Results - Material J

Specimen	Duration of test (cycles)	Pre-test condition	In situ condition		Post-test condition	Reflectance after exposure
			Cycle	Condition		
JGM-1	100	Sample surfaces flat (see Figure 73a)	0-118	No change noted (see Figures 73b and 73c)	No change noted	No change
JGN-2	1,000	Some dirt flecks and patches on reflective surface	0-1,031	No change noted	No change noted	No change
JG-1	6,000	Sample surfaces flat	0-6,000	No change noted (see Figure 73d)	No change noted	No change

Table XIX. Thermal Cycling Results - Material K

Specimen	Duration of test (cycles)	Pre-test condition	In situ condition		Post-test condition	Reflectance after exposure
			Cycle	Condition		
KG-1	100	Sample surfaces flat (see Figure 75a)	0-100	No change noted (see Figures 75c and 75d)	No change noted	No change
KGM-2	1,000	Sample surfaces flat (see Figure 75e)	0-998	No change noted (see Figure 75f)	Epoxy bonding green in some places, mainly on back surface bonding. No other change noted	No change
KGM-1	6,000	Sample surfaces flat	0-6,002	No change noted (see Figure 75b)	No change noted	No change

Table XX. Thermal Cycling Results - Material I

Specimen	Scheduled duration of test (cycles)	Pre-test condition	In situ condition		Post-test condition	Reflectance after exposure
			Cycle	Condition		
LGM-1	100	Sample convex on front face with several depressions and two small blisters (see Figure 77a)	1	One blister increased in size to 1-in. diam.		Judged not suitable for testing
			2-3	Wrinkling on front face noted		
			4-5	Degree of wrinkling and blistering increased (see Figure 77b)		
			6-100	No further changes noted (see Figure 77c)		
LGM-2	1,000	Sample appeared very slightly convex with very little or no imperfection on the front reflecting surface. When placed in vacuum, blisters developed on front surface (see Figure 77d)	1-1,000	No further change noted	Convex shape of front surface somewhat increased; blisters became dimples when sample was allowed to come to atmospheric pressure	Judged not suitable for testing
LGM-3	6,000 (test terminated at 575 cycles)	Front surface convex	1	Blister covering 75% of front surface observed during heating	Blister reached edge of face; blister no longer	Judged not suitable for testing
			2-64			
			65-575	No further change noted (see Figure 77e)		

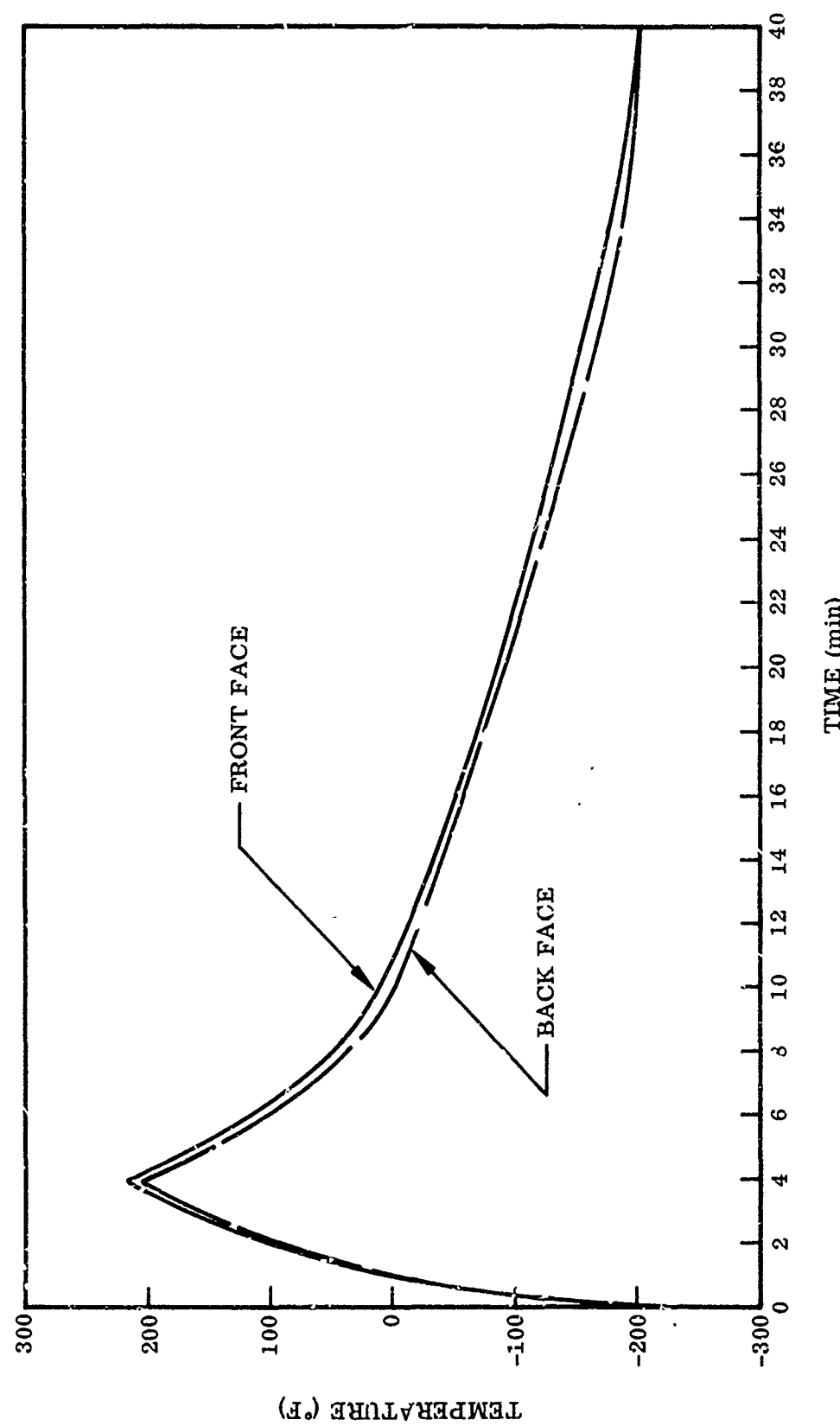
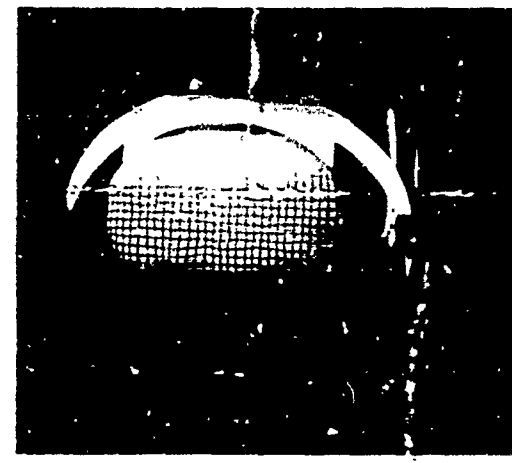


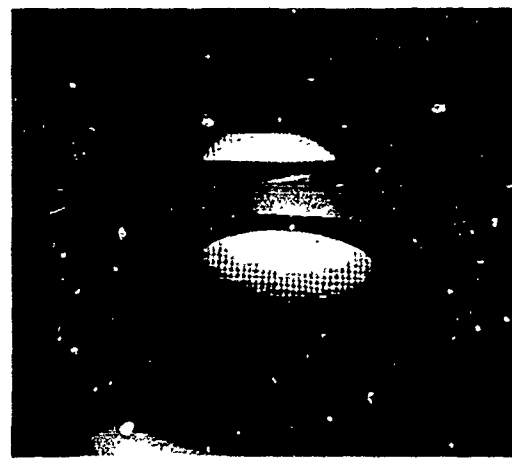
Figure 60 Temperature Histories of Front and Back Faces (One Cycle), Material A



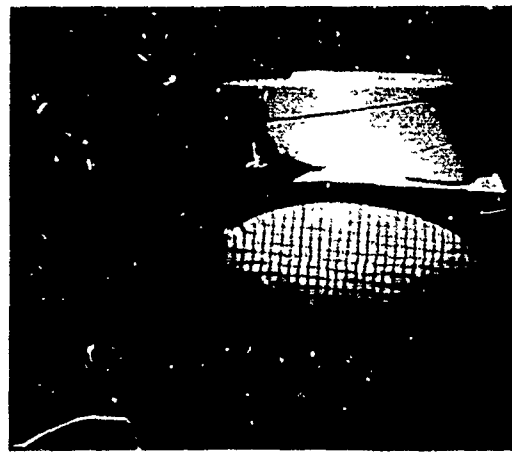
(a) Sample AGN-1, Pretest
Vacuum Condition



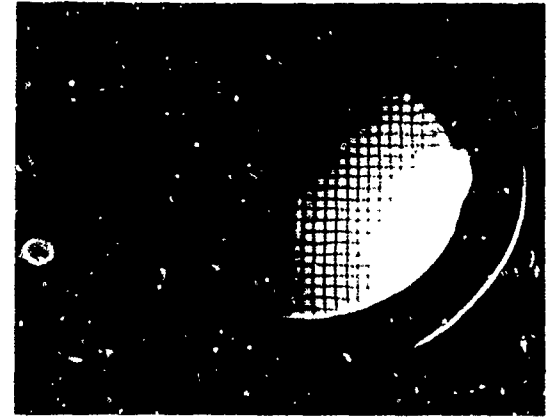
(b) Sample AGN-1, Cycle 125,
Room Temperature



(c) Sample AGM-1, Pretest
Condition



(d) Sample AGM-1, Cycle 6001,
Room Temperature



(e) Sample AGM-2,
Cycle 6001, 225° F

Figure 61 Thermal Cycling Samples, Material A

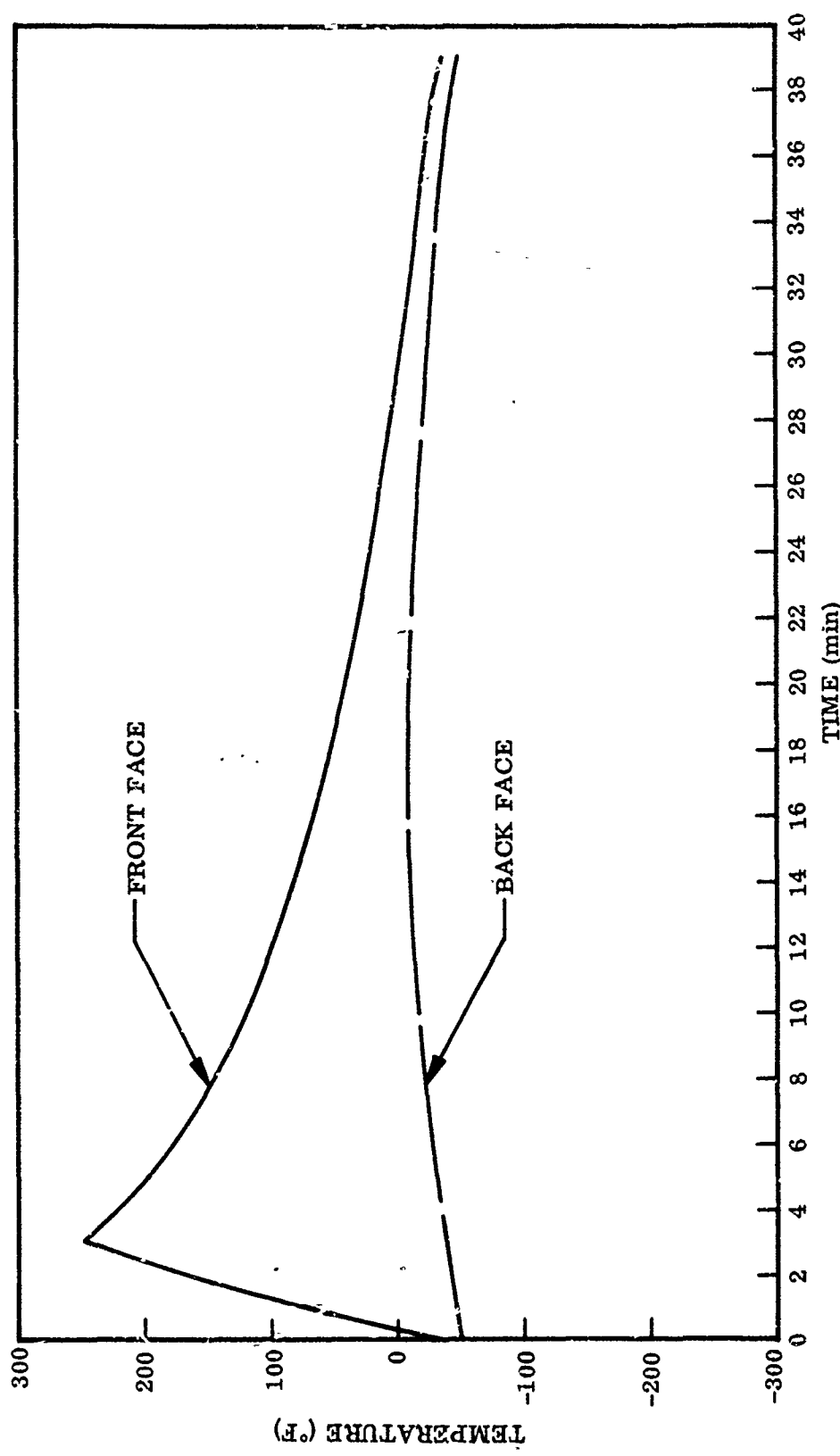


Figure 62 Temperature Histories of Front and Back Faces (One Cycle), Material B

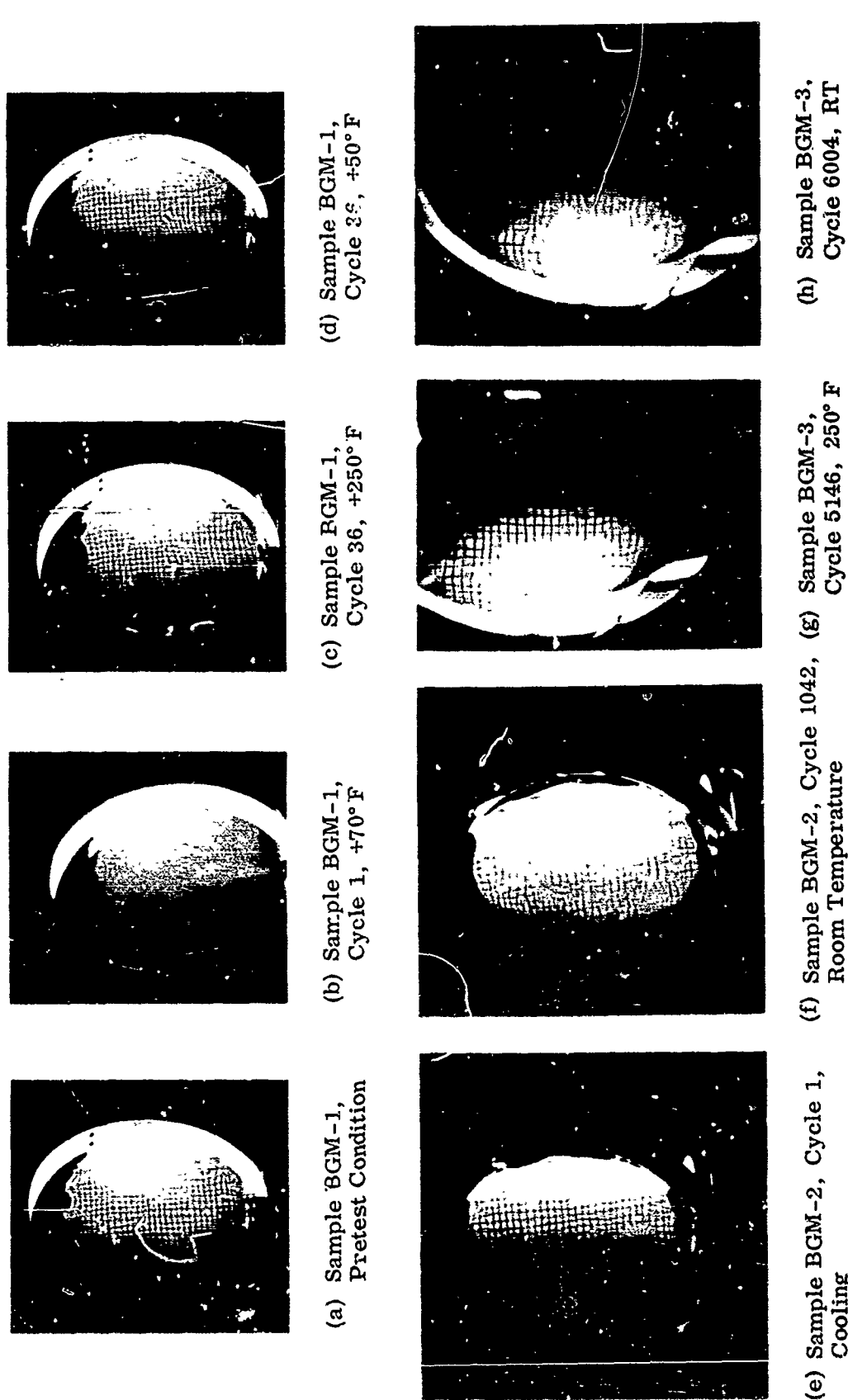


Figure 63 Thermal Cycling Samples, Material B

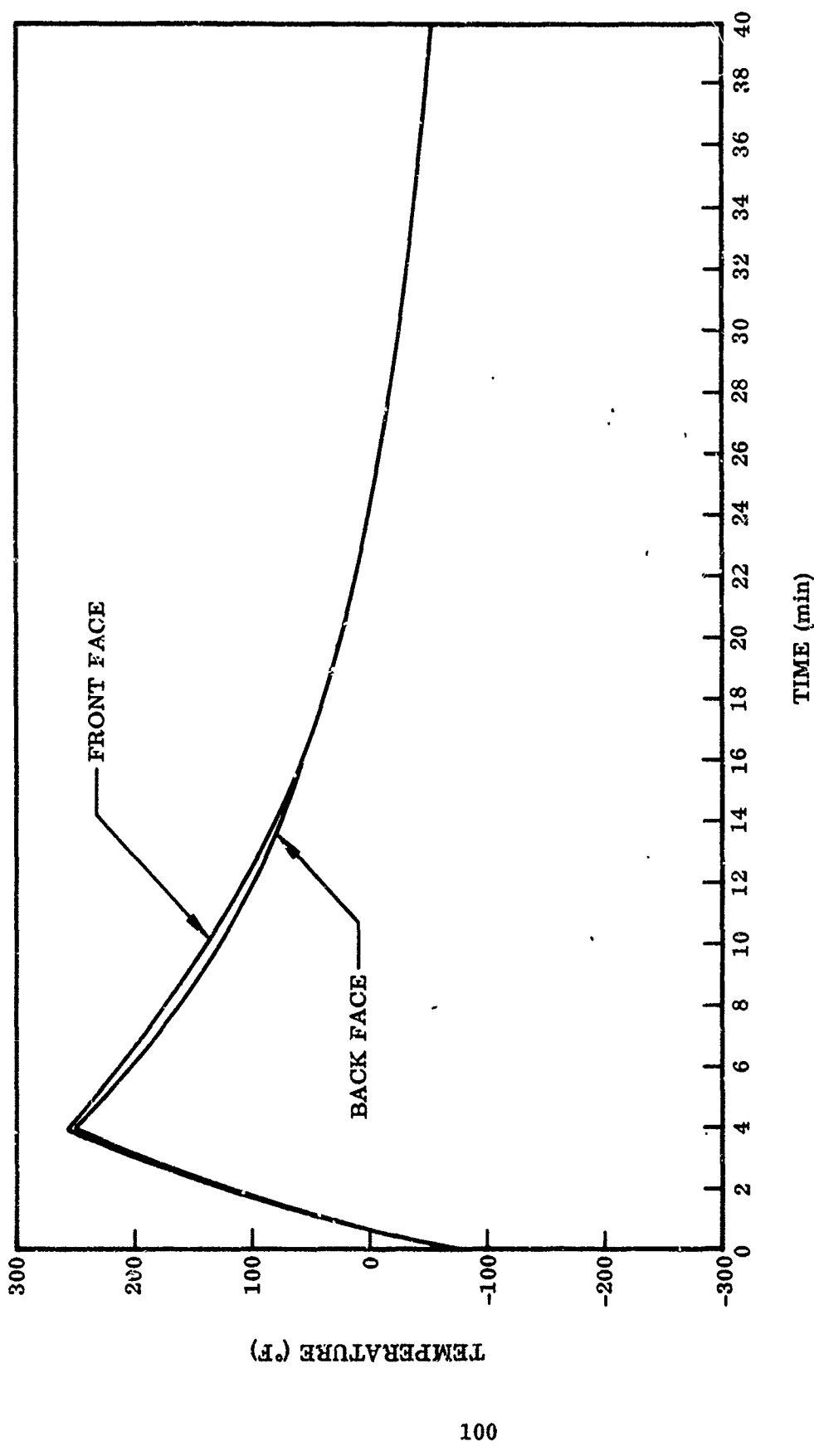
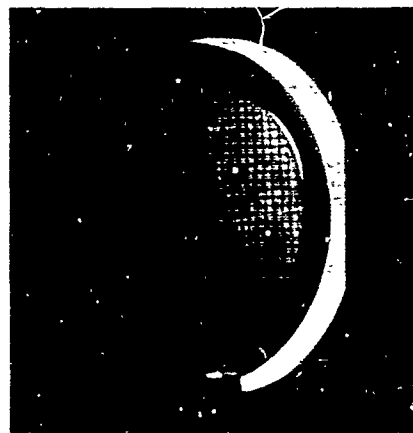
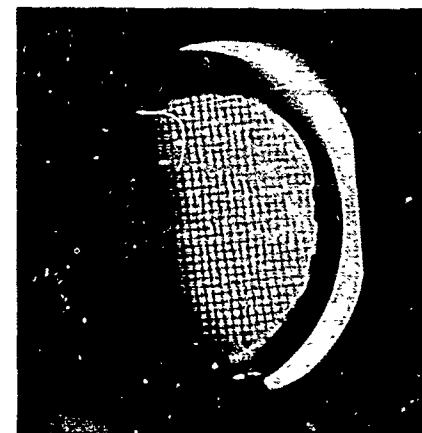


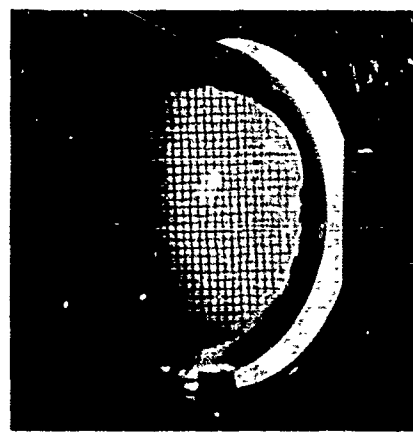
Figure 64 Temperature Histories of Front and Back Faces (Cre Cycle), Material C



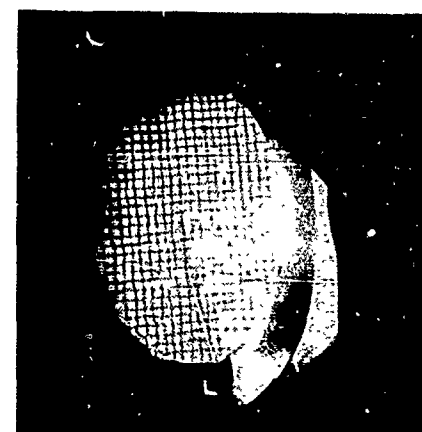
(a) Sample CG-2, Pretest Condition



(b) Sample CG-2, Cycle 104, Cold Temperature



(c) Sample CG-2, Cycle 104, Room Temperature



(d) Sample CGN-1, Cycle 1008, Low Temperature



(e) Sample CGM-3, Cycle 6000, 250° F



(f) Sample CGM-3, Cycle 6000, RT

Figure 65 Thermal Cycling Samples, Material C

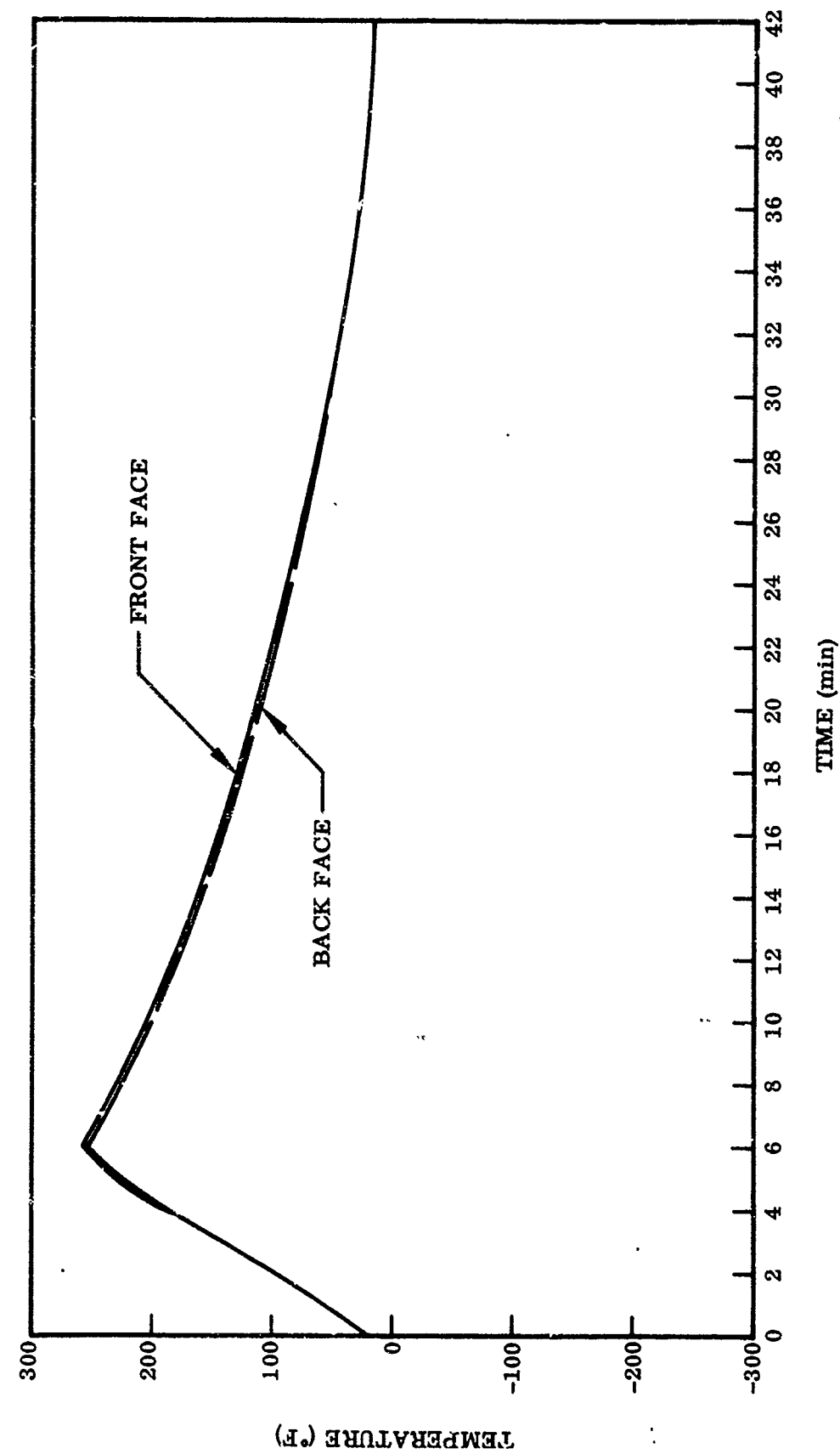
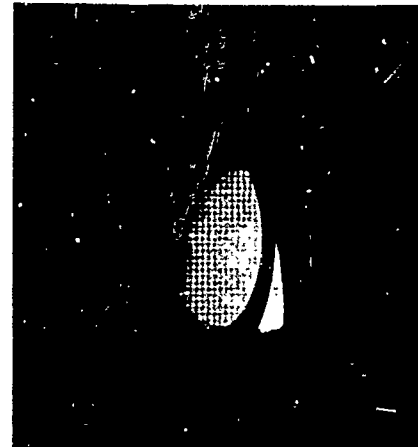


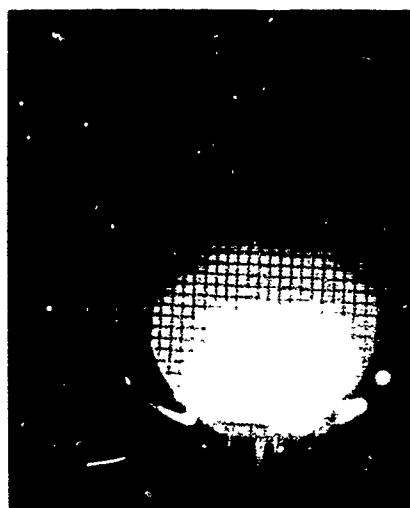
Figure 66 Temperature Histories of Front and Back Faces (One Cycle), Material D



(a) Sample DGM-1, Pretest Condition



(b) Sample DGM-1, Cycle 100, Room Temperature



(c) Sample DGN-3, Cycle 6011, 250° F



(d) Sample DGN-3, Cycle 6011, RT

Figure 67 Thermal Cycling Samples, Material D

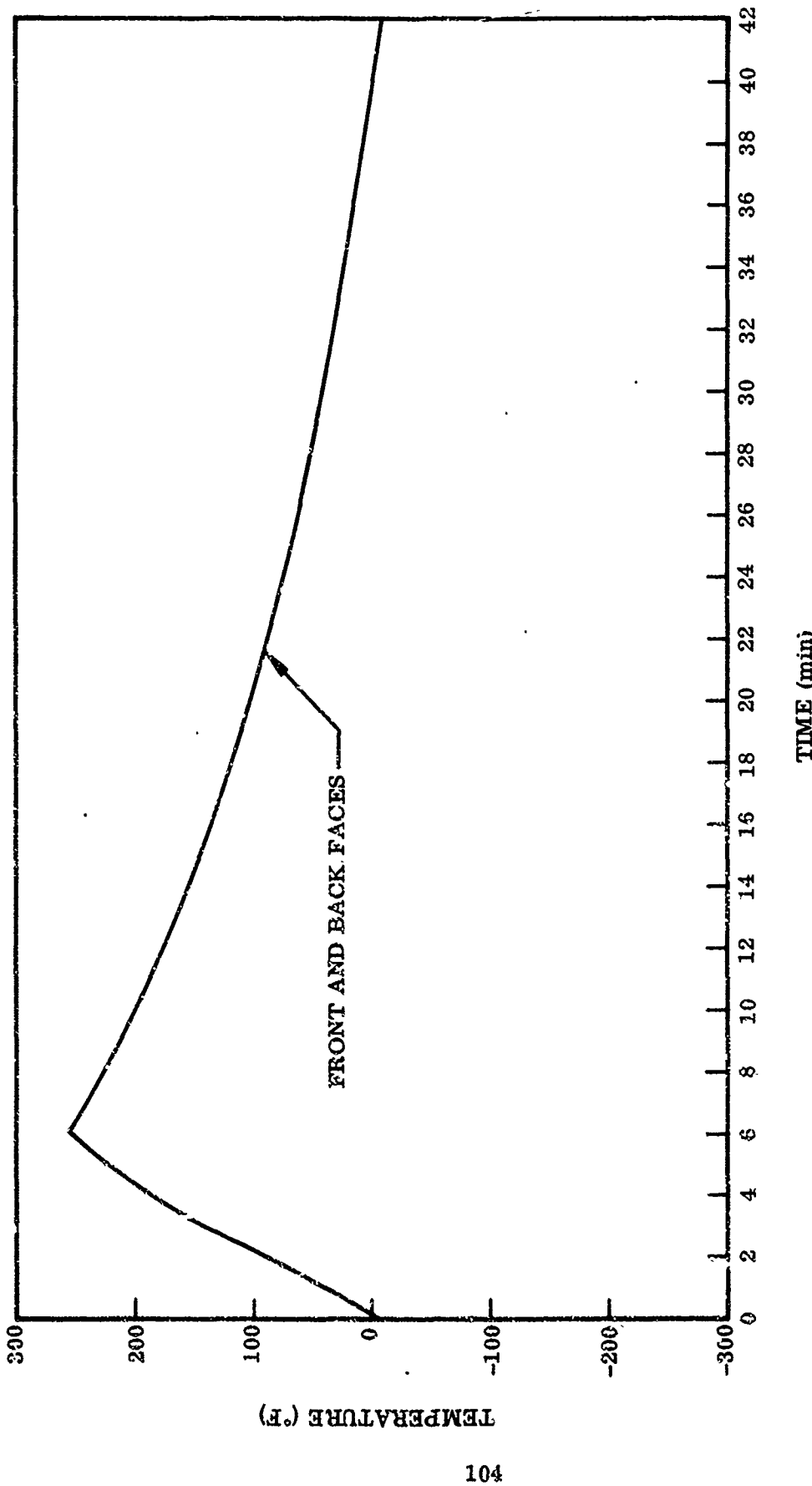
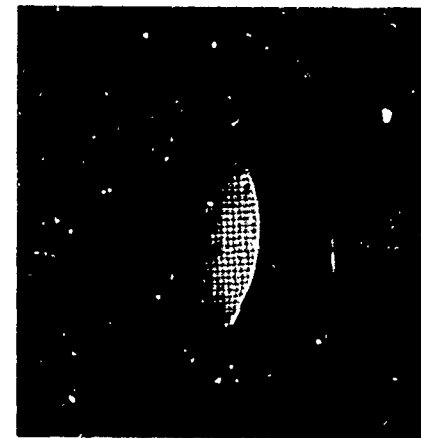


Figure 68 Temperature Histories of Front and Back Faces (One Cycle), Material E



(a) Sample EGM-1, Pretest Condition



(b) Sample EGM-1, Cycle 100, Room Temperature



(c) Sample EGM-2, Cycle 4141, 250° F

Figure 69 Thermal Cycling Samples, Material E

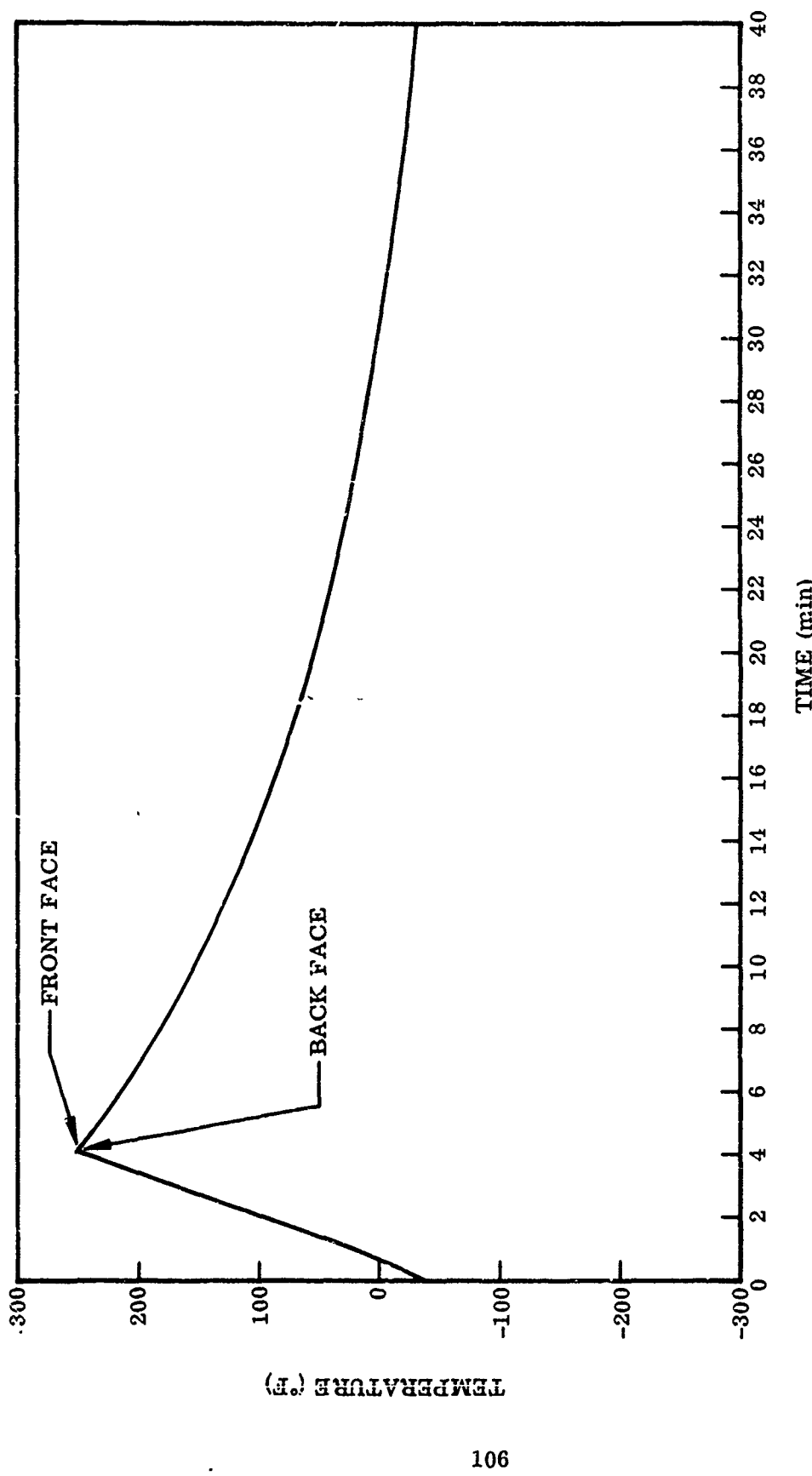
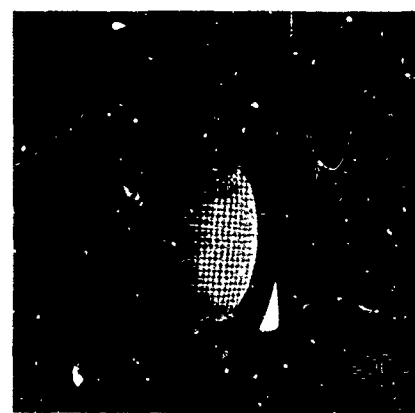


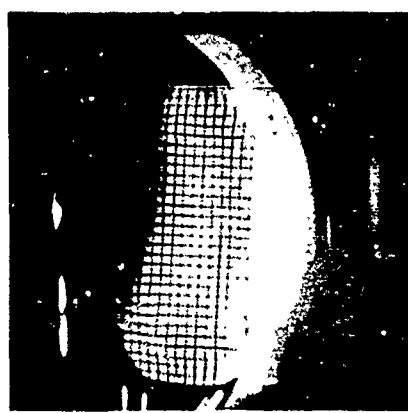
Figure 70 Temperature Histories of Front and Back Faces (One Cycle), Material F



(a) Sample FGM-1, Pretest Condition



(b) Sample FGM-1, Cycle 43



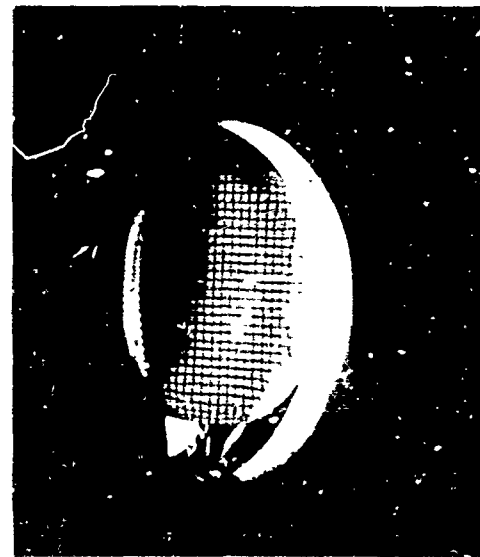
(c) Sample FGN-2, Pretest Vacuum Condition



(d) Sample FGN-2, Cycle 745,
+ 250°F



(e) Sample FGN-2, Post-Test
Showing Craze Defects



(f) Sample FGN-1, Cycle 3000, RT

Figure 71 Thermal Cycling Samples, Material F

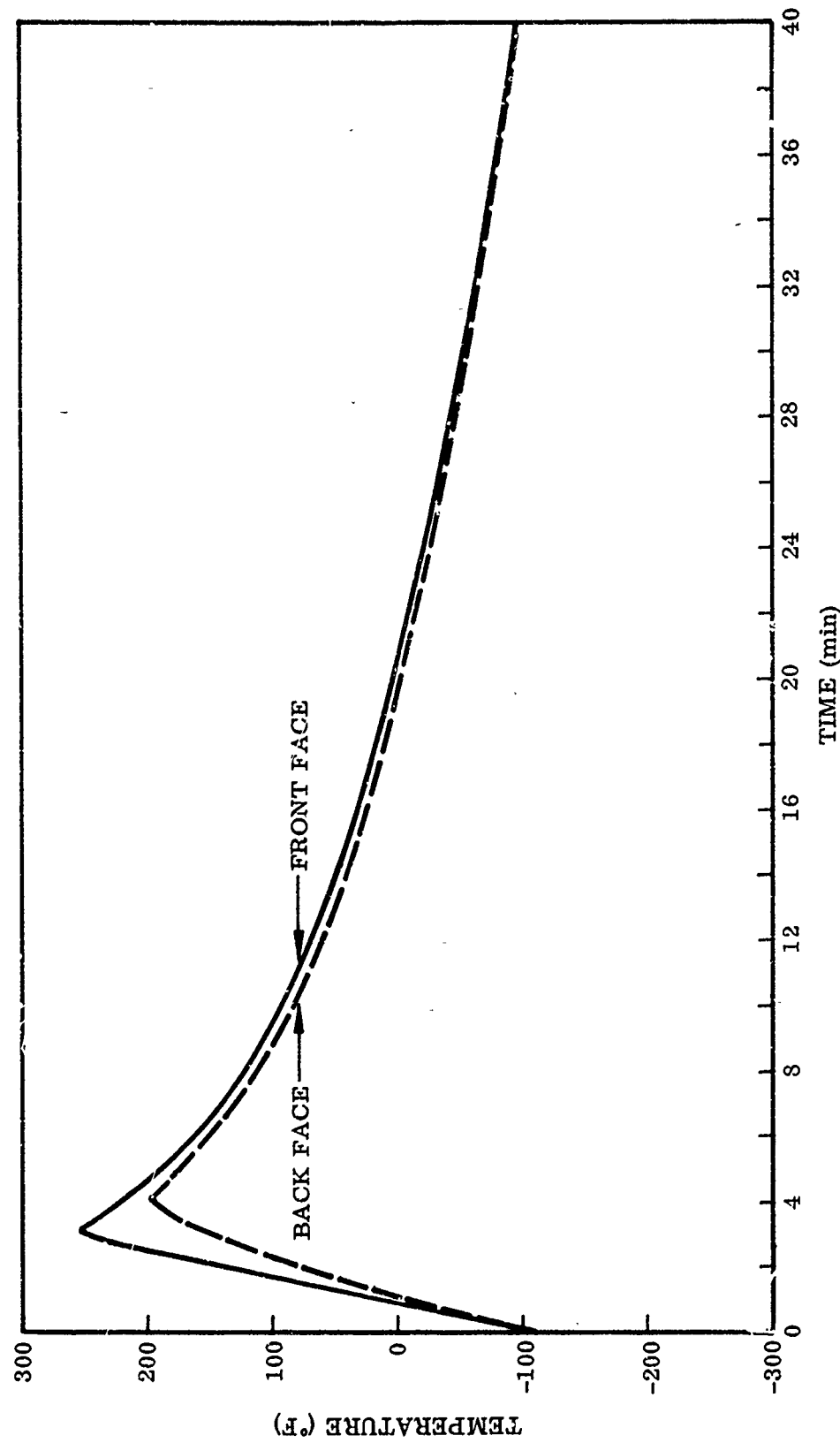
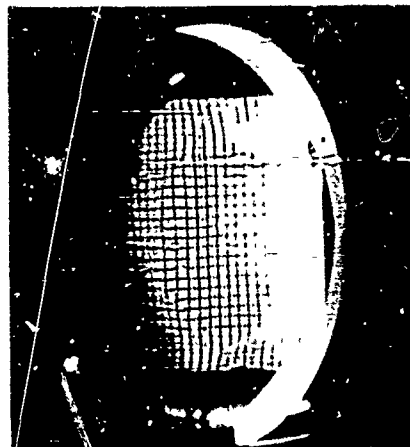
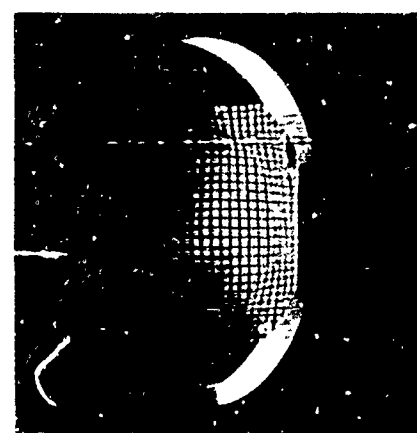


Figure 72 Temperature Histories of Front and Back Faces (One Cycle), Material J



(a) Sample JGM-1, Pretest Condition



(b) Sample JGM-1, Cycle 118, + 250°F



(c) Sample JGM-1, Cycle 118, - 70°F



(d) Sample JG-1, Cycle 6000, RT

Figure 73 Thermal Cycling Samples, Material J

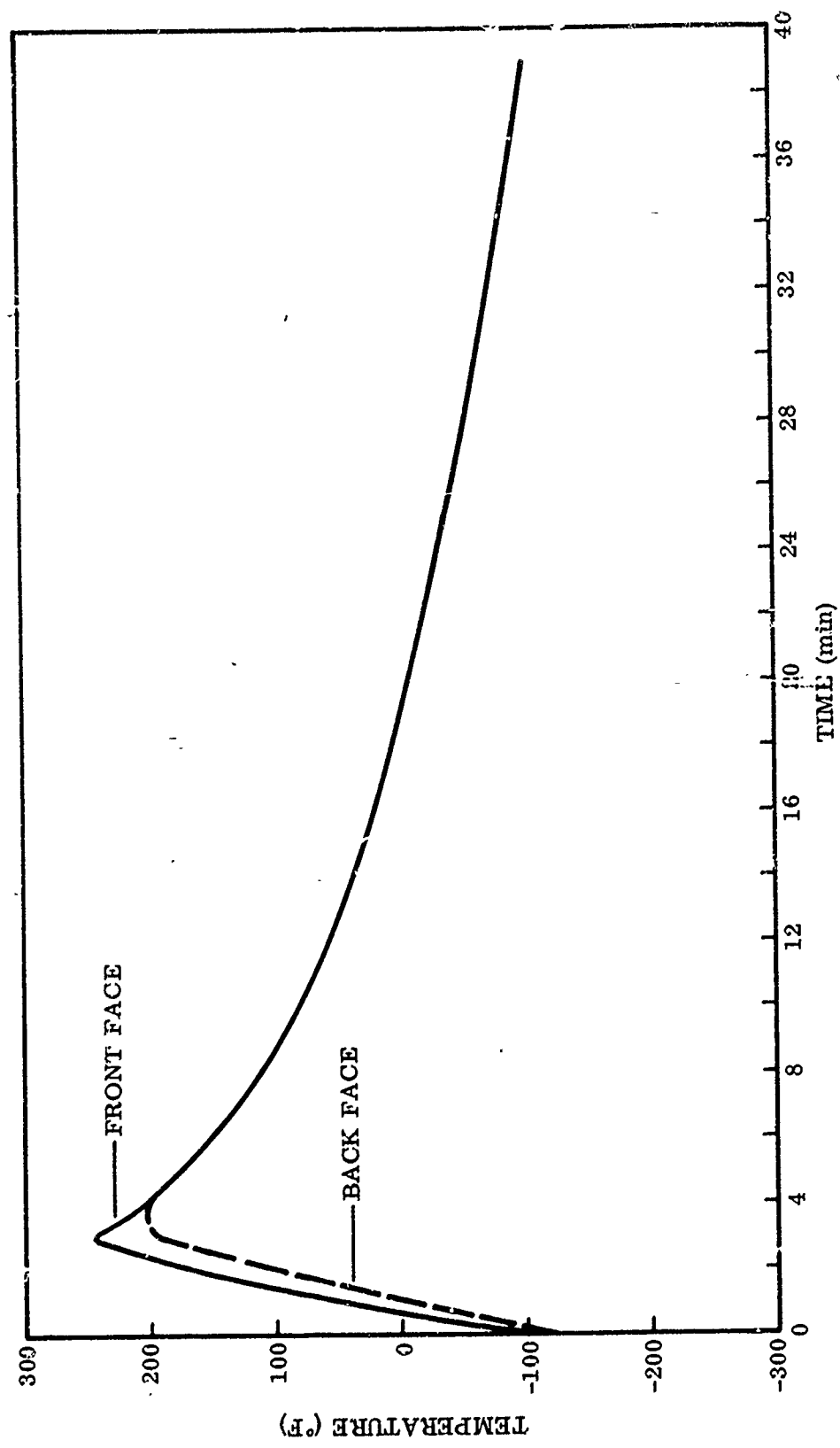
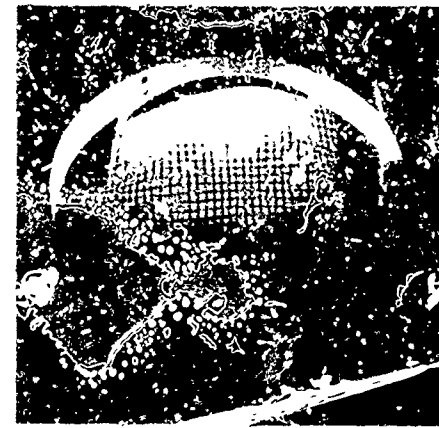
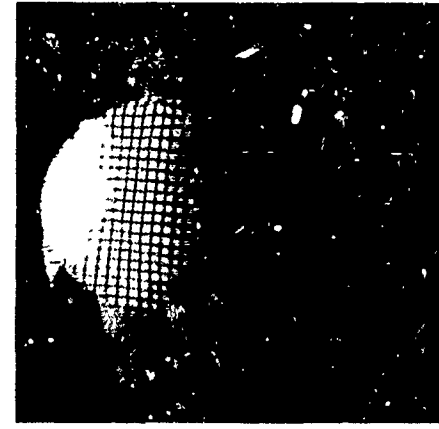


Figure 74 Temperature Histories of Front and Back Faces (in $^{\circ}$ F), Material K



(a) Sample KG-1, Pretest
Vacuum Condition



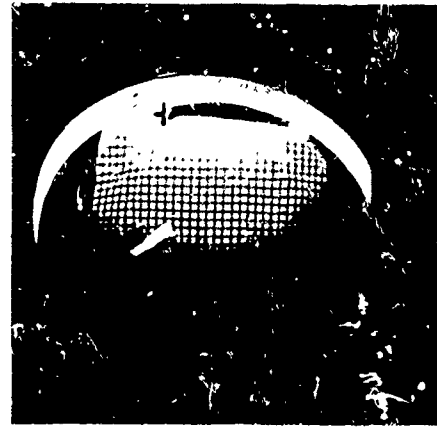
(b) Sample KGM-1,
Cycle 6002, RT



(d) Sample KG-1, Cycle 100,
Room Temperature



(c) Sample KG-1, Cycle 5,
+ 250°F



(e) Sample KGM-2, Pretest
Vacuum Condition



(f) Sample KGM-2, Cycle 1,000,
Room Temperature

Figure 75 Thermal Cycling Samples, Material K

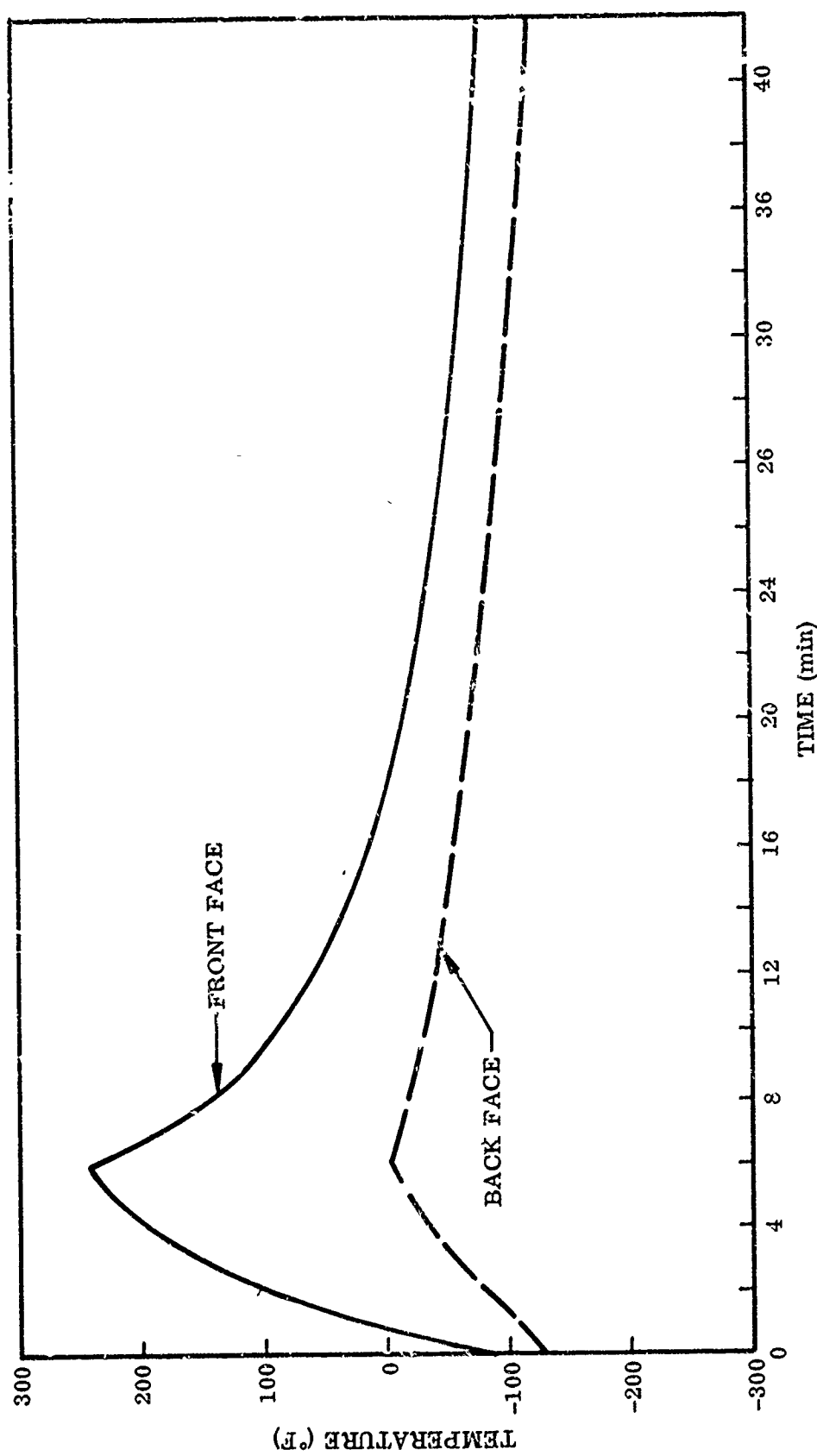
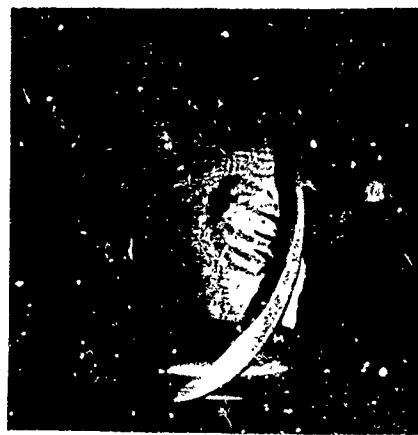


Figure 76 Temperature Histories of Front and Back Faces (One Cycle), Material L



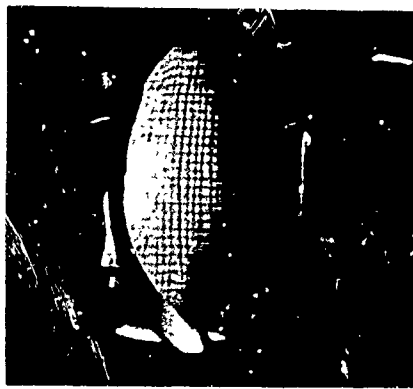
(a) Sample LGM-1, Pretest Vacuum Condition



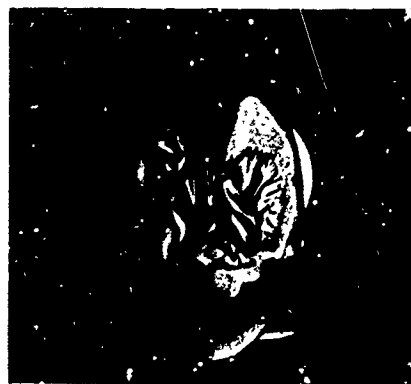
(b) Sample LGM-1, Cycle 5, Cooling



(c) Sample LGM-1, Cycle 100, Room Temperature



(d) Sample LGM-2, Pretest Condition



(e) Sample LGM-3, Post-Test Condition

Figure 77 Thermal Cycling Samples, Material L

Section III OPTICAL PROPERTIES

1. INTRODUCTION

An experimental program was conducted to determine the effects of near-ultraviolet radiation, low-energy electron irradiation, and both simultaneously on the solar reflectance of the candidate ASTEC reflector surfaces. The ultraviolet and combined exposures were conducted for periods representing up to 6 months in a 200- to 500-nm circular polar orbit. Data for electron irradiation were obtained for periods representing up to 1 year in orbit.

All tests were performed in vacuum and with samples maintained at both room temperature and +250° F. Spectral reflectance measurements were performed before and immediately after each exposure. The primary criterion for damage is change in solar reflectance, ρ_s . Room temperature emittance, ϵ , has not been observed to be affected measurably.

In order to provide engineering design data, the results of environmental studies are generally interpreted as if simulation of pertinent constituents of the orbital environment were achieved. It must be noted, however, that precise environmental simulation is never achieved in the laboratory. Some notable discrepancies are the spectral dissimilarity between natural radiation, electromagnetic and particulate, and sources suitable for screening and development studies. Also, in handling such a large number of samples, in-place optical properties measurements could not be performed economically during the irradiations. Sufficient flight data have been obtained, however, to indicate close agreement between laboratory predictions and inflight performance.

2. INITIAL OPTICAL PROPERTY MEASUREMENTS

The solar absorptance and infrared emittance were determined from measurements made upon unexposed samples to provide data for thermodynamic analyses. The environmental effects were ascertained by comparing the pre- and post-test solar reflectance values. Two types of apparatus were used to make these measurements. Each measures the energy reflected in a near-normal direction from a diffusely illuminated sample.

Near-normal reflectance from 0.28 to 1.8 μ was obtained with a Cary Model 14 double-beam spectrophotometer equipped with an integrating sphere reflectance attachment. In this device, the source energy is introduced through an aperture into a sphere with a diffuse inner surface of high reflectance. A sample placed in the wall of this inner sphere is illuminated diffusely. Energy reflected from the sample is detected and compared to that reflected from a surface of known reflectance, and the sample reflectance is computed. This reflectance curve is then multiplied by the solar spectral flux-density

curve of Johnson (10) and integrated; solar reflectance, ρ_s , is obtained by dividing the result of the above integration by the solar constant.

Near-normal spectral reflectance, $\rho_{\lambda n}$, from 1.4 to 22.0 μ , was obtained with an LMSC-constructed hohlraum and associated Perkin-Elmer Model 13 ratio-recording spectrophotometer. A hohlraum is essentially a heated-cavity reflectometer with walls at uniform temperature. In the device under discussion, the cooled sample forms part of one wall. With the exception of the solid angle subtended by the cavity aperture, the sample is irradiated uniformly from hemispherical space. Energy reflected from the sample in a near-normal direction passes out of the hohlraum aperture and is compared monochromatically with the radiosity of the hohlraum wall.

From the reciprocity theorem of Helmholtz, it can be found that the ratio of reflected energy to the radiosity of the hohlraum wall is equal to the reflectance of the sample for similarly near-normal incident unidirectional irradiation. This quantity will be referred to as near-normal spectral reflectance. The reflectance thus obtained is subtracted from 1.0 to obtain near-normal spectral absorptance ($1 - \rho_{\lambda n} = \alpha_{\lambda n}$). The absorptance curve is integrated with the blackbody curve for the temperature, t , of interest used as a weighting function. Total near-normal absorptance for blackbody energy from a source at temperature, t , is thus obtained. The result is corrected to total hemispherical absorptance, α_t , by the relationships developed by Eckert and given by Jakob, unless there is reason to suspect the surface of interest does not behave in accordance with the Eckert relationship. In any case, the best possible estimate of α_t is obtained. This is assumed equal to the total hemispherical emittance of the surface of interest when that surface is at the temperature of the blackbody for which α_t was computed.

a. Solar Absorptance and Infrared Emittance Values

Table XXI gives values of solar absorptance and emittance for the reflective surfaces in the as-received condition.

Table XXI. Solar Absorptance and Infrared Emittance

Material	Solar absorptance	Room temperature total hemispherical emittance
A	0.08	0.03
B	0.15	0.05
C	0.10	0.04
D	0.08	0.03
E	0.08	0.05
F	0.11	0.07
G	0.07	0.04
H	0.09	0.04
J	0.08	0.03
K	0.12	0.04
L	0.16	—

Spectral reflectance values for the respective samples are presented in Figures 78 through 86.

b. Comments and Interpretation of Results

The sample with the highest solar reflectance, i.e., lowest solar absorptance, is Material G; the value was 0.93. Materials A, D, E, H, and J are nearly as reflective, with values of 0.91 or 0.92. Materials B and L have a reflectance equal to or less than the total solar collector design efficiency of 85 percent.

The reflectance value for material H, which has a surface of silver with a silicon oxide coating, may not be representative for this type of surface. The basis for this statement is that the material, when received from the vendor, appeared to be somewhat tarnished, and this may have affected its reflectance adversely.

3. ULTRAVIOLET IRRADIATION

Ultraviolet radiation from the sun is a primary cause of damage to surfaces in an orbital environment. The solar reflectance of the surfaces decreases when the ultraviolet radiation produces quantum centers, which absorb solar radiation. Eighty-five percent of the solar energy is of wavelengths between 0.40 and 2.0 μ (10). This, then, is the wavelength region of greatest interest when changes in solar reflectance are considered. The principal absorption processes in this critical solar spectral region are those associated with electronic excitations; i.e., excitations in which a photon is absorbed and an electron is moved from its ground state to a state of higher energy.

a. Description of Apparatus

The source of ultraviolet radiation was a 1-kW-A-H6 (PEK Laboratories Type C) mercury-argon-arc high-pressure high-intensity lamp. Approximately 30 percent of the radiant energy of this lamp is in the 2,000 to 4,000 \AA range. By comparison, roughly 9 percent of the extraterrestrial solar spectrum is believed to lie in the same wavelength range. The lamp is water-cooled and has a quartz water jacket and velocity tube. This assembly is lowered into a quartz envelope extending into the exposure chamber from the top. The lamp assembly can be withdrawn to change lamps without disturbing the vacuum in the system.

The ultraviolet intensity is monitored with calibrated phototubes (RCA 935) that are filtered to detect energy in the 2,000 to 4,000 \AA region; Corning 7-54 filters are used to pass only near-ultraviolet radiation. In this way, only the radiation believed to produce serious damage is monitored routinely. It should be noted that the A-H6 lamp output reduces more, with time, in the short than in the long wavelength regions.

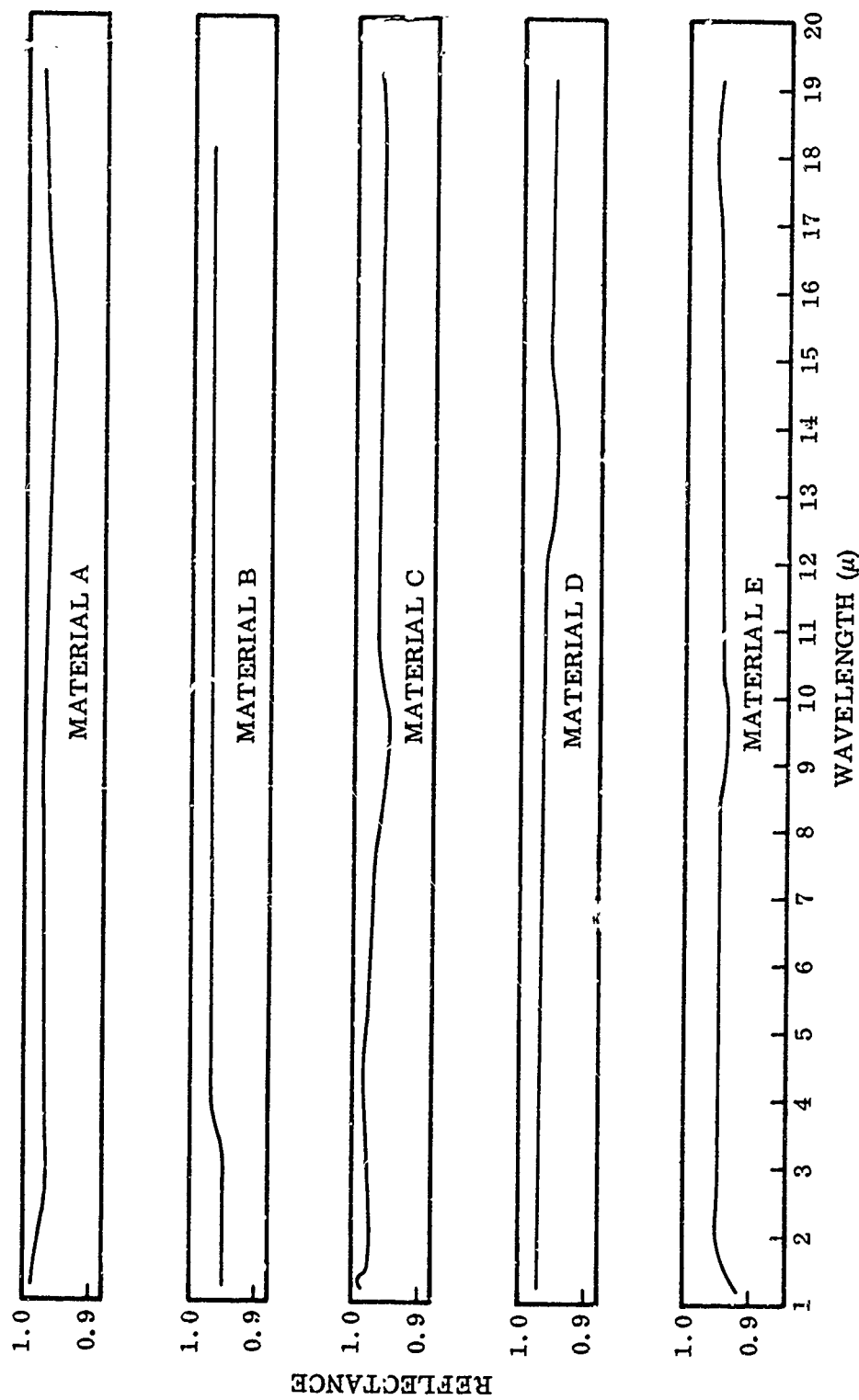


Figure 78 Spectral-Reflectance Measurements of Unexposed Surfaces, Materials A-E; 1-20 μ Region

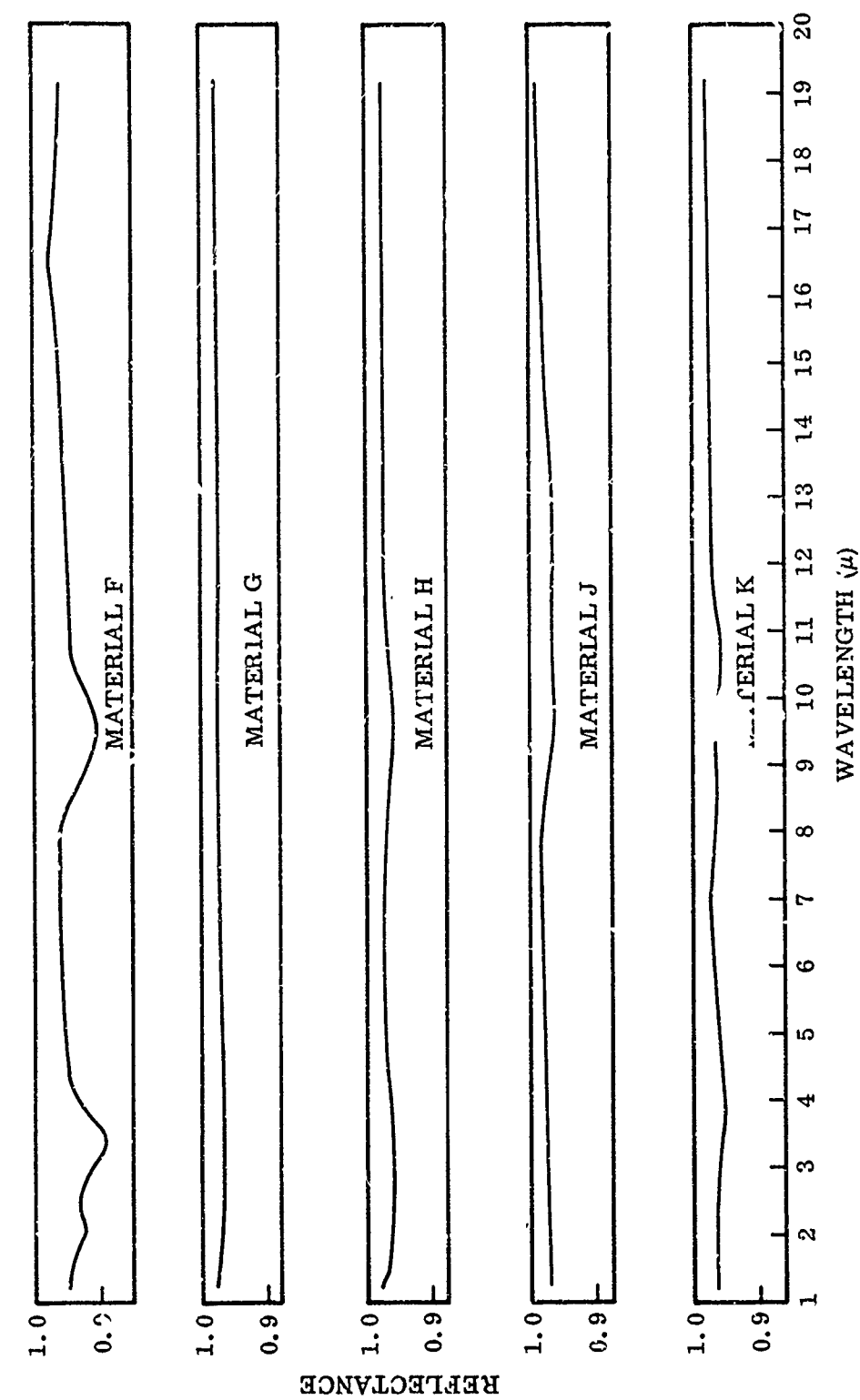


Figure 79 Spectral-Reflectance Measurements of Unexposed Surfaces, Materials F-K; 1-20 μ Region

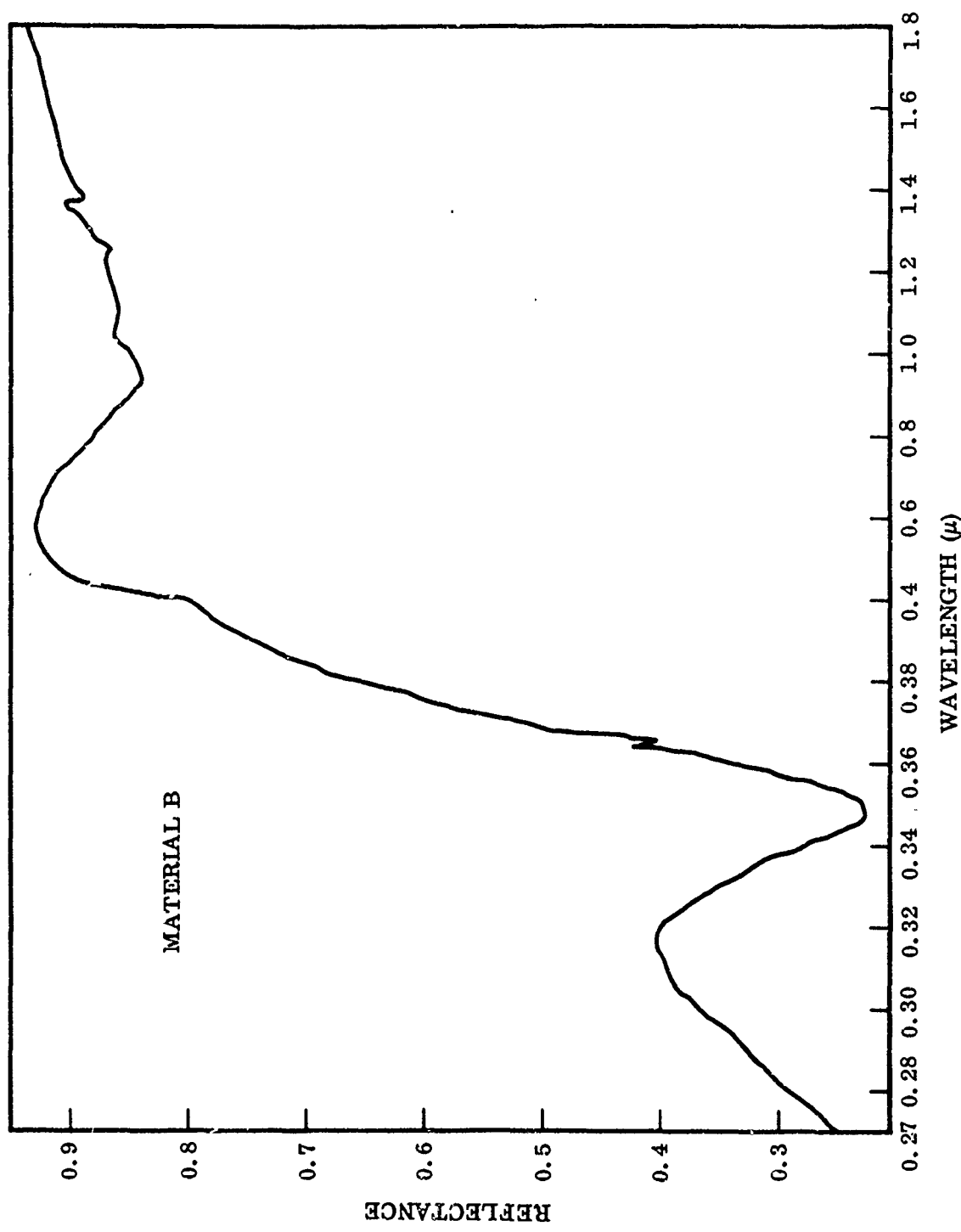


Figure 80 Spectral-Reflectance Measurements of Unexposed Surfaces, Material B; 0.27-1.8 μ Region

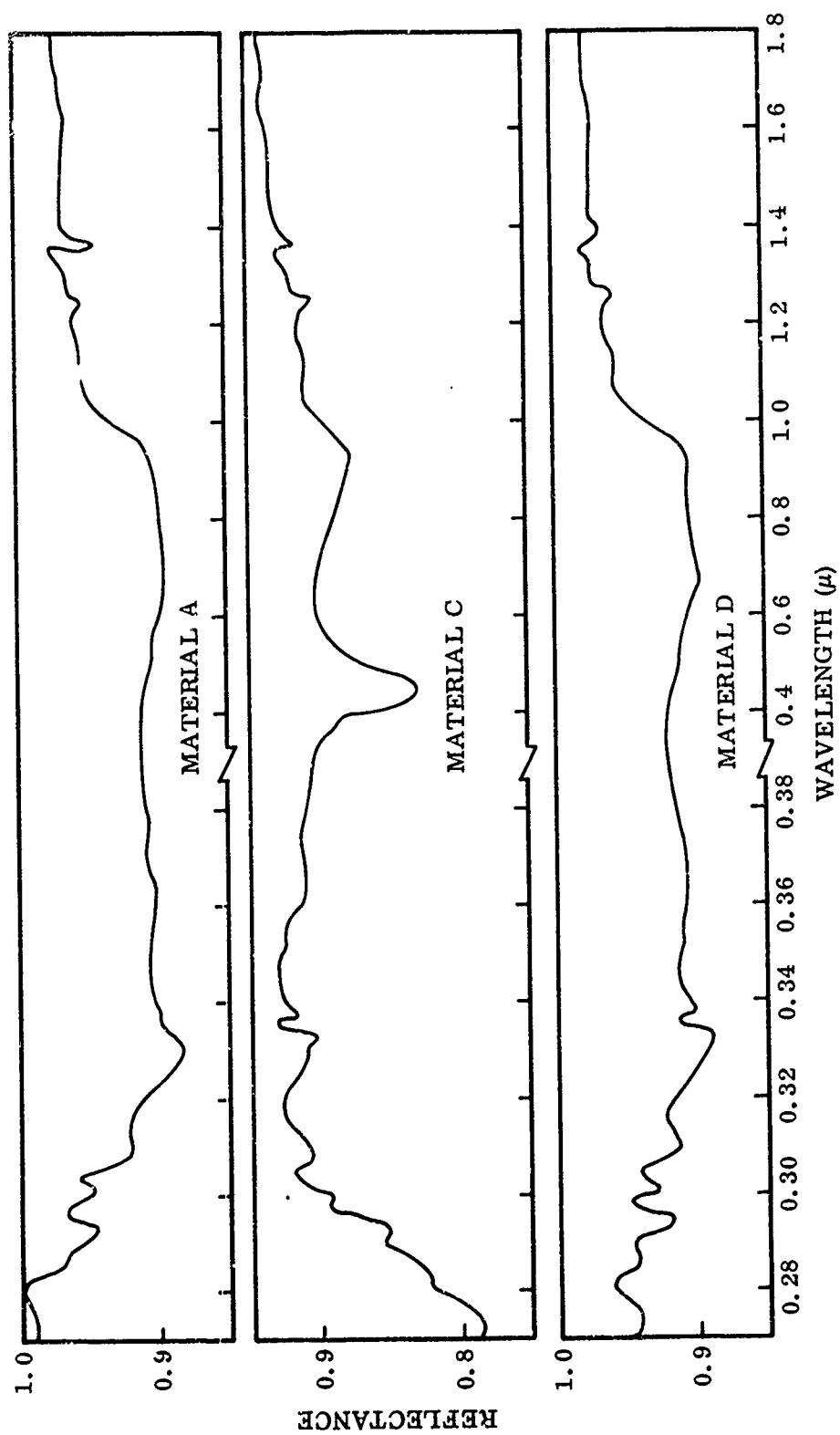


Figure 81 Spectral-Reflectance Measurements of Unexposed Surfaces, Materials A, C, and D; 0.27-1.8 μ Region

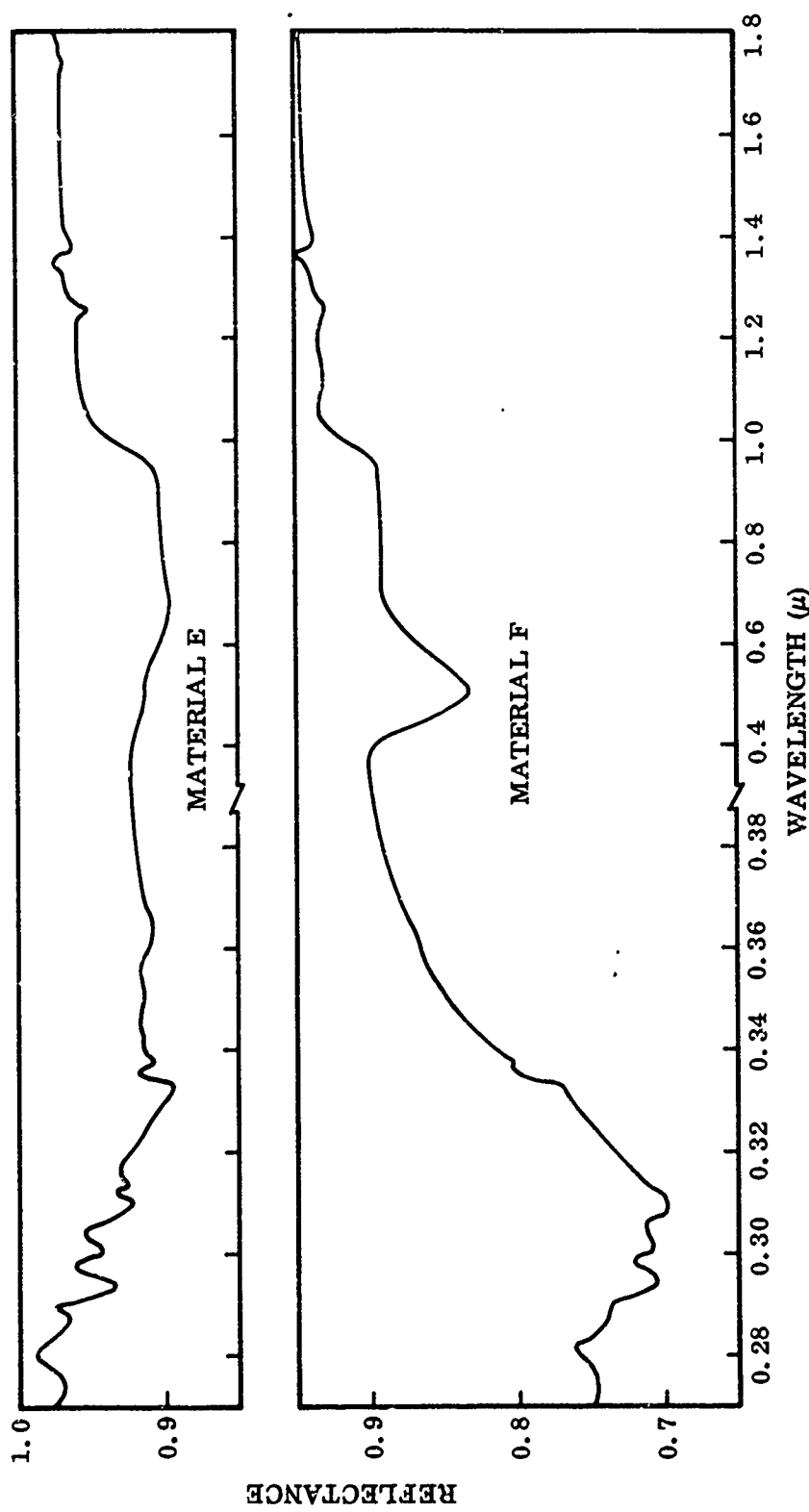


Figure 82 Spectral-Reflectance Measurements of Unexposed Surfaces, Materials E and F;
0.27-1.8 μ Region

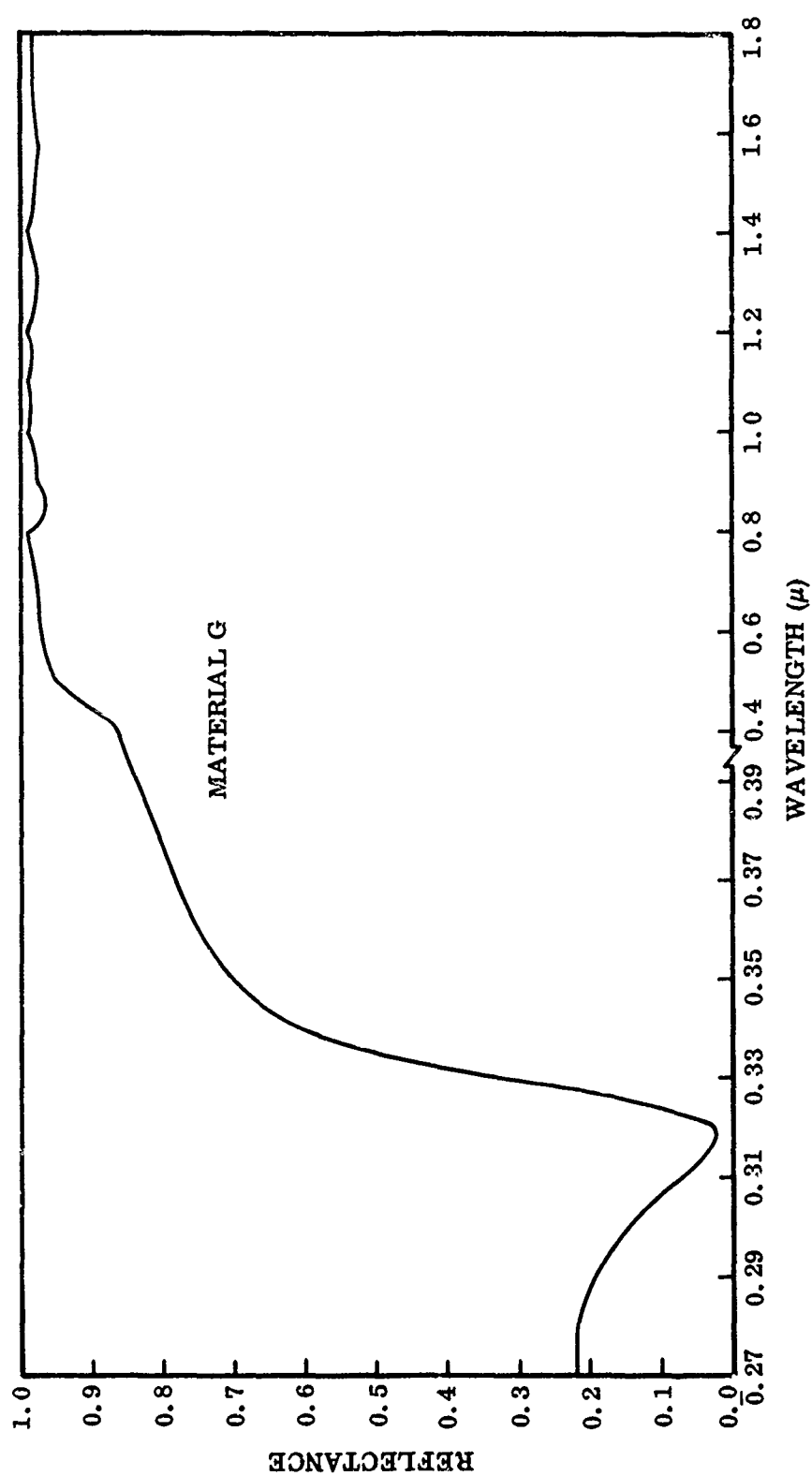


Figure 83 Spectral-Reflectance Measurements of Unexposed Surfaces, Material G; 0.27 - 1.8 μ Region

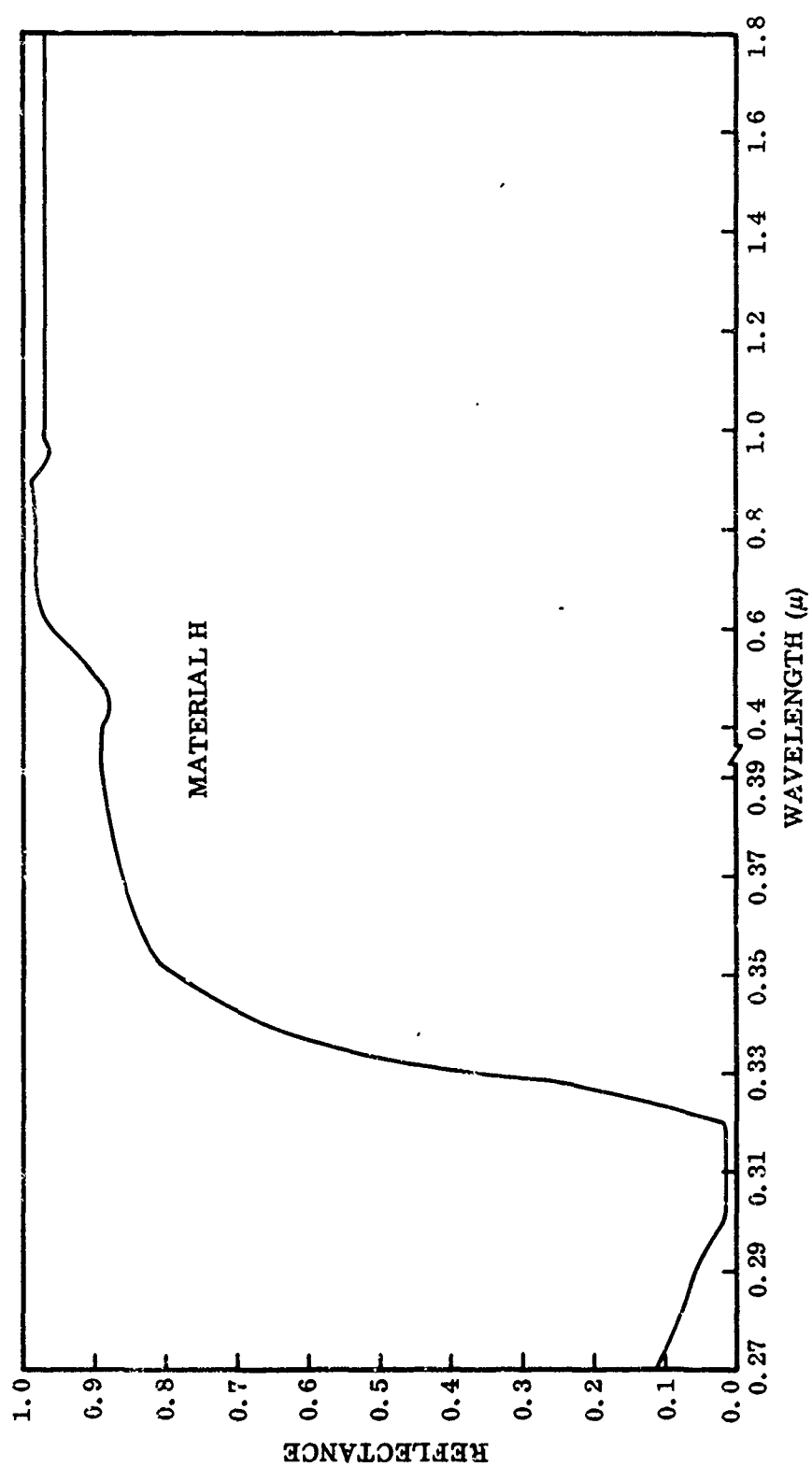


Figure 84 Spectral-Reflectance Measurements of Unexposed Surfaces, Material H: 0.27-1.8 μ Region

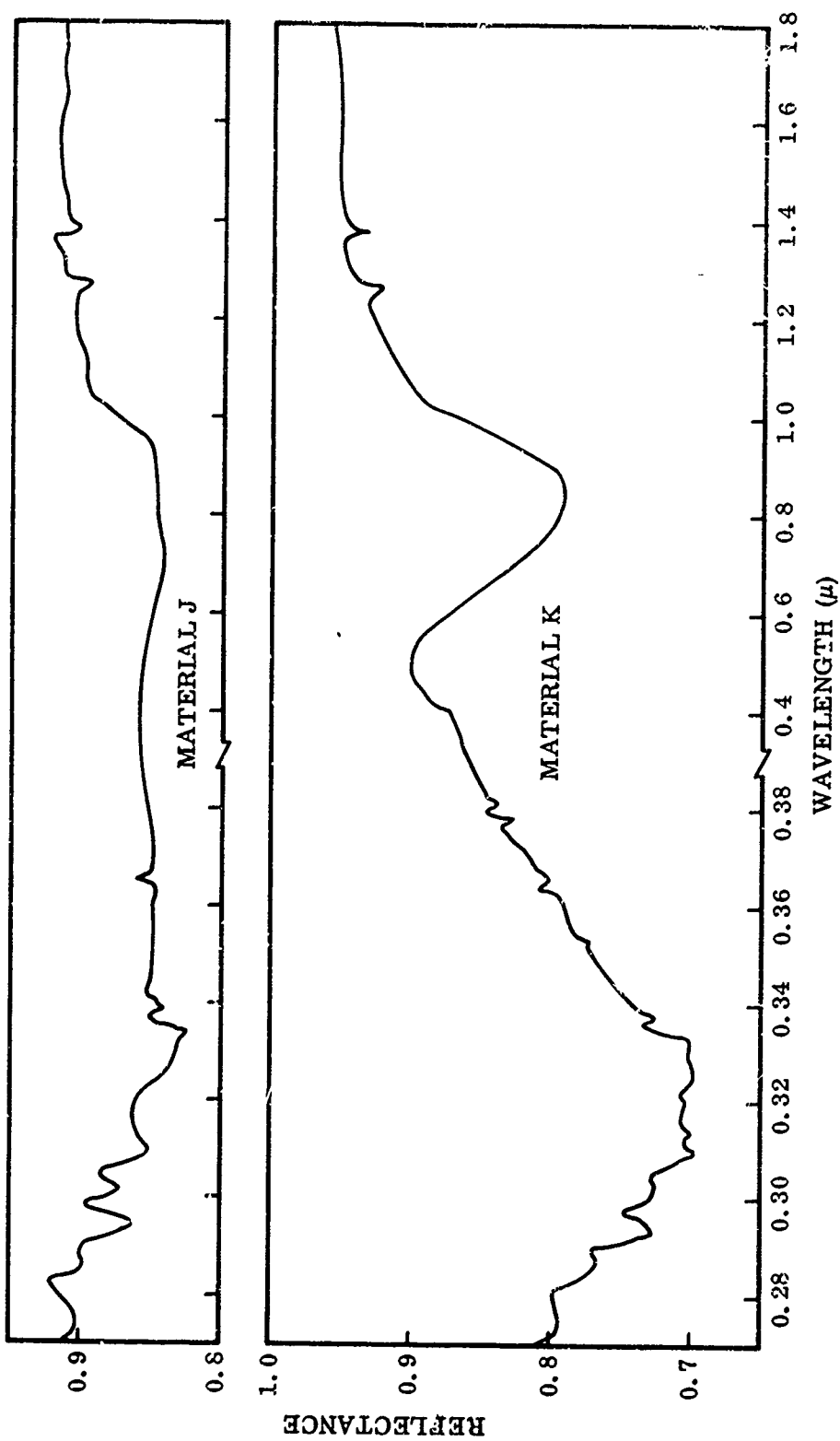


Figure 85 Spectral-Reflectance Measurements of Unexposed Surfaces, Materials J and K;
 $0.27 - 1.8 \mu$ Region

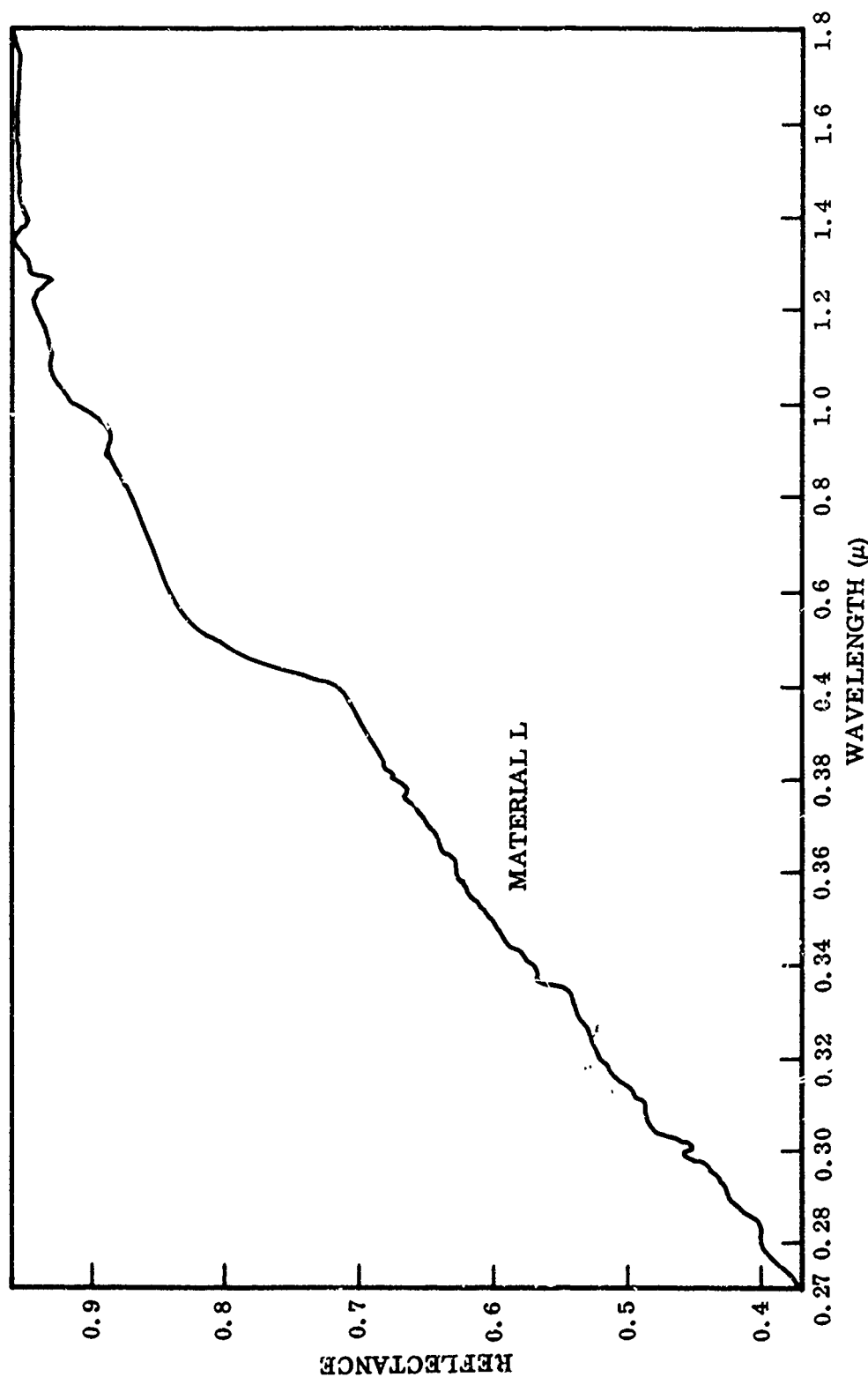


Figure 86 Spectral-Reflectance Measurements of Unexposed Surfaces, Material L; 0.27-1.8 μ Region

Neutral-density filters are used to reduce the flux density incident on the detector in order to avoid saturation of the phototube. The phototubes have been calibrated by actinometry and with a thermopile. The output of the phototubes is automatically measured and recorded for a few minutes every hour with a recording microammeter. When desired, a Corning 0-54 filter is used to compare the intensity in the 2,000 to 3,000 Å region to that in the 3,000 to 4,000 Å region.

The exposure chambers are metal bell jars 14 in. high by 14 in. in diameter mounted on 18-in. base plates. The sample holder is a water-cooled copper block viewing the ultraviolet radiation source to give a nominal six "suns" of ultraviolet energy. A "sun" of near-ultraviolet radiation is defined as the flux density of extraterrestrial solar radiation at one astronomical unit from the sun, in the wavelength interval of 2,000 to 4,000 Å. The "sun" is admittedly an unsatisfactory unit of flux density; it is used for convenience in comparing the data in this report with those of other investigators.

Normally, water is passed through copper tubes soldered to the sample holders. This maintains the specimen temperatures between 65 and 95° F. During the elevated-temperature exposures, a flow of compressed air is passed through the cooling tubes to maintain the samples at the desired temperatures.

High vacuums in the range of 10^{-7} Torr are maintained with electronic vacuum pumps using standard vacuum techniques.

b. Test Procedure

Two samples of each material were exposed to near-ultraviolet radiation in vacuum under the conditions of four total doses and two sample temperatures during exposure. One control sample of each material also was retained. The total exposures were equivalent to orbit times of 0.5, 1, 2, and 6 months (nominal).

Changes of optical properties due to ultraviolet radiation are in part dependent upon sample temperature during irradiation. Therefore, the optical stability of the reflector surfaces was determined for two temperature conditions — room temperature and +250° F. Optical property measurements were made before and immediately after the exposures.

c. Test Results

Reflectance data were obtained for samples exposed to near-ultraviolet radiation for approximately 3,500 to 4,000 sun-hr. Based upon a 200-nm circular polar orbit, this exposure represents 7 to 8 months in orbit. The data were then extrapolated to 6,000 sun-hr, or one year in orbit. Table XXII is a summary of the results of the total change in solar reflectance.

The changes in solar reflectance of the reflective samples exposed to near-ultraviolet radiation are presented in Figures 87 through 89. At each exposure condition two specimens were irradiated. Single data points on the figures represent the values for two specimens when the solar reflectance values were identical.

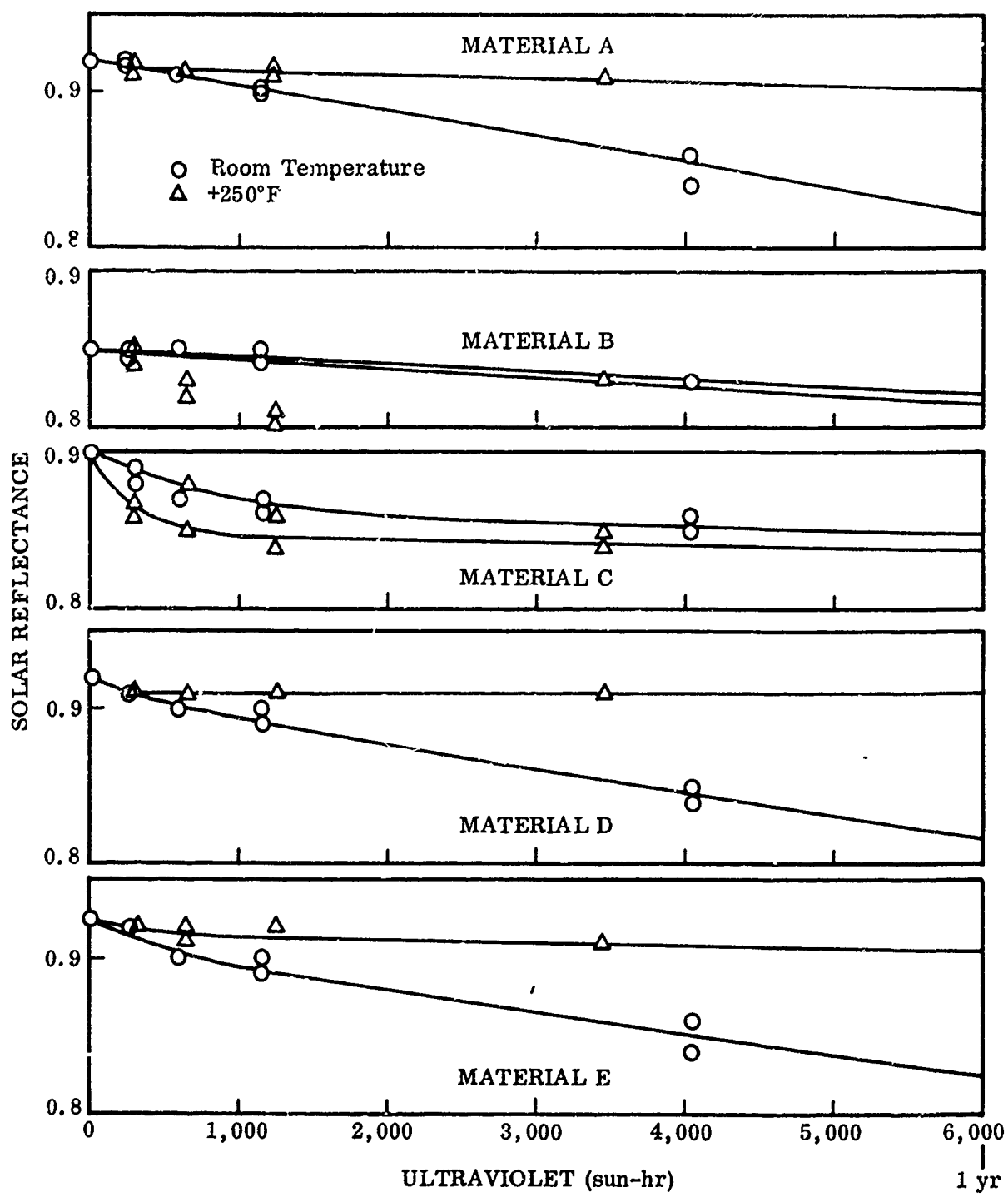


Figure 87 Ultraviolet-Radiation Damage to Reflective Surfaces, Materials A-E

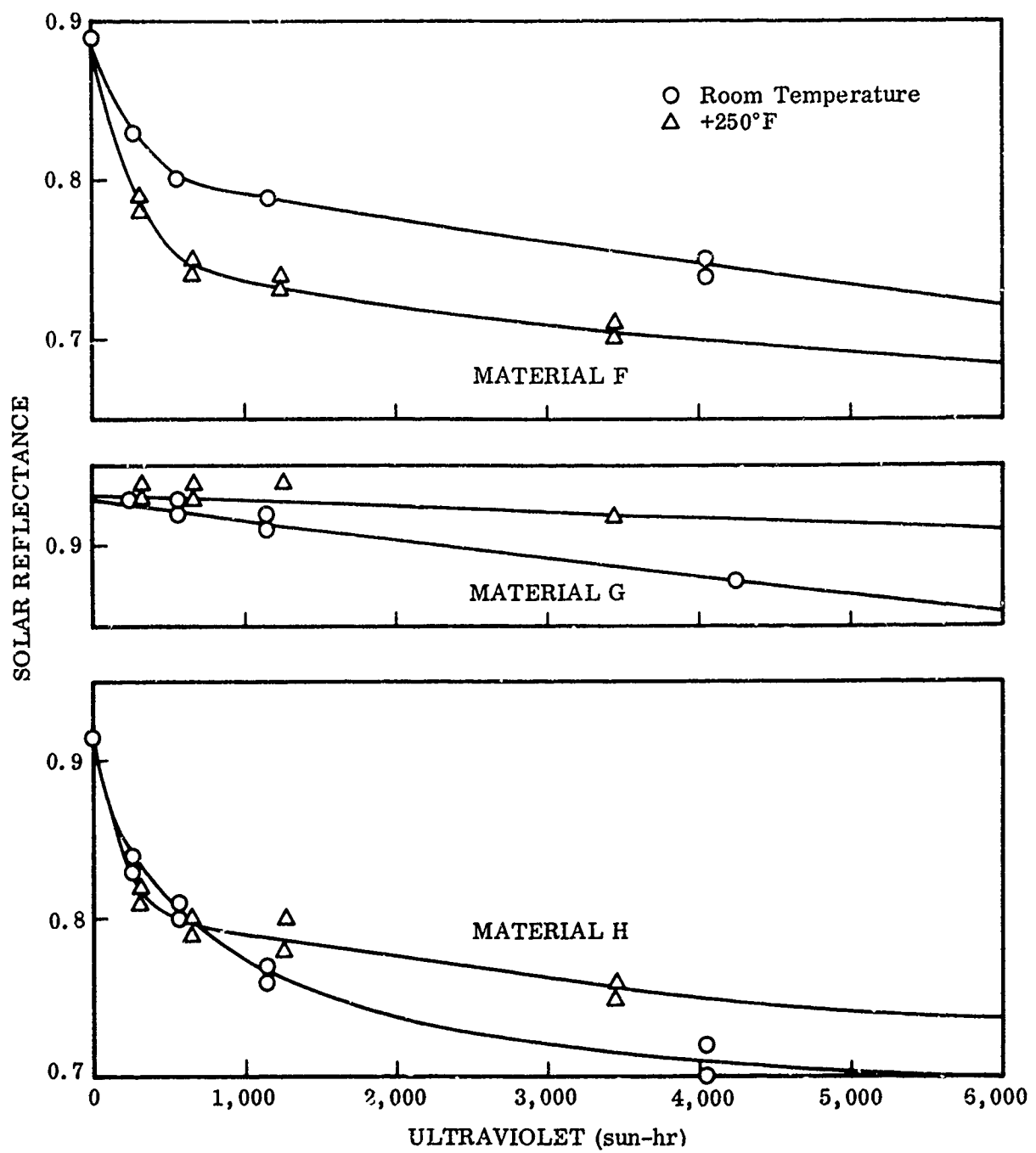


Figure 88 Ultraviolet-Radiation Damage to Reflective Surfaces, Materials F-H

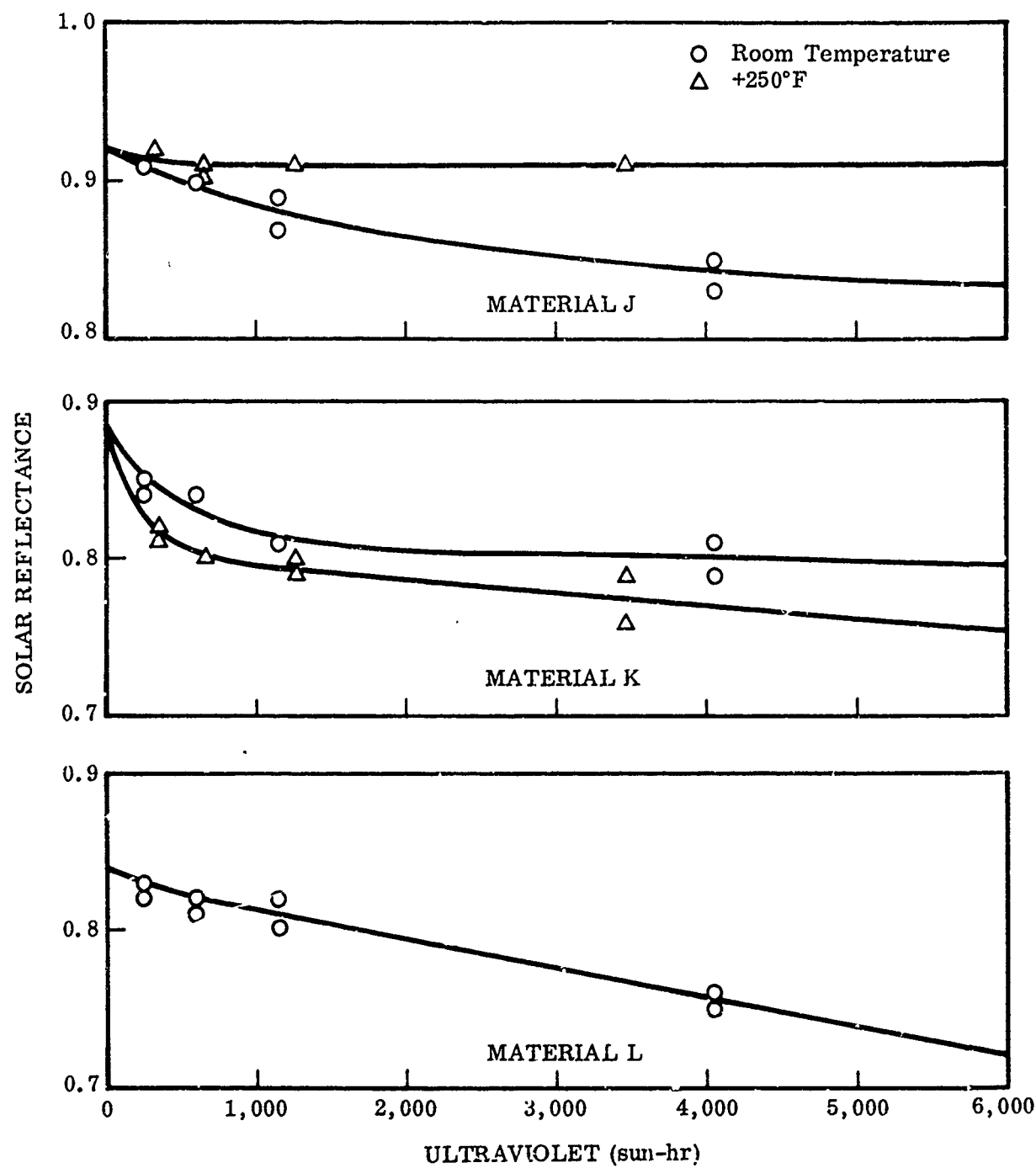


Figure 89 Ultraviolet-Radiation Damage to Reflective Surfaces, Materials J-L

Table XXII. Ultraviolet Exposure Results

Material	Initial solar reflectance	Final solar reflectance after 1-yr exposure	
		Room temperature	250° F
A	0.92	0.82	0.90
B	0.85	0.82	0.82
C	0.90	0.85	0.84
D	0.92	0.82	0.91
E	0.92	0.83	0.90
F	0.89	0.72	0.69
G	0.93	0.86	0.91
H	0.91	0.70	0.74
J	0.92	0.83	0.91
K	0.88	0.80	0.75
L	0.84	0.72	—

d. Comments and Interpretation of Results

Materials A, D, E, G, and J were found to be optically most stable in the ultraviolet environment. The degradation observed for sample H is not believed to have been representative of silver with overcoating because the samples, as received, appeared to be discolored or tarnished. It was noted that the uncoated samples were, in all cases, more stable than those with an overcoating.

4. ELECTRON BOMBARDMENT

The purpose of this test was to determine the effect of the low-energy auroral electrons found in the ASTEC environment on the reflective surfaces of the candidate materials. Samples were irradiated at an energy level of 5 kV and a flux level of 10 ergs/cm²-sec. A level of 5 kV has been determined to be the average energy level of the auroral electron stream. The average energy flux is estimated to be 1 erg/cm²-sec; this figure was raised by an order of magnitude to allow for periods of maximum activity.

Exposure times for the tests were equivalent to 2, 4, 8, and 12 months in orbit. Since irradiation was continuous, and an orbiting vehicle is within the auroral radiation zones only a small percentage of the time, it was possible to accelerate the tests greatly. Total exposure times were, respectively, 1, 2, 4, and 5 days. Each of these tests was carried out in vacuum at two temperatures - room temperature and +250° F.

a. Description of Apparatus

Test samples were placed on a copper block with water cooling and resistance heating tracings. This table was electrically isolated from ground.

The sample table was placed in a stainless-steel vacuum chamber pumped by a 1,500 liter/sec oil diffusion pump with liquid-nitrogen trapping. The operating pressure was 6×10^{-8} Torr.

The cathode consisted of an array of 70 small tungsten electron emitters, electrically in parallel. This configuration was necessary to attain a uniform electron density at the sample table surface. The cathode was suspended by insulators from a metal plate. This plate formed the top closure to a pyrex insulating section.

The configuration of this apparatus is shown in Figure 92. While this is the diagram for the combined-environment apparatus, it differs from the electron-bombardment apparatus only by the addition of the ultraviolet lamps.

b. Test Procedure

Samples were placed on the sample table with tweezers and secured with stainless-steel frames to the copper table. The table was placed in the vacuum chamber through a port and secured to a plexiglas insulator ring.

The system reached the starting operating pressure of 10^{-7} Torr within 15 min. Thereafter, the system was run continuously for the required number of days. The sample table temperature was controlled and recorded continuously. The electron current was recorded and read out every hour.

c. Test Results

Reflectance data were obtained for samples exposed to 5-keV electrons for a period representing one year in orbit, $5.8 \times 10^{15} e^-/cm^2$. Table XXIII summarizes the results by presenting the total change in solar reflectance after a year in orbit.

Table XXIII. 5-keV Electron Exposure Results

Material	Initial solar reflectance	Final solar reflectance after 1-yr exposure	
		Room temperature	+250°F
A	0.92	0.92	0.92
B	0.85	0.82	0.81
C	0.90	0.90	0.87
D	0.92	0.92	0.92
E	0.92	0.92	0.92
F	0.89	0.86	0.81
G	0.93	0.92	0.93
H	0.91	0.91	0.90
J	0.92	0.92	0.92
K	0.88	0.82	0.75

The changes in solar reflectance of the reflective samples exposed to 5-keV electron radiation are presented in Figures 90 and 91. At each exposure condition two specimens were irradiated; therefore, at times, one data point represents values for two samples.

d. Comments and Interpretation of Results

The reflective properties of most samples were damaged slightly or not at all by the radiation, the major exceptions being samples B, F, and K. It is also noteworthy that an apparent threshold for damage to the coated samples lies at about $4 \times 10^{15} \text{ e}^-/\text{cm}^2$. At lower total exposures no significant damage was observed.

5. COMBINED ENVIRONMENT

Two samples of c. h material were exposed in vacuum to the eight conditions defined by room temperature and $+250^\circ\text{F}$, and four dose levels. Simultaneous irradiation by low-energy electrons and near-ultraviolet radiation was performed to provide doses equivalent to 0.5, 1, 2, and 6 months in orbit. Actual exposure times were 2, 4, 8, and 24 days.

a. Description of Apparatus

The vacuum system, electron emission and monitoring system, and sample table were identical to those used in the electrons-only chamber. The source of near-ultraviolet radiation with monitor system was identical to that of the ultraviolet-only exposures. Two high-pressure mercury-arc lamps were located at opposite sides of the sample table to provide an approximate six-sun intensity.

A schematic diagram of the combined-environment apparatus appears in Figure 92; the apparatus is shown pictorially in Figure 93.

b. Test Procedure

These exposures were conducted in a manner identical to that of the electron exposures. The lamps were changed every 50 hr of operation. The electron current on the sample table was 3.5×10^{-8} amp to maintain equivalent total doses of electron radiation and near-ultraviolet radiation.

c. Test Results

The solar reflectance, as a function of exposure time to combined electron and ultraviolet radiation, was obtained experimentally for a representative 6-month period and extrapolated to 1 year in orbit. Table XXIV summarizes the results by presenting the total change in solar reflectance after 6 months in orbit.

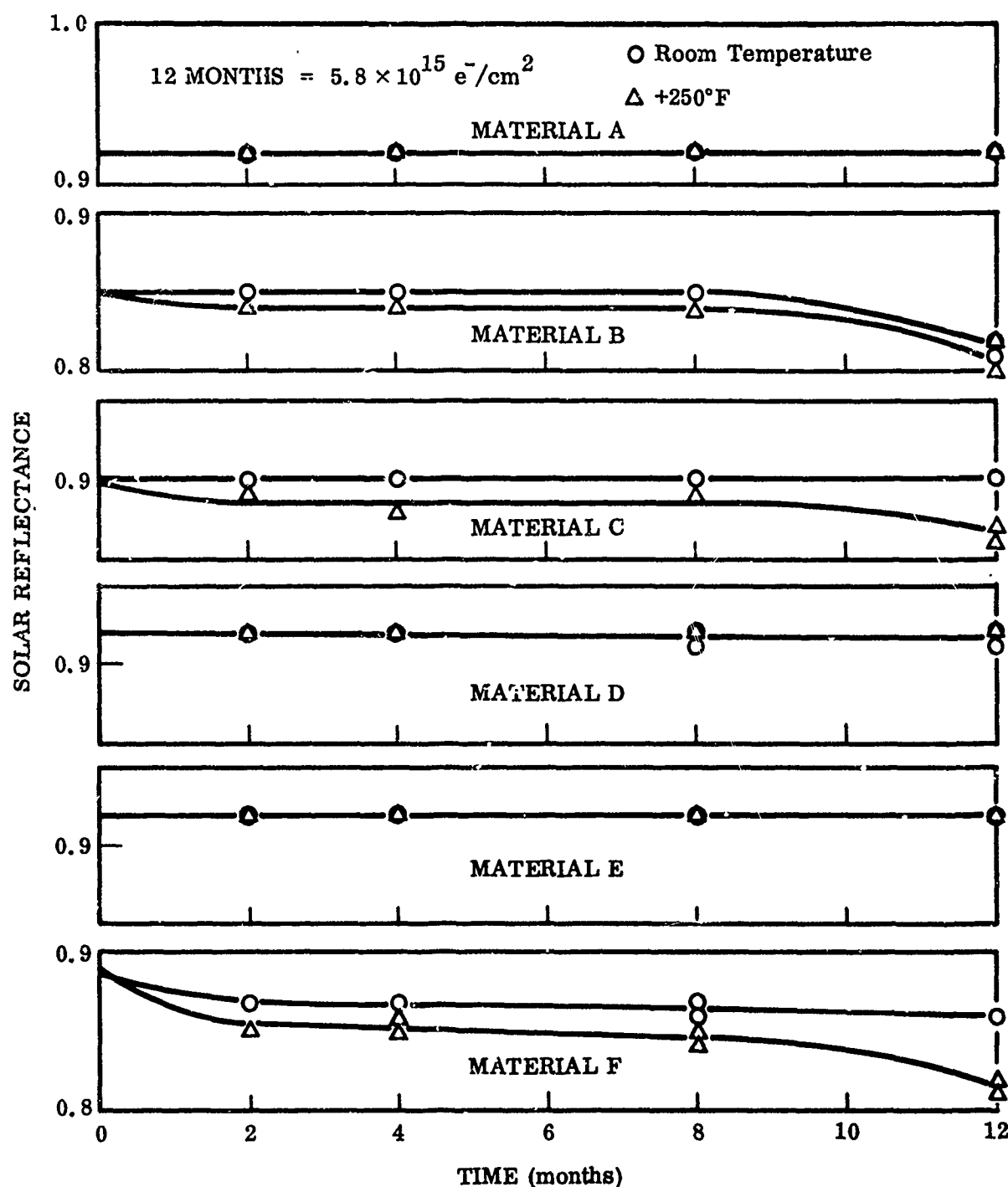


Figure 90 Damage to Reflective Surfaces Caused by 5-keV Electrons, Materials A-F

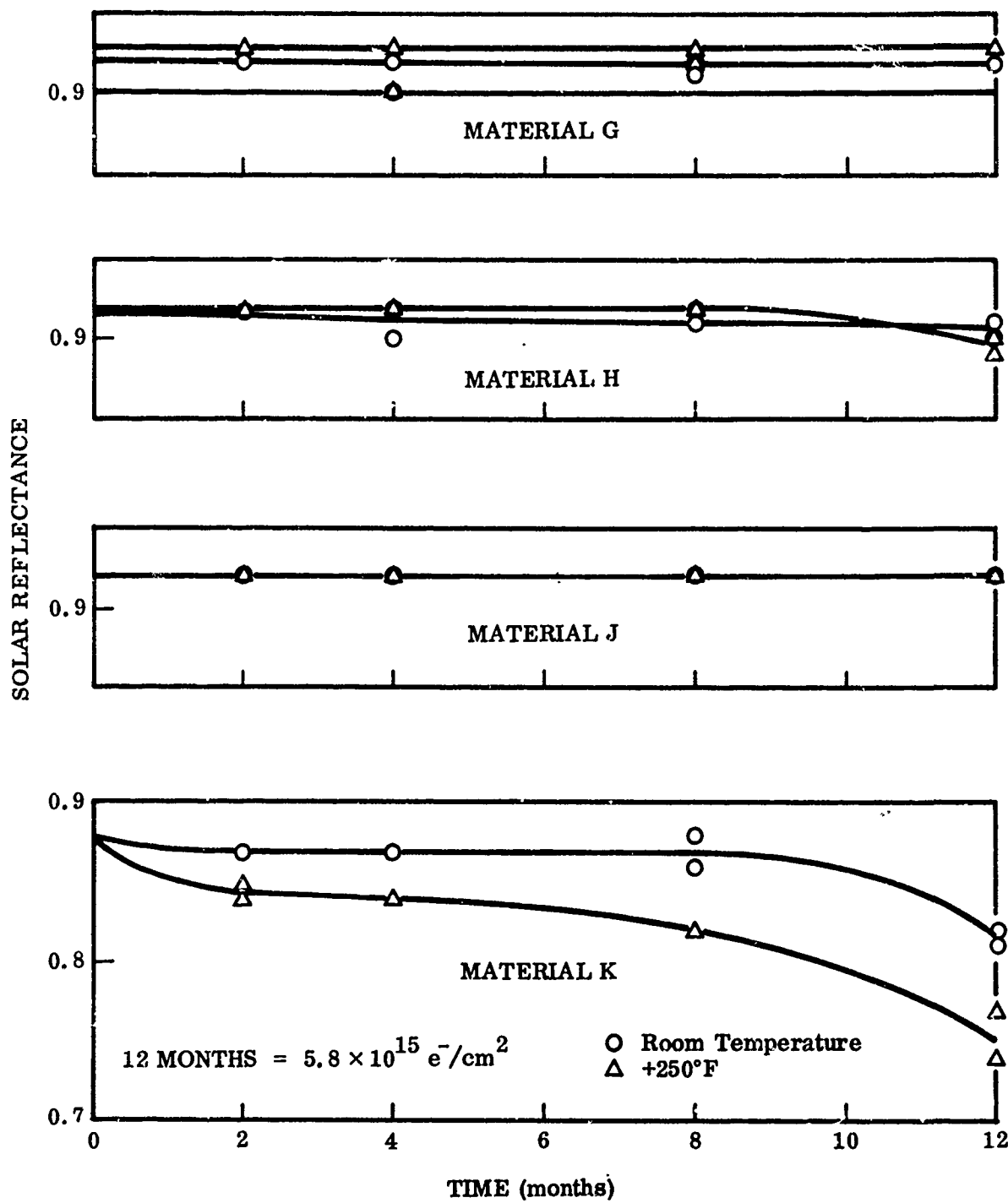


Figure 91 Damage to Reflective Surfaces Caused by 5-keV Electrons, Materials G-K

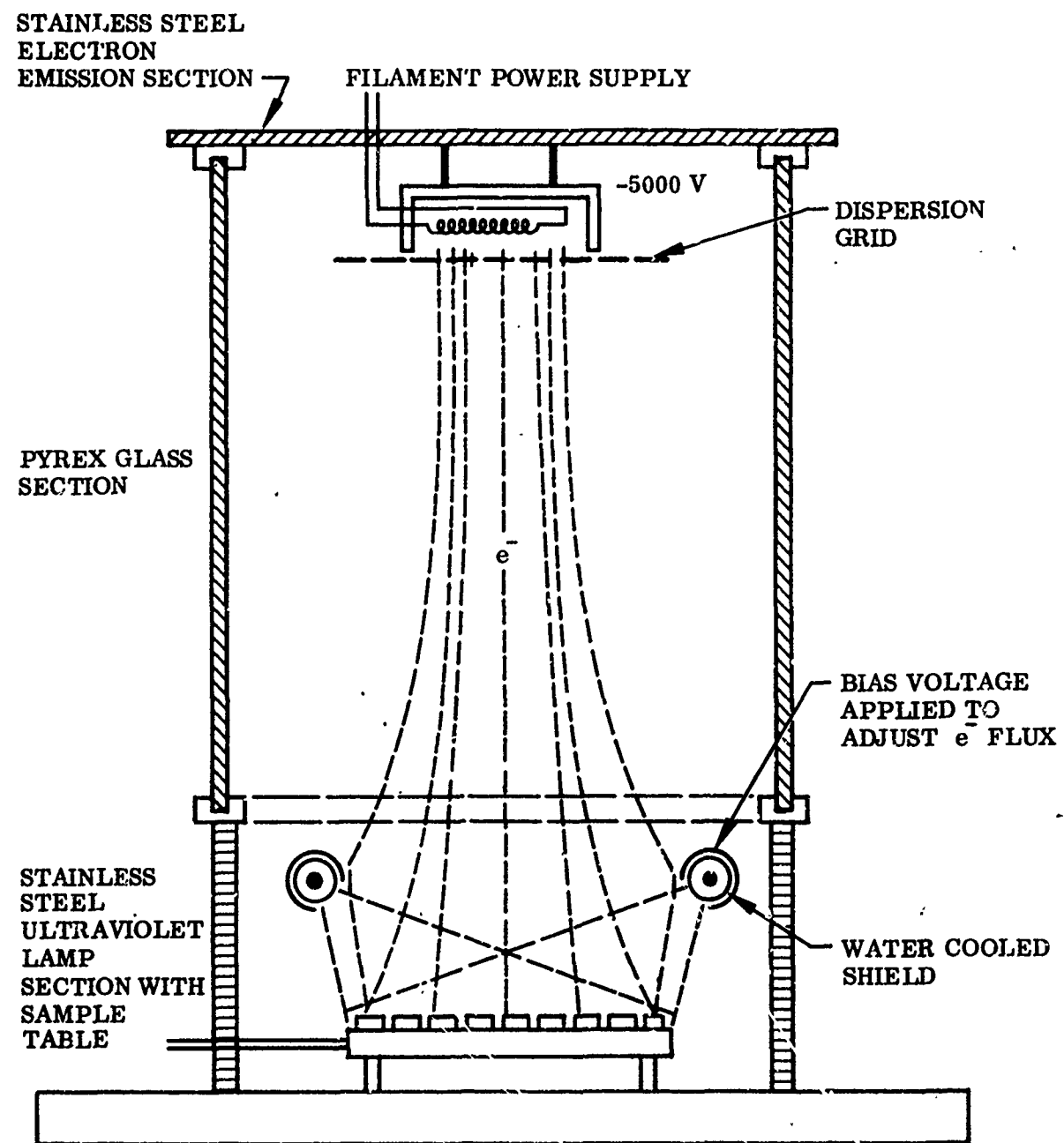


Figure 92 Combined Environment Chamber

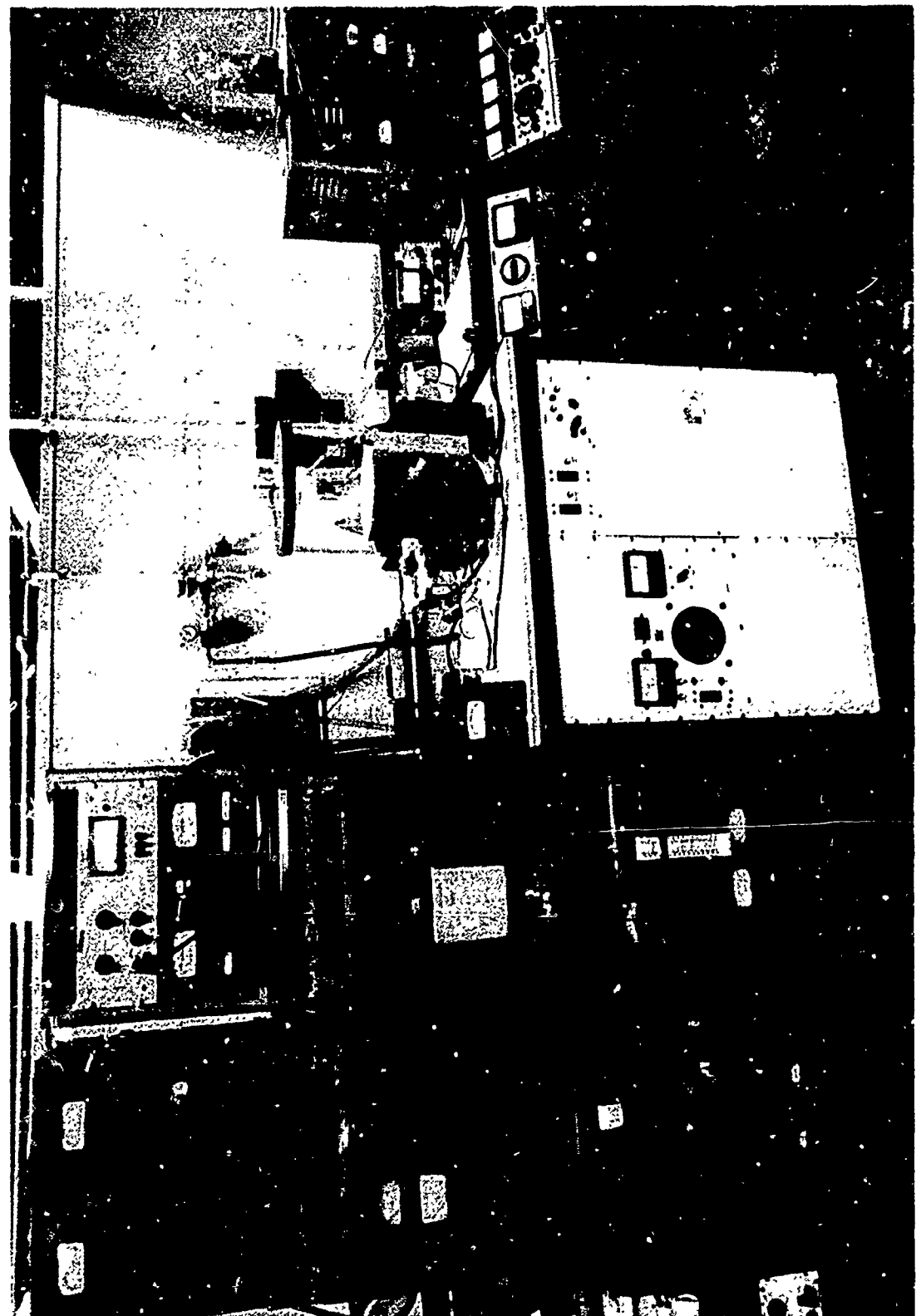


Figure 93 Combined Environment Apparatus

Table XXIV. Solar Reflectance After Combined-Environmental Exposure

Material	Solar reflectance		
	Initial	After 6-mo exposure	
		Room temperature	250° F
A	0.92	0.85	0.91
B	0.85	0.83	0.82
C	0.90	0.83	0.82
D	0.92	0.84	0.91
E	0.92	0.87	0.90
F	0.89	0.75	0.64
G	0.93	0.91	0.90
H	0.91	0.78	0.78
J	0.92	0.87	0.92
K	0.88	0.80	0.77

The changes in solar reflectance of the reflective samples exposed to the combined environment are presented in Figures 94 and 95. At each exposure condition two specimens were irradiated; at times, therefore, one data point represents values for two specimens.

d. Comments and Interpretation of Results

The superiority of the uncoated surfaces from the standpoint of withstanding the combined ultraviolet and electron environments is clearly shown in Table XXIV. Reflectance values of the five silicon-oxide-coated surfaces after 6 months' equivalent exposure at 250° F ranged from 0.82 to 0.64; the latter figures represent a decrease of 25 percentage points during the test period. In contrast, the final reflectance values of the five uncoated surfaces all were 0.90 or higher, and the maximum degradation within this group was 3 percentage points. Data for the 6-month-equivalent exposure at room temperature present a similar picture, although the differences between the bare surfaces and the coated surfaces were not so pronounced.

The extrapolated values of reflectance for the coated samples (B, C, F, H, K) (Figures 94 and 95) are conservative since these materials exhibited an electron-damage threshold after 8 months' exposure. These values represent, therefore, the highest solar reflectance which could be expected.

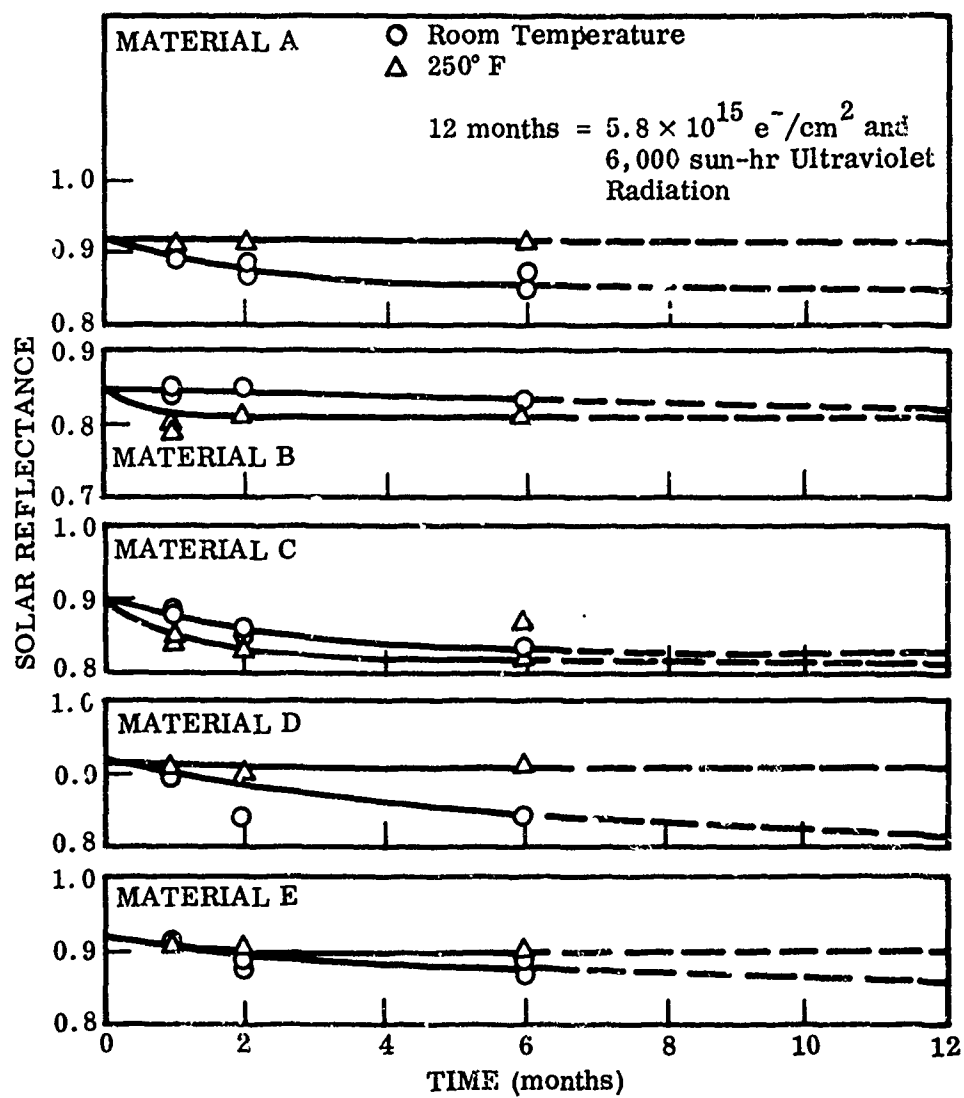


Figure 94 Damage to Reflective Surfaces Caused Simultaneously by 5-keV Electrons and Ultraviolet Radiation, Materials A-E

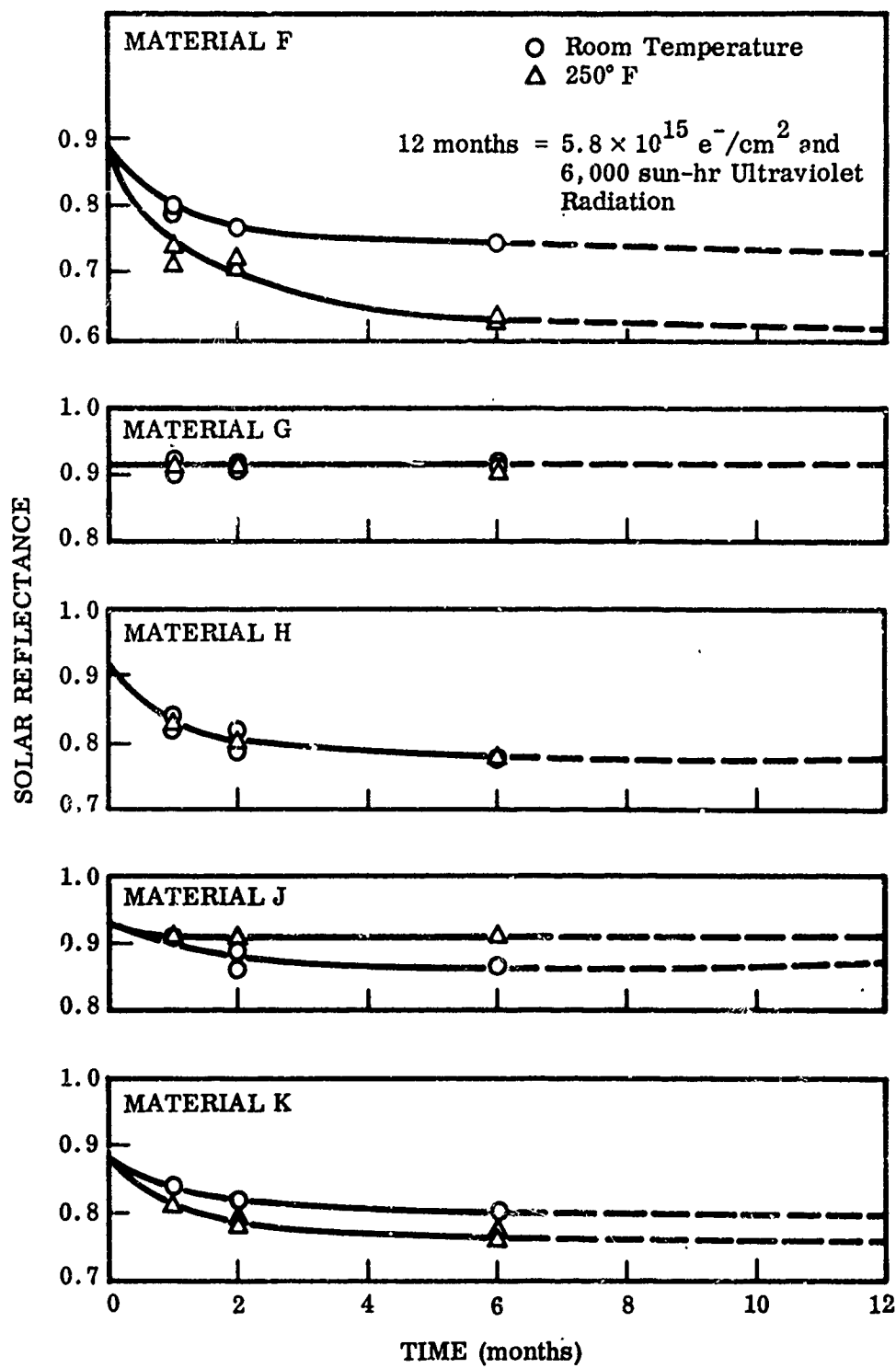


Figure 95 Damage to Reflective Surfaces Caused Simultaneously by 5-keV Electrons and Ultraviolet Radiation, Materials F-K

Section IV

MECHANICAL PROPERTIES

1. INTRODUCTION

Five types of tests were performed to determine the mechanical properties of candidate materials:

- Panel shear
- Panel bend
- Facing tension
- Facing separation
- Core compression

All these tests, except the panel-bend test, were conducted at +250°F, room temperature, and -200°F. Panel-bend tests were conducted at room temperature only.

Reduction of test data gave the various effective moduli, elastic limits, and ultimate limits of the materials, as well as average values and deviation of each minimum value from its respective average. It should be noted, however, the the modulus values in the tables appearing later in this section are "composite moduli" since the test materials are not homogeneous. The wide scatter of some data indicates, to some extent, the anomalies of these nonhomogeneous materials. Testing of a greater number of specimens and the use of statistical procedures would give more meaningful results. The number of valid tests performed upon previously unexposed specimens of each candidate material in the different test types is shown in Table XXV.

2. PANEL SHEAR

Several specimens of each candidate material were subjected to a shear test. Data from these tests indicated the maximum shear stress sustained by the specimen, the strain on the specimen at the maximum stress, the elastic limit or point beyond which permanent deformation occurred, and the shear modulus. Maximum stress

Table XXXV. Mechanical Properties Tests on Candidate Materials - Unexposed Specimens

Material	Number of valid tests									Approx. material thickness (in.)
	Panel-shear test J	Panel-bend test K	Facing-tension test L	Facing-tension test M	Core-compression test N	Core-compression test O	Core-compression test P	Core-compression test Q	Core-compression test R	
A	-200°F RT ^(a) +250°F RT ^(a) only	-200°F RT ^(a) +250°F RT ^(a) only	-200°F RT ^(a) +250°F RT ^(a)	-200°F RT ^(a) +250°F RT ^(a)	3	3	3	3	3	0.25
A	3	3	4	3	3	3	3	3	3	0.25
A	-	-	4	-	-	-	-	3	3	0.75
B	3	3	4	4 ^(b)	3	3	1	3	3	0.50
B	-	-	4	2 ^(c)	3	3	-	-	3	0.50
C	3	3	4	4	2 ^(d)	3	4	3	3	1.00
C	3	3	4	2 ^(e)	2 ^(f)	3	4	3	3	0.50
D	3	3	3	4	3 ^(f)	4	4	3	3	0.50
E	-	-	-	-	3 ^(g)	3	3	-	3	0.50
G	0	2	1	3	3	3	3	1	3	0.50
G	1	3	1	3	3	3	-	-	3	1.00
L	-	-	-	4 ^(h)	4 ⁽ⁱ⁾	-	-	-	-	1.00

(a) Room temperature

(b) Facing.

(c) Backing.

(d) With discontinuity.

(e) With seam.

(f) 0.008-in. thick.

(g) 0.004-in. thick.

(h) Longitudinal.

(i) Transverse.

is defined as the point on the characteristic stress-strain curve where the load carried by the specimen first decreases; it is calculated by dividing the load at that point by the surface area. The final strain is a measure of material deformation at maximum stress and is numerically equal to the translation between the two faces divided by the specimen thickness. The shear modulus, G , is the ratio between unit stress and unit strain while the material is still elastic and is calculated from the data by

$$G = \frac{P}{A} \frac{t}{\Delta L}$$

where P/A is the force per unit area applied to give an elastic translation, ΔL is the translation of one face with respect to the other, and t is the specimen thickness.

a. Description of Apparatus

Specimens were prepared for testing by lightly sanding the faces and backs and then cleaning them to provide a good surface for bonding to the sand-blasted shear plates with high strength epoxy. The mounted specimens were then attached to the proper mounting blocks for insertion in the testing machine. Several different size sets of mounting blocks were used on the various materials to minimize the existence of moments and to ensure that the shear force was applied directly through the center of the specimen.

The extensometer was mounted on two gage blocks cemented the correct distance apart on a shear plate and the adjacent mounting block. This device was made from thin, shaped, stainless-steel shim stock and was instrumented with a full-strain-gage bridge. Calibration was achieved by placing the extensometer in a calibration fixture and operating it over a known deflection. This calibration was performed at each of the various test temperatures.

The mounted specimen (Figures 96 and 97) was held in the test linkage by two dowel pins that also act as unidirectional universal joints. Any misalignment in the other direction was taken up in a bidirectional pivot connected in series with the assembly. A load cell (not shown in Figure 97) was included in the linkage for measuring the force carried by the specimen.

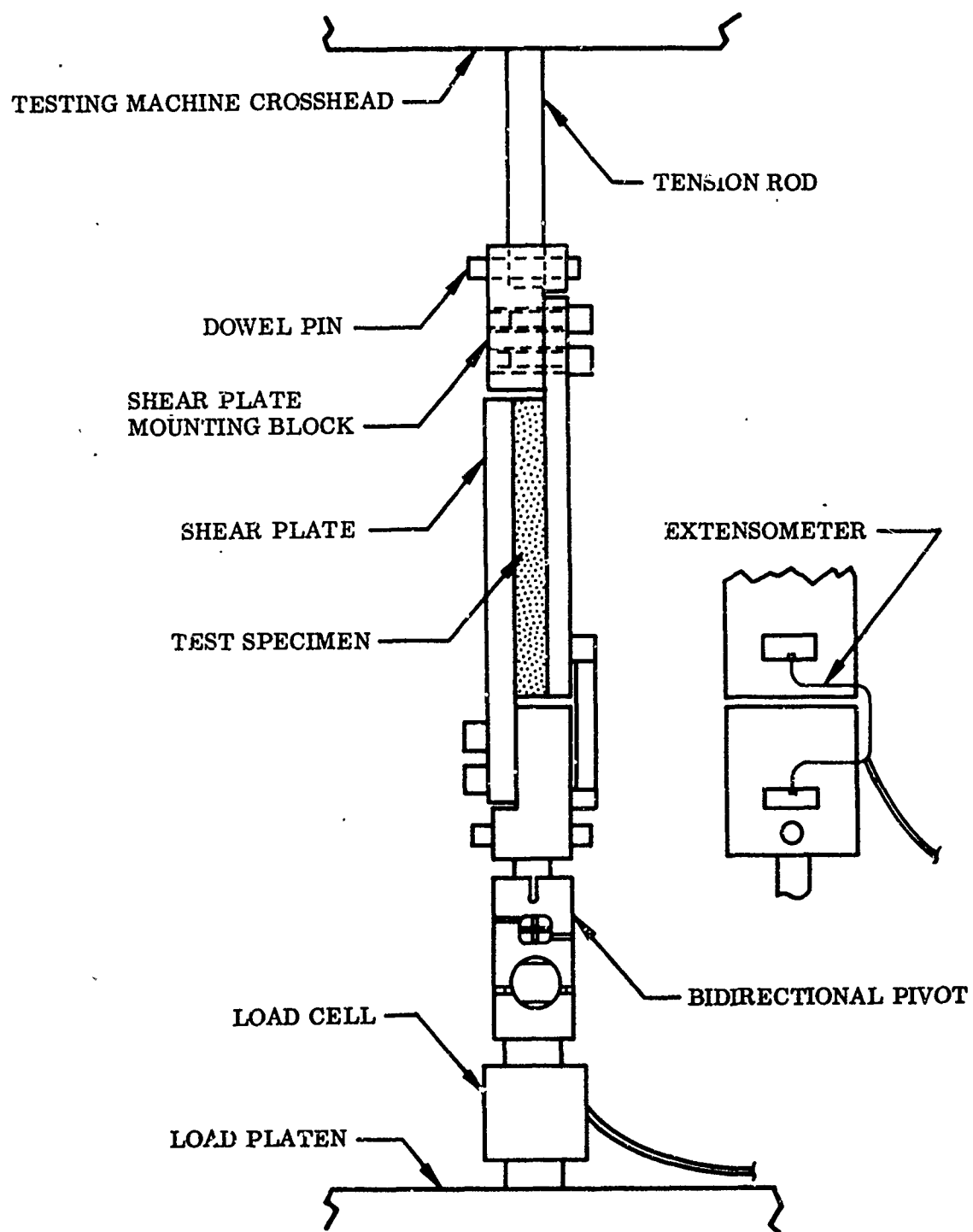


Figure 96 Panel Shear Apparatus Diagram

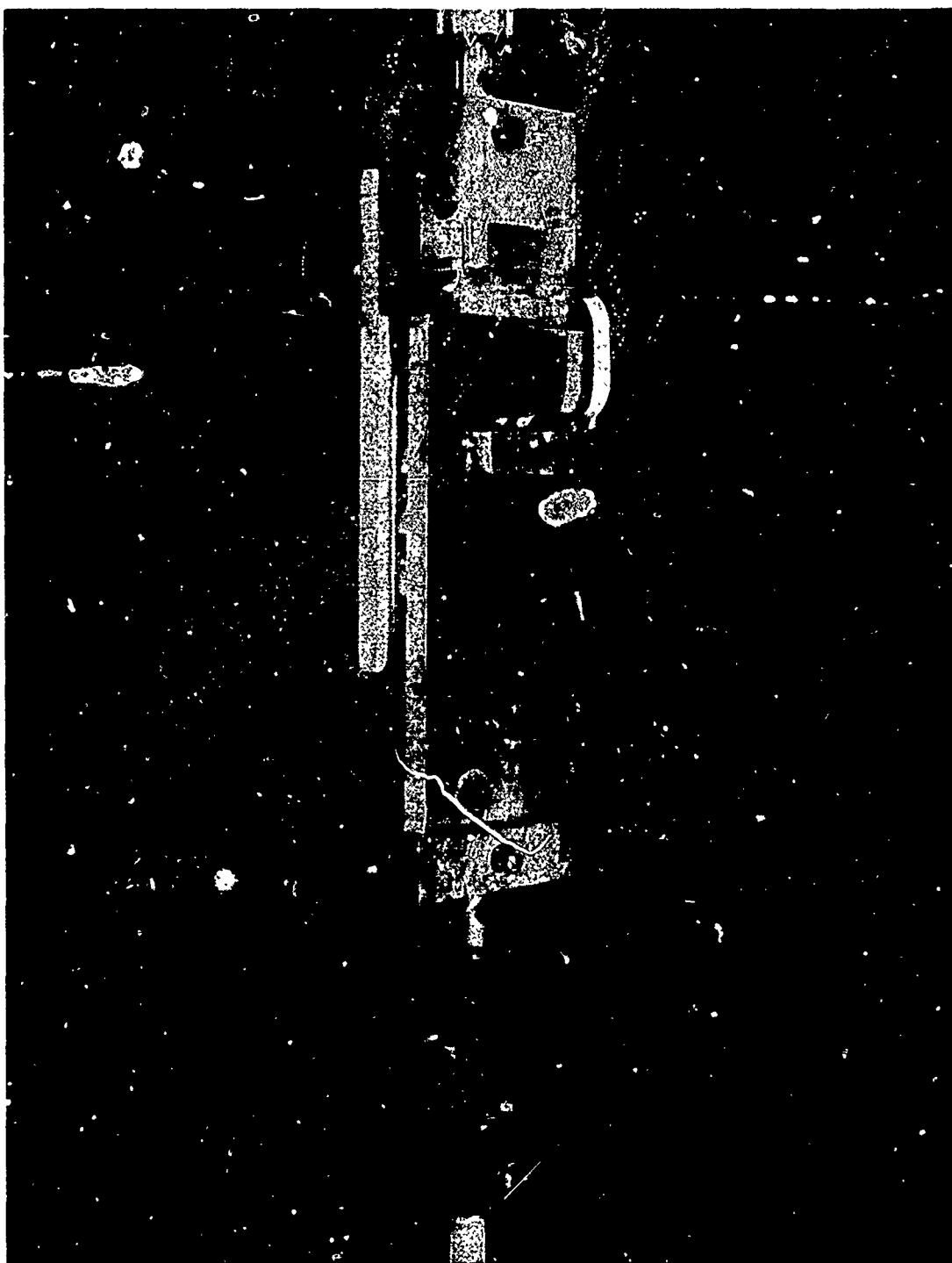


Figure 97 Panel Shear Apparatus

The testing was done in either a hydraulically operated Research Incorporated Model 6566 Universal Testing Machine with 10,000-lb capacity or a mechanically operated Baldwin-Emery Model FGT SR-4 Testing Machine with 50,000-lb capacity. The load cell and extensometer outputs were amplified, as required, by Sanborn carrier amplifiers and plotted on the Y and X axes, respectively, of a Moseley Model 2D2A XY plotter or an Electro-Instrument Model 500 XY plotter.

The +250°F tests were conducted in a small oven constructed of composition-glass insulating board and heated by temperature-controlled forced-air blowers (Figure 98). The specimens were mounted with thermocouples at the facings to monitor the temperature and were preheated in a separate chamber. Specimens were gradually heated to the desired temperature and held there during the actual test.

The -200°F tests were conducted in a special stainless-steel refrigerator cooled by liquid nitrogen (Figures 99 and 100). The specimens were instrumented as in the +250°F tests and prechilled to approximately -110°F with dry ice. Temperature during the actual test was regulated by controlling the flow of liquid nitrogen into the refrigerator.

b. Test Procedure

- (1) Measure and record specimen dimensions.
- (2) Sandblast shear plates.
- (3) Lightly sand both specimen faces (one face only on material B).
- (4) Thoroughly clean specimen and cement to shear plates with epoxy. Install thermocouples if required.
- (5) Attach mounted specimen to mounting blocks.
- (6) Mount extensometer gage blocks.
- (7) If required, preheat or prechill mounted specimen.
- (8) Install mounted specimen in test linkage. Install extensometer and connect output cable.
- (9) If required, bring oven or refrigerator to test temperature as monitored by internal thermocouples.
- (10) If required, verify and adjust load cell and extensometer scales by shunting proper transducer bridge legs with calibration resistors.
- (11) Operate testing machine to gradually apply load until specimen failure.
- (12) Remove specimen and note or measure any anomalies of the failure.

c. Test Results

Test results for the individual specimens of several materials are presented in Tables XXVI through XXX. In addition, average value and the percent deviation of the minimum value from the average are given. Average values of all materials are listed in Table XXXI.

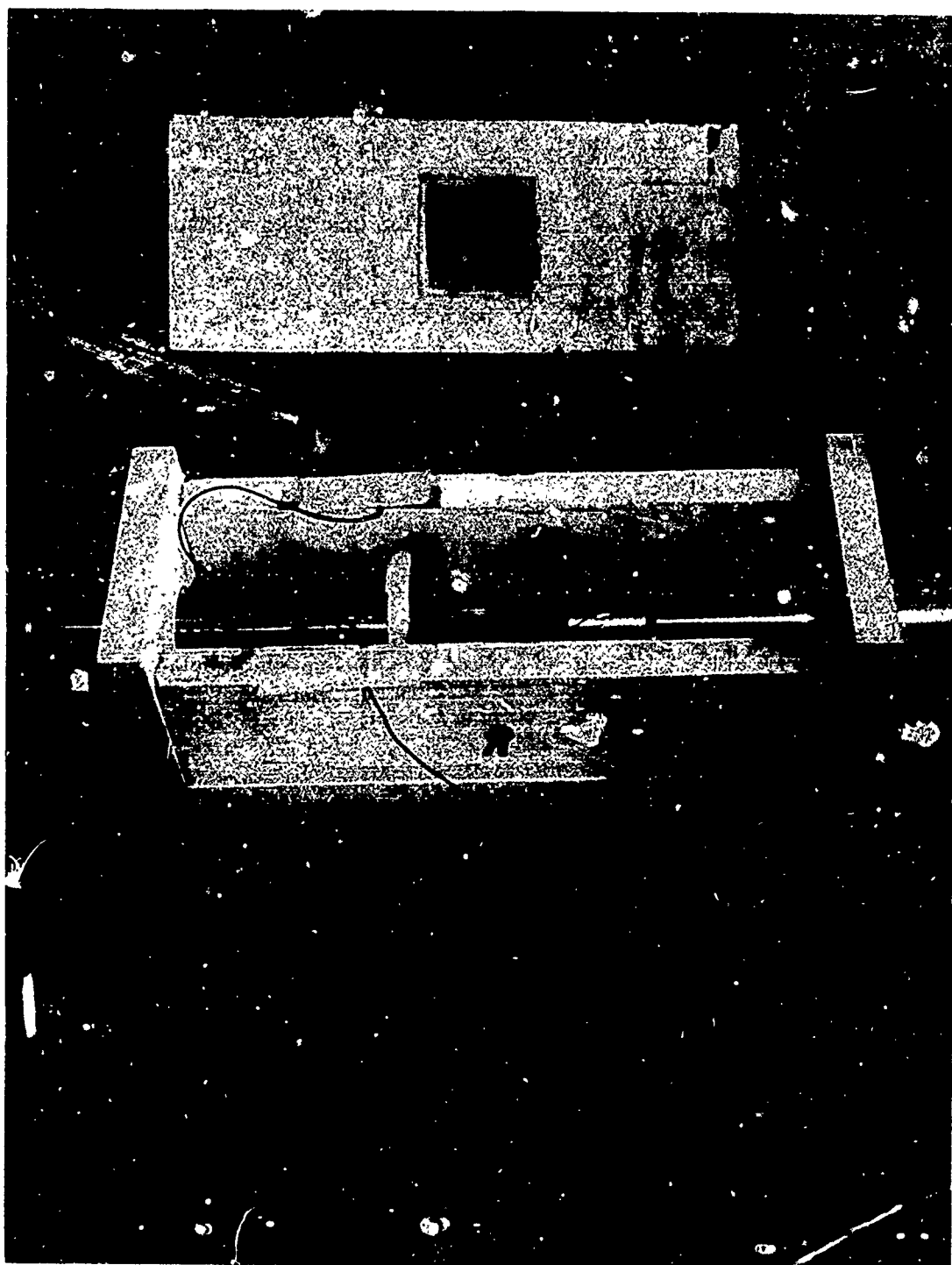


Figure 98 Elevated Temperature Oven (Shown in Core Compression Configuration)

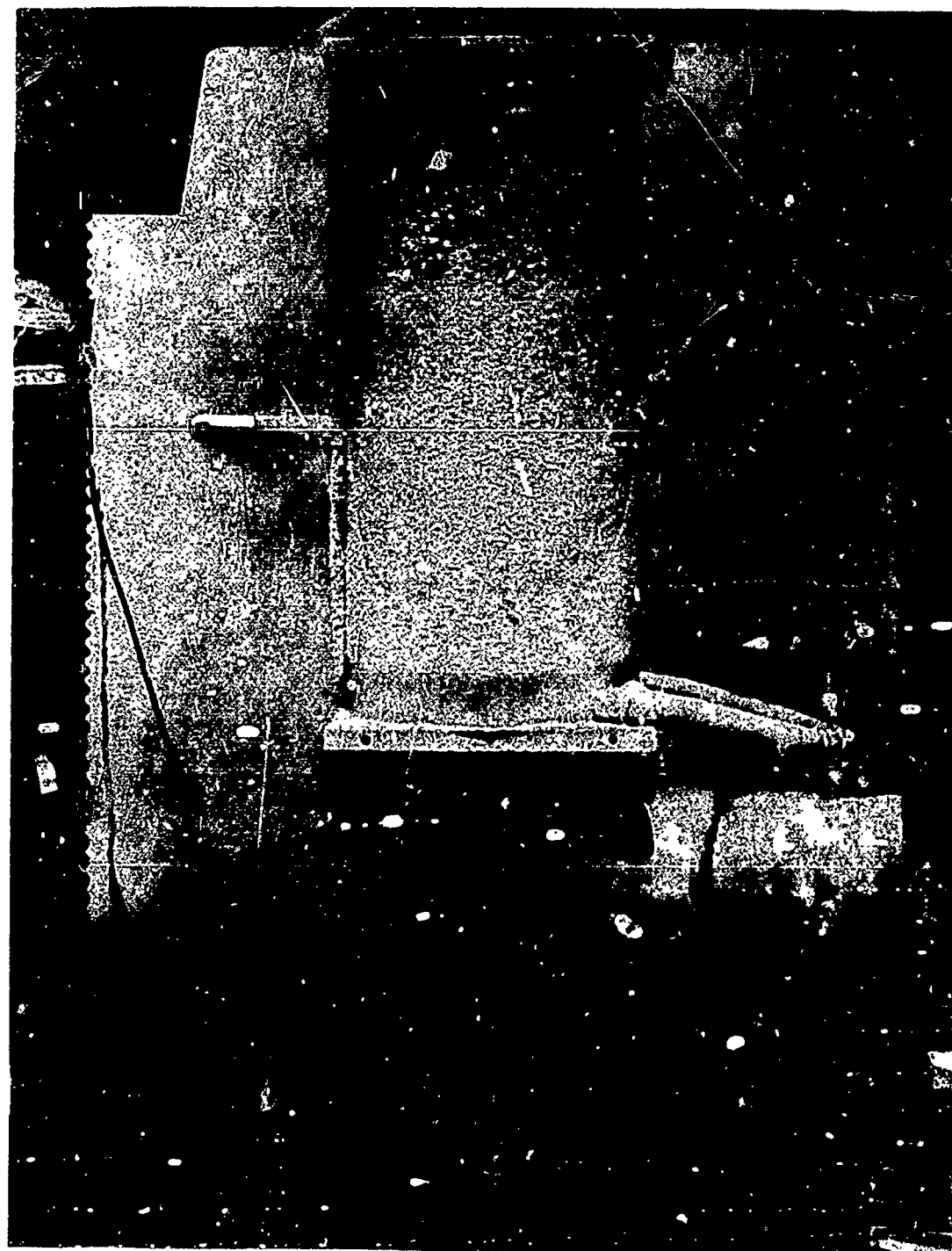


Figure 99 Cryogenic Refrigerator

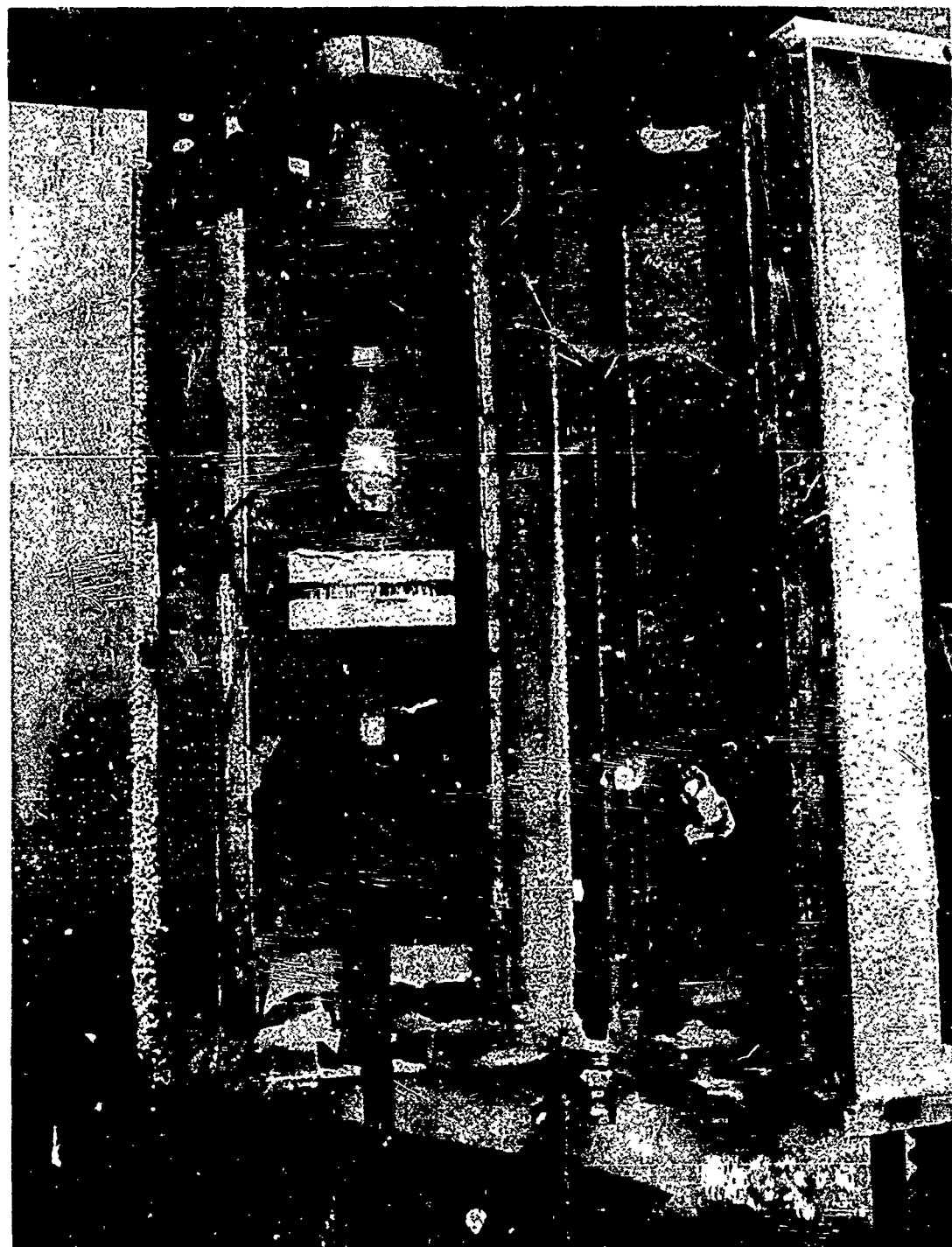


Figure 100 Cryogenic Refrigerator – Internal View
(Shown in Facing Separation Configuration)

d. Comments and Interpretation of Results

Material A (Table XXVI). Like most tested materials, this material had a relatively small data scatter at -200°F, a larger scatter at room temperature, and the greatest scatter at +250°F. The exception to this characteristic was seen in the tests with specimen AJ-3 in which the load increased to 17.8 psi and then dropped to approximately 16.7 psi. At that point, the load started increasing again until a maximum of approximately 59 psi was reached with approximately 12.7 percent strain.

Room-temperature average values in Table XXVI include AJ-3, since established criteria require that the first maximum be used to calculate maximum stress and final strain.

A failure typical of the room temperature and +250°F tests is shown in Figure 101. It should be noted that the failure occurred in the cement between the facing and the honeycomb material. Figure 102 shows that at -200°F partial failure of honeycomb material also occurred. The lightening hole shown at the top of Figure 102 is 1.5 in. in diameter. This reduces the effective shear area of the test specimen by approximately 18 percent. Under normal conditions, such holes are placed on 2.3-in. centers and effectively reduce the surface area by approximately 33 percent. Thus any honeycomb material in this area contributes very little to the strength of the material.

Table XXVI. Material A - Panel-Shear Test

Temperature	Specimen designation	Modulus G (psi)	Elastic limit (psi)	Maximum stress (psi)	Final strain (%)
-200°F	AJ-8	4.25×10^3	30.1	111.4	4.00
	AJ-9	4.51×10^3	47.5	87.8	5.06
	AJ-10	3.83×10^3	25.3	80.9	4.42
	Average	4.20×10^3	35.6	93.4	4.49
	Deviation	(8.8%)	(17.7%)	(3.1%)	(10.9)
Room temperature	AJ-1	3.12×10^3	13.50	56.5	6.78
	AJ-2	2.86×10^3	7.01	115.2	7.90
	AJ-3	2.69×10^3	8.50	17.8	1.09
	Average	2.89×10^3	9.67	63.2	5.26
	Deviation	(6.9%)	(17.2%)	(71.9%)	(78.9)
+250°F	AJ-6	2.20×10^3	3.31	5.06	0.46
	AJ-7	4.38×10^3	3.99	4.69	2.98
	AJ-8	1.19×10^3	1.59	3.69	1.60
	Average	2.92×10^3	2.96	4.48	1.68
	Deviation	(59.2%)	(46.2%)	(17.6%)	(72.6)

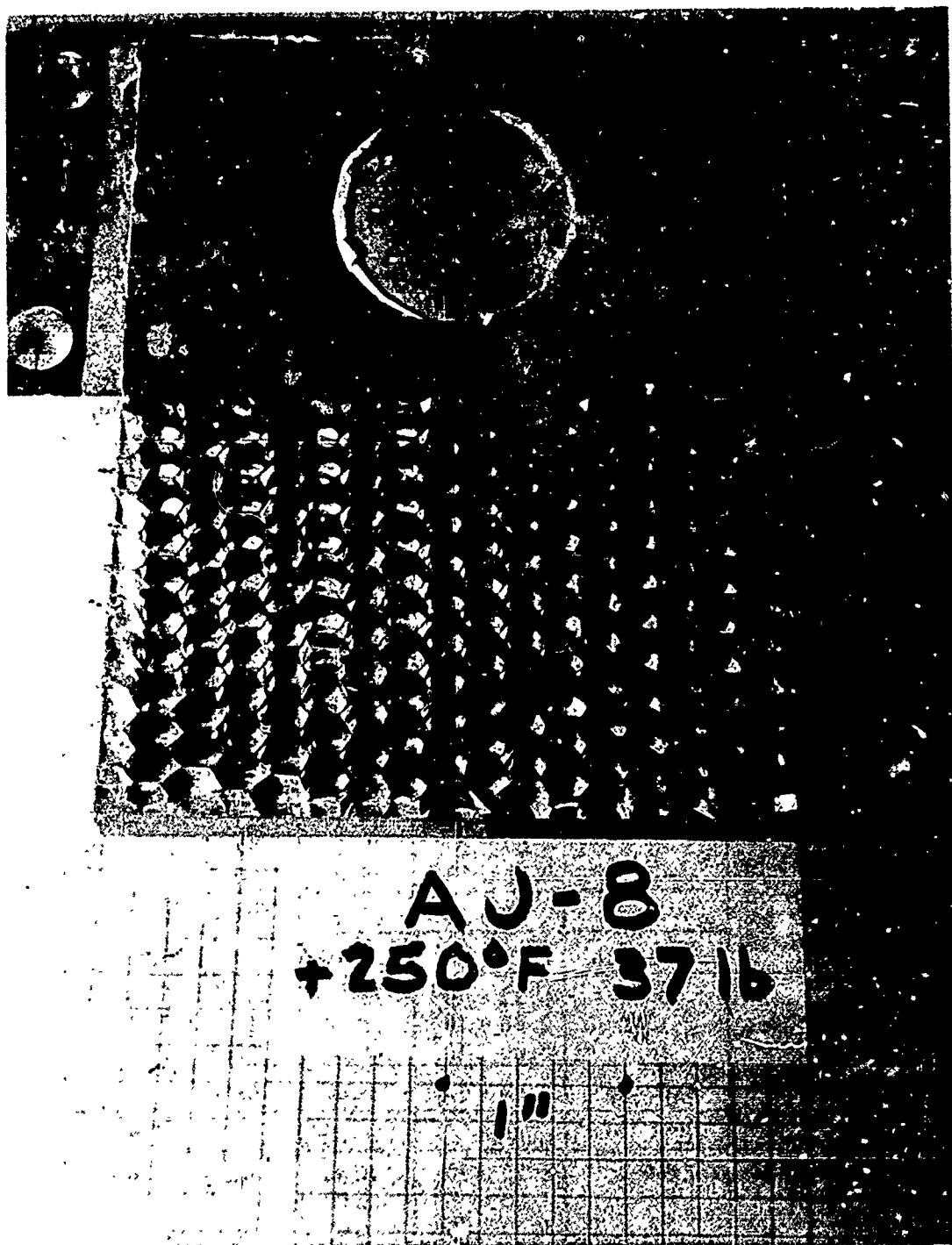


Figure 101 Material A (AJ-8) – Panel Shear

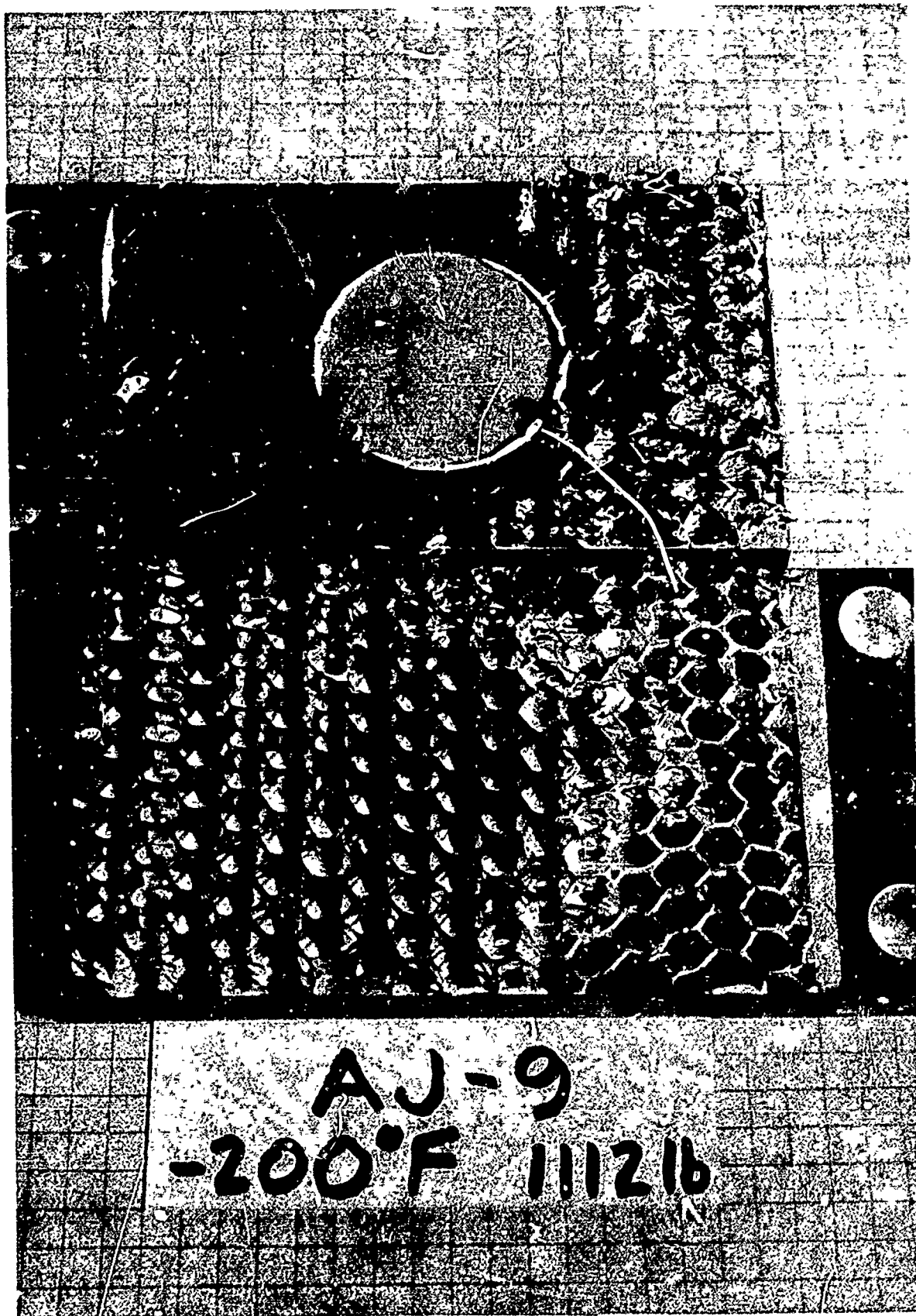


Figure 102 Material A (AJ-9) – Panel Shear

Material B (Table XXVII). The properties of this material, a plastic foam sandwiched between an electroformed nickel facing and a thin mylar backing, are given in Table XXVII. Examination of the failure modes in this material (Figures 103, 104, and 105) indicate that the glue bond between the foam and the mylar backing deteriorates severely with cold and the foam itself becomes the weakest component with increasing temperature.

Table XXVII. Material B - Panel-Shear Test

Temperature	Specimen designation	Modulus G (psi)	Elastic limit (psi)	Maximum stress (psi)	Final strain (%)
-200° F	BJ-6	222	2.82	4.32	2.40
	BJ-9	462	1.15	2.13	1.04
	BJ-10	216	2.24	3.23	1.66
	Average	300	2.07	3.23	1.70
Room temperature	Deviation	(28.0%)	(44.4%)	(34.1%)	(38.8)
	BJ-1	753	1.32	6.01	2.68
	BJ-2	251	7.67	7.67	3.19
	BJ-3	216	7.70	7.70	3.58
+250° F	Average	407	5.56	7.13	3.15
	Deviation	(47.0%)	(78.9%)	(15.7%)	(14.9)
	BJ-4	152	1.17	7.55	6.37
	BJ-5	148	2.86	6.87	5.44
	BJ-11	290	-	12.14	5.04
	Average	197	2.02	8.85	5.62
	Deviation	(24.9%)	(42.1%)	(22.4%)	(10.3)

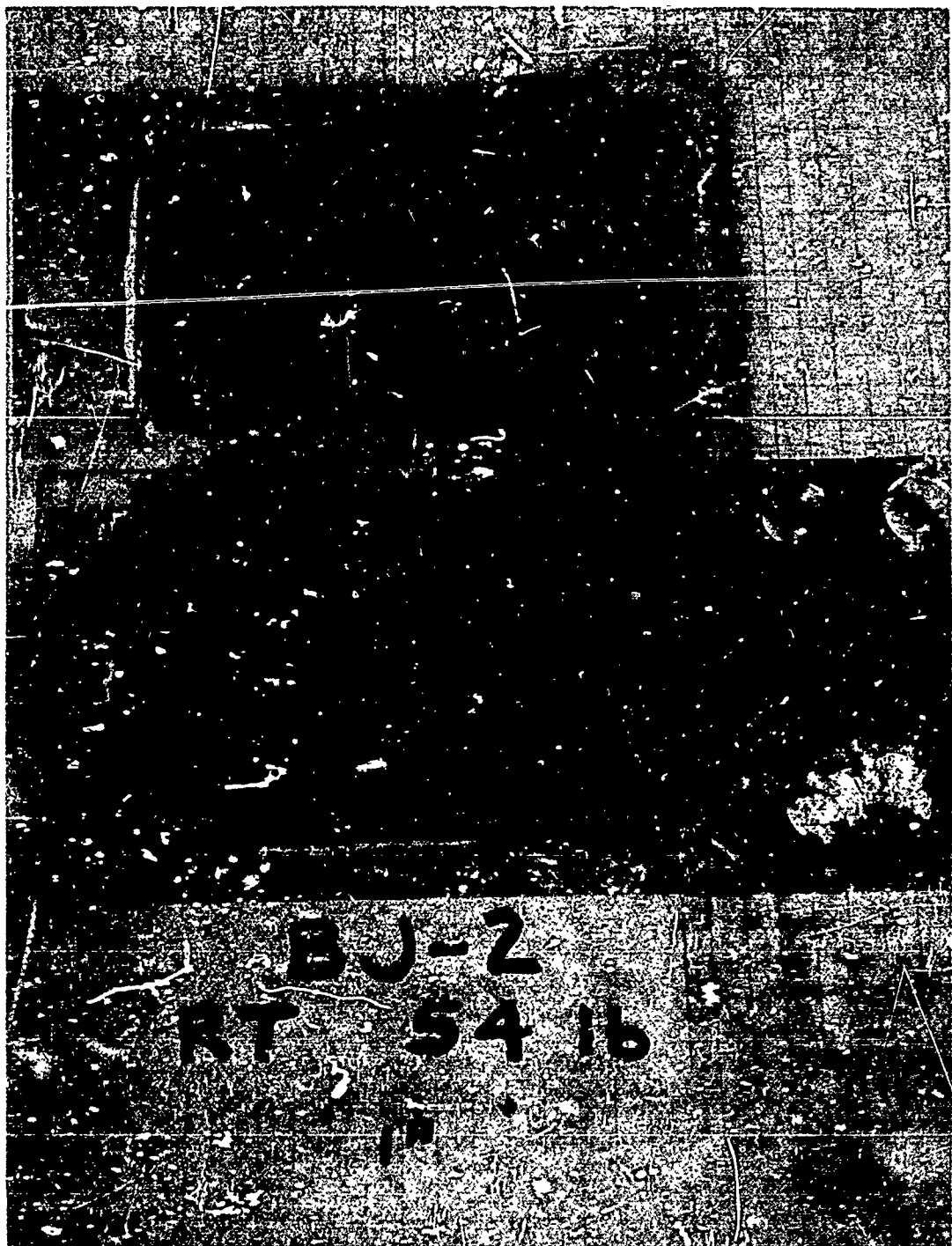
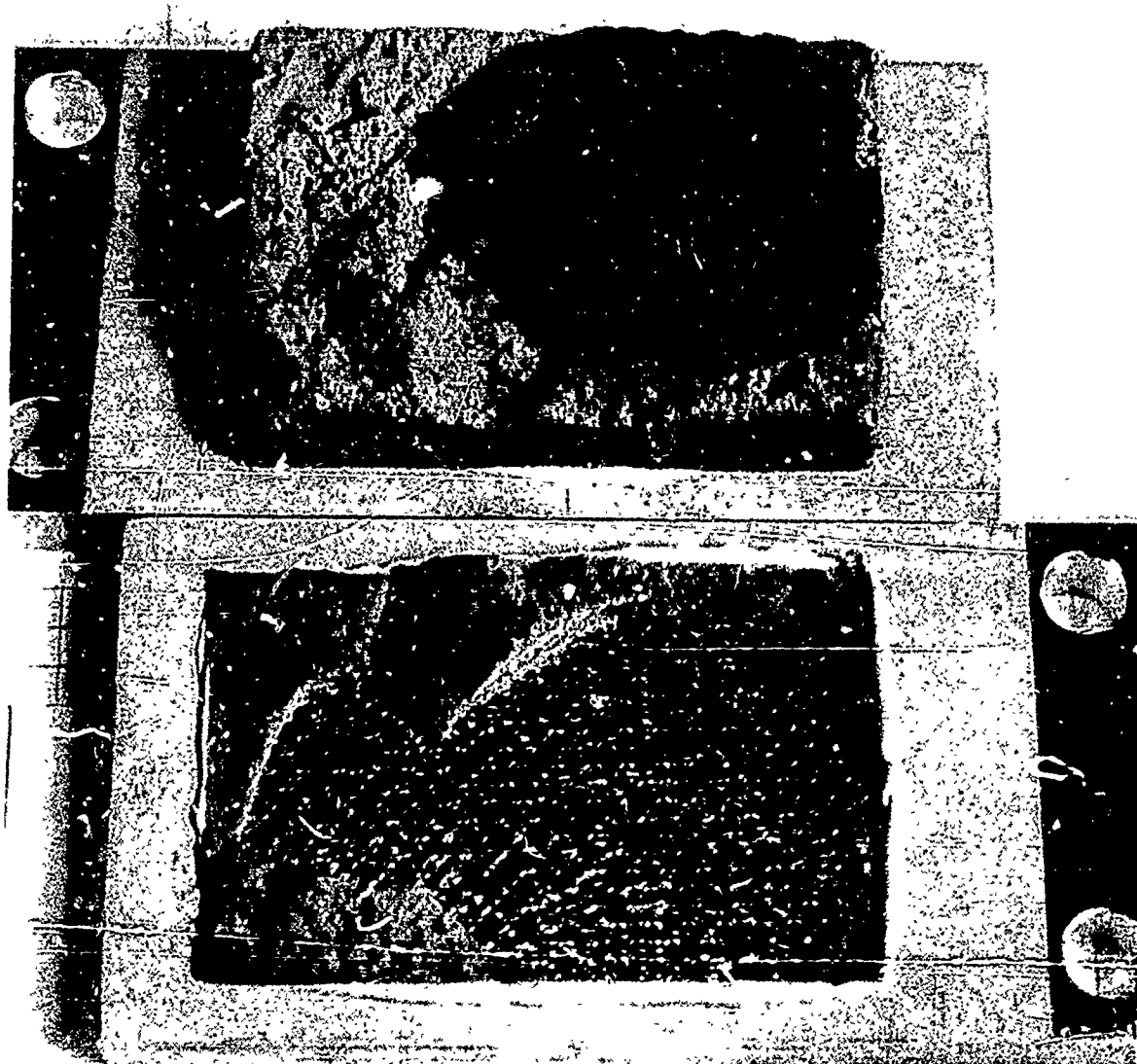


Figure 103 Material B (BJ-2) -- Panel Shear



BJ-6
-200°F 26 LB

Figure 104 Material R (BJ-6) - Panel Shear

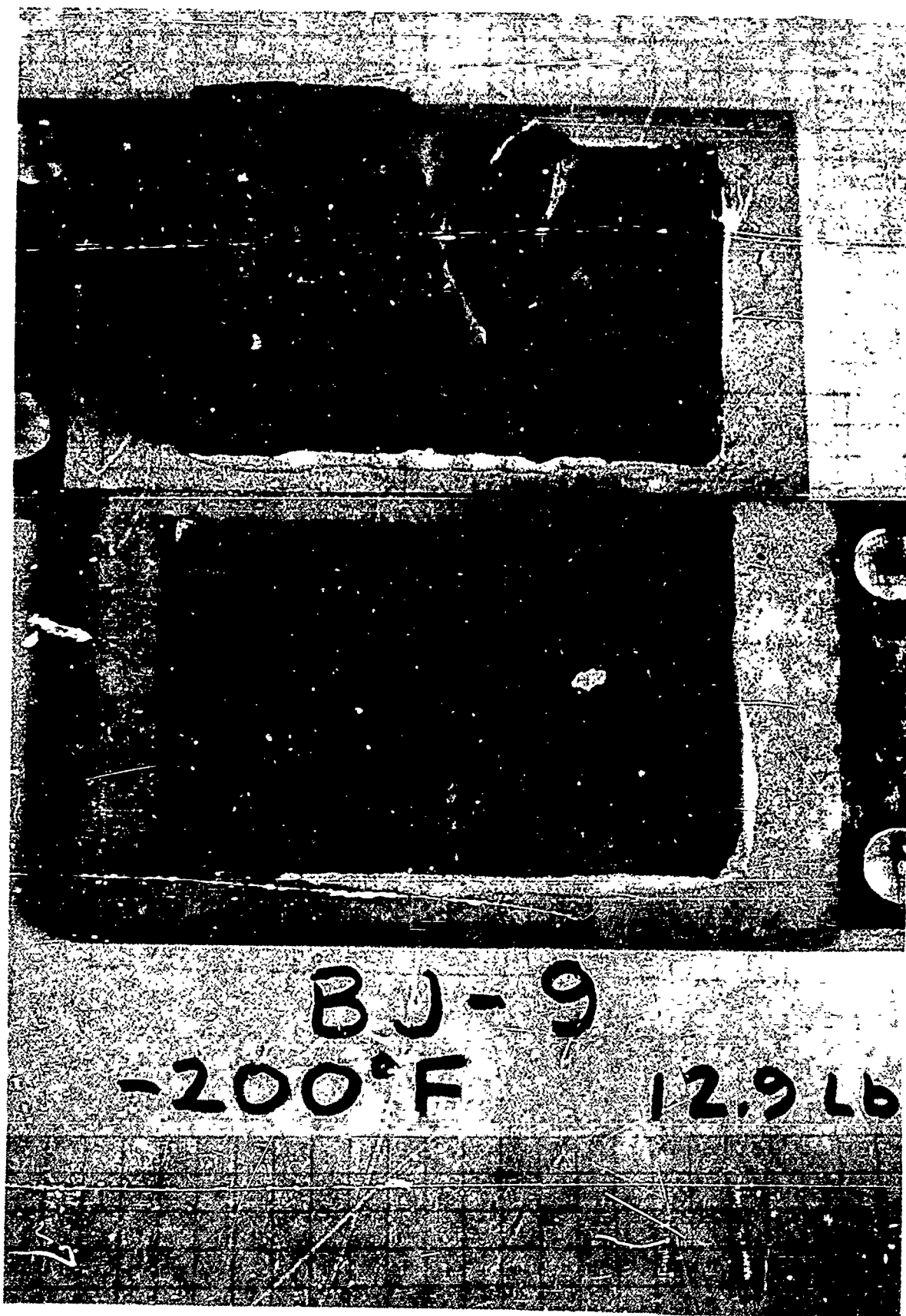


Figure 105 Material B (BJ-9) – Panel Shear

Material C (Table XXVIII). This material exhibits fairly uniform qualities at -200°F and room temperature but seems to deteriorate at the facing-honeycomb glue line at +250°F as seen in Figures 106 and 107. This fact is indicated in the data by the sharp decrease in modulus and maximum stress at elevated temperature.

Table XXVIII. Material C - Panel-Shear Test

Temperature	Specimen designation	Modulus G (psi)	Elastic limit (psi)	Maximum stress (psi)	Final strain (%)
-200° F	CJ-7	6.08×10^3	147	248	5.73
	CJ-8	7.66×10^3	121	246	5.26
	CJ-9	7.58×10^3	56.8	245	6.96
	Average	7.11×10^3	108	246	5.98
	Deviation	(14.5%)	(47.2%)	(0.4%)	(13.7)
Room temperature	CJ-1	6.78×10^3	26.6	205	9.49
	CJ-2	7.12×10^3	38.7	212	6.18
	CJ-3	5.66×10^3	19.3	206	5.94
	Average	6.52×10^3	28.2	208	7.20
	Deviation	(13.2%)	(31.6%)	(1.4%)	(17.5)
+250° F	CJ-4	2.49×10^3	21.40	53.5	8.16
	CJ-6	—	—	54.5	1.56
	CJ-13	3.26×10^3	22.60	71.3	6.22
	CJ-14	2.59×10^3	16.75	76.0	4.90
	Average	2.78×10^3	20.25	63.8	5.25
	Deviation	(11.6%)	(20.9%)	(16.2%)	(70.3)



Figure 106 Material C (CJ-3) – Panel Shear

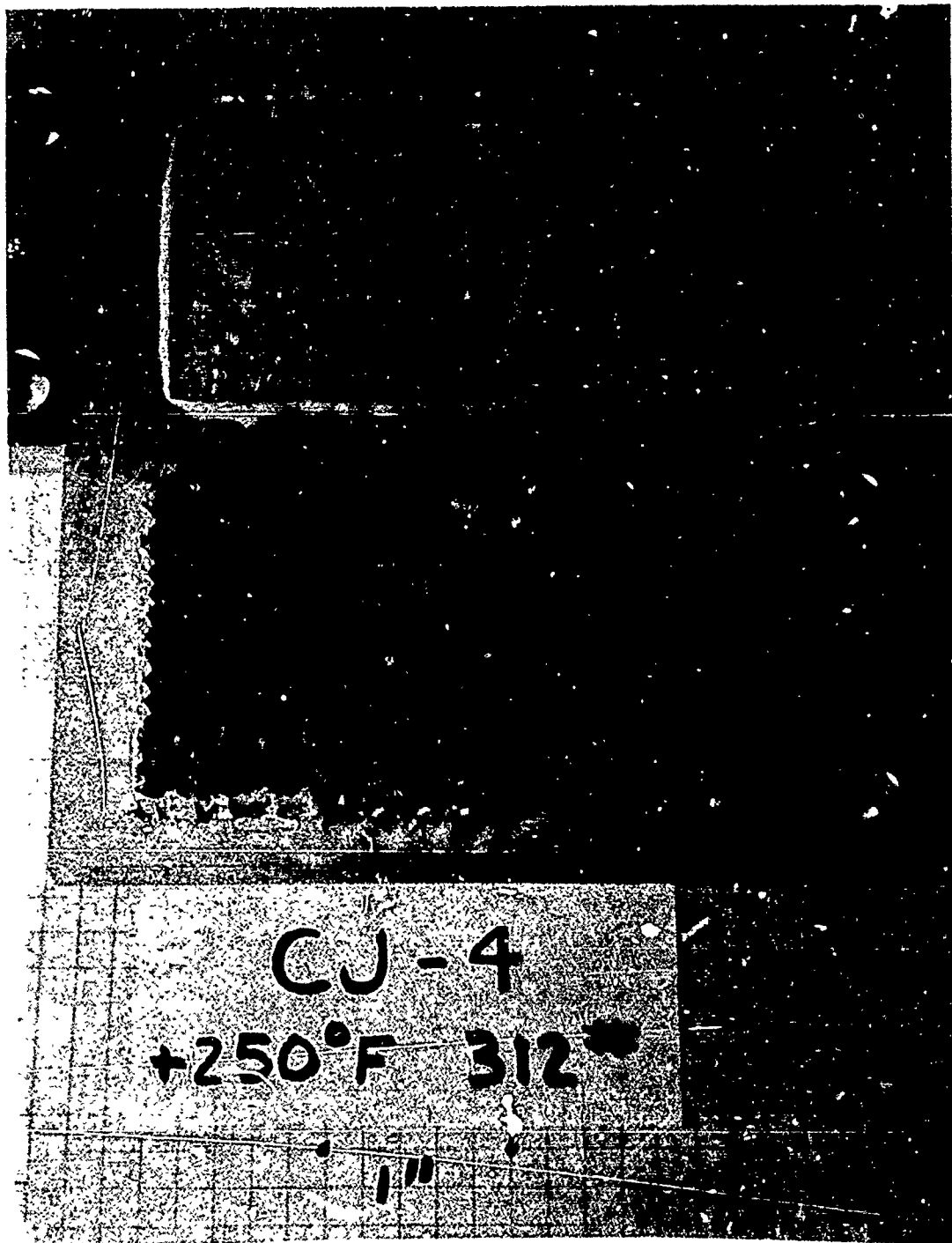


Figure 107 Material C (CJ-4) – Panel Shear

Material D (Table XXIX). This material, while demonstrating specimen uniformity by the very small data scatter, appears to decay quite rapidly as temperature is increased. At -200°F, fairly high maximum stress and modulus were noted and failure was caused by cell buckling. However, at room temperature these values had dropped by more than 50 percent and the failures occurred at the glue line. At +250°F the modulus and maximum stress had dropped further to approximately 5 percent of the values at -200°F. The failure mode at +250°F was the same as at room temperature and is shown in Figures 108 and 109. It should be noted that there was no correlation possible between the failure of Figure 108 where the cement partially remained on the facing and Figure 109 where no cement remained on the facing. These two types of failures seemed to occur randomly at both +250°F and room temperature.

Table XXIX. Material D – Panel-Shear Test

Temperature	Specimen designation	Modulus G (psi)	Elastic limit (psi)	Maximum stress (psi)	Final strain (%)
-200°F	DJ-7	5.83×10^3	22.3	86.1	2.43
	DJ-8	5.69×10^3	25.0	92.8	2.31
	DJ-9	4.71×10^3	26.6	91.3	2.85
	Average	5.41×10^3	24.6	90.1	2.53
Room temperature	Deviation	(12.9%)	(9.4%)	(4.4%)	(8.7)
	DJ-1	2.52×10^3	13.40	46.8	8.17
	DJ-2	2.29×10^3	12.25	44.3	9.40
	DJ-3	2.21×10^3	14.40	38.6	7.18
	Average	2.34×10^3	13.35	43.2	8.58
+250°F	Deviation	(5.5%)	(7.9%)	(10.7%)	(16.3)
	DJ-4	830	2.82	6.15	1.06
	DJ-5	2,300	2.18	5.58	0.55
	DJ-6	1,530	1.71	5.22	0.52
	Average	1,553	2.24	5.65	0.71
	Deviation	(46.6%)	(23.6%)	(7.6%)	(26.8)

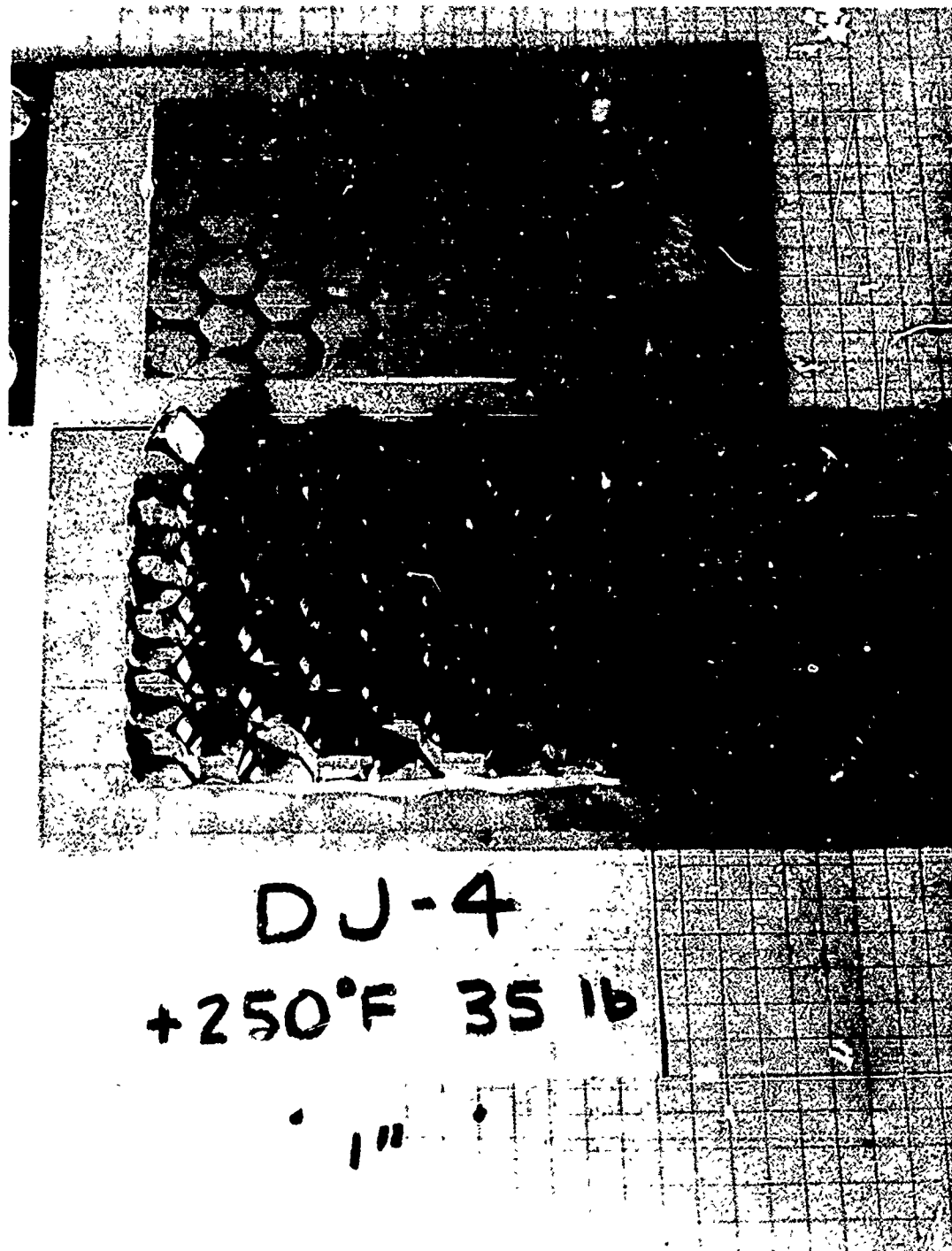


Figure 108 Material D (DJ-4) – Panel Shear



Figure 109 Material D (DJ-6) – Panel Shear

Material G (Table XXX). Data obtained for this material indicate that the material glue line deteriorates very badly at elevated temperatures. Further deterioration in the form of glue-line brittleness was noted in the -200°F tests. Lack of samples at the various temperatures was caused by the extreme fragility of the material, which would often fail during the heating or cooling process or even while the specimen was being prepared for test.

Table XXX. Material G – Panel-Shear Test

Temperature	Specimen designation	Modulus G (psi)	Elastic limit (psi)	Maximum stress (psi)	Final strain (%)	Thickness (in.)
-200°F	GJ-14	588	1.00	1.00	0.17	1.0
Room temperature	GJ-1	555	3.08	5.10	1.72	0.5
	GJ-2	—	—	5.50	1.41	0.5
	GJ-18	349	1.21	2.50	0.96	1.0
	GJ-19	330	—	2.77	1.15	1.0
+250°F	GJ-3	—	—	(a)	—	0.5
	GJ-12	—	—	(a)	—	1.0

(a) Failure occurred with approximately 3-lb fixture weight.

Table XXXI. Panel-Shear-Test Summary

Temperature	Material designation	Modulus G Average (psi)	Modulus G Deviation (%)	Elastic limit Average (psi)	Elastic limit Deviation (%)	Maximum stress Average (psi)	Maximum stress Deviation (%)	Final strain Average (%)	Final strain Deviation (%)
-200°F	A	4.20 × 10 ³	8.8	35.6	17.7	93.4	3.1	4.49	10.9
	B	300	28.0	2.07	44.4	3.23	34.1	1.70	38.8
	C	7.11 × 10 ³	14.5	108.0	47.2	246	0.4	5.98	13.7
	D	5.41 × 10 ³	12.9	24.6	9.4	90.1	4.4	2.53	8.7
	G(a)	588	—	1.00	—	1.00	—	0.17	—
Room temperature	A	2.89 × 10 ³	6.9	9.67	17.2	63.2	71.9	5.26	78.9
	B	407	47.0	5.56	78.9	7.13	15.7	3.15	14.9
	C	6.52 × 10 ³	13.2	28.2	31.6	208	1.4	7.20	17.5
	D	2.34 × 10 ³	5.5	13.35	7.9	43.2	10.7	8.58	16.3
	G(a)	340	2.9	1.21	—	2.64	5.3	1.05	8.6
+250°F	A	2.92 × 10 ³	59.2	2.96	46.2	4.48	17.6	1.68	72.6
	B	197	24.9	2.02	42.1	8.85	22.4	5.62	10.3
	C	2.78 × 10 ³	11.6	20.25	20.9	63.8	16.2	5.25	70.3
	D	1,553	46.6	2.24	23.6	5.65	7.6	0.71	26.8
	G(b)	—	—	—	—	—	—	—	—

(a) 1.00-in. thick specimens.

(b) No valid tests completed.

3. PANEL BEND

Panel-bend tests of the candidate materials were conducted at room temperature only. In this test, two-point loading of a simply supported beam produced a pure bending moment of uniform magnitude over a central section of the specimen. Deflection was measured with respect to loading points. A plot of deflection versus the load gives a measure of resistance of the beam to bending (EI). This value EI must be divided by b (the width of the beam) to provide a means for comparing the different candidate materials. EI/b is thus the bending stiffness per unit width.

It should be emphasized that E in the term EI/b represents the usual material property known as Young's modulus and I is the geometrical property called the moment of inertia. In this instance, the two are inseparable because all candidate materials consisted of at least two different materials and had a somewhat ill-defined geometry, especially in the vicinity of the facing where the greatest contribution to the numerical value of I takes place. The following expression is used for determining EI from the experimental data:

$$EI = \frac{PL^3}{56.3\Delta}$$

where P and Δ are the total load and corresponding central deflection, L is the span of the beam, and the constant 56.3 applies to a simple beam with half the load P applied at the beam's third points. Other parameters derived from the data were the maximum elastic moment (M_e) per unit width,

$$\frac{M_e}{b} = \frac{P_e L}{6b}$$

where P_e is the elastic limit load, and the ultimate moment (M_u) per unit width

$$\frac{M_u}{b} = \frac{P_u L}{6b}$$

where P_u is the maximum load sustained by the beam.

a. Description of Apparatus

The apparatus used in the panel-bend tests is shown in Figures 110 and 111. The specimen is placed between four hard steel rollers and subjected to a total load, P , as measured by the load cell. The deflection at the center of the specimen is measured by means of a blade deflectometer. Proper load bearing and alignment is provided by the bidirectional pivot located between the load cell and the specimen. An X-Y plot is made of the deflection versus total load. The four small columns around the bidirectional pivot in Figure 111 carry no load and are in place merely to prevent excess moments in the load cell in case the specimen fails suddenly. As in the panel-shear

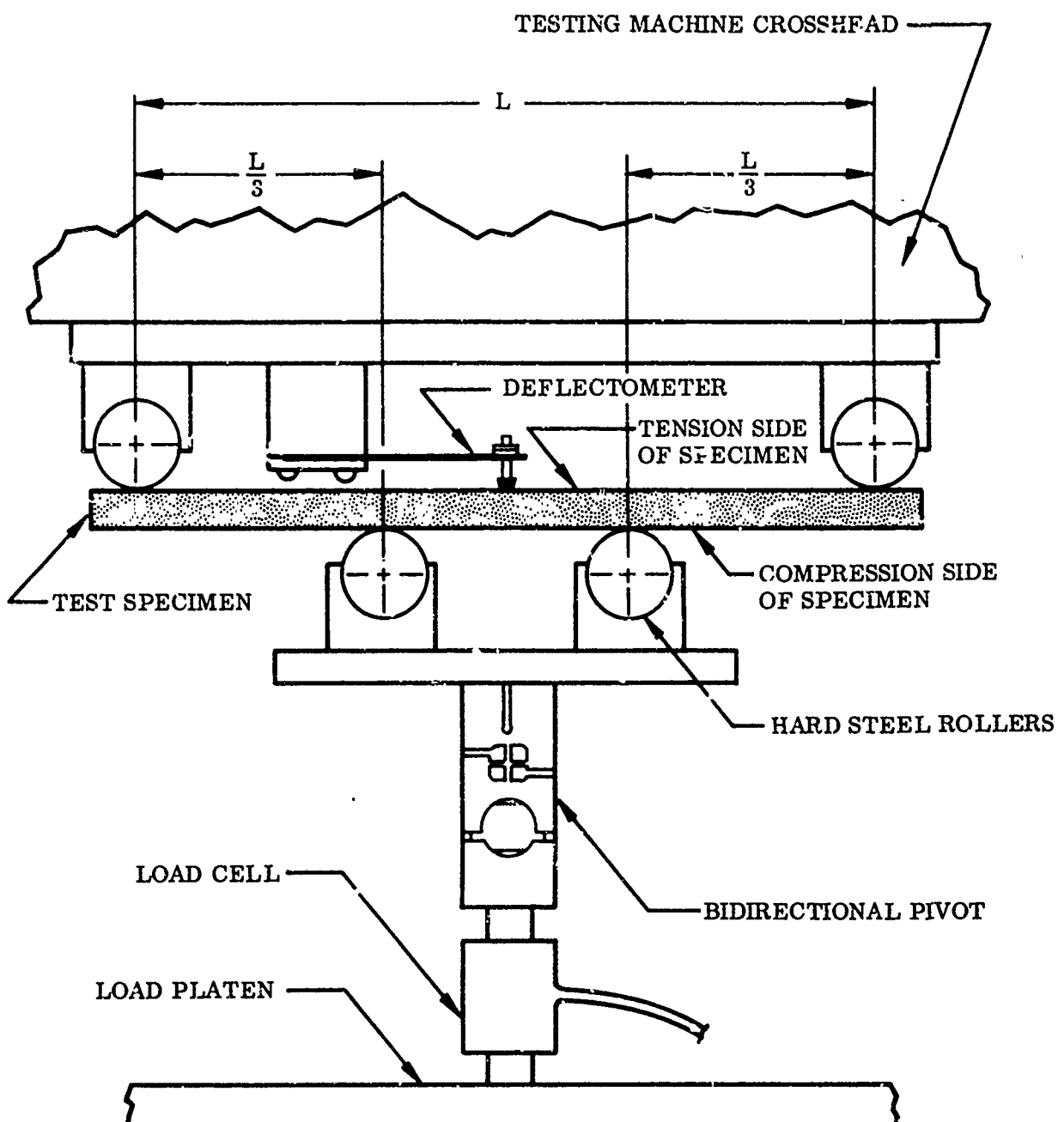


Figure 110 Panel Bend Apparatus Diagram

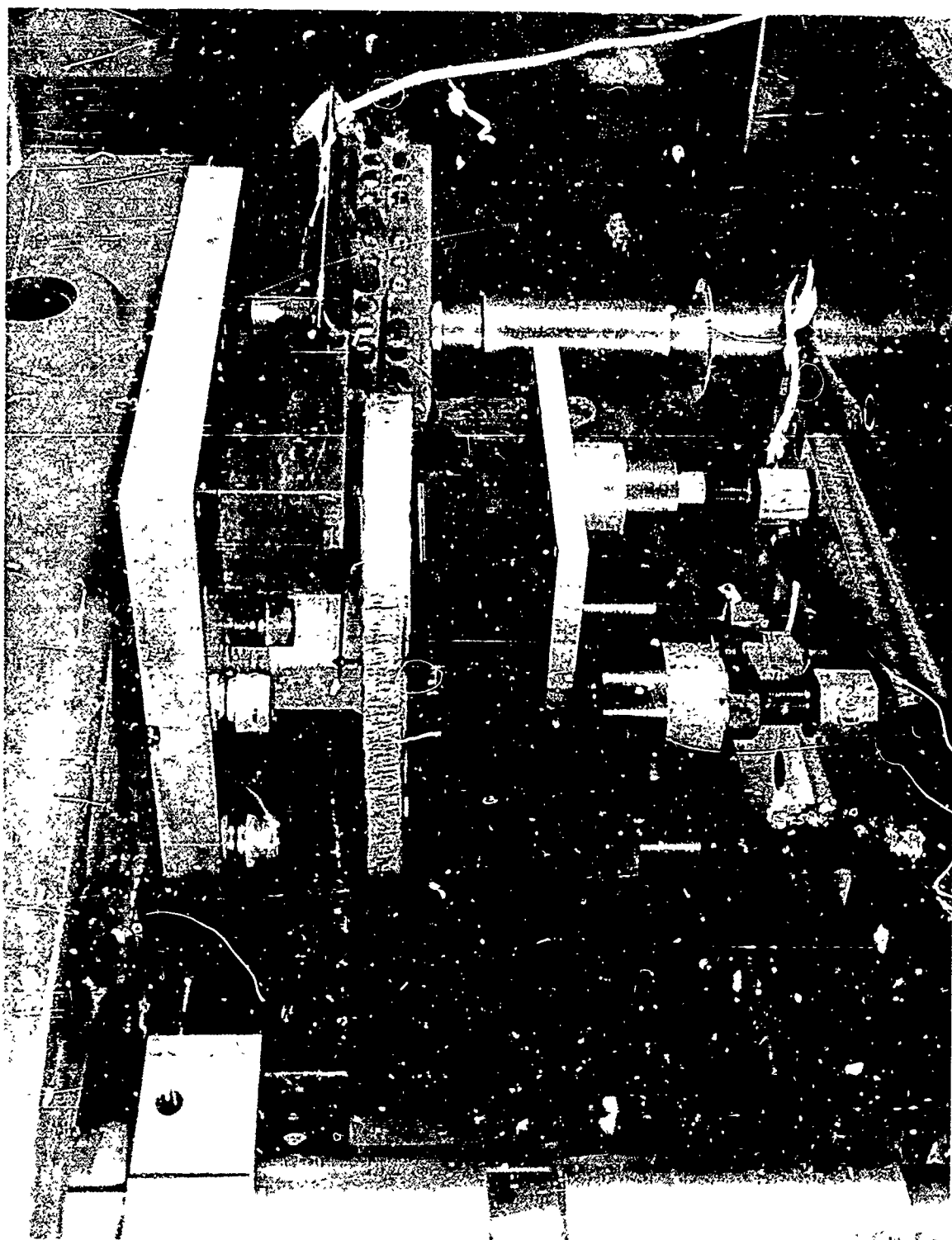


Figure 111 Panel Bend Apparatus

tests, the load cell and deflectometer signals were amplified, as required, with Sanborn carrier amplifiers and recorded on a Moseley 2D2A or Electro-Instruments 500 XY plotter.

b. Test Procedure

- (1) Measure and record average specimen thickness, width, and length.
- (2) Adjust outer hard-steel rollers for proper distance, $L = 6.00, 9.00$, or 12.00 in., depending on specimen size.
- (3) Adjust inner hard-steel rollers for proper spacing $L/3 = 2.00, 3.00$, or 4.00 in.
- (4) If required, verify and adjust load cell and deflectometer scales by shunting proper transducer bridge legs with calibration resistors.
- (5) Operate testing machine to apply load gradually until specimen failure or machine travel limits are reached.
- (6) Examine tested specimen for failure mode and any anomalies that may be present.

c. Test Results

Test results for the six tested materials are shown in Tables XXXII to XXXVII for the individual specimens and collectively in Table XXXVII. Nonsymmetrical specimens were subjected to bending in both directions as noted on the individual data sheets. However, only the weakest bending mode is tabulated in Table XXXVIII.

d. Comments and Interpretation of Results

Material A (Table XXXII). As can be seen in Table XXXII, the 0.75-in.-thick material is far superior to the 0.25-in.-thick material. In both cases, the weakest bending mode was that which placed the back face (or facing with the cutouts) in compression (cutouts down in Figure 110). The different types of failures are illustrated in Figures 112 and 113. Specimens AK-1 and AK-3, tested with the back face in compression, failed by back-face buckling where the cutout produced the narrowest section. Specimens AK-2, AK-4, and AK-6, tested with the back face in tension, failed by a tensile fracture of the facing, again coincident with the center of a cutout. Specimens AK-5, AK-7, and AK-8, tested with the back face in compression, failed by back-face buckling coincident with the centers of the two inner cutouts.

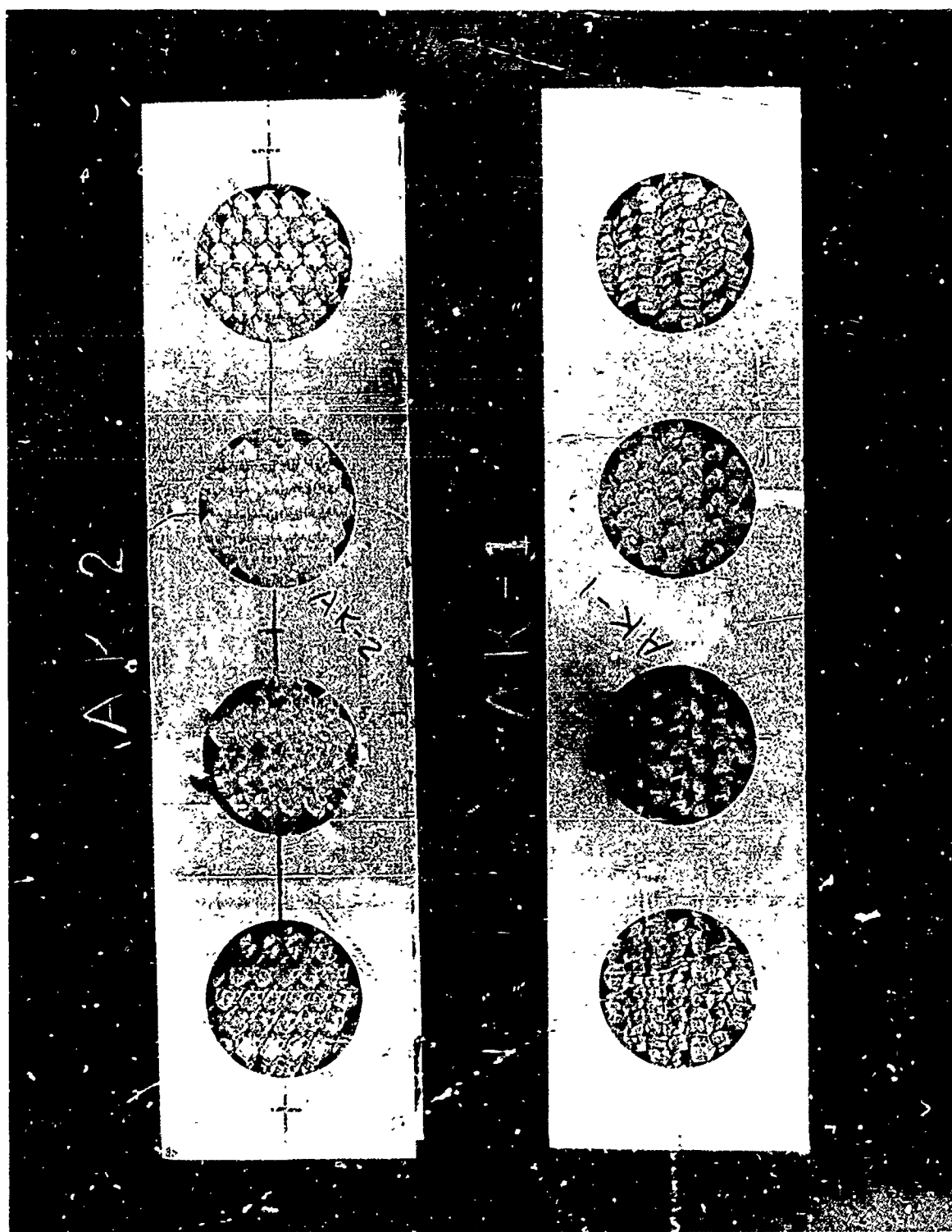


Figure 112 Material A (AK 1,2) – Panel Bend

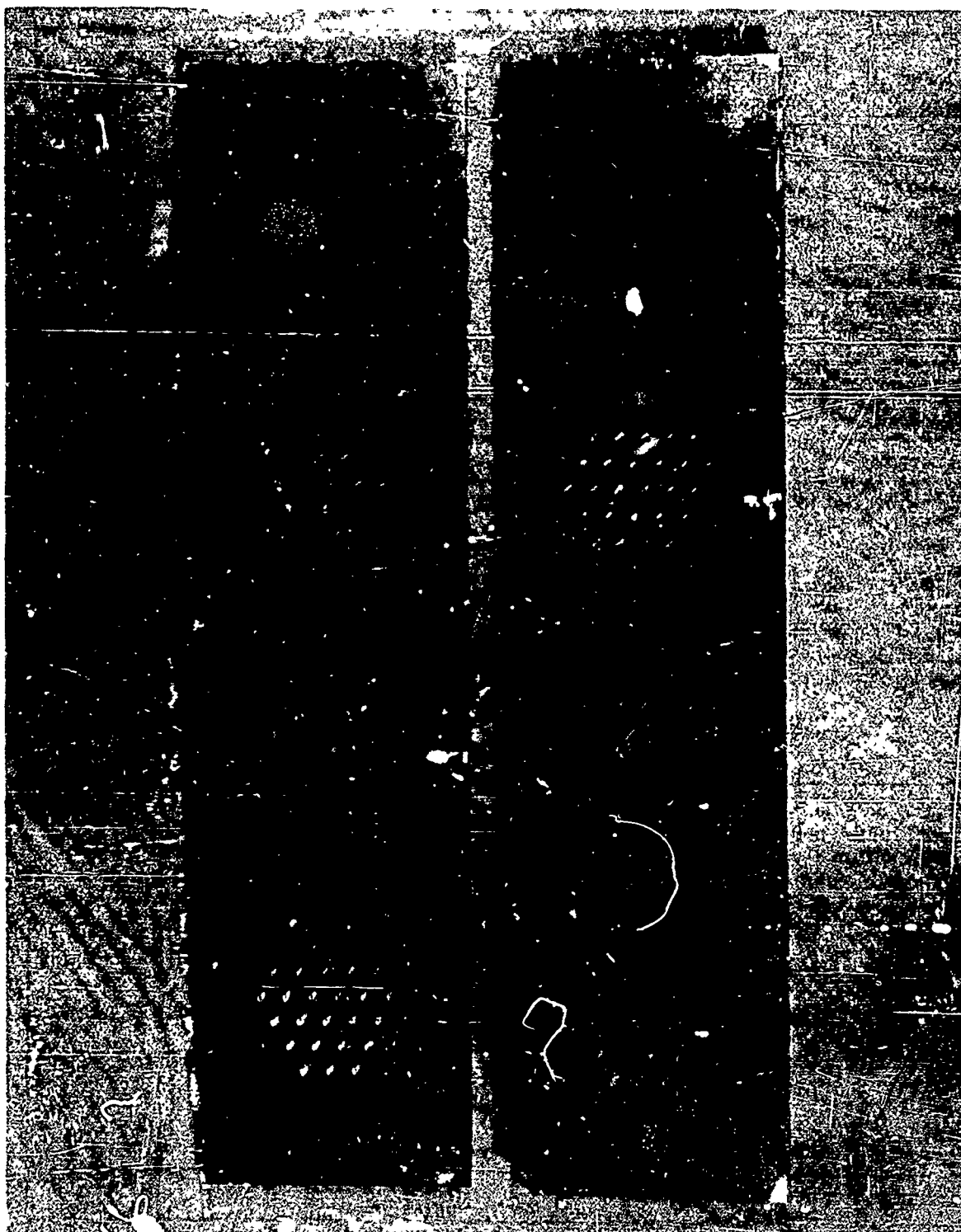


Figure 113 Material A (AK-5, 6) – Panel Bend

Table XXXII. Material A - Panel-Bend Test

Specimen designation	Beam width, b (in.)	Beam span, L (in.)	EI/b (in. 2 -lb/in.)	M_e/b (lb)	M_u/b (lb)	Tension face	Thickness (~ in.)
AK-2	2.50	9	7,350	34.5	54.0	Nonreflecting	0.75
AK-4	2.50	9	7,520	30.0	54.8	Nonreflecting	
AK-1	2.50	9	6,200	16.2	20.2	Reflecting	
AK-3	2.50	9	5,600	9.9	16.3	Reflecting	
Average ^(a)	—	—	5,900	13.0	18.2		
AK-6	2.50	9	905	9.90	18.20	Nonreflecting	0.25
AK-5	2.50	9	835	4.80	7.02	Reflecting	
AK-7	2.50	9	642	4.20	6.12	Reflecting	
AK-8	2.50	9	785	2.40	5.82	Reflecting	
Average ^(a)	—	—	754	3.80	6.32		

(a) Average is for weakest bending mode of each parameter.

Material B (Table XXXIII). The major difficulty with this material, as evidenced by Figures 114 and 115, is the anomalies in the foam filler that are probably caused by either insufficient or improper mixing. As can be seen in the data (Table XXXIII), eight specimens were tested: four were approximately 1-in. thick and four were approximately 0.5-in. thick. Of these eight, all except BK-3 and BK-4 failed as a

Table XXXIII. Material B - Panel-Bend Test

Specimen designation	Beam width, b (in.)	Beam span, L (in.)	EI/b (in. 2 -lb/in.)	M_e/b (lb)	M_u/b (lb)	Tension face	Thickness (~ in.)
BK-2	1.97	9	1,062	12.9	20.1	Nonreflecting	1.0
BK-3	2.00	9	932	11.6	16.7	Nonreflecting	
BK-1	2.00	9	1,360	14.2	18.5	Reflecting	
BK-4	2.02	9	1,450	9.8	16.7	Reflecting	
Average ^(a)	—	—	1,405	12.0	17.6		
BK-6	2.00	9	380	3.0	13.5	Nonreflecting	0.50
BK-8	2.02	9	440	5.9	13.2	Nonreflecting	
BK-5	2.00	9	528	7.5	13.4	Reflecting	
BK-7	2.02	9	399	8.6	11.6	Reflecting	
Average ^(a)	—	—	410	4.4	12.5		

(a) Average is for weakest bending mode of each parameter.

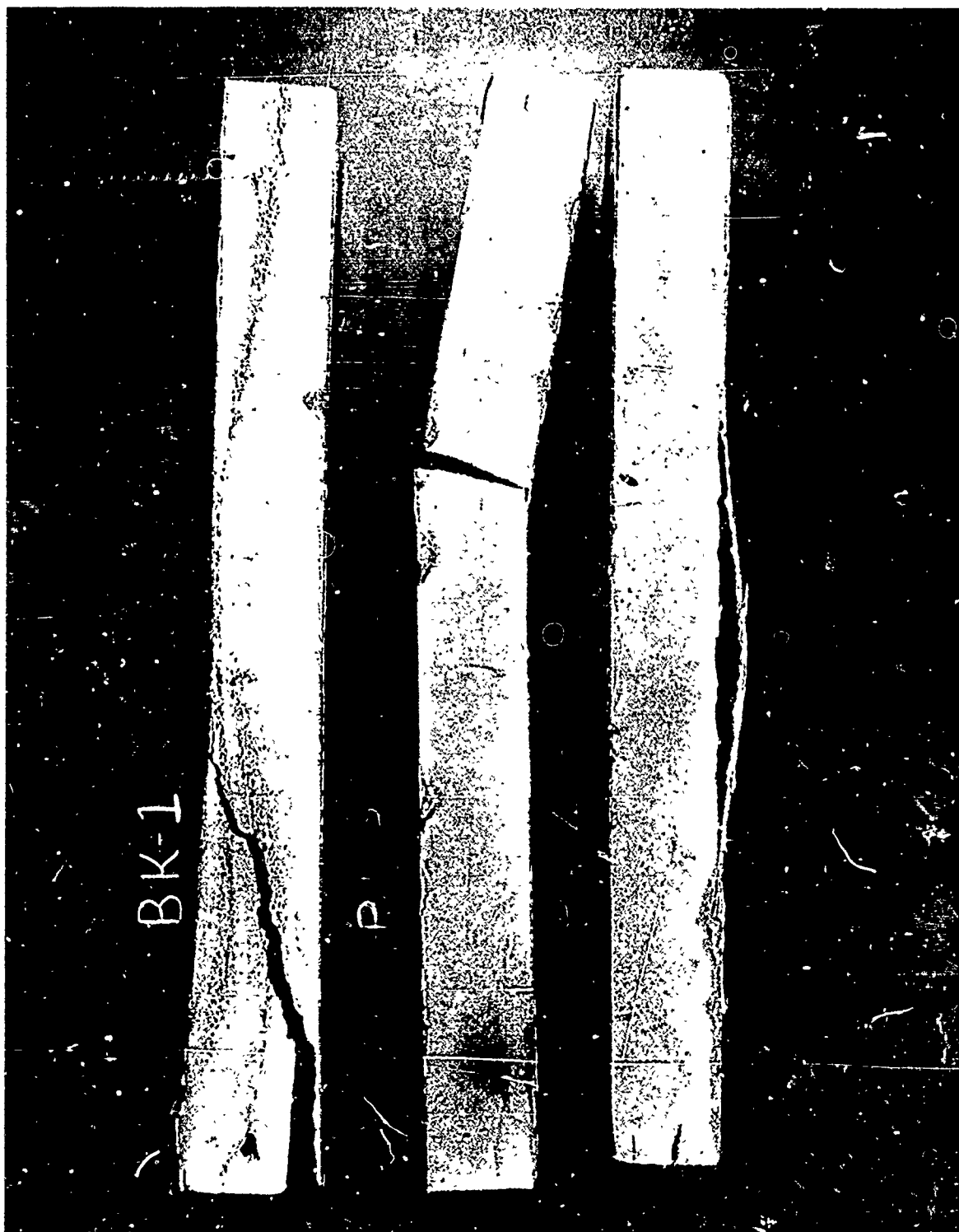


Figure 114 Material B (BK-1, 3, 4) – Panel Bend



Figure 115 Material B (BK-6, 7, 8) – Panel Bend

result of foam shearing at a visible defect in the foam. Visual inspection of BK-3 and BK-4 in Figure 114 indicates no apparent anomalies. Specimen BK-4, in which the reflective face was placed in tension, failed because of tensile failure in the filler near the non-reflecting surface. Specimen BK-3, however, failed by tensile failure of the non-reflecting side when that side was placed in tension. Examination of the data shows that the weakest bending mode was that with the nonreflecting surface in tension.

Material C (Table XXXIV). This material, although it possesses a lower bending stiffness than some of the other materials, had the highest elastic and ultimate moments of all the candidate materials. Specimens CK-1 through CK-4 failed by localized inter-cellular facing buckling (Figure 116). Specimens CK-5 and CK-6 were specimens with a discontinuity. CK-5 failed by buckling at a discontinuity that was in the tension face. Specimens CK-7 and CK-8 were specimens that had facing material seams. CK-7, with the nonreflecting side in tension, failed by buckling of the compression facing at a point removed from the seam. CK-8, with the nonreflecting side in compression, failed by buckling immediately adjacent to the seam. The values presented in summary Table XXXVIII are for specimens CK-1 through CK-4 only.

Table XXXIV. Material C – Panel-Bend Test

Specimen designation	Beam width, b (in.)	Beam span, L (in.)	$\frac{EI/b}{\text{in. } 2\text{-lb}} \text{ in.}$	M_e/b (lb)	M_u/b (lb)	Tension face
CK-1	2.00	9	1,230	23.2	35.2	Back
CK-2	1.95	9	1,200	19.2	20.5	Front
CK-3	1.95	9	1,120	18.5	20.2	Front
CK-4	2.00	9	1,150	15.0	19.1	Front
Average	—	—	1,175	19.0	23.7	
CK-5	1.25	6	1,420	19.2	28.0	(a)
CK-6	1.28	6	1,210	10.5	11.9	(b)
CK-7	1.36	6	1,300	22.0	27.8	(c)
CK-8	1.28	6	1,290	16.8	18.1	(d)

- (a) Specimen with discontinuity in compression.
- (b) Specimen with discontinuity in tension.
- (c) Specimen with lap joint; reflecting surface in compression.
- (d) Specimen with lap joint; reflecting surface in tension.



Figure 116 Material C (CK-1, 2, 3, 4) — Panel Bend

Material D (Table XXXV). All four specimens of this material failed by localized inter-cellular buckling of the compression facing as shown in Figure 117. Results of the tests (Table XXXV) indicate that the material, although high in bending stiffness, has fairly low elastic and ultimate moments.

Table XXXV. Material D – Panel-Bend Test

Specimen designation	Beam width, b (in.)	Beam span, L (in.)	$\frac{EI/b}{(in.^2-lb)} \frac{in.}{in.}$	M_e/b (lb)	M_u/b (lb)	Tension face
DK-1	1.98	9	3,580	6.1	11.8	(a)
DK-2	1.98	9	2,920	9.1	10.8	(a)
DK-3	1.98	9	2,900	9.1	10.2	(a)
DK-4	1.98	9	3,290	6.8	9.9	(a)
Average	--	--	3,172	7.8	10.7	

(a) Symmetrical specimens.

Material G (Table XXXVI). This material failed typically by general facing buckling at very small loads. In addition to the facing buckling, several supporting cups pulled loose in two of the specimens, GK-3 and GK-5. Failure of a typical specimen, GK-1, is shown in Figure 118.

Table XXXVI. Material G – Panel-Bend Test

Specimen designation	Beam width, b (in.)	Beam span, L (in.)	$\frac{EI/b}{(in.^2-lb)} \frac{in.}{in.}$	M_e/b (lb)	M_u/b (lb)	Tension face	Thickness (~ in.)
GK-1 ^(a)	16.0	12.0	15.9	0.137	0.331	Nonreflecting	1
GK-3 ^(b)	16.0	12.0	28.4	0.181	0.390	Nonreflecting	
GK-2 ^(a)	16.0	12.0	17.3	0.140	0.264	Reflecting	
Average ^(c)	--	--	20.5	0.153	0.328		
GK-5 ^(d)	16.0	12.0	24.4	0.112	0.150	Nonreflecting	0.5
GK-7 ^(d)	16.0	12.0	37.2	0.050	0.425	Nonreflecting	
GK-6 ^(d)	16.0	12.0	23.2	0.138	0.134	Reflecting	
Average ^(c)	--	--	28.3	0.100	0.236		

(a) No specimen failure. Test was stopped when equipment limits of approximately 0.5-in. deflection were reached.

(b) Four cups of 24 unbonded at time of failure.

(c) All specimens used for averages.

(d) One cup unbonded at time of failure.

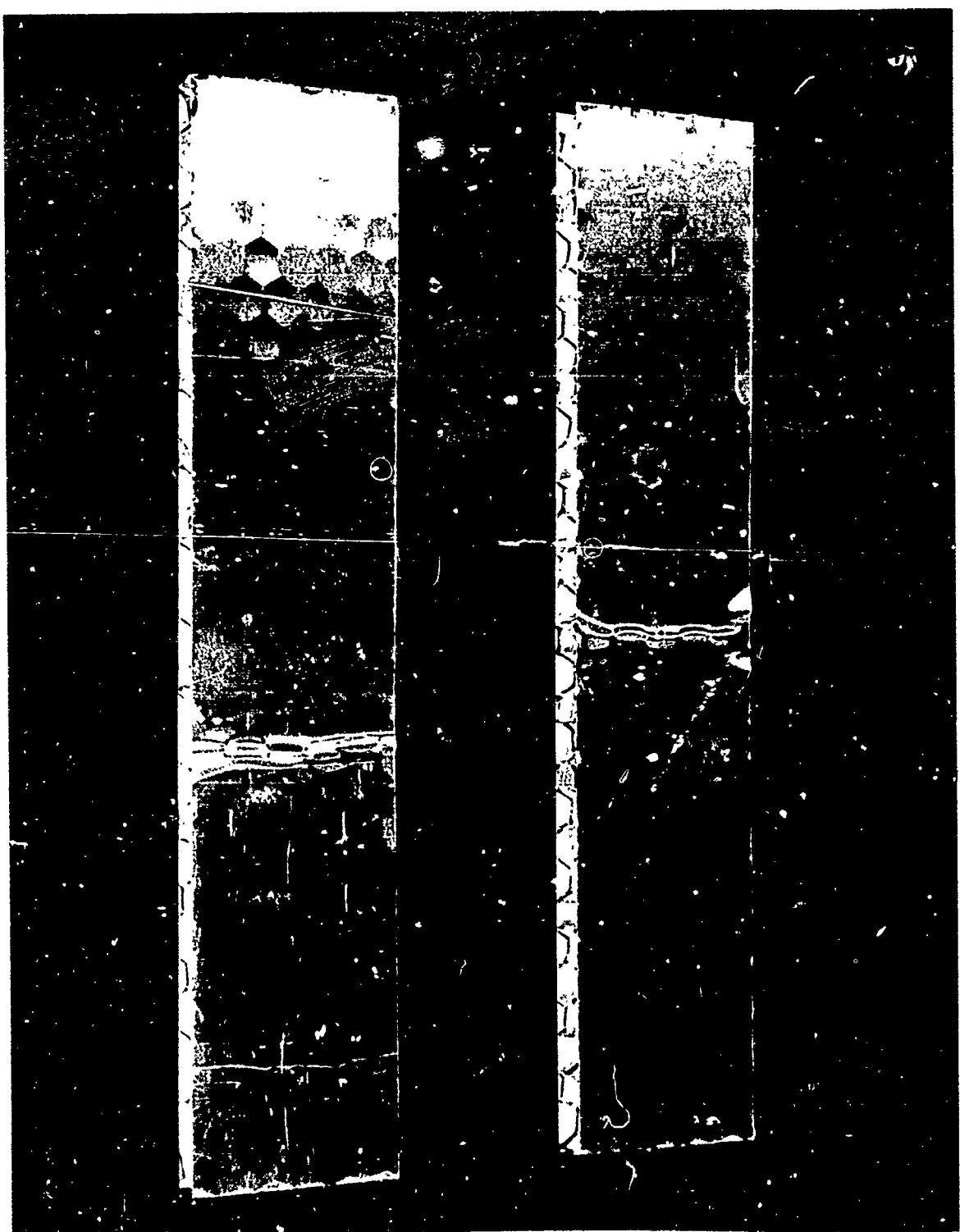


Figure 117 Material D (DK-1, 4) — Panel Bend

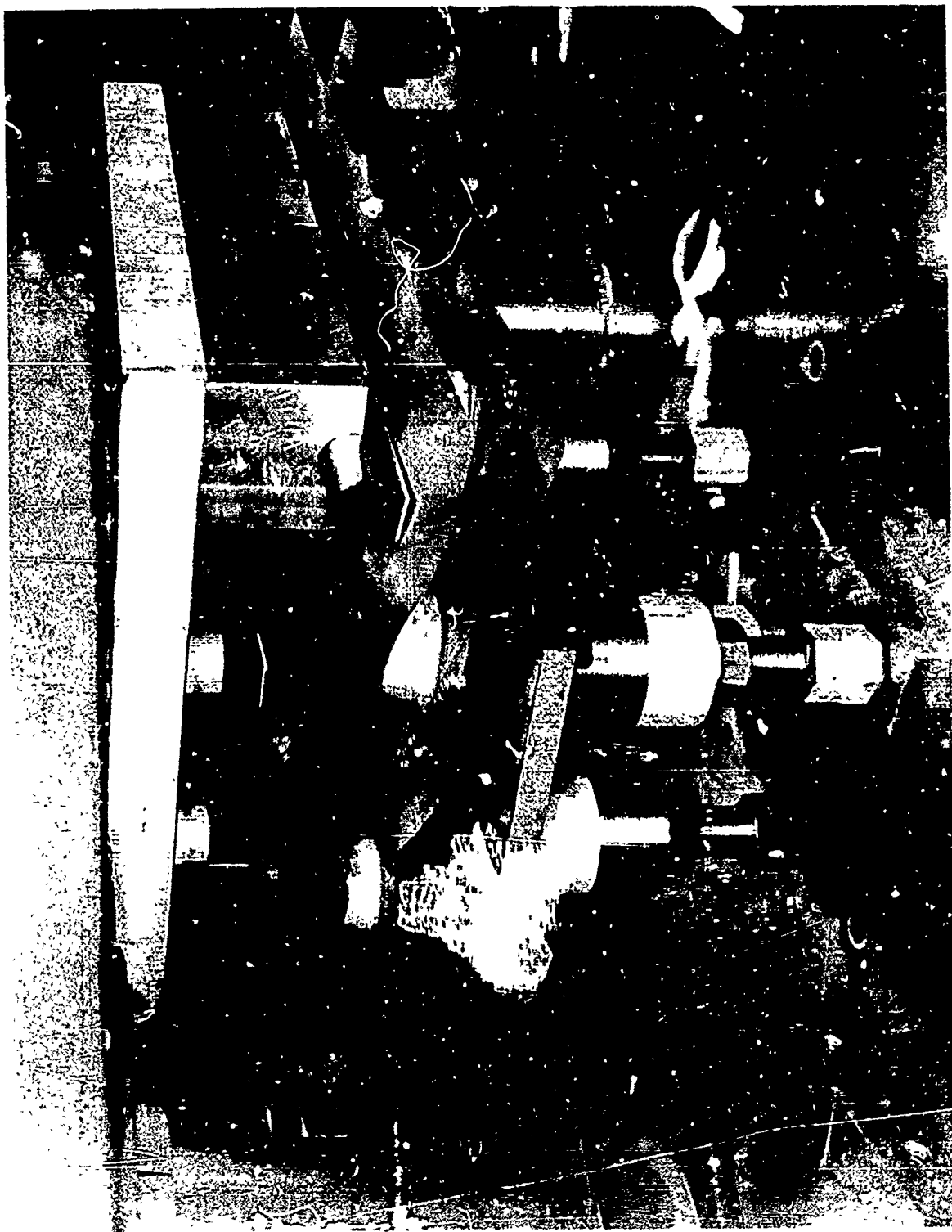


Figure 118 Material G (GK-1) - Panel Bend

Material L (Table XXXVII). This material, because the filler material was arranged in rows, had greatly different characteristics when bending occurred about the two different major axes. When bending occurred about the axis normal to the fibrous rows, the values given in Table XXXVII for LK-1 through LK-4 resulted. However, when bending occurred about the axis parallel to the fibrous rows, the values dropped drastically, as may be seen for specimens LK-5 through LK-8. Figure 119 illustrates a test of one of the latter specimens in which the testing machine limitation of approximately 0.5-in. deflection was reached. For all specimens, the weakest bending mode was that which placed the nonreflecting surface in compression.

Table XXXVII. Material L - Panel-Bend Test

Specimen designation	Beam width, b (in.)	Beam span, L (in.)	EI/b (in. ² -lb/in.)	M_e/b (lb)	M_u/b (lb)	Tension face
LK-1 ^(a)	2.11	9	76	1.99	6.97	Nonreflecting
LK-2 ^(a)	2.10	9	116	1.43	2.34	Reflecting
LK-3 ^(a)	2.05	9	65	0.81	1.43	Reflecting
LK-4 ^(a)	2.07	9	81	1.16	2.55	Reflecting
Average ^(b)	—	—	87	1.13	2.11	
LK-5 ^(c)	1.35	6	5.8	0.81	1.14	Reflecting
LK-6 ^(c)	1.28	6	8.6	1.17	1.39	Nonreflecting
LK-7 ^(c)	1.28	6	5.8	0.63	0.78	Reflecting
LK-8 ^(c)	1.30	6	7.1	0.73	0.85	Reflecting
Average ^(b)	—	—	6.2	0.72	0.92	

(a) Fibrous rows normal to bend axis.

(b) Averages for specimens with reflecting face in tension.

(c) Fibrous rows parallel to bend axis.

Table XXXVIII. Panel-Bend-Test Summary

Material designation	Approx. material thickness (in.)	EI/b (in. ² -lb/in.)	M_e/b (in.-lb/in.)	M_u/b (in.-lb/in.)	Failure type ^(a)
A	0.75	5,900	13.0	18.2	LFB
A	0.25	754	3.80	6.32	LFB
B	1.00	1,405	12.0	17.6	CSF
B	0.50	410	4.4	12.5	CSF
C	0.30	1,175	19.0	23.7	LFB
D	0.50	3,172	7.8	10.7	LFB
G	1.00	20.5	0.15	0.33	EFD
G	0.50	28.3	0.10	0.24	EFD
L	0.75	6.2	0.72	0.92	LFB

(a) LFB = Local facing buckling; CSF = Core shear fracture;

EFD = Excessive facing distortion.

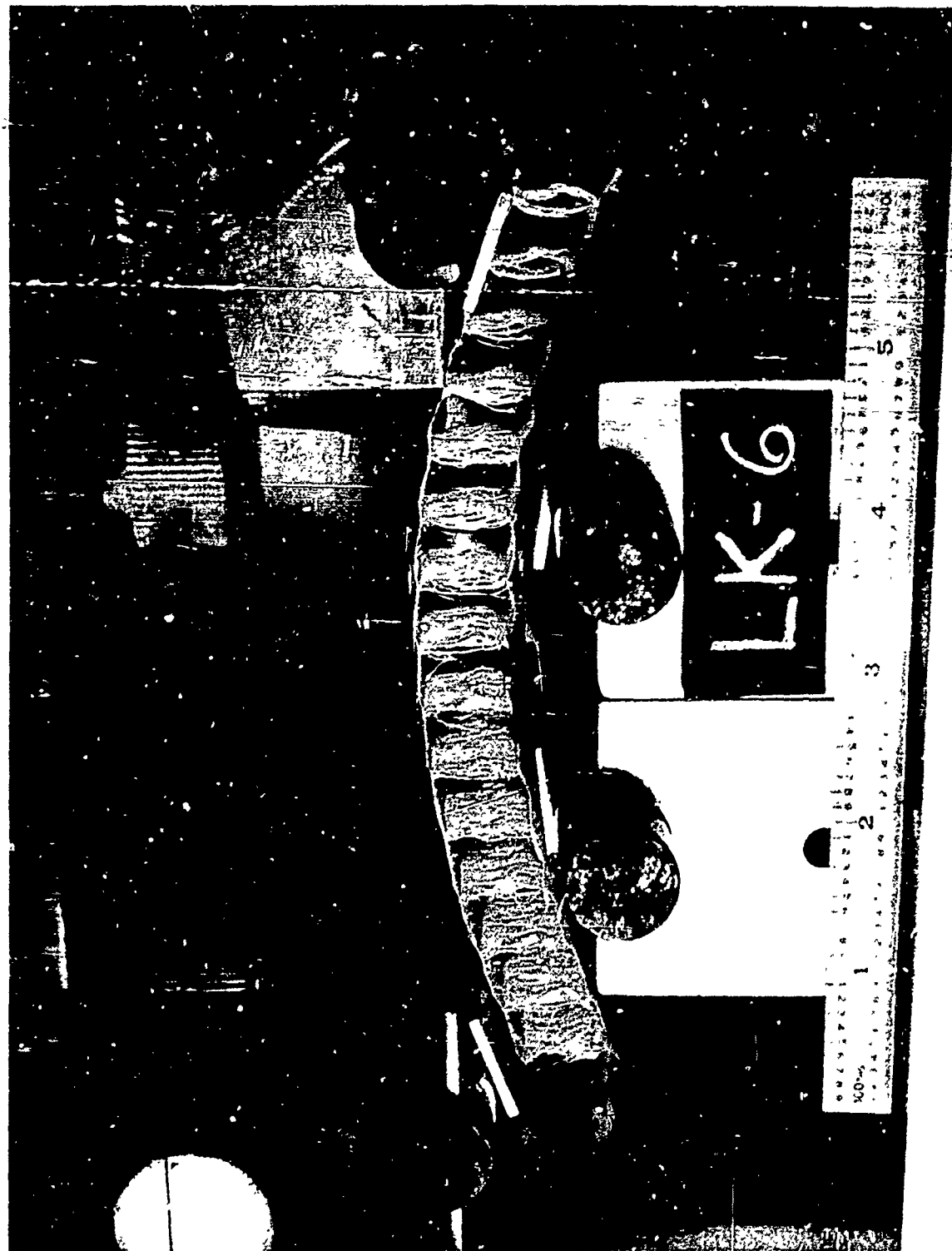


Figure 119 Material L (LK-6) - Panel Bend

4. FACING TENSION

Facing tension tests were performed on facing materials (and backing materials if different from the facing) of the candidate materials to determine the modulus of elasticity, elastic limit, maximum stress, and final strain. These tests were performed at -200° F, room temperature, and +250° F. Metallic materials were tested at a strain rate of 0.5 percent per minute while nonmetallic materials were tested at a rate of 10 percent per minute to avoid material creep.

The modulus of elasticity, E , was calculated from the stress-strain curve by the relation,

$$E = \frac{P}{A\epsilon}$$

where P is the load, A is the cross-sectional area, and ϵ is the strain at load P .

a. Description of Apparatus

Specimen and Specimen Grips. Specimens were cut to the configuration shown in Figure 26 by shaping rectangular pieces of the facing material between two templates and removing the excess material with a razor blade. The thickness of the shaped specimens was then measured to an accuracy of ± 0.00005 in. by taking the average of readings at three places along the gage length. At the time of the test, the specimen was mounted in grips as shown in Figure 121. From left to right in the figure are the following items:

- One-half of the extensometer pair that measured the elongation of the specimen
- Extensometer crossbars with alignment rods that were spaced exactly to the extensometer gage length, 2.000 in.
- Second-half of the extensometer pair
- Specimen grips with alignment rods
- Mounted specimen with crossbars and extensometers installed

Extensometers. The extensometers used were made from thin stainless-steel shim stock bent into the shape shown in Figure 121 and then instrumented with one-half of a strain gage bridge on each clip. The output signal of the clips was then calibrated at each temperature before and after testing by applying a known deflection.

Loading Frame. The loading frame shown in Figure 122 was constructed to allow close control of the strain rate as well as accurate measurement of very small loads. The latter requirement was necessary because the maximum load on some specimens was as high as 300 lb while it was only 1 lb on others. A variable speed dc-drive motor with a built-in speed reducer was used to drive a small screw jack that applied strain to the specimen. The tensile load was measured by the load cell in series in the

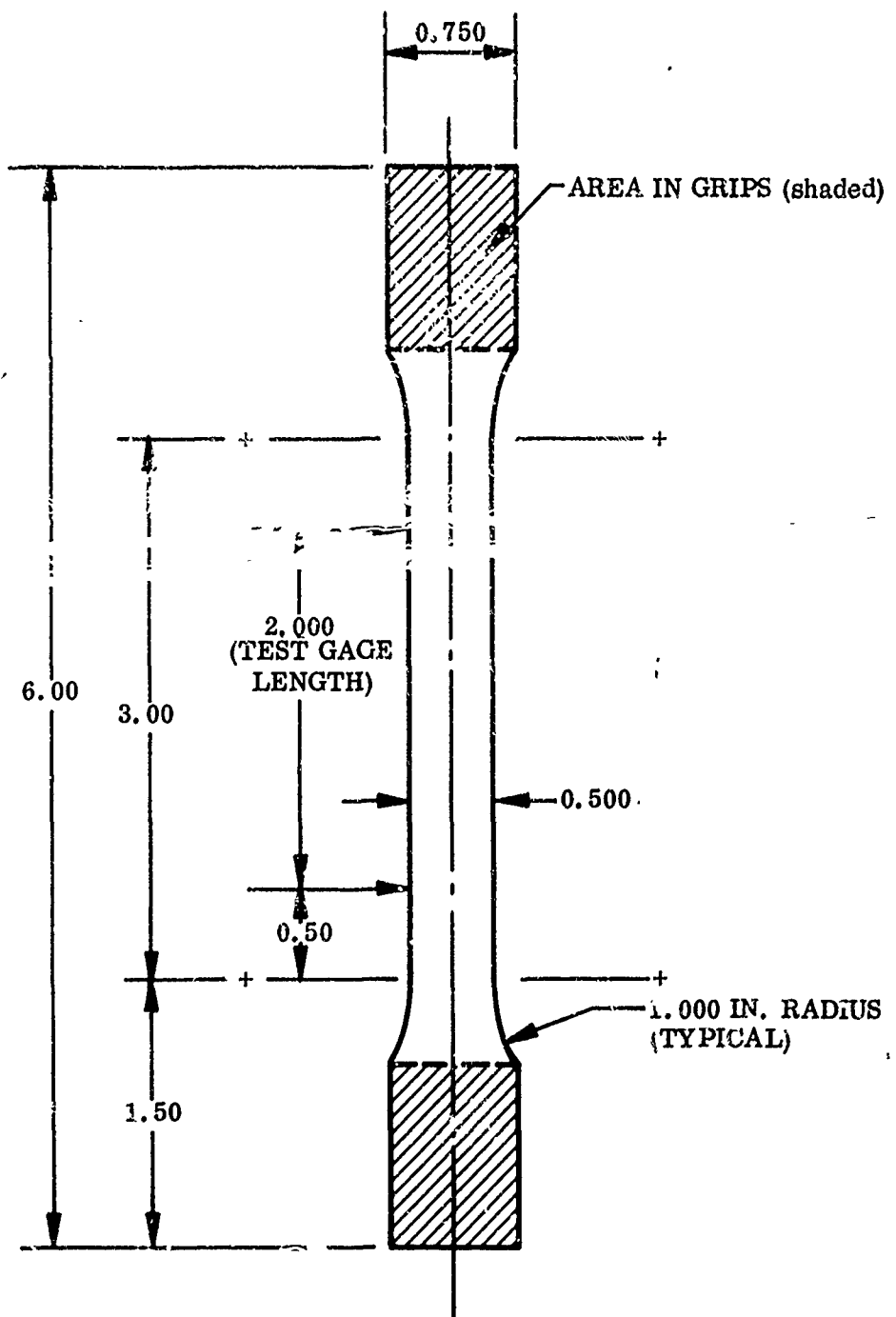


Figure 120 Facing Tension – Specimen Detail



Figure 121 Facing Tension Test - Specimen Grips

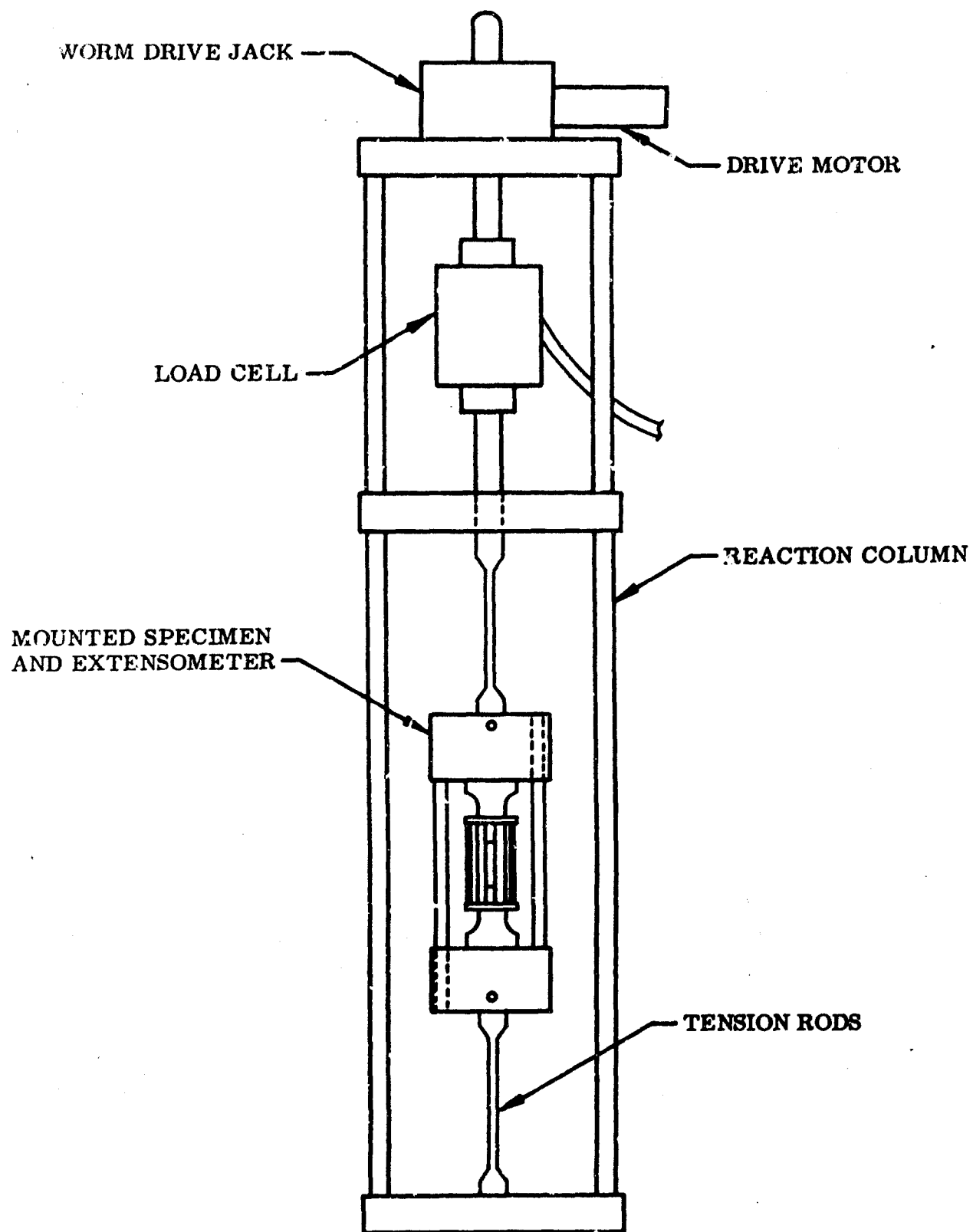


Figure 122 Facing Tension Apparatus Diagram

specimen. The output of this load cell was amplified by a Sanborn carrier amplifier and recorded on the Y axis of an XY plotter. The thin tension rods approximately 0.1 in. in diameter, in series with the specimen, served to minimize any moments due to minor misalignments. The lower half of the loading frame was placed in the oven or refrigerator, as required, and was easily removable to allow changing specimens.

b. Test Procedure

- (1) Place specimen blank between templates and shape by removing excess material with a sharp knife or razor blade.
- (2) Measure and record specimen width and thickness in three places along the 2-in. gage length.
- (3) Mount specimen in grips and install crossbars.
- (4) If required, adjust input voltage to drive motor and gear chain to get proper strain rate for material being tested.
- (5) Place mounted specimen in loading frame between tension rods and secure with dowel pins.
- (6) Mount extensometers between crossbars using caution to ensure that extensometers are centered on specimen and properly seated on crossbars.
- (7) For +250° and -200° F tests only, place frame in oven (or refrigerator) and bring to temperature. Hold temperature for the duration of test.
- (8) If required, verify and adjust load cell and extensometer scales by shunting proper transducer bridge legs with calibration resistors.
- (9) If required, start drive motor and continue monitoring temperature until specimen failure.
- (10) Remove specimen, inspect for and record any failure anomalies.

c. Test Results

The results of the facing tension tests performed on the candidate materials are shown in Tables XXXIX - XLIII. Average values for all of the materials are listed in Table XLIV.

d. Comments and Interpretation of Results

Material A (Table XXXIX). A typical failure for this material is shown in Figure 123. This material, used for both facing and backing, exhibits the slight deterioration of characteristics with increasing temperature usually found in soft aluminum alloys. At room temperature, no definite elastic limit could be assigned, so the 0.2 percent offset yield strength is given. This is the stress sustained by the material when it has reached 0.2 percent nonelastic strain.

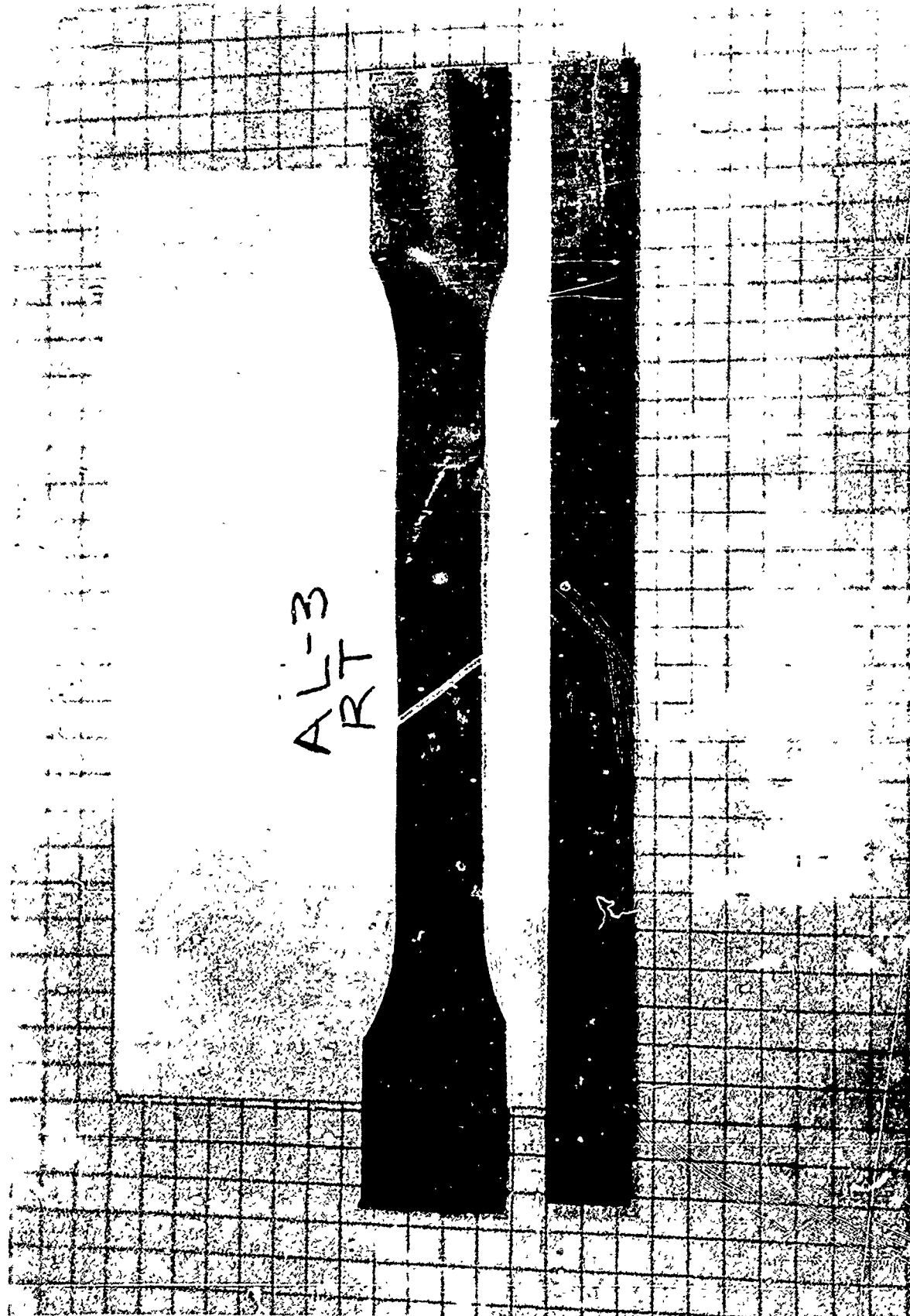


Figure 123 Material A (AL-3) – Facing Tension

Table XXXIX. Material A - Facing-Tension Test

Temperature	Specimen designation	Modulus E (psi)	Elastic limit (psi)	Maximum stress (psi)	Final strain (%)
-200° F	AL-7	11.7×10^6	25.0×10^3	43.5×10^3	8.14
	AL-8	13.4×10^6	31.5×10^3	44.7×10^3	6.64
	AL-9	17.5×10^6	31.5×10^3	46.2×10^3	7.52
	Average	14.2×10^6	29.3×10^3	44.8×10^3	7.19
Room temperature(a)	Deviation	(17.6%)	(14.7%)	(2.9%)	(7.6)
	AL-1	10.5×10^6	35.5×10^3	38.0×10^3	3.85
	AL-2	10.4×10^6	35.5×10^3	38.2×10^3	4.50
	AL-3	9.6×10^6	36.3×10^3	40.4×10^3	4.25
	Average	10.2×10^6	35.8×10^3	38.7×10^3	4.20
+250° F	Deviation	(5.9%)	(0.8%)	(1.8%)	(8.3)
	AL-4	9.1×10^6	17.3×10^3	37.8×10^3	2.28
	AL-5	10.7×10^6	14.0×10^3	37.7×10^3	2.74
	AL-6	8.9×10^6	18.0×10^3	37.7×10^3	2.38
	Average	9.6×10^6	16.2×10^3	37.7×10^3	2.47
	Deviation	(7.3%)	(13.6%)	(0.1%)	(7.7)

(a) The 0.2 percent offset yield strength at room temperature is given instead of the elastic limit.

Material B (Table XL). This material has an electroformed nickel front-facing and a very thin (0.0003-in. average) "quilted" mylar back-facing. The nickel front-facing has a modulus that is higher than any of the other materials in this program. Because of this, the modulus determination was somewhat less accurate - the sensitivity of the extensometer was not sufficient to measure the very small strains. However, the average values shown follow the expected trend. The modulus shows a drop of approximately 25 percent from -200 to +250°F as do the maximum stress and elastic limit values. In addition, the reflective plating partially flaked off at -200°F as can be seen in Figure 124. The thin backing material shows extreme deterioration with increasing temperature by the drop of approximately 95 percent in modulus value from -200 to +250°F. These tests indicate that the high-test temperature is close to the temperature at which the material disintegrates structurally.

Table XL. Material B - Facing-Tension Test

Temperature	Specimen designation	Modulus E (psi)	Elastic limit (psi)	Maximum stress (psi)	Final strain (%)
$-200^{\circ}\text{ F}^{(a)}$	BL-8	39.3×10^6	—	139×10^3	—
	BL-9	31.6×10^6	62.2×10^3	135×10^3	—
	BL-11	—	—	155×10^3	2.95
	BL-12	38.9×10^6	50.0×10^3	166×10^3	2.55
	Average	36.6×10^6	56.1×10^3	149×10^3	2.75
Room temperature ^(a)	Deviation	(1.4%)	(10.9%)	(9.4%)	(7.3%)
	BL-1	25.3×10^6	50.0×10^3	107×10^3	1.20
	BL-2	—	—	100×10^3	5.30
	BL-4	42.3×10^6	—	102×10^3	3.40
	Average	33.8×10^6	50.0×10^3	103×10^3	3.30
$+250^{\circ}\text{ F}^{(a)}$	Deviation	(25.1%)	—	(2.9%)	(63.6%)
	BL-5	31.4×10^6	28.6×10^3	100×10^3	1.05
	BL-6	24.9×10^6	41.3×10^3	110×10^3	2.05
	BL-7	24.7×10^6	41.4×10^3	115×10^3	1.86
	Average	27.0×10^6	37.1×10^3	108×10^3	1.70
$-200^{\circ}\text{ F}^{(b)}$	Deviation	(8.5%)	(22.9%)	(7.4%)	(38.2%)
	BL-24	0.85×10^6	9.33×10^3	24.5×10^3	3.42
	BL-25	1.14×10^6	9.33×10^3	22.8×10^3	2.80
	BL-26	1.09×10^6	13.30×10^3	26.9×10^3	3.30
	Average	1.03×10^6	10.69×10^3	24.7×10^3	3.17
Room temperature ^(b)	Deviation	(17.5%)	(12.7%)	(7.7%)	(11.7%)
	BL-13	0.476×10^6	3.66×10^3	7.20×10^3	4.50
	BL-14	0.430×10^6	1.73×10^3	8.73×10^3	5.90
	BL-15	0.480×10^6	2.10×10^3	7.53×10^3	5.30
	Average	0.462×10^6	2.50×10^3	7.82×10^3	5.23
$+250^{\circ}\text{ F}^{(b)}$	Deviation	(6.9%)	(30.8%)	(7.9%)	(14.0%)
	BL-20	46.3×10^3	3.5×10^3	6.20×10^3	18.2
	BL-21	47.0×10^3	4.0×10^3	5.90×10^3	17.5
	BL-23	60.0×10^3	5.0×10^3	7.47×10^3	16.0
	Average	51.1×10^3	4.2×10^3	6.52×10^3	17.2
	Deviation	(7.4%)	(16.7%)	(9.5%)	(7.0%)

(a) Facing material.

(b) Backing material.

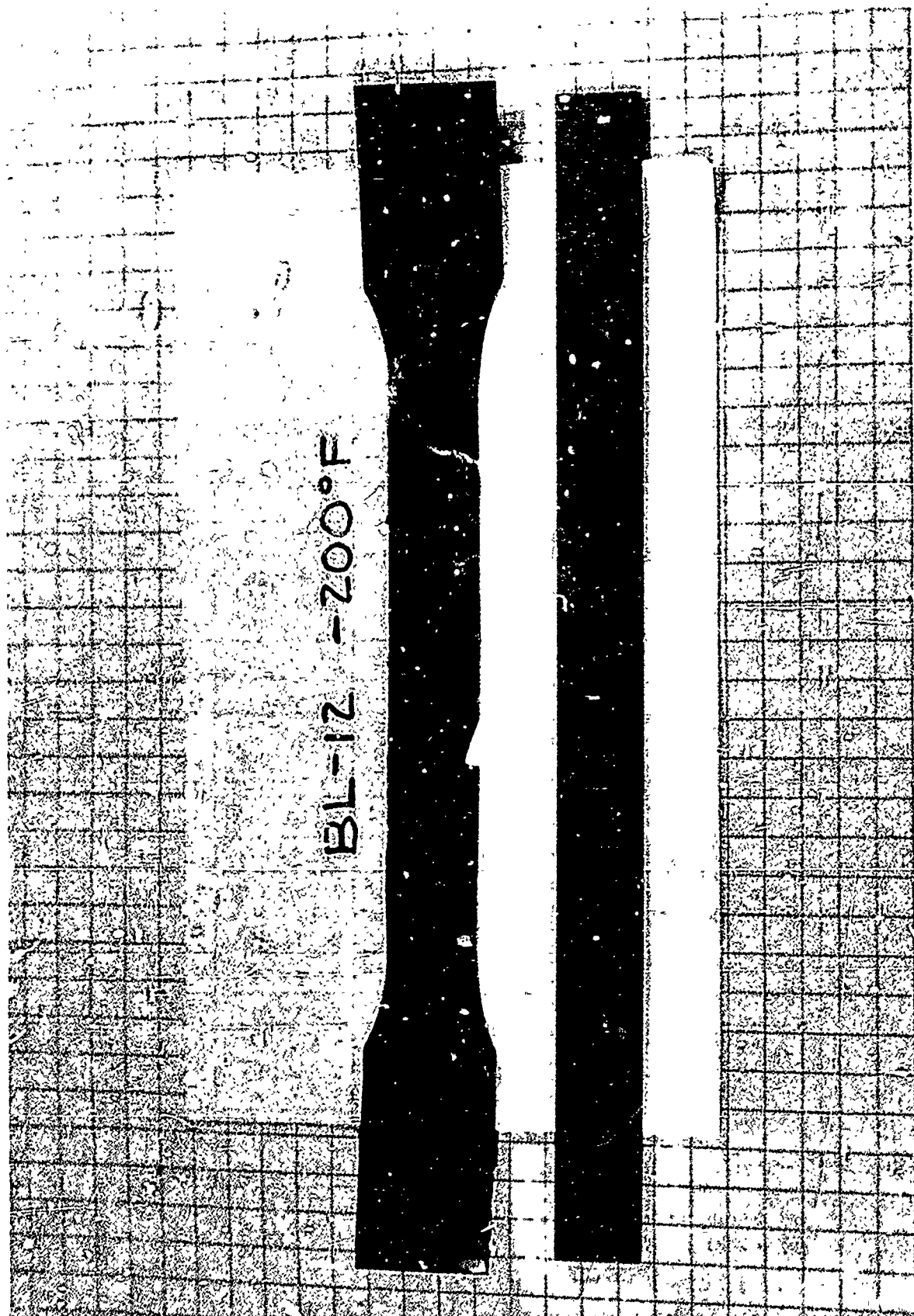


Figure 124 Material B (BL-12) – Facing Tension

Material C (Table XLI). This material, an aluminum alloy, is used both for facing and backing. As may be seen in the data, the values generally decrease with increasing temperature. At room temperature, no definite values for the elastic limit could be assigned, so the 0.2 percent offset yield strength is given. A typical failure is shown in Figure 125.

Table XLI. Material C - Facing-Tension Test

Temperature	Specimen designation	Modulus E (psi)	Elastic limit (psi)	Maximum stress (psi)	Final Strain (%)
-200° F	CL-9	11.65×10^6	21.7×10^3	53.1×10^3	7.50
	CL-10	10.30×10^6	39.4×10^3	54.9×10^3	5.12
	CL-11	12.10×10^6	22.8×10^3	54.9×10^3	7.07
	Average	11.35×10^6	28.0×10^3	54.3×10^3	6.56
Room temperature(a)	Deviation	(9.2%)	(26.0%)	(2.2%)	(21.9)
	CL-1	10.20×10^6	43.2×10^3	47.0×10^3	4.70
	CL-2	8.35×10^6	42.0×10^3	47.0×10^3	6.00
	CL-3	9.37×10^6	42.9×10^3	45.8×10^3	3.60
	CL-4	9.38×10^6	41.9×10^3	45.9×10^3	3.90
	Average	9.32×10^6	42.5×10^3	46.4×10^3	4.55
+250° F	Deviation	(10.4%)	(1.4%)	(1.3%)	(18.7)
	CL-5	11.00×10^6	—	42.0×10^3	1.19
	CL-6	10.80×10^6	17.2×10^3	43.2×10^3	4.48
	CL-7	9.35×10^6	20.6×10^3	44.0×10^3	3.90
	CL-8	9.12×10^6	25.4×10^3	44.2×10^3	3.50
	Average	10.07×10^6	21.1×10^3	43.3×10^3	3.27
	Deviation	(9.4%)	(18.5%)	(3.0%)	(63.7)

(a) The 0.2 percent offset yield strength at room temperature is given instead of the elastic limit.

Material D (Table XLII). Aluminum alloy facing and backing of approximately 0.008-in. and 0.004-in. thickness, respectively, were used to construct this material. Values obtained show that the properties generally deteriorate slightly with increase in temperature except for the modulus of elasticity of the 0.008-in. facing material. This value decreased from the room temperature value at both -200 and +250° F. Also, as would be expected, a slightly higher final strain was experienced with the thicker material. Examples of typical failures may be seen in Figure 126; specimen DL-2 is the facing and specimen DL-14 is the backing.

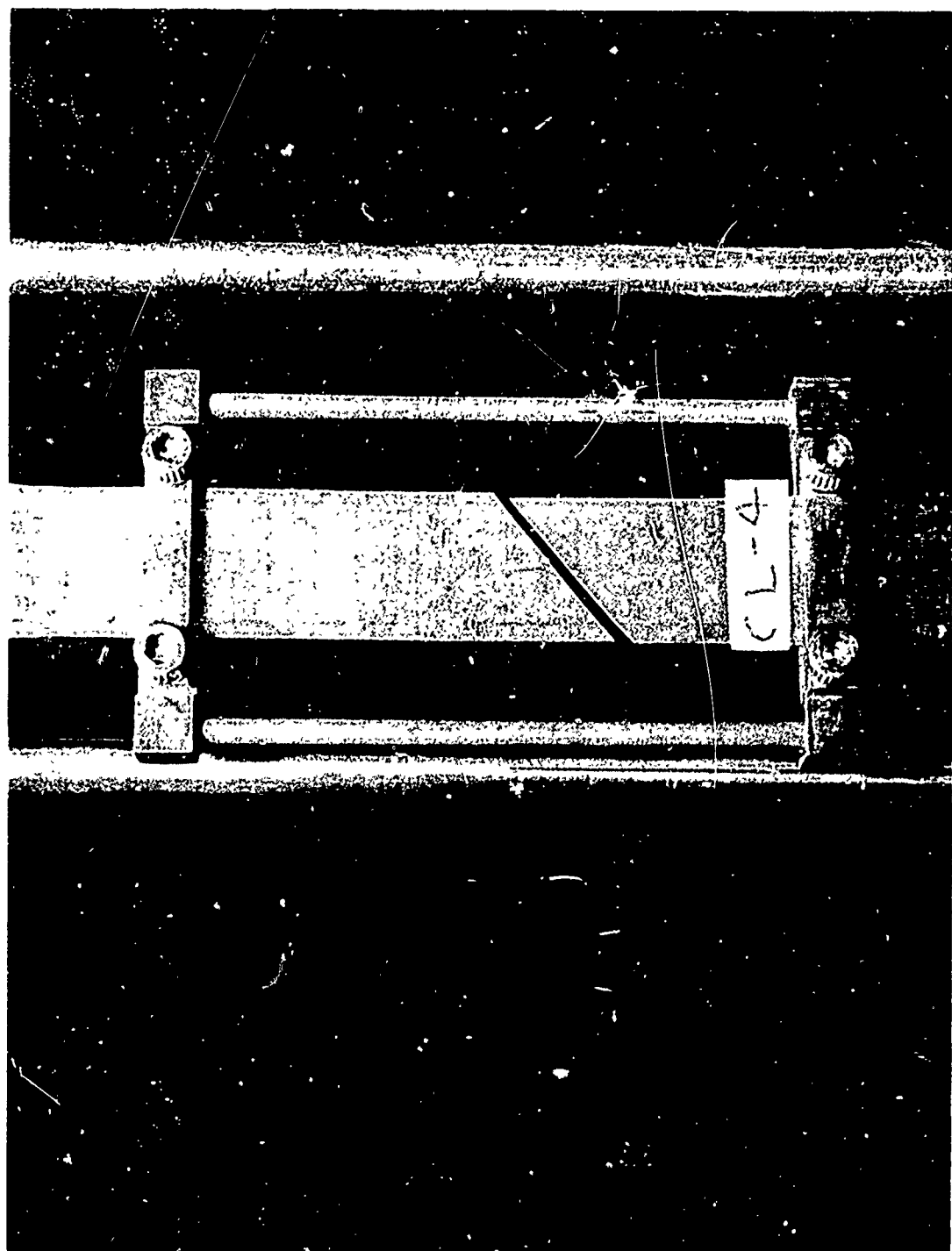


Figure 125 Material C (CL-4) – Facing Tension

Table XLII. Material D - Facing-Tension Test

Temperature	Specimen designation	Modulus E (psi)	Elastic limit (psi)	Maximum stress (psi)	Final strain (%)
-200° F(a)	DL-9	3.99×10^6	9.88×10^3	21.9×10^3	>13.0
	DL-10	4.56×10^6	6.66×10^3	22.3×10^3	17.0
	DL-11	7.13×10^6	6.42×10^3	21.6×10^3	13.9
	Average	5.23×10^6	7.65×10^3	21.9×10^3	--
Room temperature(a)	Deviation	(23.7%)	(16.2%)	(1.4%)	--
	DL-1	7.80×10^6	4.94×10^3	19.0×10^3	19.3
	DL-2	8.50×10^6	8.40×10^3	15.0×10^3	>14
	DL-3	7.76×10^6	5.83×10^3	15.4×10^3	12.8
+250° F(a)	DL-4	8.05×10^6	6.42×10^3	15.8×10^3	>14
	Average	8.03×10^6	6.40×10^3	16.3×10^3	--
	Deviation	(3.4%)	(29.6%)	(8.0%)	--
	DL-5	4.42×10^6	5.00×10^3	13.9×10^3	20.2
-200° F(b)	DL-6	2.29×10^6	5.19×10^3	13.3×10^3	13.2
	DL-7	4.18×10^6	4.94×10^3	14.2×10^3	20.6
	DL-8	5.32×10^6	3.21×10^3	13.7×10^3	13.7
	Average	4.05×10^6	4.58×10^3	13.8×10^3	16.9
Room temperature(b)	Deviation	(43.5%)	(29.9%)	(3.6%)	(21.9)
	DL-19	11.35×10^6	5.81×10^3	21.4×10^3	16.3
	DL-20	11.40×10^6	6.20×10^3	22.4×10^3	15.6
	DL-21	7.14×10^6	7.75×10^3	22.2×10^3	10.2
+250° F(b)	Average	9.96×10^6	6.59×10^3	22.0×10^3	14.0
	Deviation	(28.3%)	(11.8%)	(2.7%)	(27.1)
	DL-13	7.96×10^6	3.02×10^3	15.1×10^3	>14
	DL-14	8.01×10^6	5.22×10^3	15.3×10^3	12.9
	DL-15	9.70×10^6	4.88×10^3	15.5×10^3	14.9
	Average	8.56×10^6	4.37×10^3	15.3×10^3	--
	Deviation	(7.0%)	(30.9%)	(0.7%)	--
	DL-16	3.94×10^6	3.72×10^3	13.0×10^3	6.1
	DL-17	2.45×10^6	4.65×10^3	13.2×10^3	13.0
	DL-18	4.70×10^6	4.57×10^3	13.3×10^3	10.5
	Average	3.70×10^6	4.31×10^3	13.2×10^3	9.9
	Deviation	(33.8%)	(13.7%)	(1.5%)	(38.4)

(a) Facing material \approx 0.008 in. thick.(b) Backing material \approx 0.004 in. thick.

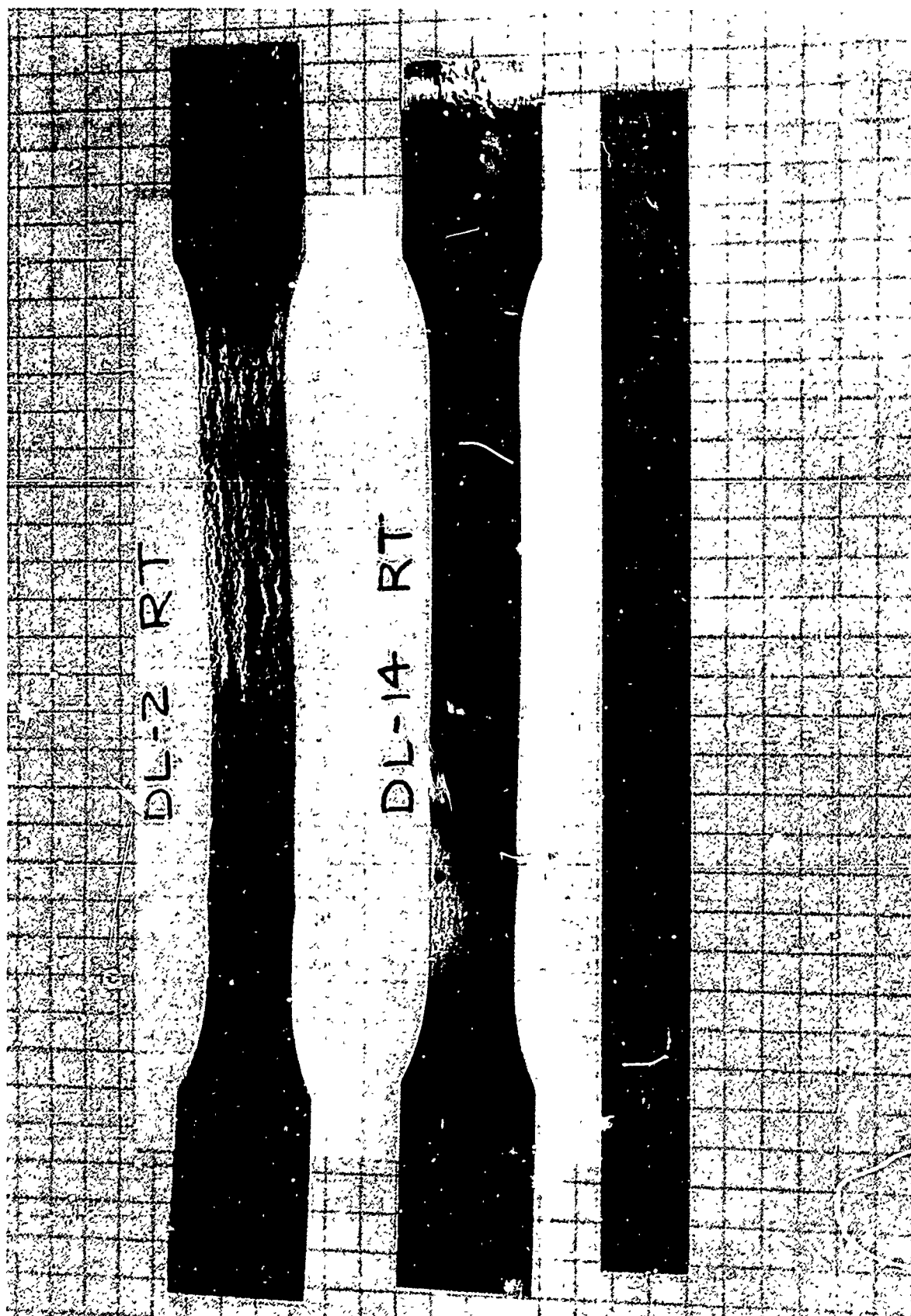


Figure 126 Material D (DL-2, 14) – Facing Tension

Material G (Table XLIII). This facing material, an electroformed nickel, behaved like the other nickel facing material tested; it was extremely strong at -200°F and deteriorated by approximately 30 percent at $+250^{\circ}\text{F}$. Again, the strength of the material prevented obtaining some values of elastic limit because of lack of resolution. A typical failure is shown in Figure 127.

Table XLIII. Material G - Facing-Tension Test

Temperature	Specimen designation	Modulus E (psi)	Elastic limit (psi)	Maximum stress (psi)	Final strain (%)
-200°F	GL-8	—	—	152×10^3	4.40
	GL-9	47.8×10^6	31.4×10^3	152×10^3	4.20
	GL-10	—	—	154×10^3	3.60
	Average	47.8×10^6	—	153×10^3	4.07
Room temperature	Deviation	—	—	(0.6%)	(11.6)
	GL-2	18.2×10^6	22.7×10^3	111×10^3	2.30
	GL-3	—	—	123×10^3	3.98
	GL-4	—	—	121×10^3	3.70
	Average	18.2×10^6	—	118×10^3	3.33
$+250^{\circ}\text{F}$	Deviation	—	—	(5.9%)	(31.0)
	GL-5	16.4×10^6	20.0×10^3	100×10^3	2.85
	GL-6	18.9×10^6	20.0×10^3	—	—
	GL-7	18.4×10^6	23.6×10^3	108×10^3	2.75
	Average	17.9×10^6	21.2×10^3	104×10^3	2.80
	Deviation	(8.4%)	(6.0%)	(3.8%)	(1.8)

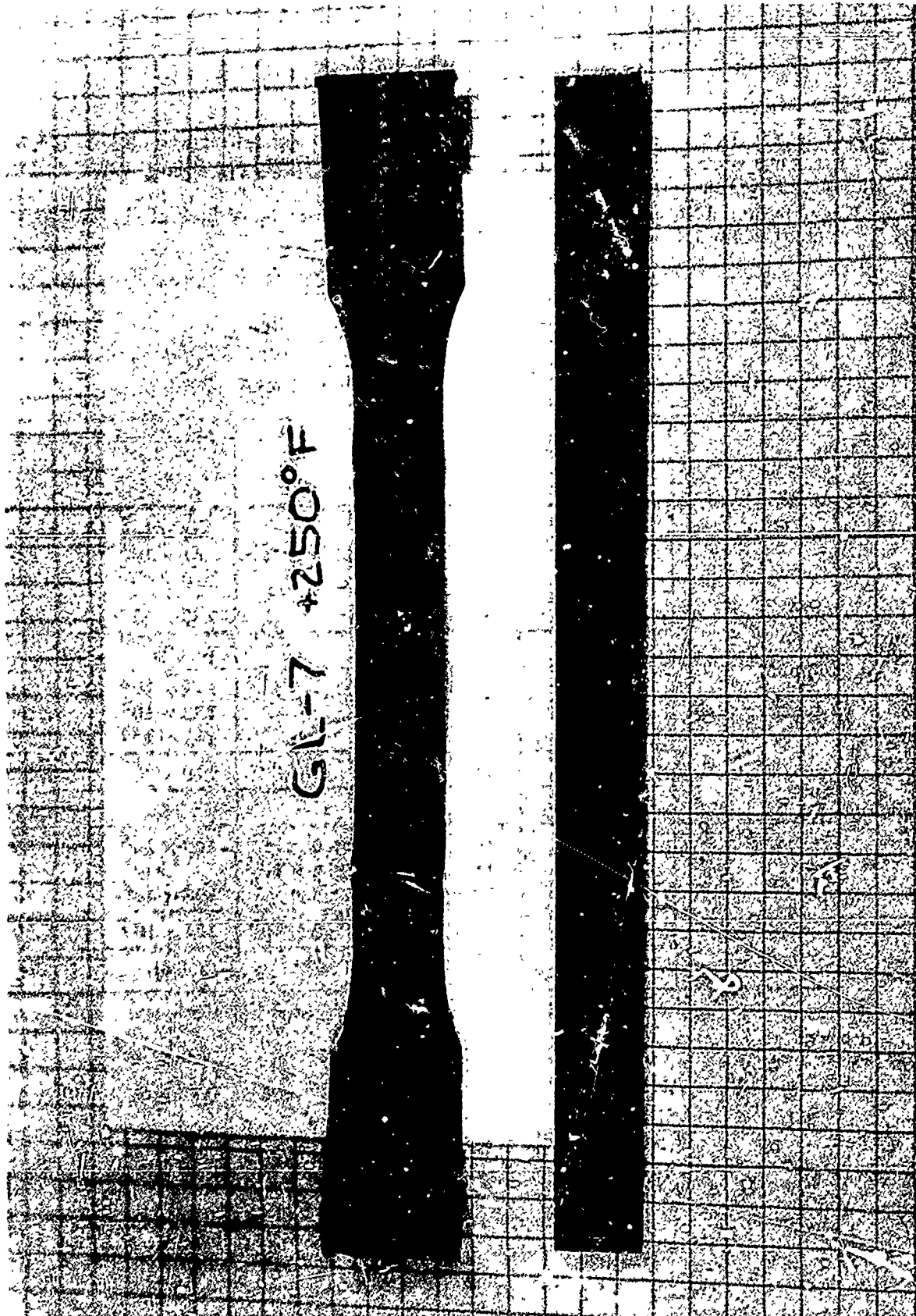


Figure 127 Material G (GL-7) – Facing Tension

Table XLIV. Facing-Tension-Test Summary

Temperature	Material designation	Modulus		Elastic limit		Maximum stress		Final strain	
		Average (psi)	Deviation (%)	Average (psi)	Deviation (%)	Average (psi)	Deviation (%)	Average (%)	Deviation (%)
-200°F	A	14.2 × 10 ⁶	17.6	29.3 × 10 ³	14.7	44.8 × 10 ³	2.9	7.19	7.6
	B(a)	36.6 × 10 ⁶	1.4	56.1 × 10 ³	10.9	149 × 10 ³	9.4	2.75	7.3
	B(b)	1.03 × 10 ⁶	17.5	10.69 × 10 ³	12.7	24.7 × 10 ³	7.7	3.17	11.7
	C	11.35 × 10 ⁶	9.2	28.0 × 10 ³	26.0	54.3 × 10 ³	2.2	6.56	21.9
	D(a)	5.23 × 10 ⁶	23.7	7.65 × 10 ³	16.2	21.9 × 10 ³	1.4	>13	-
	D(b)	9.96 × 10 ⁶	28.3	6.59 × 10 ³	11.8	22.0 × 10 ³	2.7	14.0	27.1
	G	47.8 × 10 ⁶	-	31.4 × 10 ³	-	153 × 10 ³	0.6	4.07	11.6
Room temperature	A	10.2 × 10 ⁶	5.9	35.8 × 10 ³	0.8	38.7 × 10 ³	1.8	4.20	8.3
	F(a)	33.8 × 10 ⁶	25.1	50.0 × 10 ³	-	103 × 10 ³	2.9	3.30	63.6
	B(b)	0.462 × 10 ⁶	6.9	2.50 × 10 ³	30.8	7.82 × 10 ³	7.9	5.23	14.0
	C	9.32 × 10 ⁶	10.4	42.5 × 10 ³	1.4	46.4 × 10 ³	1.3	4.55	18.7
	D(a)	8.03 × 10 ⁶	3.4	6.40 × 10 ³	29.6	16.3 × 10 ³	8.0	>14	-
	D(b)	8.56 × 10 ⁶	7.0	4.37 × 10 ³	30.9	15.3 × 10 ³	0.7	>14	-
	G	18.2 × 10 ⁶	-	22.7 × 10 ³	-	118 × 10 ³	5.9	3.33	31.0
+250°F	A	9.6 × 10 ⁶	7.3	16.2 × 10 ³	13.6	37.7 × 10 ³	0.1	2.47	7.7
	R(a)	27.0 × 10 ⁶	8.5	37.1 × 10 ³	22.9	108 × 10 ³	7.4	1.70	38.2
	B(b)	0.0511 × 10 ⁶	7.4	4.2 × 10 ³	16.7	6.52 × 10 ³	9.5	17.2	7.0
	C	10.07 × 10 ⁶	9.4	21.1 × 10 ³	18.5	43.3 × 10 ³	3.0	3.27	63.7
	D(a)	4.05 × 10 ⁶	43.5	4.58 × 10 ³	29.9	13.8 × 10 ³	3.6	16.9	21.9
	D(b)	3.70 × 10 ⁶	33.8	4.31 × 10 ³	13.7	13.2 × 10 ³	1.5	9.9	38.4
	G	17.9 × 10 ⁶	8.4	21.2 × 10 ³	6.0	104 × 10 ³	3.8	2.80	1.8

(a) Facing.
(b) Backing.

5. FACING SEPARATION

The facing separation tests were run to determine the properties of the core material in tension and the strength of the core-to-facing bond line. Aluminum plates 1/2-in. thick and 3-in. in diameter were bonded to each face of circular specimens taken from flat panel stock. Threaded holes at the center of each aluminum plate permitted the application of a tensile force normal to the plane of the panel and concentric with the circular specimen. Hysol 1-C epoxy cement was used between the plates and the specimen. The data were obtained as a load-deflection or stress-strain curve. From this curve, a "composite modulus of elasticity," elastic limit, maximum stress, and final strain were determined. The test was performed on specimens at room temperature, +250°F, and -200°F. The term "composite" is used because the core material was not homogeneous, and the modulus was, therefore, that of a solid homogeneous material which, in this loading configuration, would produce the same stress-strain curve.

Facing separation tests also were performed upon candidate-material samples which had been previously exposed to the thermal/vacuum environment and thermal cycling. The purpose of these tests was to determine the effects of such exposure upon the core material and the facing bond. Test procedures were the same as those used for the unexposed specimens, except that tests were performed only at room temperature.

a. Description of Apparatus

The test apparatus is shown in Figures 128 and 129. The tests were performed in a hydraulically operated Research Incorporated Model 6566 Universal Testing Machine with 10,000-lb capacity. A bidirectional pivot was incorporated to minimize angular misalignments. The specimen was attached between the load cell and a slip joint that facilitated specimen installation in the linkage. A deflectometer (strain-gage instrumented cantilever) was used to measure the extension of specimen. A second strain-gage bridge on the deflectometer was used to provide a feedback signal to the machine controller to obtain a uniform deflecting rate. The deflectometer and load cell signals were amplified by Sanborn carrier amplifiers, as required, and then recorded on an X-Y plotter.

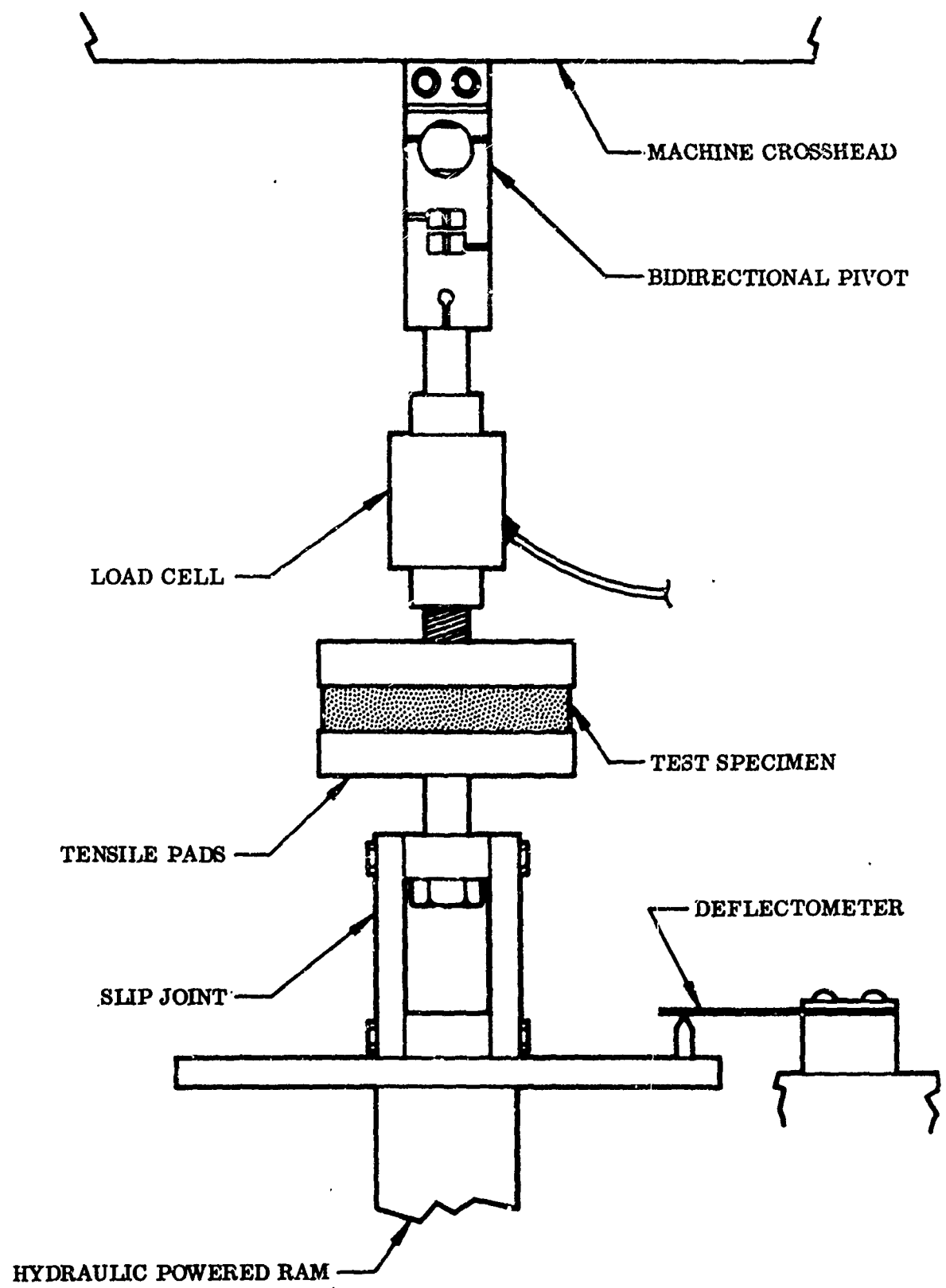


Figure 128 Facing Separation Apparatus Diagram

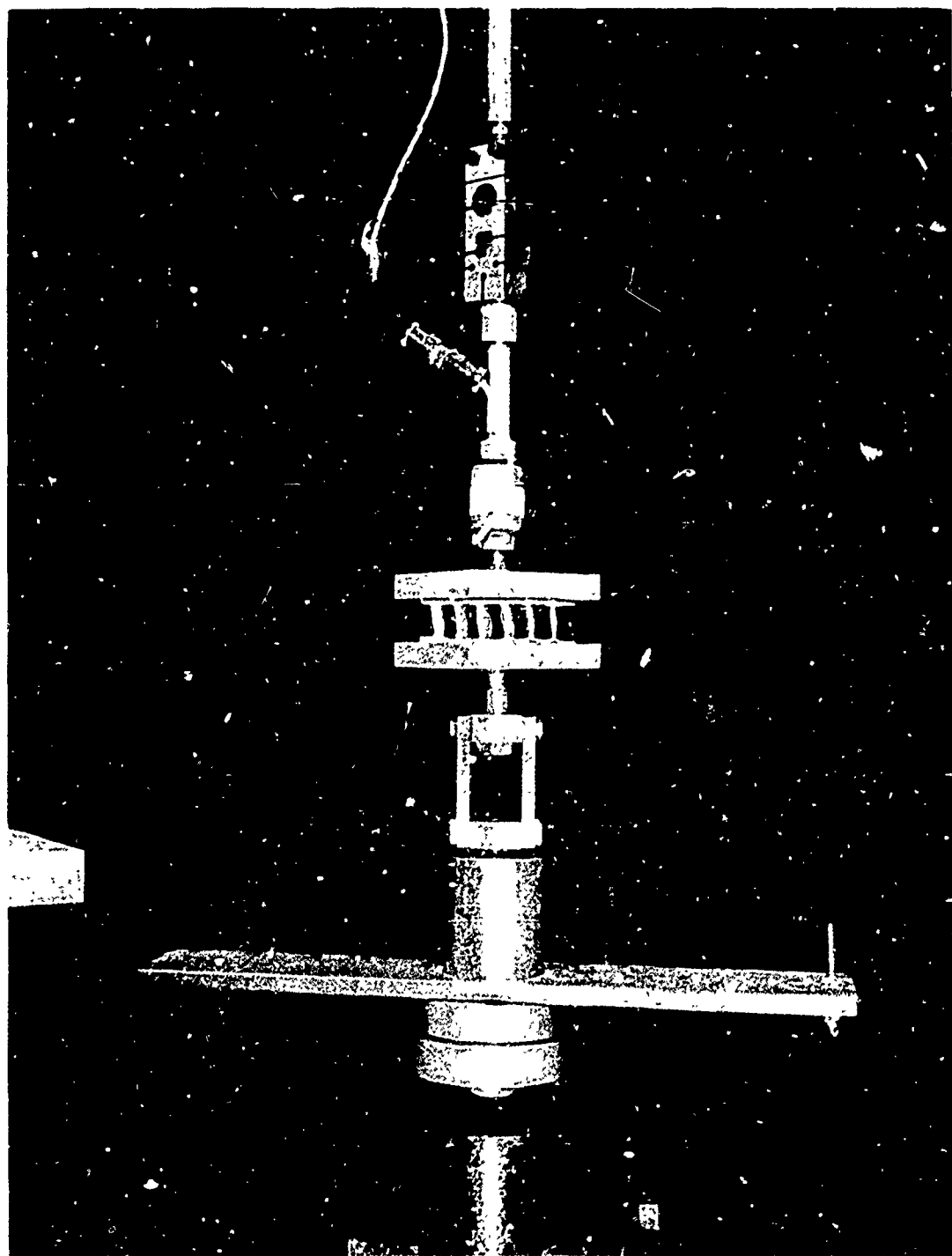


Figure 129 Facing Separation Apparatus

b. Test Procedure

- (1) Measure and record specimen thickness and diameter.
- (2) On metal-faced specimens, sand lightly to obtain suitable bonding surface.
- (3) Mount specimen between sand-blasted tensile pads using epoxy and allow to cure. For -200 and +250° F specimens only, mount two thermocouples between specimen face and tensile pad. Use extreme care to maintain concentricity between specimen and tensile pads.
- (4) For -200 and +250° F specimens only, prechill or preheat specimen as required.
- (5) Check calibration of load cell and deflectometer and adjust if necessary.
- (6) Operate testing machine to apply load to produce desired uniform strain rate until specimen failure.

c. Test Results

The results of the facing separation tests are listed for the candidate materials in Tables XLV through XLIX. Average values for all of the materials are shown in Table L.

d. Comments and Interpretation of Results

Unexposed Specimens

Material A (Table XLV). This material had a large data scatter at all temperatures. A typical failure is shown in Figure 130. In all cases, it was the nonreflecting surface glue bond that failed because of the lightening cutouts.

Material B (Table XLVI). This material exhibited identical failure characteristics in this test as in the panel-shear test. Figure 131 shows a foam failure that was typical at room temperature and +250° F. Figure 132 shows the failure, at -200° F, in which the facing or backing separated at the glue line. Figure 133 shows a similar failure that occurred while the specimen was being brought down to -200° F with an approximate fixture load of 3 lb. It was noted that anomalies in the foam contributed greatly to weakening the specimen and, therefore, contribute in part to the large data scatter.

Material C (Table XLVII). This material exhibited somewhat peculiar characteristics in that the lowest modulus and highest final strain occurred at -200° F. At this temperature, core tensile failure occurred as shown in Figure 134 as opposed to the glue-line failures noted at higher temperatures (Figure 135). At +250° F, maximum stress and elastic limit values exhibit the typical deterioration seen in all metallic specimens.

Table XLV. Material A - Facing-Separation Test

Unexposed Specimens

Temperature	Specimen designation	Modulus E (psi)	Elastic limit (psi)	Maximum stress (psi)	Final strain (%)
-200°F	AM-7	2.92×10^3	87.9	87.9	3.06
	AM-8	4.46×10^3	122.0	122.0	2.81
	AM-9	4.50×10^3	102.3	109.0	2.52
	Average	3.99×10^3	104.1	106.3	2.80
Room temperature	Deviation	(26.8%)	(15.6%)	(17.3%)	(10.0)
	AM-1	1.35×10^3	132.0	132.0	9.76
	AM-2	5.50×10^3	84.9	110.0	2.23
	AM-3	4.33×10^3	43.0	47.8	1.29
	Average	3.73×10^3	86.6	96.6	4.43
+250°F	Deviation	(63.8%)	(51.5%)	(50.5%)	(71.3)
	AM-4	1.09×10^3	11.20	11.90	1.50
	AM-5	128	2.77	2.77	2.18
	AM-6	732	4.33	5.44	1.04
	Average	650	6.10	6.70	1.57
	Deviation	(80.3%)	(54.6%)	(58.7%)	(33.8)

Exposed Specimens

Specimen	Previous exposure	Modulus E (psi)	Elastic limit (psi)	Maximum stress (psi)	Final strain (%)
AFM-1	Thermal/vacuum environment (100 hr)	2.79×10^3	159	159	5.89
AFM-3	Thermal/vacuum environment (1,000 hr)	3.82×10^3	241	252	6.71
AF-2	Thermal/vacuum environment (6,000 hr)	11.10×10^3	209	286	2.80
AFM-2	Thermal/vacuum environment (6,000 hr)	5.09×10^3	197	223	4.30
AGN-1	Thermal cycling (100 cycles)	3.34×10^3	108.6	108.6	3.23
AGM-1	Thermal cycling (1,000 cycles)	4.57×10^3	170	199	4.43
AGM-3	Thermal cycling (6,000 cycles)	4.75×10^3	142	173	3.92
AGM-2	Thermal cycling (214 cycles)	4.90×10^3	160	214	4.90

NOTE: Specimen AGM-2 was initially scheduled to undergo 6,000 cycles. Testing was terminated after 214 cycles because of electronic difficulties which resulted in the specimen's being maintained at 290°F for approximately 16 hr.

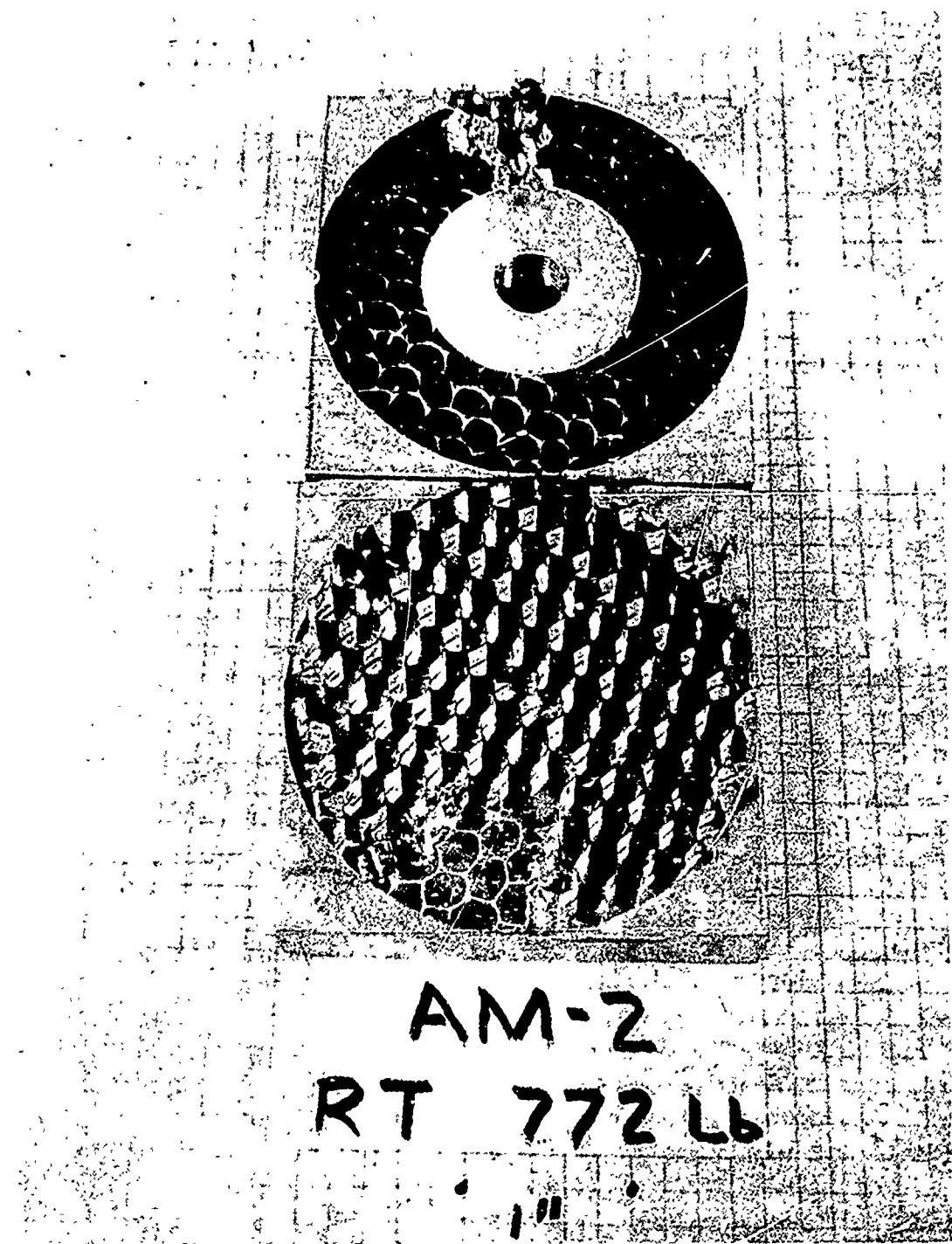


Figure 130 Material A (AM-2) - Facing Separation

Table XLVI. Material B - Facing-Separation Test

Unexposed Specimens

Temperature	Specimen designation	Modulus E (psi)	Elastic limit (psi)	Maximum stress (psi)	Final strain (%)
-200° F	BM-10(a) BM-8(a) (b)	179 —	2.97 —	2.97 —	1.45 —
Room temperature	BM-1(a)	660	4.88	5.81	1.04
	BM-2(a)	526	2.20	2.61	0.96
	BM-3(a)	583	8.94	8.94	1.52
	Average	590	5.34	5.79	1.17
+250° F	Deviation	(10.8%)	(58.2%)	(55.0%)	(18.0)
	BM-4(c)	426	8.69	8.69	2.04
	BM-5(c)	177	3.55	4.33	2.73
	BM-6(c)	194	3.92	4.66	2.56
	Average	266	5.39	5.89	2.44
	Deviation	(33.5%)	(34.2%)	(26.5%)	(16.4)

Exposed Specimens

Specimen	Previous exposure	Modulus E (psi)	Elastic limit (psi)	Maximum stress (psi)	Final strain (%)
BFM-1	Thermal/vacuum environment (100 hr)	—	—	0.705	—
BFB-3	Thermal/vacuum environment (1,000 hr)	593	5.68	5.68	0.99
BFM-3	Thermal/vacuum environment (1,000 hr)	417	4.52	4.52	1.08
BFM-2	Thermal/vacuum environment (6,000 hr)	331	4.23	4.23	1.28
BGM-1	Thermal cycling (100 cycles)	487	7.75	7.75	1.59
BGM-2	Thermal cycling (1,000 cycles)	522	5.83	6.42	1.29

(a) Glue-line failure.

(b) Specimen failed while cooling and is listed for report reference only.

(c) Foam fracture failure.



Figure 131 Material B (BM-6) – Facing Separation



Figure 132 Material B (BM-10) – Facing Separation

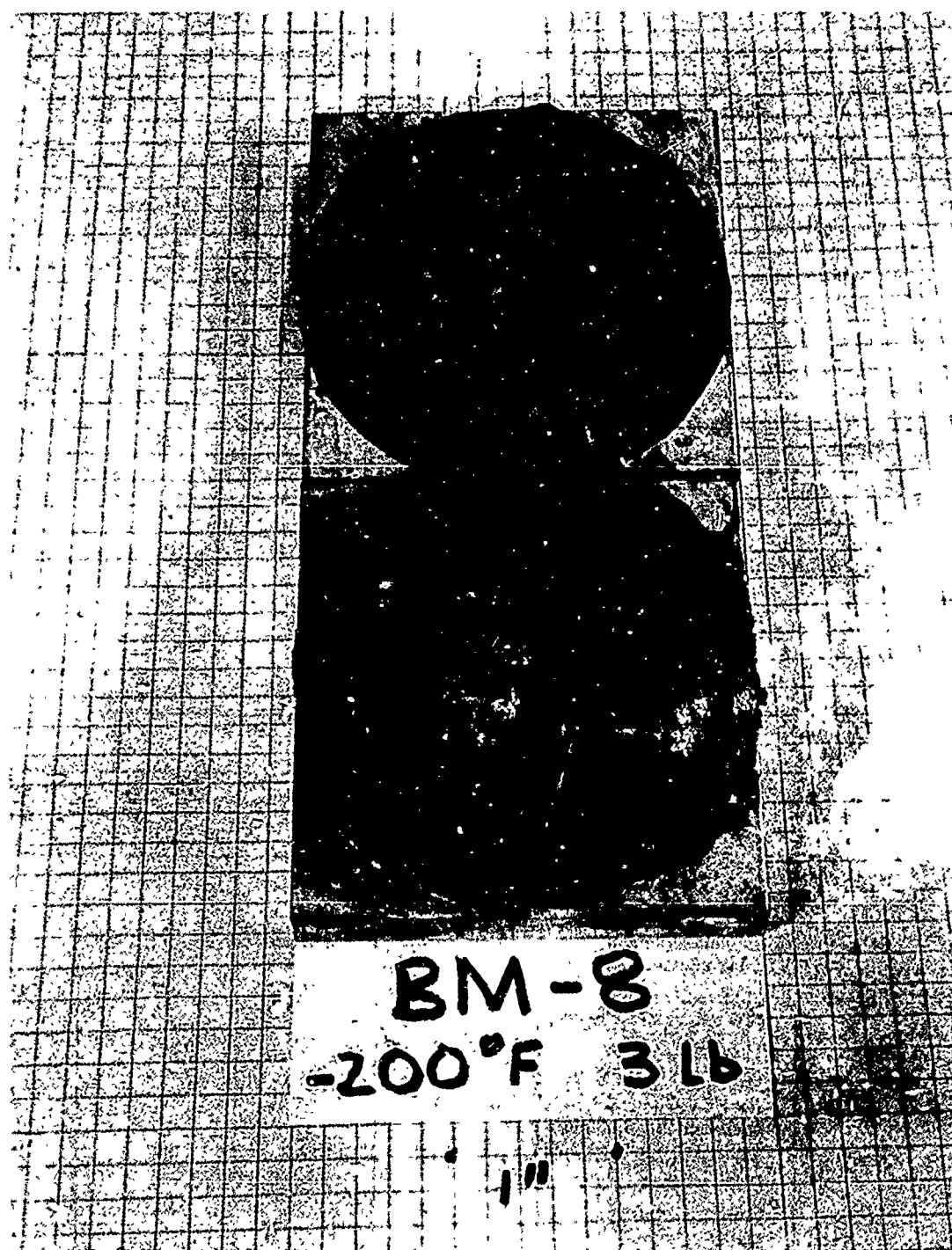


Figure 133 Material B (BM-8) – Facing Separation

Table XLVII. Material C - Facing-Separation Test

Unexposed Specimens

Temperature	Specimen designation	Modulus E (psi)	Elastic limit (psi)	Maximum stress (psi)	Final strain (%)
-200°F	CM-7(a)	4.46×10^3	---	---	---
	CM-8(a)	4.08×10^3	512	550	16.8
	CM-9(a)	3.80×10^3	564	573	14.5
	Average	4.11×10^3	538	561	15.6
Room temperature	Deviation	(7.6%)	(4.8%)	(2.0%)	(7.1%)
	CM-1(a)	11.5×10^3	237	322	3.30
	CM-2(b)	12.2×10^3	139	---	---
	CM-3(a)	15.8×10^3	167	230	1.90
+250°F	Average	13.2×10^3	181	271	2.60
	Deviation	(12.9%)	(23.2%)	(16.7%)	(29.6%)
	CM-4(c)	9.25×10^3	102	125	2.08
	CM-10(c)	9.41×10^3	120	145	2.33
	CM-11(c)	10.55×10^3	128	140	2.48
	Average	9.74×10^3	117	137	2.30
	Deviation	(5.0%)	(12.8%)	(8.7%)	(9.6%)

Exposed Specimens

Specimen	Previous exposure	Modulus E (psi)	Elastic limit (psi)	Maximum stress (psi)	Final strain (%)
CFM-1	Thermal/vacuum environment (100 hr)	3.08×10^3	155	349	14.4
CF-3	Thermal/vacuum environment (1,000 hr)	5.01×10^3	301	364	8.3
CFM-3	Thermal/vacuum environment (1,000 hr)	2.47×10^3	326	360	15.0
CF-2	Thermal/vacuum environment (6,000 hr)	5.75×10^3	297	332	5.75
CFM-2	Thermal/vacuum environment (6,000 hr)	6.65×10^3	291	351	5.62
CG-2	Thermal cycling (100 cycles)	3.95×10^3	360	396	10.5
CGN-1	Thermal cycling (1,000 cycles)	5.93×10^3	362	390	9.53
CGM-3	Thermal cycling (6,000 cycles)	6.27×10^3	295	346	5.75

(a) Core-material tensile failure.

(b) Test-equipment failure; maximums not recorded.

(c) Glue-line failure.



Figure 134 Material C (CM-7) - Facing Separation



Figure 135 Material C (CM-11) - Facing Separation

Material E (Table XLVIII). Examination of the data obtained for this material indicates that the material is fairly well balanced at room temperature but has different failure modes at the extreme temperatures. The material was the strongest at -200° F, and failure occurred at room temperature by separation of the reflective surface from the facing as shown in Figure 136. However, at +250° F, all failures occurred at the glue line, and all values were greatly reduced. At room temperature, one specimen failed at the glue line (EM-5, Figure 137) and the other two (EM-3 and EM-4) failed as at -200° F (by separation of the reflective surface).

Material G (Table XLIX). This material failed by bond tensile failure at all temperatures. Because of the nature of the material, it was not possible to get enough data for a good sampling. Specimens would either fail during preparation or during prechilling or preheating under the approximately 1.5 lb of fixture weight. Because of the total lack of any structural value, no real test was possible and nothing further can be said about the data.

Exposed Specimens

Because of the fragmentary character of the data, few meaningful generalizations can be made as to the effects of exposure to thermal/vacuum environment or thermal cycling. The following tentative conclusions are presented:

Material A (Table XLV). Both the elastic limit and the maximum stress increased significantly with exposure time. This appears to have been due to changes in the properties of the epoxy bond during the previous exposure.

Material B (Table XLVI). This material appears to have been affected little from a structural standpoint by either thermal/vacuum exposure or thermal cycling. (However, partial separation of the reflective surface occurred during both tests.)

Material C (Table XLVII). The modulus of elasticity of this material decreased to less than half that of the unexposed specimens, while the elastic limit, the maximum stress, and the final strain increased substantially. The material, in other words, became less stiff, more plastic. As in the case of Material A, this appears to have been due to changes in the properties of the epoxy bond.

Materials D, E, and F (Table XLVIII). The behavior of these materials was similar to that of Material C, except that the modulus of elasticity did not clearly decrease. Here again, changes in the epoxy bond appear to have been the reason.

Materials G through K (Table XLIX). No statement can be made regarding the data for these materials.

Table XLVIII. Materials D-F - Facing-Separation Test

Unexposed Specimens

Temperature	Specimen designation	Modulus E (psi)	Elastic limit (psi)	Maximum stress (psi)	Final strain (%)
-200°F	EM-7(a)	13.4×10^3	100.0	100.0	0.78
	EM-8(a)	15.9×10^3	76.4	76.4	0.48
	EM-9(a)	10.2×10^3	147.5	147.5	1.48
	Average	13.2×10^3	108.0	108.0	0.91
Room temperature	Deviation	(22.7%)	(30.2%)	(30.2%)	(47.3)
	EM-3(a)	6.38×10^3	23.5	23.5	0.38
	EM-4(a)	9.94×10^3	16.2	21.9	0.32
	EM-5(b)	5.47×10^3	11.3	47.3	---
+250°F	Average	7.26×10^3	17.0	30.9	0.35
	Deviation	(24.6%)	(33.5%)	(29.1%)	(8.6)
	EM-1(b)	1.11×10^3	4.50	5.3	0.65
	EM-2(b)	1.16×10^3	7.45	8.02	0.84
	EM-6(b)	1.58×10^3	5.45	9.38	0.87
	Average	1.28×10^3	5.80	7.80	0.85
	Deviation	(13.3%)	(22.4%)	(29.6%)	(1.2)

Exposed Specimens

Specimen	Previous exposure	Modulus E (psi)	Elastic limit (psi)	Maximum stress (psi)	Final strain (%)
DGM-1	Thermal cycling (100 cycles)	6.05×10^3	58.7	90.0	1.95
EFM-1	Thermal/vacuum environment (100 hr)	5.60×10^3	81.0	160	4.02
EFM-3	Thermal/vacuum environment (1,000 hr)	7.26×10^3	210	292	4.53
EF-2	Thermal/vacuum environment (6,000 hr)	8.16×10^3	158	181	2.46
EFM-2	Thermal/vacuum environment (6,000 hr)	8.97×10^3	102	204	2.63
EGM-1	Thermal cycling (100 cycles)	4.05×10^3	60.2	82.8	3.27
FGM-1	Thermal cycling (100 cycles)	3.85×10^3	64.0	76.7	2.41
FG-1	Thermal cycling (1,000 cycles)	4.44×10^3	57.8	84.5	2.70
FGN-2(c)	Thermal cycling (1,246 cycles)	5.58×10^3	72.5	99.8	3.04

(a) Plating failure.

(b) Glue-like failure.

(c) Initially scheduled to undergo 6,000 cycles. Testing was terminated after 1,246 cycles when vacuum was lost as result of frozen seal.

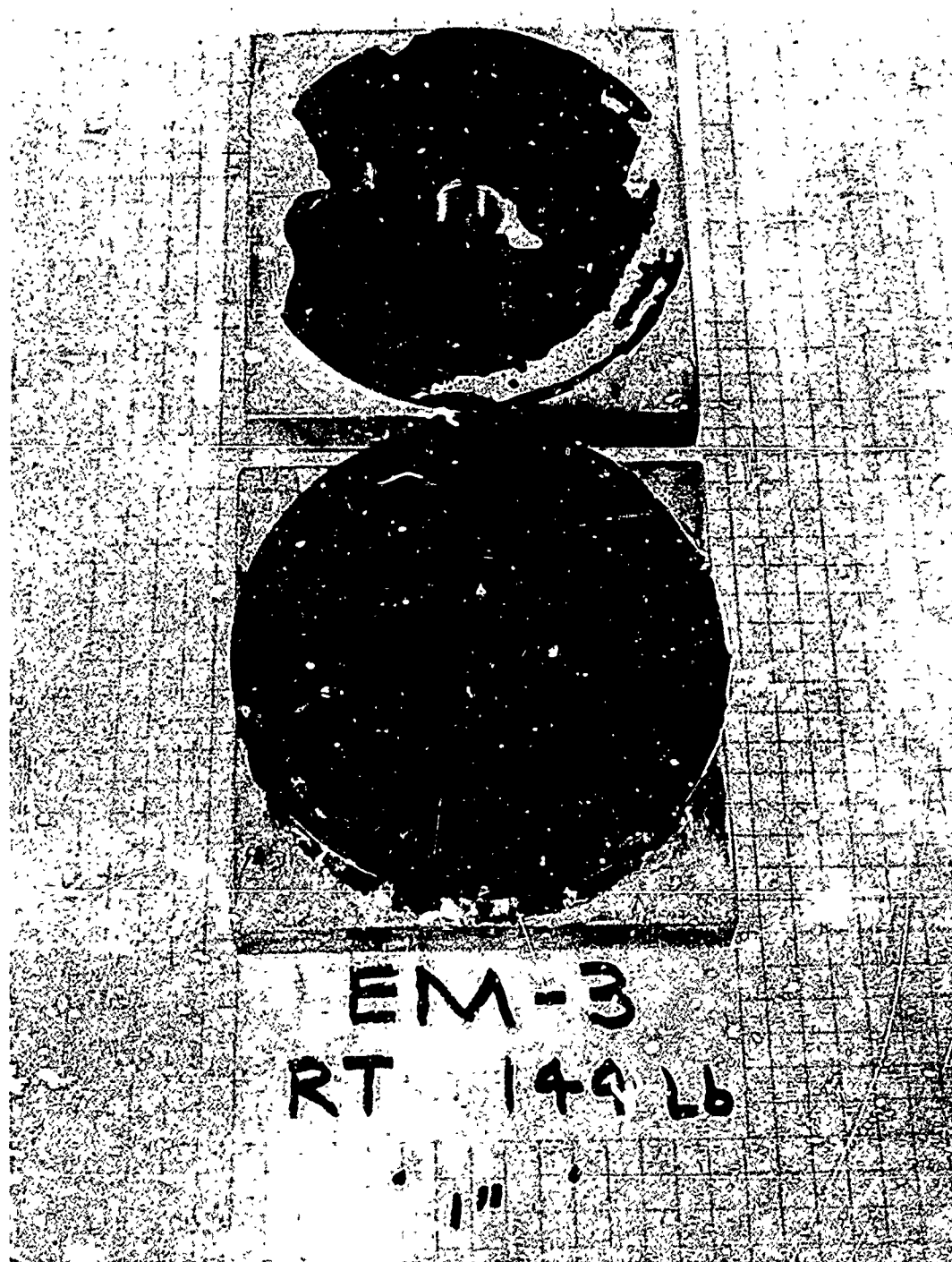


Figure 136 Material E (EM-3) – Facing Separation

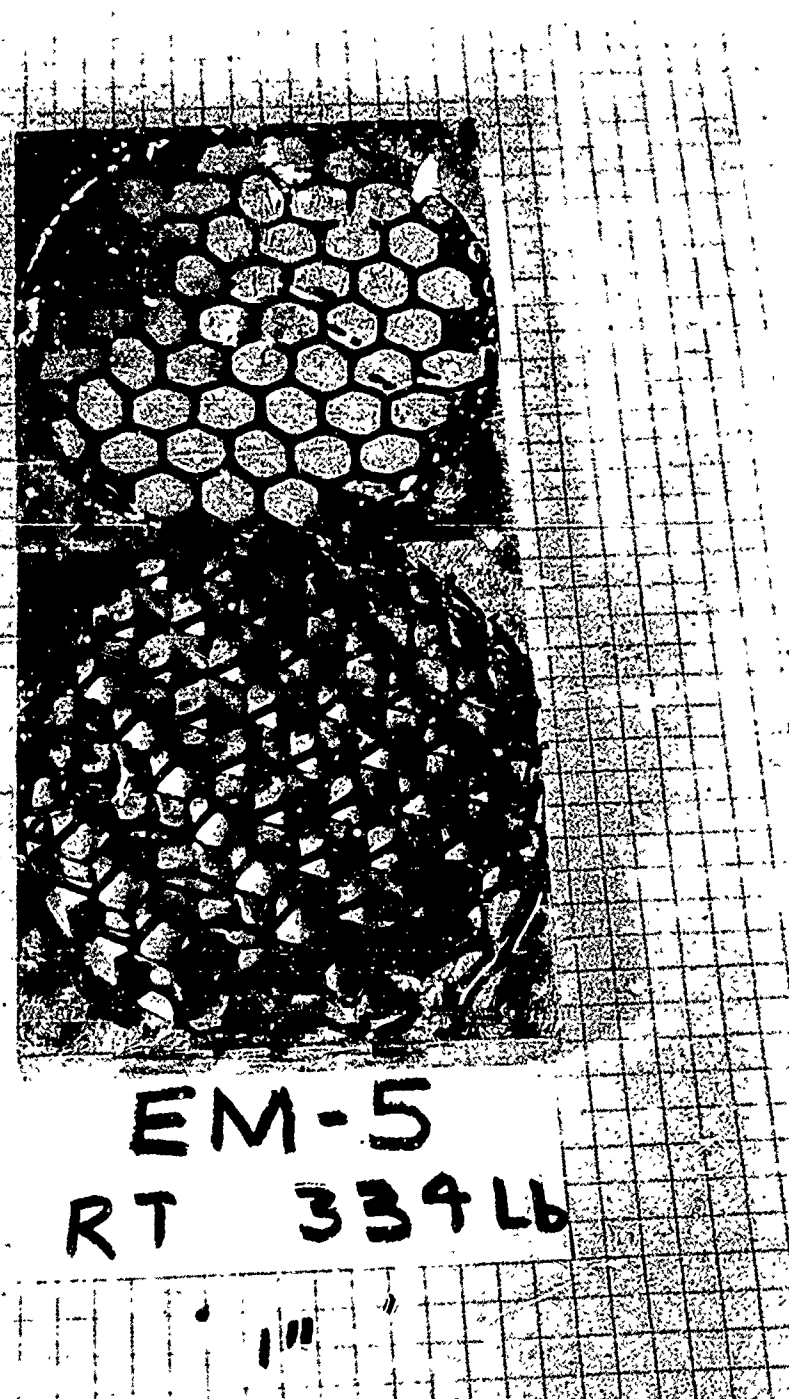


Figure 137 Material E (EM-5) - Facing Separation

Table XLIX. Materials G-K - Facing-Separation Test

Unexposed Specimens

Temperature	Specimen designation	Modulus E (psi)	Elastic limit (psi)	Maximum stress (psi)	Final strain (%)
-200° F	GM-11	1.05×10^3	3.25	3.25	0.29
Room temperature	GM-1	672	3.34	3.34	0.57
	GM-2	24.2	0.475	0.600	3.09
	Average	348.1	1.92	1.97	1.83
	Deviation	(93%)	(75.5%)	(69.5%)	(68.8)
+250° F	GM-4	292	1.00	1.00	0.57

Exposed Specimens

Specimen	Previous exposure	Modulus E (psi)	Elastic limit (psi)	Maximum stress (psi)	Final strain (%)
GFM-3	Thermal/vacuum environment (1,000 hr)	74.6	2.87	2.87	3.78
GFM-2	Thermal/vacuum environment (6,000 hr)	603	5.00	7.60	1.46
JGM-1	Thermal cycling (100 cycles)	306	4.05	4.05	1.32
JGN-2	Thermal cycling (1,000 cycles)	174	1.53	2.11	1.34
KG-1	Thermal cycling	457	4.25	4.25	0.93

Table I. Facing-Separation-Test Summary — Unexposed Specimens

Temperature	Material designation	Modulus		Elastic limit		Maximum stress		Final strain	
		Average (psi)	Deviation (%)	Average (psi)	Deviation (%)	Average (psi)	Deviation (%)	Average (%)	Deviation (%)
-200°F	A	3.99×10^3	26.8	104.1	15.6	106.3	17.3	2.80	10.0
	B	179	—	2.97	—	2.97	—	1.45	—
	C	4.11×10^3	7.6	538	4.8	561	2.0	15.6	7.1
	E	13.2×10^3	22.7	108	30.2	108	30.2	0.91	47.3
	G	1.05×10^3	—	3.25	—	3.25	—	0.29	—
Room temperature	A	3.73×10^3	63.8	86.6	51.5	96.6	50.5	4.43	71.3
	B	590	19.8	5.34	58.8	5.79	55.0	1.17	18.0
	C	13.2×10^3	12.9	181	23.2	276	16.7	2.60	29.6
	E	7.26×10^3	24.6	17.0	33.5	30.9	29.1	0.35	8.6
	G	348.1	93	1.92	75.5	1.97	69.5	1.83	68.8
+250°F	A	650	30.3	6.10	54.6	6.70	58.7	1.57	33.8
	B	266	33.5	5.39	34.2	5.89	26.5	2.44	16.4
	C	9.74×10^3	5.0	117	12.8	137	8.7	2.30	9.6
	E	1.28×10^3	13.3	5.80	22.4	7.80	29.6	0.85	1.2
	G	292	—	1.00	—	1.00	—	0.57	—

6. CORE COMPRESSION

The core compression tests were run to determine characteristics of candidate materials when subjected to a compression load normal to the plane of the panel. Data were obtained in the form of a load-deflection or stress-strain curve. From this curve, the equivalent compression modulus, elastic limit, maximum stress, and final strain at maximum stress were calculated. The point of maximum stress and final strain was defined as the point where decreasing load first occurred. Again, it is emphasized that only an "equivalent" modulus is intended, since the materials were not solid, continuous, or homogeneous.

Core compression tests also were performed upon candidate-material samples which had been previously exposed to the thermal/vacuum environment or to thermal cycling. The purpose was to determine the effects of the exposure upon the materials' resistance to compression load. Test procedures were the same as those used for the unexposed specimens, except that tests were performed only at room temperature.

a. Description of Apparatus

The test apparatus is shown schematically in Figure 138. The specimen under test was placed between two platens, one of which has a spherical seat to accommodate any materials with nonparallel facings. For the +250 and -200° F tests, thermocouple instrumented "gruyere" or thermal transmutation blocks were placed on either side of the specimen to transfer the heat or cold being carried by the surrounding air to the specimen. The platens were supported by 2-in. diameter stainless-steel compression columns in the +250° F and room temperature tests and by similar phenolic columns in the -200° F tests. Compression on the specimen was measured by a load cell at the base of the compression column while a calibrated deflector measured the movement of the platens.

The load cell and deflectometer signals were amplified by Sanborn carrier amplifiers, as required, and recorded on an X-Y plotter as the load was applied. In the case of the phenolic compression columns used at -200° F, the final data were compensated for compressive shortening of the columns.

Figure 98 shows the apparatus used at +250° F. The gruyere blocks, compression columns, platens, and forced-air heaters can be seen as can the deflectometer, which is just visible in the lower righthand corner.

b. Test Procedure

- (1) Measure and record average specimen thickness and dimension.
- (2) Center specimen between platens (or gruyere blocks for +250 and -200° F tests).
- (3) For +250 and -200° F tests only, bring specimen to temperature as indicated by thermocouples in face of gruyere blocks.
- (4) Operate testing machine to gradually apply load until specimen failure.

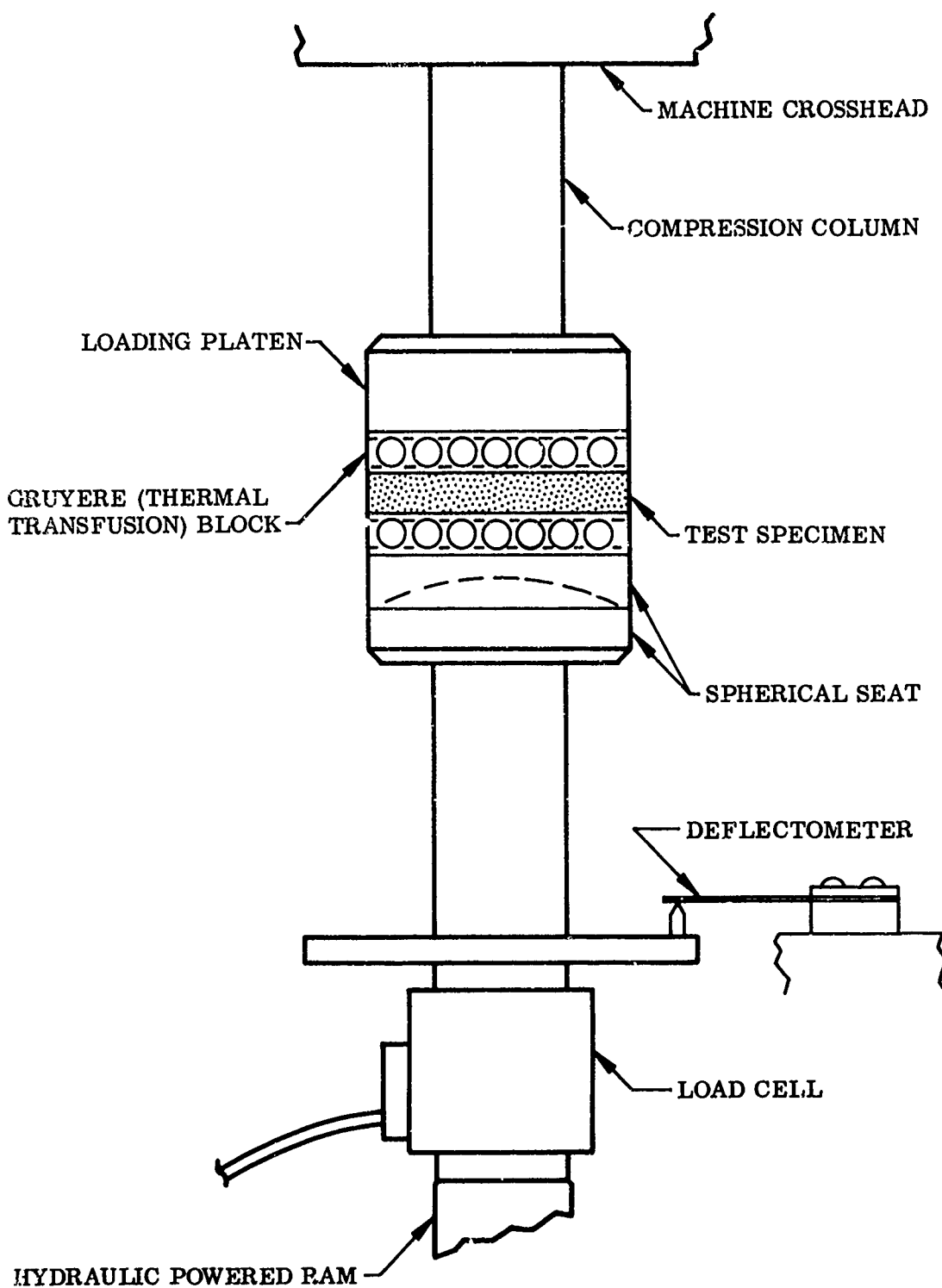


Figure 138 Core Compression Apparatus Diagram

c. Test Results

Test results for the several materials are shown individually in Tables LI through LV and collectively in Table LVI.

d. Comments and Interpretation of Results

Unexposed Specimens

Material A (Table LI). Samples of two thicknesses were tested, and the results shown in Table LI indicate clearly that the thinner material has a greater load-carrying capacity in normal compression. This is because failure results from buckling of the cell walls, and buckling strength increases as the length of the element decreases. Typical failures are shown in Figures 139 and 140. Both sizes exhibited strongest qualities at room temperature and weakened considerably at both +250 and -200° F. As in other tests of this material, the lightening hole lowered the material strength greatly, because the core in the area of the hole never contacts the compressing face and hence carries no load until the surrounding area has buckled.

Material B (Table LII). One-half and 1-in. thick specimens were tested with no notable differences in characteristics. Failure occurred by crushing of the foam cells that was not readily visible, since the actual cells are only a few thousandths of an inch in diameter.

Material C (Table LIII). The values obtained for this material were maximum at room temperature and showed greatest deterioration at -200° F. The large scatter in the data at room temperature was due to the lack of resolution of the extensometer measuring transducers even at very high sensitivity — this material was very rigid and deflected very little. In all cases, failure occurred by cell wall buckling as shown in Figure 141.

Material D (Table LIV). This material exhibited the rather odd characteristics of highest equivalent core modulus at +250° F and deterioration as the temperature was decreased. However, the greatest load-carrying capacity was at room temperature. Typical failures of this material are shown in Figure 142. It should be stated that load-carrying capacity is the more important quality in this configuration.

Material G (Table LV). This material has very erratic and poor characteristics, as may be verified from the data. Typical failure, as shown in Figure 143, occurred by buckling of the inner core "cups."

Exposed Specimens

The paucity of data makes it impossible to draw firm conclusions with regard to the effects of exposure to thermal/vacuum environment or thermal cycling. It appears, however, that in the case of the honeycomb structures (Materials A, C, and D-F; Tables LI, LIII, and LIV), the modulus of elasticity increased somewhat, or at any rate did not decrease; while the final strain decreased greatly. Values for Material B (Table LII), except for final strain, were lower than the corresponding values for unexposed specimens of the same materials, suggesting that the resistance to core compression of the phenolic foam is adversely affected by thermal/vacuum environment. The inferior structural properties of Material G (Table LV) do not appear to have been greatly affected by exposure to this environment.

The values presented in Table LIV for Material F (sample FGN-1) are much lower than would be expected for this material, judging by the corresponding values for the previously exposed specimens of materials D and E, and by the results of the facing separation tests performed on exposed specimens of Material F (Table XLVIII). It must be concluded that (1) the specimen itself was faulty, or (2) a malfunction of the test apparatus occurred during thermal cycling, resulting in damage to the specimen.

Table LI. Material A - Core-Compression Test
Unexposed Specimens

Temperature	Specimen designation	Modulus E (psi)	Elastic limit (psi)	Maximum stress (psi)	Final strain (%)
-200° F ^(a)	AN-7	3.84×10^3	28.0	32.8	1.39
	AN-8	3.07×10^3	27.1	29.9	1.02
	AN-9	2.28×10^3	23.2	29.5	1.57
	Average	3.06×10^3	26.1	30.7	1.33
Room temperature ^(a)	Deviation	(25.5%)	(11.1%)	(4.0%)	(23.3)
	AN-1	3.33×10^3	48.0	67.5	2.83
	AN-2	4.60×10^3	44.4	71.0	2.54
	AN-3	9.09×10^3	52.8	63.0	1.15
+250° F ^(a)	Average	5.67×10^3	48.4	67.2	2.17
	Deviation	(41.3%)	(8.3%)	(6.3%)	(47.7)
	AN-4	3.96×10^3	22.2	54.7	2.48
	AN-5	2.74×10^3	—	56.2	2.66
-200° F ^(b)	AN-6	2.53×10^3	42.8	51.2	2.56
	Average	3.08×10^3	32.5	54.0	2.57
	Deviation	(17.8%)	(31.7%)	(5.2%)	(3.5)
	AN-20	2.86×10^3	23.8	30.0	1.06
Room temperature ^(b)	AN-21	8.08×10^3	34.8	34.8	0.19
	AN-22	6.80×10^3	45.5	45.5	0.67
	Average	5.91×10^3	34.7	36.8	0.64
	Deviation	(51.6%)	(31.4%)	(18.5%)	(70.3)
+250° F ^(b)	AN-23	6.43×10^3	—	117.6	2.59
	AN-24	7.92×10^3	101.5	115.0	2.45
	AN-26	6.37×10^3	80.2	115.9	3.56
	Average	6.91×10^3	90.8	116.2	2.87
	Deviation	(7.8%)	(11.7%)	(1.0%)	(14.6)
	AN-16	1.68×10^3	32.8	37.7	2.40
	AN-17	2.50×10^3	31.6	64.1	5.61
	AN-18	4.20×10^3	39.1	60.7	3.79
	AN-19	1.76×10^3	31.1	52.5	4.70
	Average	2.53×10^3	33.6	53.7	4.12
	Deviation	(33.6%)	(7.4%)	(29.8%)	(41.7)

(a) Approximately 0.75-in. thick.

(b) Approximately 0.25-in. thick.

Table LI --- Continued

Exposed Specimens

Specimen	Previous exposure	Modulus E (psi)	Elastic limit (psi)	Maximum stress (psi)	Final strain (%)
AF-1	Thermal/vacuum environment (100 hr)	6.97×10^3	104	111	—
AFN-1	Thermal/vacuum environment (100 hr)	8.70×10^3	110	110	1.71
AF-3	Thermal/vacuum environment (1,000 hr)	7.37×10^3	97.7	109.4	1.94
AFN-3	Thermal/vacuum environment (1,000 hr)	10.2×10^3	110	133	1.58
AFN-2	Thermal/vacuum environment (6,000 hr)	9.73×10^3	131	140	1.59

Note: Specimens were approximately 0.25-in. thick. Data should be compared with results of tests on unexposed specimens of same thickness.



Figure 139 Material A (AN-1, 5) – Core Compression



Figure 140 Material A (AN-13) – Core Compression

Table LII. Material B - Core-Compression Test
Unexposed Specimens

Temperature	Specimen designation	Modulus E (psi)	Elastic limit (psi)	Maximum stress (psi)	Final strain (%)
-200° F ^(a)	BN-8	102	2.87	2.87	2.90
	BN-9	132	2.83	2.83	2.10
	BN-10	143	2.68	2.68	1.82
	Average	126	2.79	2.79	2.27
Room temperature ^(a)	BN-1	540	9.20	11.70	3.10
	BN-2	506	8.85	8.85	1.76
	BN-3	378	6.45	7.34	2.00
	BN-4	590	6.55	7.65	1.42
	Average	503	7.76	8.88	2.07
+250° F ^(a)	BN-5	683	6.57	7.04	1.45
	BN-6	309	4.37	4.37	1.40
	BN-7	285	4.42	-	-
	Average	426	5.12	5.70	1.42
-200° F ^(b)	BN-21	573	5.76	5.76	1.02
	BN-22	327	8.17	8.17	2.50
	BN-23	298	3.34	3.34	1.15
	Average	399	5.76	5.76	1.56
Room temperature ^(b)	BN-13	493	8.72	9.87	1.85
	BN-14	440	8.16	10.60	2.83
	BN-15	410	10.20	11.40	2.90
	BN-16	513	8.01	8.01	1.55
+250° F ^(b)	Average	464	8.77	9.97	2.28
	Deviation	(25.3%)	(42.0%)	(42.0%)	(34.6)
	BN-17	249	5.95	-	-
	BN-18	257	6.12	7.60	3.20
	BN-19	379	5.27	9.00	3.20
	BN-20	378	7.65	-	-
	Average	316	6.25	8.30	3.20
	Deviation	(21.2%)	(15.7%)	(8.4%)	(0)

(a) Approximately 0.5-in. thick.

(b) Approximately 1.0-in. thick.

Table LII --- Continued

Exposed Specimens

Specimen	Previous exposure	Modulus E (psi)	Elastic limit (psi)	Maximum stress (psi)	Final strain (%)
BFN-1	Thermal/vacuum environment (100 hr)	271	5.33	6.49	2.64
BFN-3	Thermal/vacuum environment (1,000 hr)	331	5.02	5.42	1.67
BFN-2	Thermal/vacuum environment (6,000 hr)	209	4.60	5.94	2.00

Note: Specimens were approximately 0.5-in. thick. Data should be compared with results of tests on unexposed specimens of same thickness.

Table LIII. Material C - Core-Compression Test
Unexposed Specimens

Temperature	Specimen designation	Modulus E (psi)	Elastic limit (psi)	Maximum stress (psi)	Final strain (%)
-200°F	CN-9	2.41×10^3	83	98	4.92
	CN-10	4.73×10^3	124	162	3.74
	CN-11	2.55×10^3	108	152	9.13
	Average	3.23×10^3	105	137	5.93
	Deviation	(25.4%)	(20.9%)	(28.5%)	(37.0)
Room temperature	CN-1	5.43×10^3	198	272	3.14
	CN-2	13.5×10^3	276	305	2.54
	CN-14	5.27×10^3	208	238	6.00
	Average	8.07×10^3	227	272	3.93
	Deviation	(22.3%)	(12.8%)	(12.5%)	(35.4)
+250°F	CN-6	5.30×10^3	213	213	9.58
	CN-7	5.83×10^3	200	200	7.78
	CN-8	—	—	203	—
	Average	5.56×10^3	206	205	8.68
	Deviation	(4.7%)	206	(4.1%)	(10.3)

Exposed Specimens

Specimen	Previous exposure	Modulus E (psi)	Elastic limit (psi)	Maximum stress (psi)	Final strain (%)
CF-1	Thermal/vacuum environment (100 hr)	10.65×10^3	257	257	2.36
CFN-3	Thermal/vacuum environment (1,000 hr)	11.05×10^3	246	282	2.98
CFN-2	Thermal/vacuum environment (6,000 hr)	9.50×10^3	196	227	2.61

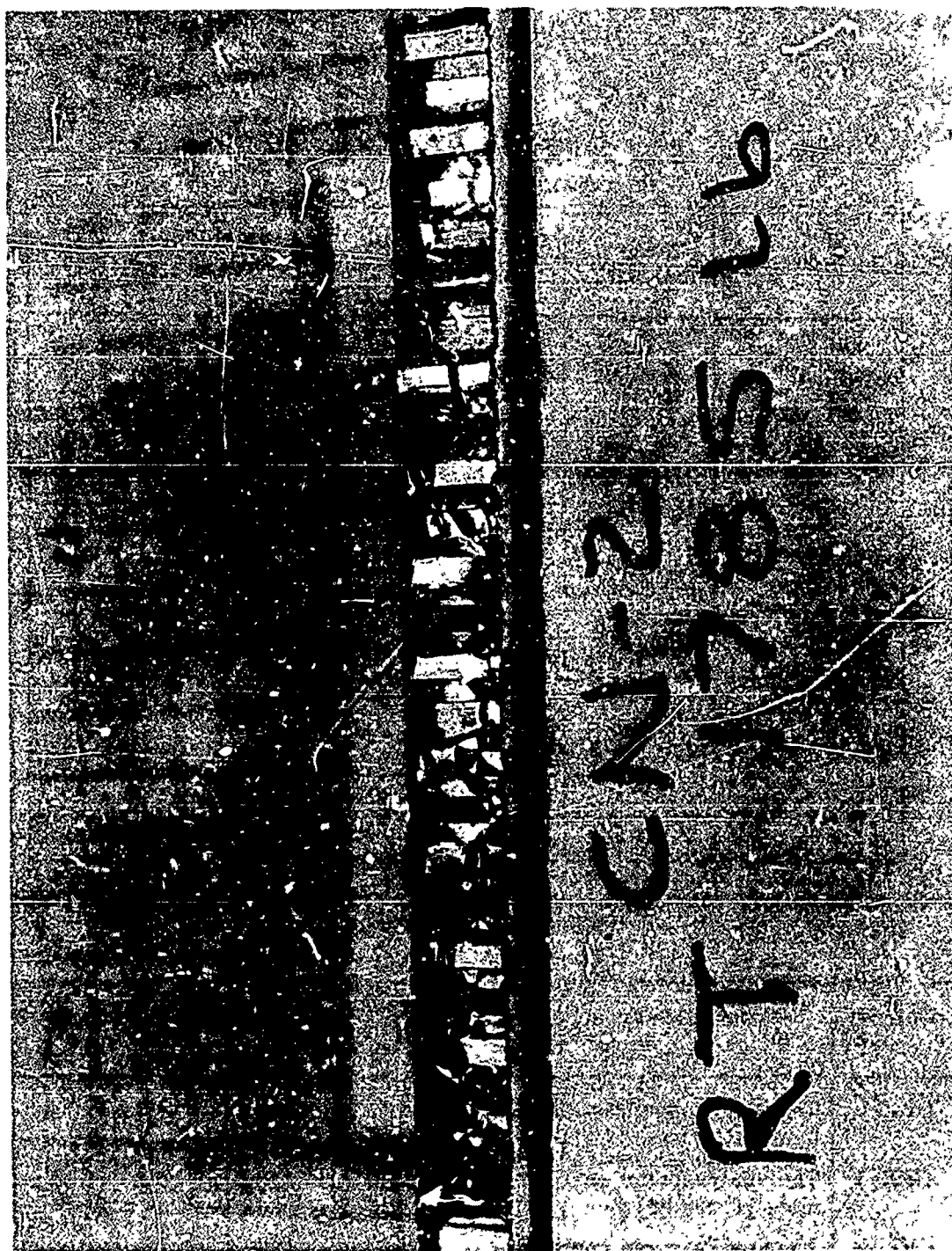


Figure 141 Material C (CN-2) – Core Compression

Table LIV. Materials D-F - Core-Comprression Test

Unexposed Specimens

Temperature	Specimen designation	Modulus E (psi)	Elastic limit (psi)	Maximum stress (psi)	Final strain (%)
-200° F	DN-7	1.55×10^3	44.6	47.8	4.92
	DN-8	5.00×10^3	43.4	57.8	1.37
	DN-9	---	63.5	67.6	---
	Average	3.28×10^3	50.5	57.7	3.16
Room temperature	Deviation	(52.7%)	(14.1%)	(17.2%)	(56.5)
	DN-1	4.22×10^3	53.5	83.1	3.84
	DN-2	4.53×10^3	43.9	89.3	5.30
	DN-3	3.35×10^3	44.8	84.8	4.32
+250° F	Average	4.03×10^3	47.4	85.7	4.49
	Deviation	(16.8%)	(7.4%)	(3.0%)	(14.5)
	DN-4	6.20×10^3	32.5	51.8	11.88
	DN-5	8.30×10^3	57.3	66.3	9.64
	DN-6	8.64×10^3	51.3	54.7	6.96
	Average	7.71×10^3	47.0	57.6	9.49
	Deviation	(19.6%)	(30.8%)	(11.8%)	(26.7)

Exposed Specimens

Specimen	Previous exposure	Modulus E (psi)	Elastic limit (psi)	Maximum stress (psi)	Final strain (%)
DGN-1	Thermal cycling (1,000 cycles)	4.72×10^3	69.5	71.5	1.62
DGN-3	Thermal cycling (6,000 cycles)	8.93×10^3	76.8	82.8	1.04
EF-1	Thermal/vacuum environment (100 hr)	3.85×10^3	---	82.5	0.92
EFN-1	Thermal/vacuum environment (100 hr)			Test equipment failure - no data	
EF-3	Thermal/vacuum environment (1,000 hr)	13.8×10^3	91.8	95.6	0.71
EFN-3	Thermal/vacuum environment (1,000 hr)	9.88×10^3	76.5	87.1	0.94
EFN-2	Thermal/vacuum environment (6,000 hr)	6.52×10^3	76.7	83.9	1.45
EGN-3	Thermal cycling (1,000 cycles)	7.09×10^3	80.5	88.4	1.41
FGN-1	Thermal cycling (3,000 cycles)	0.91×10^3	11.5	18.4	2.40

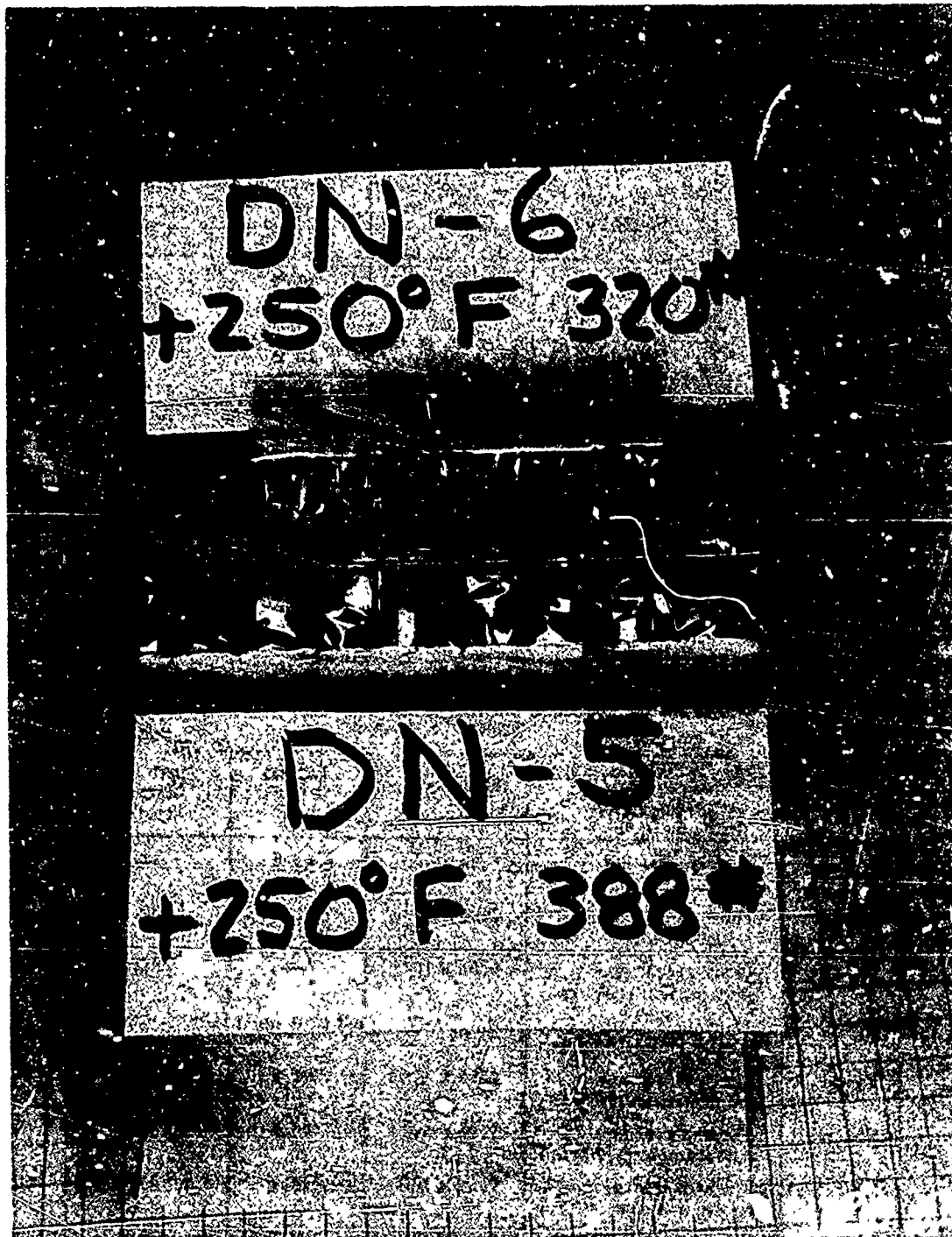


Figure 142 Material D (DN-5,6) – Core Compression

Table LV. Material G – Core-Compression Test
Unexposed Specimens

Temperature	Specimen designation	Modulus E (psi)	Elastic limit (psi)	Maximum stress (psi)	Final strain (%)
-200° F(a)	GN-7	530	2.74	2.74	0.52
	GN-8	295	3.22	3.60	1.37
	GN-9	518	4.45	4.78	0.97
	Average	448	3.47	3.71	0.95
Room temperature(a)	Deviation	(34.1%)	(21.1%)	(26.1%)	(45.3)
	GN-1	577	3.99	4.53	0.83
	GN-2	553	1.62	2.05	0.44
	GN-3	381	1.39	2.19	0.85
+250° F(a)	Average	504	2.33	2.92	0.71
	Deviation	(24.6%)	(40.3%)	(29.8%)	(38.0)
	GN-4	226	1.62	2.25	1.15
	GN-5	488	2.62	3.46	0.83
-200° F(b)	GN-6	280	2.00	2.92	1.16
	Average	331	2.08	2.88	1.05
	Deviation	(31.7%)	(22.1%)	(19.8%)	(20.9)
	GN-18	136	3.30	3.30	2.45
Room temperature(b)	GN-19	97	2.06	2.06	2.21
	GN-20	100	2.19	2.19	2.21
	Average	111	2.52	2.52	2.29
	Deviation	(11.7%)	(18.3%)	(18.3%)	(3.5)
+250° F(b)	GN-13	138	1.38	2.21	1.81
	GN-16	308	1.84	2.50	1.00
	GN-21	103	1.51	1.67	1.72
	Average	183	1.58	2.13	1.51
	Deviation	(43.7%)	(12.7%)	(21.6%)	(33.8)
	GN-14	173	1.06	1.44	0.89
	GN-15	113	0.94	1.47	2.32
	GN-17	172	0.91	0.91	0.55
	Average	156	0.97	1.27	1.25
	Deviation	(27.6%)	(6.2%)	(28.4%)	(56.0)

(a) Approximately 1.0-in. thick.

(b) Approximately 0.5-in. thick

Table LV --- Continued
Exposed Specimens

Specimen	Previous exposure	Modulus E (psi)	Elastic limit (psi)	Maximum stress (psi)	Final strain (%)
GF-1	Thermal/vacuum environment (100 hr)	138	2.32	2.94	2.62
GFN-1	Thermal/vacuum environment (100 hr)	115	2.50	2.75	2.55
GF-3	Thermal/vacuum environment (1,000 hr)	127	2.19	2.50	2.10
GFN-3	Thermal/vacuum environment (1,000 hr)	163	1.94	1.94	1.26
GFN-2	Thermal/vacuum environment (6,000 hr)	127	0.71	0.71	0.52

Note: Specimens were approximately 0.5-in. thick. Data should be compared with results of tests on unexposed specimens of same thickness.

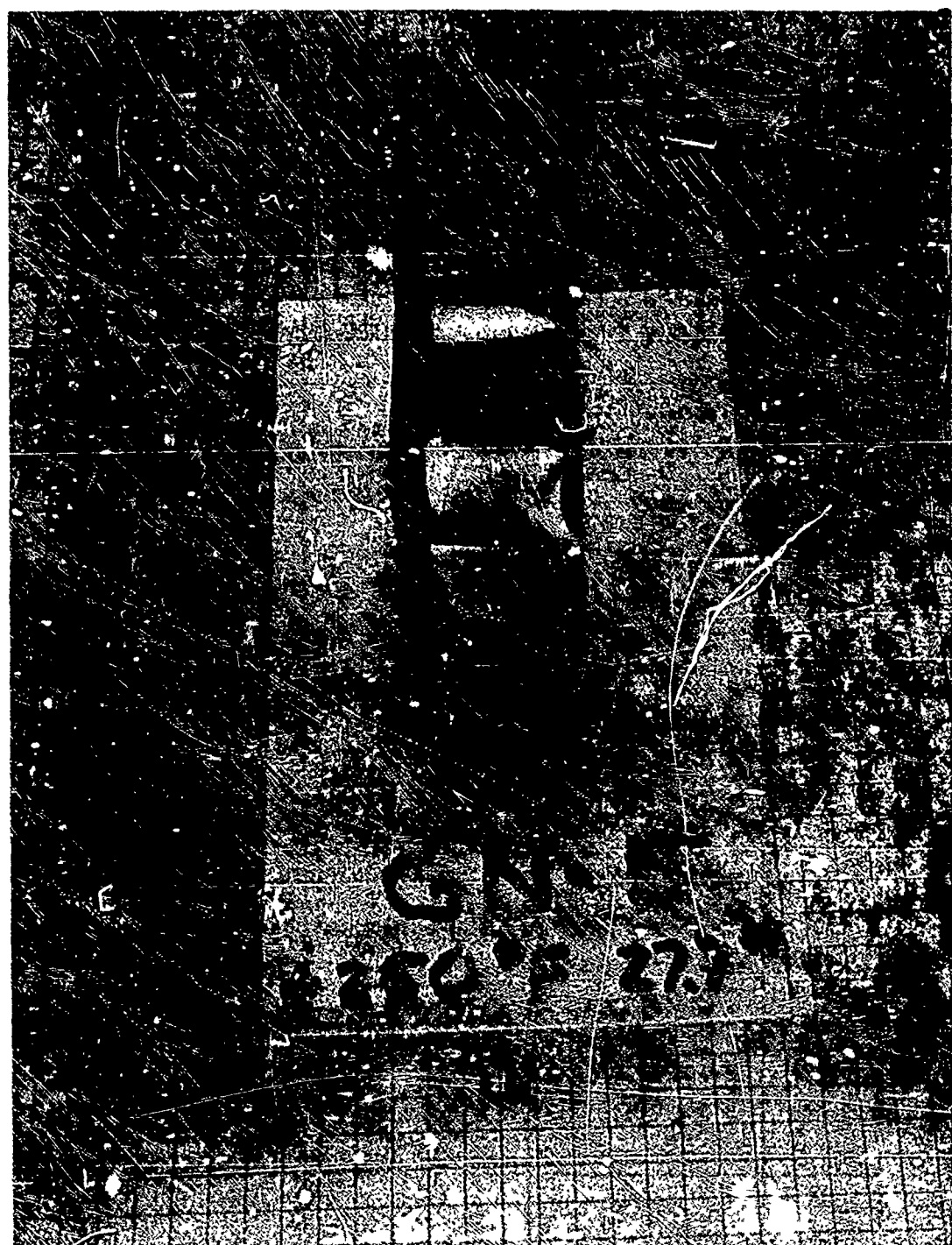


Figure 143 Material G (GN-5) - Core Compression

Table LVI. Core-Compression-Test Summary - Unexposed Specimens

Temperature	Material designation	Modulus Average (psi)	Deviation (%)	Elastic limit Average (psi)	Deviation (%)	Maximum stress Average (psi)	Deviation (%)	Final strain Average (%)	Deviation (%)
-200°F	A(a)	3.06 × 10 ³	25.5	26.1	11.1	30.7	4.0	1.33	23.3
	A(b)	5.91 × 10 ³	51.6	34.7	31.4	36.8	18.5	0.64	70.3
	B(c)	126	19.0	2.79	3.9	2.79	3.9	2.27	19.8
	B(d)	399	25.3	5.76	42.0	5.76	42.0	1.56	34.6
	C	3.23 × 10 ³	25.4	105	20.9	137	28.5	5.93	37.0
	D	3.28 × 10 ³	52.7	50.5	14.1	57.7	17.2	3.15	56.5
	G(d)	448	34.1	3.47	21.1	3.71	26.1	0.95	45.3
	G(c)	111	11.7	2.52	18.3	2.52	18.3	2.29	3.5
Room temperature	A(a)	5.67 × 10 ³	41.3	48.4	8.3	67.2	6.3	2.17	47.7
	A(b)	6.91 × 10 ³	7.8	90.8	11.7	116.2	1.0	2.87	14.6
	B(c)	503	24.8	7.76	16.9	8.88	17.3	2.07	31.4
	B(d)	4.64	11.6	8.77	8.7	9.97	19.7	2.28	32.0
	C	8.07 × 10 ³	22.8	227	12.8	272	12.5	3.93	35.4
	D	4.03 × 10 ³	16.8	47.4	7.4	85.7	3.0	4.49	14.5
	G(d)	504	24.6	2.33	40.3	2.92	29.8	0.71	38.0
	G(c)	183	43.7	1.58	12.7	2.13	21.6	1.51	33.8
+250°F	A(a)	3.08 × 10 ³	17.8	32.5	31.7	54.0	5.2	2.57	3.5
	A(b)	2.53 × 10 ³	33.6	33.6	7.4	53.7	29.8	4.12	41.7
	B(c)	426	33.1	5.12	14.7	5.70	23.4	1.42	1.4
	B(d)	316	21.2	6.25	15.7	8.30	8.4	3.20	0.0
	C	5.56 × 10 ³	4.7	—	—	205	4.1	8.68	10.3
	D	7.71 × 10 ³	19.6	47.0	30.8	57.6	11.8	9.49	26.7
	G(d)	331	31.7	2.08	22.1	2.88	19.8	1.05	20.9
	G(c)	156	27.6	0.97	6.2	1.27	28.4	1.25	56.0

(a) 0.75-in. thick. (b) 0.25-in. thick. (c) 0.5-in. thick. (d) 1.0-in. thick.

Section V CONCLUSIONS

The more significant test results, from the standpoint of making comparative evaluations of the candidate materials, are given in Table LVII. This table is intended to be used only for general reference and comparative purposes; for a thorough evaluation, the test results presented in the discussions of the individual tests should be consulted. In particular, the mechanical-properties data given in this section are averages and tell nothing about scatter among different samples of the same material, which in some instances was substantial.

The following comments generally appear to be justified with regard to the candidate materials:

1. None of the materials tested is ideally suited, in all respects, for use in the ASTEC solar collector. The best one from a structural standpoint does not have the best reflective surface. On the other hand, the material which showed to best advantage in the optical-properties testing has a highly unsatisfactory structure. The types of tests selected for the candidate material evaluation were adequate for collector-material comparison.
2. From a structural standpoint, the true honeycomb configurations are far superior to the other types. The lowest value recorded for a true honeycomb structure in the mechanical-properties testing (apart from the facing-tension test, which did not involve the complete structure) was higher than the highest value recorded for a structure of a nonhoneycomb type. The present test series was intended to provide a basis for comparing the candidate collector materials, rather than judging them against predetermined standards. The parameters measured for each material contained fairly wide bands of scatter. Thus, for the three samples tested under similar conditions, little is known about the distribution of the scatter about the average. In fact, three samples do not provide a basis for an average value which is to be used as a design criterion.
3. Materials with bare metal reflective surfaces have greater reflectance than those with silicon oxide overcoatings, and in addition proved to be significantly more stable in the ASTEC environment. The initial reflectance of the uncoated surfaces is above 0.90 in all cases, whereas only one of the coated surfaces exceeds 90 percent reflectance. The materials which showed the greatest degradation in the ASTEC environment, moreover, all have silicon oxide overcoatings.
4. The test program did not provide sufficient information regarding the effect upon reflectance of simultaneous exposure to ultraviolet radiation and low-energy electrons. The longest of the four test periods, 24 days, provided a dose equivalent

to 6 months in orbit. In the electrons-only exposure (subsection III.4), however, it was found that an apparent threshold for damage to the coated surfaces is reached after 8 months in orbit. Accordingly, little confidence can be placed in the extrapolated values shown in Figures 94 and 95 for reflectance after 12 months in orbit.

5. Specific test observations for each material tested, through Material K, are as follows.

- Material A. This material appears to be less desirable so far as its structural properties are concerned than Material C, but it is greatly superior to any of the nonhoneycombs. Its low values compared to Material C in this phase of the test program seem to be due wholly to the "lightening" holes in the backing material, which degrade its performance out of all proportion to the weight saving. Its reflective surface, vacuum-deposited aluminum with no over-coating, ranks near the top. Not only is its initial reflectance relatively high (92 percent), but there was degradation below the 85-percent ASTEC design-goal collector efficiency in only one of the environmental tests to which the reflective surface was subjected (ultraviolet exposure at room temperature). A possible problem relating to the use of Material A for a full-size solar collector stems from the two-component strippable protective coating used by the vendor. When the coating was removed, a residue remained upon the reflective surface which, if not eliminated before environmental exposure, would have caused a severe decrease in reflectance. Though the residue was easily removed from test specimens by washing the surface with distilled water and air drying, its removal from large surfaces might prove to be more difficult. The subcoat appears to be a green-dyed polyvinyl alcohol, similar or equivalent to Thalco 500G (Thalco, Inc.). The gray topcoat is a blend of polyvinyl acetate and polyvinyl chloride, including plasticizers, aluminum powder, carbon black, and titanium dioxide, similar or equivalent to Delchem X3181 (Pennsalt Chemical Corporation).
- Material B. The properties of this material suggest that its suitability for the ASTEC solar collector is at best doubtful. It proved to be quite unsound in the mechanical-properties testing, and its initial reflectance (0.85) was the lowest of any candidate material tested. (At the same time, its optical properties were among the most stable in the ASTEC environment.) The reflective surface blistersed severely and partially separated from the core material during thermal-cycling tests. This appears to have been due to the fact that the phenolic foam core contracts with increasing temperature, whereas the metallic surface expands. Finally, it should be noted that this material appears to exceed the maximum weight specified in the ASTEC solar collector design specifications (0.3 lb/ft²).
- Material C. This apparently is the most structurally desirable of the candidate materials. It was found to have high strength throughout all of the mechanical-properties tests, and its deterioration with changing temperature was relatively slight. Its initial reflectance (0.90) is close to the top among materials with silicon oxide overcoatings, although 2 or 3 percentage points below that of the

Table LVII. Summary of Candidate Materials Test Results

		Mechanical properties																						
		Panel bend (Weakest bending mode)		Facing tension						Facing separation						Core compression								
Elastic limit (psi)			Bending stiffness (in. ² -lb/in.)		Elastic moment (in.-lb/in.)		Elastic modulus (psi)			Elastic limit (psi)			Composite modulus (psi)			Elastic limit (psi)			Composite modulus (psi)			Elastic limit (psi)		
T	RT	+250°F	R1	RT	-200°F	RT	+230°F	-200°F	RT	+250°F	-200°F	RT	+250°F	RT	+200°F	RT	+250°F	-200°F	RT	+250°F	RT	+250°F		
9.47	2.95	59x0 (0.75 in. thick)	13.0 (0.75 in. thick)	14.2x10 ⁶	10.2x10 ⁶	9.6x10 ⁶	29.4x10 ³	35.5x10 ³	16.2x10 ³	3.99x10 ³	3.73x10 ³	650	104.1	56.6	6.10	3.05x10 ³	5.67x10 ³	3.08x10 ³	26.1 (0.75 in. thick)	48.4 (0.75 in. thick)	32.5 (0.75 in. thick)	90.8 (0.75 in. thick)	33.6 (0.75 in. thick)	
5.58	2.02	14x5 (1.0 in. thick)	12.0 (1.0 in. thick)	36.8x10 ⁶	33.8x10 ⁶	27.0x10 ⁶	50.1x10 ³	50.0x10 ³	37.1x10 ³	179	390	266	2.97	5.34	5.39	126 (0.5 in. thick)	503 (0.5 in. thick)	426 (0.5 in. thick)	2.79 (0.5 in. thick)	7.76 (0.5 in. thick)	5.12 (0.5 in. thick)	8.77 (1.0 in. thick)	6.25 (1.0 in. thick)	
28.2	20.25	1175 (0.3 in. thick)	19.0 (0.3 in. thick)	11.35x10 ⁶	9.32x10 ⁶	10.07x10 ⁶	23.0x10 ³	42.5x10 ³	21.1x10 ³	4.11x10 ³	13.2x10 ³	9.74x10 ³	538	161	117	3.23x10 ³	8.07x10 ³	5.56x10 ³	105	227	206			
13.35	3.24	3172 (0.5 in. thick)	7.8 (0.5 in. thick)	3.23x10 ⁶	3.03x10 ⁶	4.03x10 ⁶	7.6x10 ³	4.40x10 ³	4.58x10 ³	3.2x10 ³	7.26x10 ³	1.28x10 ³	108	17.0	5.80	3.28x10 ³	4.03x10 ³	7.71x10 ³	50.0	47.4	47.0			
Same as D	Same as D	Same as D	Same as D	Same as D	Same as D	Same as D	Same as D	Same as D	Same as D	Same as D	Same as D	Same as D	Same as D	Same as D	Same as D	Same as D	Same as D	Same as D	Same as D	Same as D	Same as D			
Same as D	Same as D	Same as D	Same as D	Same as D	Same as D	Same as D	Same as D	Same as D	Same as D	Same as D	Same as D	Same as D	Same as D	Same as D	Same as D	Same as D	Same as D	Same as D	Same as D	Same as D	Same as D			
1.31	---	20.8 (1.0 in. thick)	0.15 (1.0 in. thick)	47.8x10 ⁶	10.2x10 ⁶	17.9x10 ⁶	31.4x10 ³	22.7x10 ³	21.2x10 ³	1.05x10 ³	346.1	292	3.25	..92	1.00	448 (1.0 in. thick)	504 (1.0 in. thick)	331 (1.0 in. thick)	3.47 (1.0 in. thick)	2.35 (1.0 in. thick)	2.08 (1.0 in. thick)	1.58 (0.5 in. thick)	0.27 (0.5 in. thick)	
Same as G	Same as G	Same as G	Same as G	Same as G	Same as G	Same as G	Same as G	Same as G	Same as G	Same as G	Same as G	Same as G	Same as G	Same as G	Same as G	Same as G	Same as G	Same as G	Same as G	Same as G	Same as G			
Same as G	Same as G	Same as G	Same as G	Same as G	Same as G	Same as G	Same as G	Same as G	Same as G	Same as G	Same as G	Same as G	Same as G	Same as G	Same as G	Same as G	Same as G	Same as G	Same as G	Same as G	Same as G			
Same as G	Same as G	Same as G	Same as G	Same as G	Same as G	Same as G	Same as G	Same as G	Same as G	Same as G	Same as G	Same as G	Same as G	Same as G	Same as G	Same as G	Same as G	Same as G	Same as G	Same as G	Same as G			

uncoated materials. Its optical stability is relatively quite good. However, its reflectance fell several points below the 85-percent design goal for the ASTEC solar collector after simultaneous exposure to ultraviolet radiation and low-energy electrons for a period equivalent to 6 months in orbit.

- Material D. This material has generally good structural qualities and fairly high strength, although it had relatively low values in some of the tests at some temperatures. Its reflective surface is relatively very good, all test values being practically the same as those for Material A.
- Material E. The structure of this material is identical to that of Material D. Its reflective surface, differing from that of Material D only in the epoxy sublayer used, behaved much like that of Material D and possibly is slightly superior; the maximum degradation in the ASTEC environment for Material E (uv exposure) was 9 percentage points, compared with 10 points or more for Material D. The epoxy sublayer used in Material E lost much less weight in vacuum than the one used in Material D at all temperatures except 500° F.
- Material F. This material also has the same structure as Material D. Its reflective qualities, however, are much inferior to those of both Materials D and E; its initial reflectance is 3 percentage points lower, and it showed severe degradation (to 0.64) when exposed simultaneously to low-energy electrons and near ultraviolet radiation at 250° F for a period equivalent to 6 months. It thus appears to be the least desirable of these three materials.
- Material G. This material, identical in structure to Materials H, J, and K, had by far the lowest values in the mechanical-properties testing. Some specimens, in fact, could not be tested at all because the structure failed during preparation for testing. Its reflective surface, which was not overcoated, appears to be better than that of any other candidate material. Initial reflectance is the highest (0.93), and reflectance did not degrade to less than 0.86 in any of the environmental tests. The initial reflectance corresponds to other test data obtained independently.
- Material H. Structurally identical to Material G, the reflective properties of this material were less desirable. Though its initial reflectance (0.91) was higher than that of any other material with a coated surface, severe degradation was observed in certain of the environmental tests. Reflectance was 0.70 after ultraviolet exposure at room temperature for a period equivalent to 1 year, and below 0.80 after ultraviolet exposure at 250° F and combined-environment exposure for periods equivalent to 1 year and 6 months, respectively.
- Material J. Structurally identical to Material G, this material also proved to have a less desirable reflective surface. Its initial reflectance is a point lower, and it degraded somewhat more in the simulated ASTEC environments.
- Material K. The comments made for Material H apply also to this material, although the pattern of degradation in the ASTEC environments was somewhat different.

Section VI RECOMMENDATIONS

While the Candidate Materials Laboratory Tests appear to have provided sufficient information for a comparative evaluation of the materials, there is need for additional testing of the material or materials selected by the Air Force for further development. The following recommendations, insofar as practicable, follow the order of the conclusions.

1. Conclusion 1 would suggest that other tests, of lesser importance in this test program and perhaps not necessary at all for certain prototype designs, may become necessary after a design has been selected. These tests include the following:

Edgewise compression (of a sandwich)
Torsional stiffness (on varying widths of a panel) and creep characteristics
Thermophysical properties of complete collector petal assemblies
Venting characteristics of material sections selected

The purpose of the last test would be to ensure that rapid changes in pressure and temperature during the ascent condition will not lead to partial or complete destruction of the honeycomb petals due to insufficient venting.

2. It is recommended that a more extensive program of mechanical-properties tests, involving more specimens for each test type and temperature, be run on those materials selected for collector development. A standard deviation which is a large percentage of the reported mean would suggest that the allowable stresses used in design be lower than would be used if the standard deviation were small.
3. Consideration should be given to the use of bare metal reflecting surfaces, or the use of an inert reflecting material, on the full-scale collector selected for flight-test development and operational service. This recommendation follows from conclusion 3.
4. From conclusion 4, the effect upon reflectance of simultaneous exposure to ultraviolet radiation and low-energy electrons for periods longer than 8 months is uncertain. An investigation therefore should be made on the collector materials chosen for development to determine the degree of their optical stability in the combined environment, for a period equivalent to 1 year in orbit. This will be especially important if one or more of the materials has a silicon oxide overcoating.

Section VII
REFERENCES

1. P. J. Kendall, J. P. Moran, and T. E. Chappell, A Method for Predicting Thermal Response in Sandwich Panels, Tech. Doc. Rept. ASD-TDR-63-306, May 1963
2. R. T. Swann, Calculated Effective Thermal Conductivities of Honeycomb Sandwich Panels, NASA TN D-171, Dec 1959
3. R. T. Swann, Analysis of Effective Thermal Conductivities of Honeycomb-Core and Corrugated-Core Panels, NASA TN D-714, April 1961
4. P. J. Kendall and J. I. Gonzales, An Analytical Model for Predicting Thermal Response in Honeycomb Sandwich Panels, AIAA Paper No. 64-258, June 1964
5. M. L. Minges, Proceedings of the Fourth Conference on Thermal Conductivity, San Francisco, Calif., Oct 1964
6. A. Goldsmith, T. E. Waterman, H. J. Hirschhorn, Thermophysical Properties of Solid Materials, WADC Tech. Rep. 58-476, Vol. 1, Nov 1960
7. D. C. Ginnings, "Thermal Properties of Aluminum Oxide From 0° to 1200° K," J. Res. NBS, Vol. 57, No. 2, 1956
8. K. K. Kelley, USBM Bulletin, No. 54
9. W. Bradshaw, A. Gleason, A. Wilder, and J. Robinson, "Evaluation of Mariner Shroud Material," Lockheed Missiles & Space Company, Jan 1965
10. F. S. Johnson, "The Solar Constant," J. Meteorol., 11, 431-439, 1954

Appendix I
TEST RESULTS - CANDIDATE MATERIAL A

Presented in this appendix are the results of all laboratory tests performed on Material A. Discussions of the tests, descriptions of test apparatus, test procedures and conditions, and interpretations of test results, covered elsewhere in this report, are not repeated here.

Material A is an aluminum honeycomb structure, with epoxy-bonded aluminum front and back sheets. Its reflective surface is aluminum, vacuum-deposited on an aluminum substrate.

Results of the following tests are given in this appendix:

- Weight loss in vacuum (epoxy adhesive)
- Long-term thermal/vacuum exposure (composite structure)
- Thermal conductance of composite structures
- Behavior under thermal cycling
- Ultraviolet irradiation at room temperature and +250°F
- Exposure to low-energy electrons at room temperature and +250°F
- Exposure to combined environment (uv + e⁻) at room temperature and +250°F
- Panel shear (-200°F, room temperature, and +250°F)
- Panel bend
- Facing tension (-200°F, room temperature, and +250°F)
- Facing separation (-200°F, room temperature, and +250°F)
- Core compression (-200°F, room temperature, and +250°F)

See Figures 144 through 147 and Tables LVIII through LXVI.

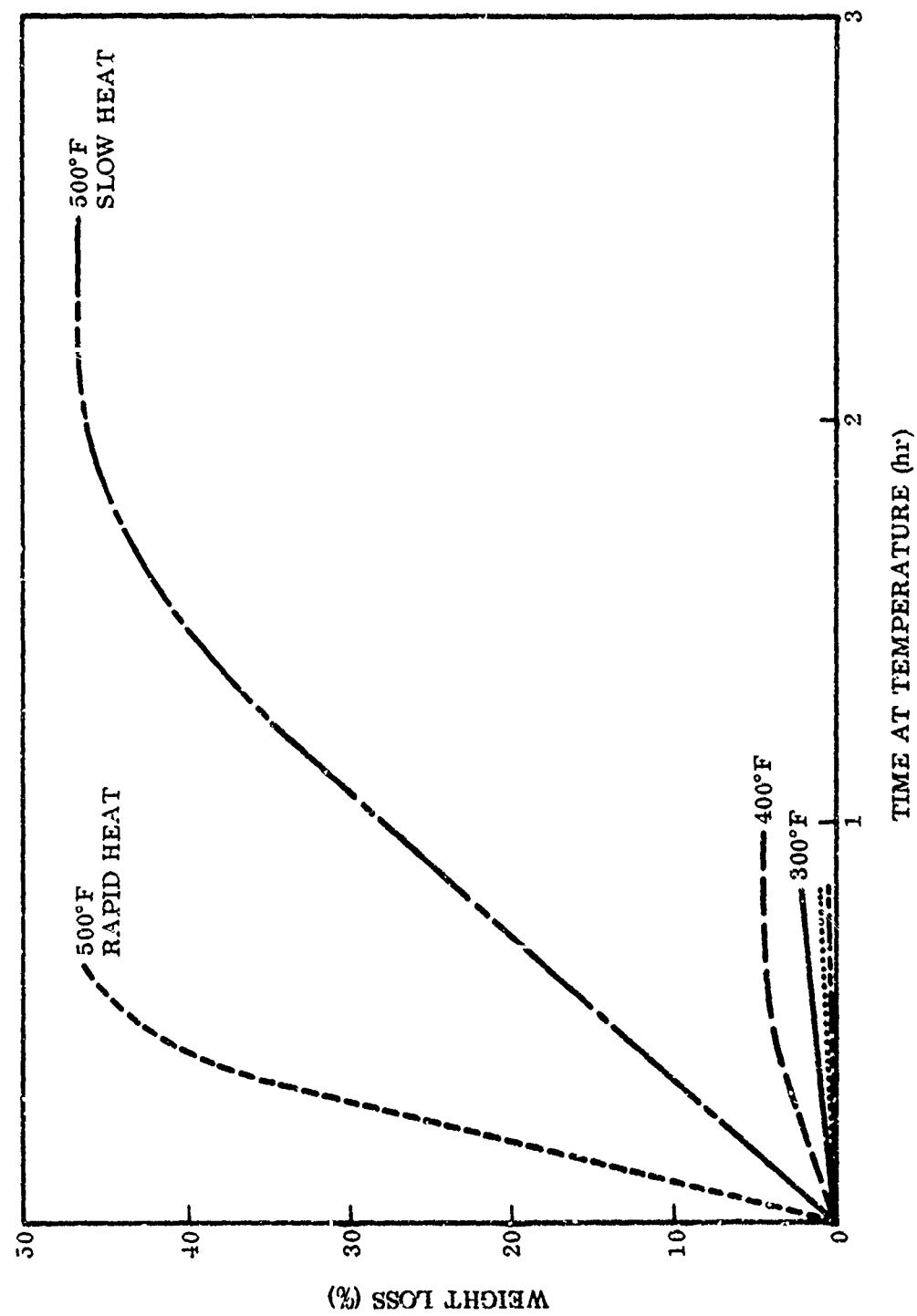


Figure 144 Weight Loss Versus Time at Temperature, Epoxy Adhesive

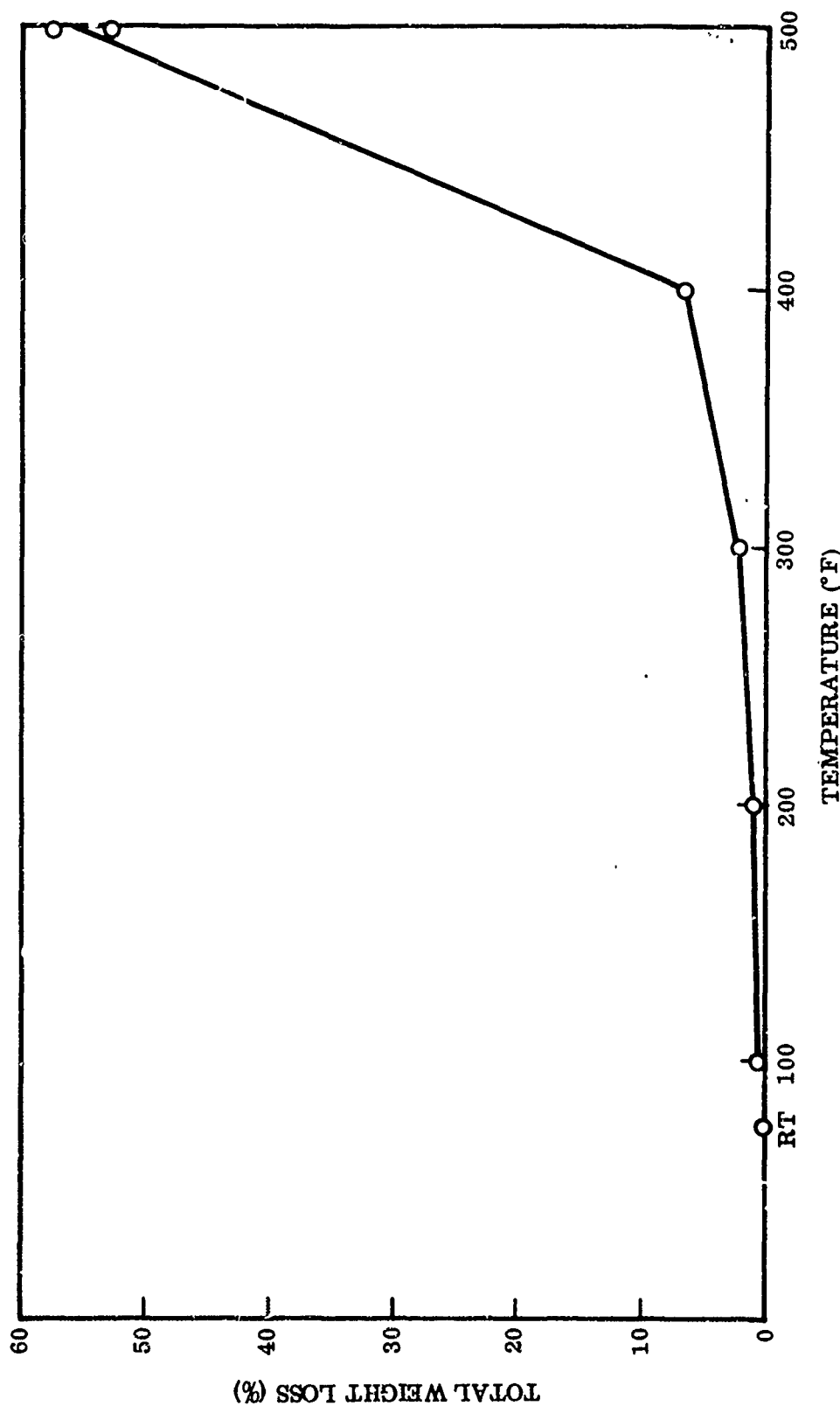


Figure 145 Equilibrium Weight Loss as a Function of Temperature, Epoxy Adhesive

Table LVIII. Short-Term Weight Loss in Vacuum, Epoxy Adhesive

Test conditions		Cumulative weight loss (%)	Maximum short-term temperature stability	Comments
Temperature (° F)	Total time (min)			
100	48	0.29	400° F	
200	96	0.71		
300	144	1.72		
400	214	6.2		
500	362	52.4		Bloated, porous brown residue at 500° F

Table LIX. Long-Term Thermal/Vacuum Exposure, Composite Structure

Specimen	Weight before (g)	Weight after (g)	Weight loss (g)	Change (%)	Post-test appearance
100-hour test					
AF-1	3.8228	3.7942	0.0286	0.75	Slight flow of bonding agent
AFM-1	3.7475	3.7162	0.0313	0.835	Same as AF-1
AFN-1	3.7890	3.7582	0.0308	0.81	Same as AF-1
1,000-hour test					
AF-3	3.7940	3.7451	0.0489	1.29	Slight flow of bonding agent
AFM-3	4.000	3.9261	0.0739	1.84	Same as AF-3
AFN-3	3.9278	3.8703	0.0575	1.46	Same as AF-3
6,000-hour test					
AF-2	3.7978	3.7302	0.0676	1.78	Slight flow of bonding agent
AFM-2	3.8238	3.7457	0.0781	2.04	Same as AF-2
AFN-2	3.9290	3.8482	0.0808	2.06	Same as AF-2

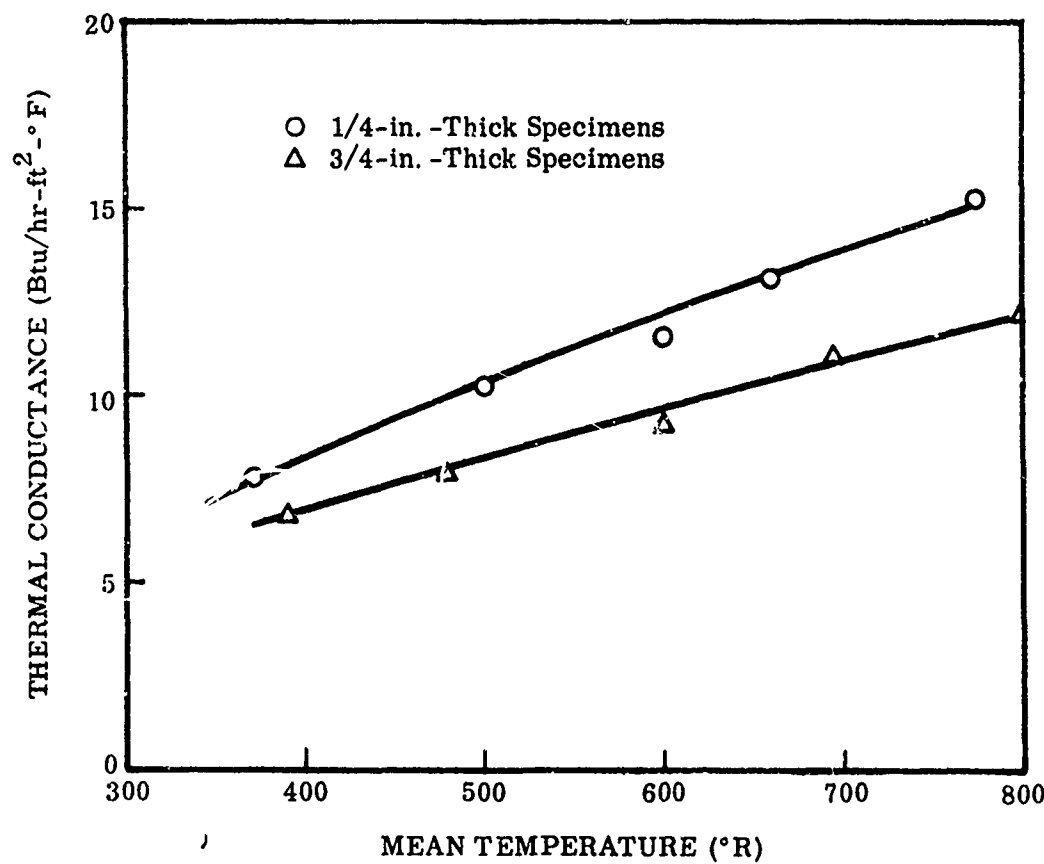


Figure 146 Thermal Conductance of Composite Structures

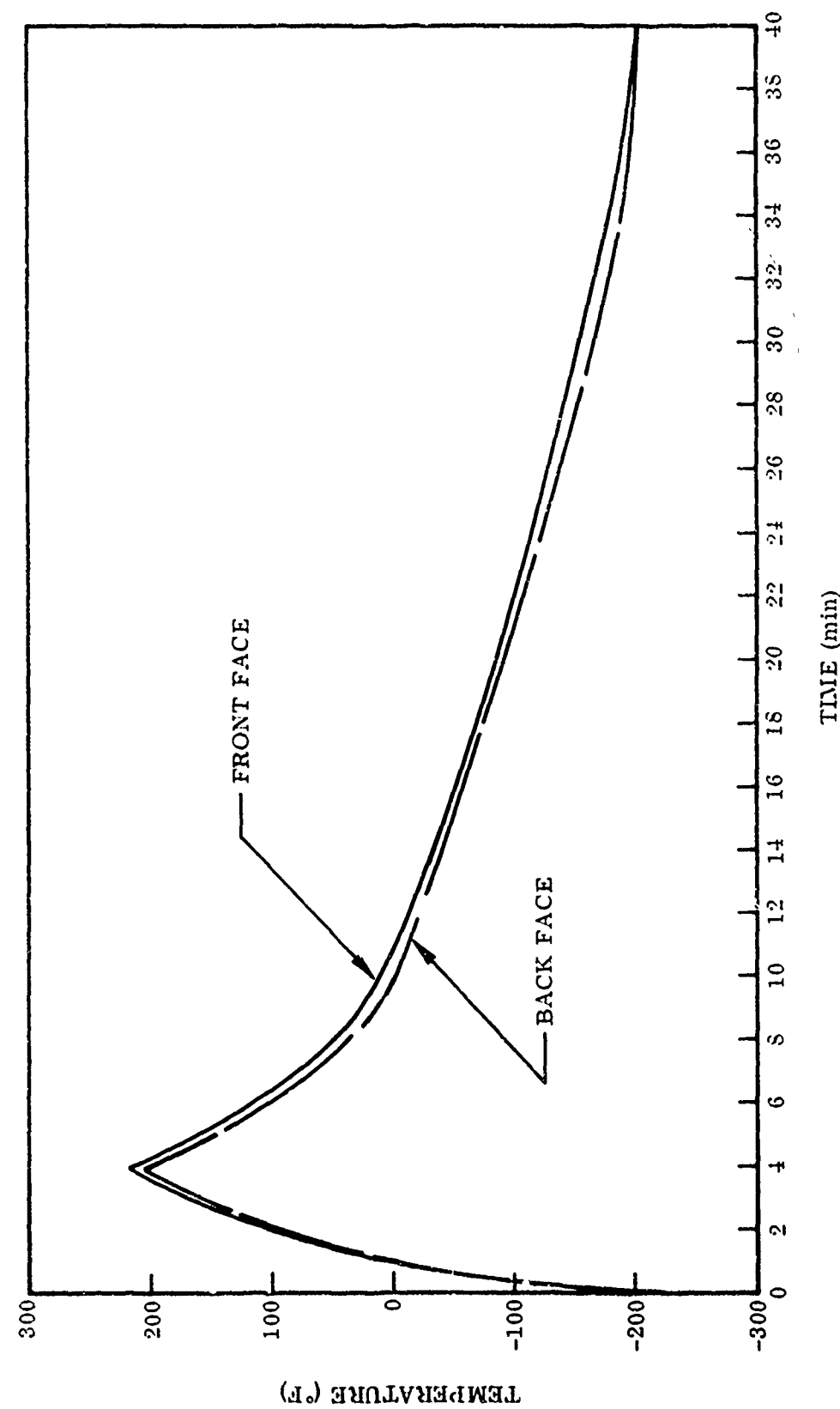


Figure 147 Temperature Histories of Front and Back Faces During Thermal Cycling

Table LX Behavior Under Thermal Cycling, Composite Structure

Specimen	Duration of test (cycles)	Pre-test condition	In situ condition		Post-test condition	Reflectance after exposure
			Cycle	Condition		
AGN-1	100	Surfaces flat (see Figure 61a)	0-125	No change noted (see Figure 61b)	No change noted	No change
AGM-1	1,000	Front surface flat; no honey-comb structure shows through (see Figure 61c)	0-4	No change noted	No change noted	No change
			67	Surface appears wavy when cool		
			68-1,007	No further change noted (see Figure 61d)		
AGM-2	6,000	Front surface flat; no honey-comb structure shows through	0-6,002	Surface appears wavy when cool, flat when heated (see Figure 61e)	No change noted	No change

Table LXI. Summary of Optical-Properties Test Results

Exposure	Solar Reflectance
Pre-test condition	0.92
Ultraviolet radiation (1-yr equivalent)	
RT	0.82
250° F	0.90
5 keV electrons (1-yr equivalent)	
RT	0.92
250° F	0.92
Combined environment (6-mo equivalent)	
RT	0.85
250° F	0.91

Table LXII. Panel-Shear Test, Composite Structure

Temperature	Specimen designation	Modulus G (psi)	Elastic limit (psi)	Maximum stress (psi)	Final strain (%)
-200° F	AJ-8	4.25×10^3	30.1	111.4	4.00
	AJ-9	4.51×10^3	47.5	87.8	5.06
	AJ-10	3.83×10^3	29.3	80.9	4.42
	Average	4.20×10^3	35.6	93.4	4.49
	Deviation	(8.8%)	(17.7%)	(3.1%)	(10.9%)
Room temperature	AJ-1	3.12×10^3	13.50	56.5	6.78
	AJ-2	2.86×10^3	7.01	115.2	7.90
	AJ-3	2.69×10^3	8.50	17.8	1.09
	Average	2.89×10^3	9.67	63.2	5.26
	Deviation	(6.9%)	(17.2%)	(71.9%)	(78.9%)
+250° F	AJ-6	2.20×10^3	3.31	5.06	0.46
	AJ-7	4.38×10^3	3.99	4.69	2.98
	AJ-8	1.19×10^3	1.59	3.69	1.60
	Average	2.92×10^3	2.96	4.48	1.68
	Deviation	(59.2%)	(46.2%)	(17.6%)	(72.6%)

Table LXIII. Panel-Bend Test, Composite Structure

Specimen designation	Beam width, b (in.)	Beam span, L (in.)	$\frac{EI/b}{in.^2-lb}$ in.	M_e/b (lb)	M_u/b (lb)	Tension face	Thickness (~ in.)
AK-2	2.50	9	7,350	34.5	54.0	Nonreflecting	0.75
AK-4	2.50	9	7,520	30.0	54.8	Nonreflecting	
AK-1	2.50	9	6,200	16.2	20.2	Reflecting	
AK-3	2.50	9	5,600	9.9	16.3	Reflecting	
Average(a)		—	5,900	13.0	18.2		
AK-6	2.50	9	905	9.90	18.20	Nonreflecting	0.25
AK-5	2.50	9	835	4.80	7.02	Reflecting	
AK-7	2.50	9	642	4.20	6.12	Reflecting	
AK-8	2.50	9	785	2.40	5.82	Reflecting	
Average(a)			754	3.80	6.32		

(a) Average is for weakest bending mode of each parameter.

Table LXIV. Facing-Tension Test, Facing Material

Temperature	Specimen designation	Modulus E (psi)	Elastic limit (psi)	Maximum stress (psi)	Final strain (%)
-200° F	AL-7	11.7×10^6	25.0×10^3	43.5×10^3	8.14
	AL-8	13.4×10^6	31.5×10^3	44.7×10^3	6.64
	AL-9	17.5×10^6	31.5×10^3	46.2×10^3	7.52
	Average	14.2×10^6	29.3×10^3	44.8×10^3	7.19
Room temperature (a)	Deviation	(17.6%)	(14.7%)	(2.9%)	(7.6)
	AL-1	10.5×10^6	35.5×10^3	38.0×10^3	3.85
	AL-2	10.4×10^6	35.5×10^3	38.2×10^3	4.50
	AL-3	9.6×10^6	36.3×10^3	40.4×10^3	4.25
	Average	10.2×10^6	35.8×10^3	38.7×10^3	4.20
+250° F	Deviation	(5.9%)	(0.8%)	(1.8%)	(8.3)
	AL-4	9.1×10^6	17.3×10^3	37.8×10^3	2.28
	AL-5	10.7×10^6	14.0×10^3	37.7×10^3	2.74
	AL-6	8.9×10^6	18.0×10^3	37.7×10^3	2.38
	Average	9.6×10^6	16.2×10^3	37.7×10^3	2.47
	Deviation	(7.3%)	(13.6%)	(0.1%)	(7.7)

(a) The 0.2 percent offset yield strength at room temperature is given instead of the elastic limit.

Table LXV. Facing-Separation Test, Composite Structure

Unexposed Specimens

Temperature	Specimen designation	Modulus E (psi)	Elastic limit (psi)	Maximum stress (psi)	Final strain (%)
-200°F	AM-7	2.32×10^3	87.9	87.9	3.36
	AM-8	4.46×10^3	122.0	122.0	2.81
	AM-9	4.50×10^3	102.3	109.0	2.52
	Average	3.99×10^3	104.1	106.3	2.80
	Deviation	(26.8%)	(15.6%)	(17.3%)	(10.0)
Room temperature	AM-1	1.35×10^3	132.0	132.0	9.76
	AM-2	5.50×10^3	84.9	110.0	2.23
	AM-3	4.33×10^3	43.0	47.8	1.29
	Average	3.73×10^3	86.6	96.6	4.43
	Deviation	(63.8%)	(51.5%)	(50.5%)	(71.3)
+250°F	AM-4	1.09×10^3	11.20	11.90	1.50
	AM-5	128	2.77	2.77	2.18
	AM-6	732	4.33	5.44	1.04
	Average	650	6.10	6.70	1.57
	Deviation	(80.3%)	(54.6%)	(58.7%)	(33.8)

Exposed Specimens

Specimen	Previous exposure	Modulus E (psi)	Elastic limit (psi)	Maximum stress (psi)	Final strain (%)
AFM-1	Thermal/vacuum environment (100 hr)	2.79×10^3	159	159	5.89
AFM-3	Thermal/vacuum environment (1,000 hr)	3.82×10^3	241	252	6.71
AF-2	Thermal/vacuum environment (6,000 hr)	11.10×10^3	209	286	2.80
AFM-2	Thermal/vacuum environment (6,000 hr)	5.09×10^3	197	223	4.30
AGN-1	Thermal cycling (100 cycles)	3.34×10^3	108.6	108.6	3.23
AGM-1	Thermal cycling (1,000 cycles)	4.57×10^3	170	199	4.43
AGM-3	Thermal cycling (6,000 cycles)	4.75×10^3	142	173	3.92
AGM-2	Thermal cycling (214 cycles)	4.90×10^3	160	214	4.90

NOTE: Specimen AGM-2 was initially scheduled to undergo 6,000 cycles. Testing was terminated after 214 cycles because of electronic difficulties which resulted in the specimen's being maintained at 200°F for approximately 16 hr.

Table LXVI. Core-Compression Test Composite Structure
Unexposed Specimens

Temperature	Specimen designation	Modulus E (psi)	Elastic limit (psi)	Maximum stress (psi)	Final strain (%)
-200° F(a)	AN-7	3.84×10^3	28.0	32.8	1.39
	AN-8	3.07×10^3	27.1	29.9	1.02
	AN-9	2.28×10^3	23.2	29.5	1.57
	Average	3.06×10^3	26.1	30.7	1.33
Room temperature(a)	Deviation	(25.5%)	(11.1%)	(4.0%)	(23.3)
	AN-1	3.33×10^3	48.0	67.5	2.83
	AN-2	4.60×10^3	44.4	71.0	2.54
	AN-3	9.09×10^3	52.8	63.0	1.15
+250° F(a)	Average	5.67×10^3	48.4	67.2	2.17
	Deviation	(41.3%)	(8.3%)	(6.3%)	(47.7)
	AN-4	3.96×10^3	22.2	54.7	2.48
	AN-5	2.74×10^3	—	56.2	2.66
-200° F(b)	AN-6	2.53×10^3	42.8	51.2	2.56
	Average	3.08×10^3	32.5	54.0	2.57
	Deviation	(17.8%)	(31.7%)	(5.2%)	(3.5)
	AN-20	2.86×10^3	23.8	30.0	1.06
Room temperature(b)	AN-21	8.08×10^3	34.8	34.8	0.19
	AN-22	6.80×10^3	45.5	45.5	0.67
	Average	5.91×10^3	34.7	36.8	0.64
	Deviation	(51.6%)	(31.4%)	(18.5%)	(70.3)
+250° F(b)	AN-23	6.43×10^3	—	117.6	2.59
	AN-24	7.92×10^3	101.5	115.0	2.45
	AN-26	6.37×10^3	80.2	115.9	3.56
	Average	6.91×10^3	90.8	116.2	2.87
+250° F(b)	Deviation	(7.8%)	(11.7%)	(1.0%)	(14.6)
	AN-16	1.68×10^3	32.8	37.7	2.40
	AN-17	2.50×10^3	31.6	64.1	5.61
	AN-18	4.20×10^3	39.1	60.7	3.79
+250° F(b)	AN-19	1.76×10^3	31.1	52.5	4.70
	Average	2.53×10^3	33.6	53.7	4.12
	Deviation	(33.6%)	(7.4%)	(29.8%)	(41.7)

(a) Approximately 0.75-in. thick.

(b) Approximately 0.25-in. thick.

Table IXVI --- Continued

Exposed Specimens

Specimen	Previous exposure	Modulus E (psi)	Elastic limit (psi)	Maximum stress (psi)	Final strain (%)
AF-1	Thermal/vacuum environment (100 hr)	6.92×10^3	161	111	—
AFN-1	Thermal/vacuum environment (200 hr)	8.70×10^3	110	120	1.71
AF-3	Thermal/vacuum environment (1,000 hr)	7.37×10^3	57.7	199.4	1.94
AF-5	Thermal/vacuum environment (1,000 hr)	10.2×10^3	111	133	1.58
AFN-2	Thermal/vacuum environment (6,000 hr)	9.73×10^3	131	140	1.59

Note: Specimens were approximately 0.25-in. thick. Data should be compared with results of tests on unexposed specimens of same thickness.

Appendix II
TEST RESULTS - CANDIDATE MATERIAL B

Presented in this appendix are the results of all laboratory tests performed on Material B. Discussions of the tests, descriptions of test apparatus, test procedures and conditions, and interpretations of test results, covered elsewhere in this report, are not repeated here.

Material B consists of electroformed nickel sheet, backed with phenolic foam. Its reflective surface is aluminum vacuum-deposited on a nickel substrate, with a silicon-oxide overcoating. The back surface is epoxy-bonded, aluminized mylar.

Results of the following tests are given in this appendix:

- Weight loss in vacuum (foam structure)
- Long-term thermal/vacuum exposure
- Thermal conductance of composite structure
- Thermal expansion (reflective surface, foam structure, back surface)
- Heat capacity (foam structure and back surface)
- Behavior under thermal cycling
- Ultraviolet irradiation at room temperature and +250°F
- Exposure to low-energy electrons at room temperature and +250°F
- Exposure to combined environment (uv + e⁻) at room temperature and +250°F
- Panel shear (-200°F, room temperature, and +250°F)
- Panel bend
- Facing tension (-200°F, room temperature, and +250°F)
- Facing separation (-200°F, room temperature, and +250°F)
- Core compression (-200°F, room temperature, and +250°F)

See Figures 148 through 160 and Tables LXVII through LXXV.

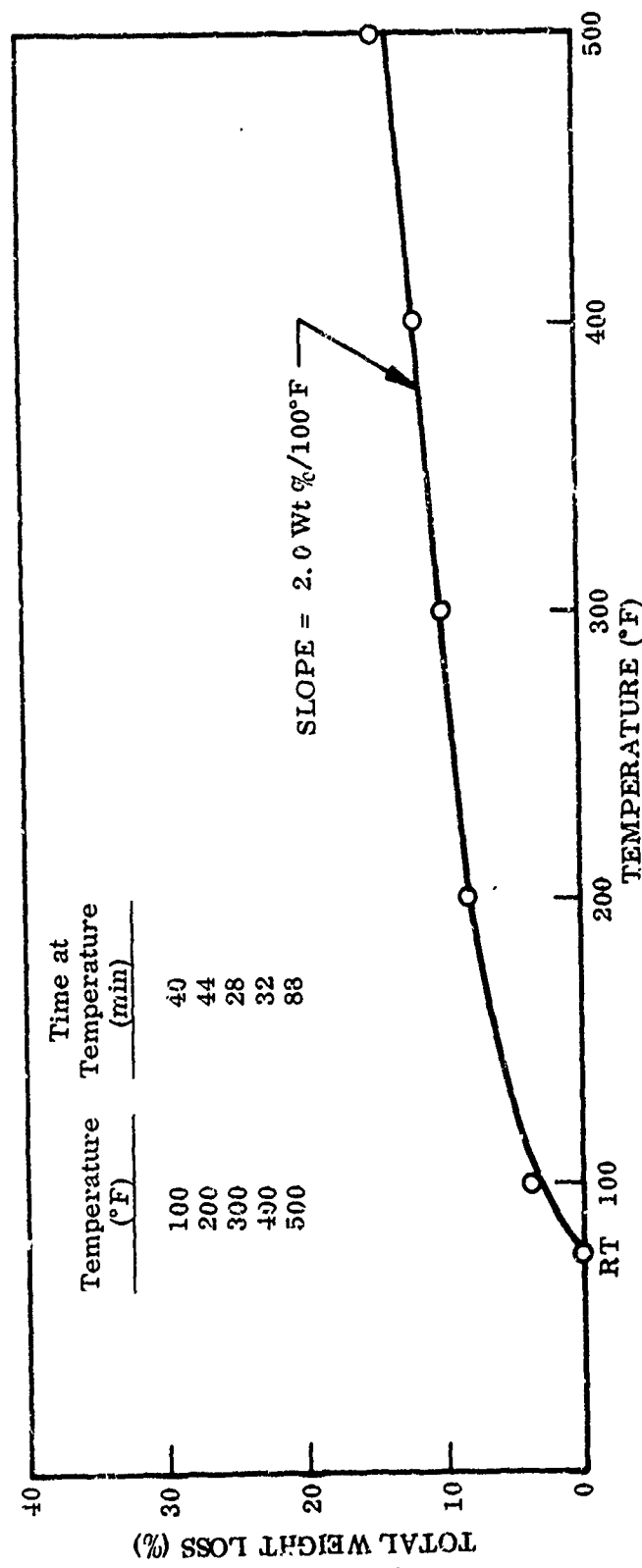


Figure 148 Equilibrium Weight Loss Versus Temperature, Foam Structure

Table LXVII. Short-Term Weight Loss in Vacuum, Foam Structure

Test conditions		Cumulative weight loss (%)	Maximum short-term temperature stability	Comments
Temperature (° F)	Total time (min)			
100	48	3.7	500° F; sample slightly discolored at 500° F	Most weight loss is adsorbed water evolved below 200° F
200	97	7.8		
300	151	9.6		
400	205	11.4	considerable structural strength lost	
500	322	14.2		

Table LXVIII. Long-Term Thermal/Vacuum Exposure, Composite Structure

Specimen	Weight before (g)	Weight after (g)	Weight loss (g)	Change (%)	Post-test appearance
100-hour Test					
BFB-1	7.7580	7.5024	0.2556	3.30	No change
BFM-1	9.6278	9.3366	0.2912	3.01	No change
BFN-1	7.6182	7.3710	0.2472	3.24	No change
1,000-hour Test					
BFB-3	8.6695	8.3245	0.3450	3.98	Smooth face, slightly discolored
BFM-3	9.0251	8.7235	0.2916	3.23	Same as BFB-3
BFN-3	8.1627	7.8823	0.2804	3.43	Smooth face pulled away from structure in one spot; slight discoloration
6,000-hour Test					
BFB-2	10.1970	9.8276	0.3694	3.62	No change
BFM-2	8.5144	8.1630	0.3514	4.13	No change
BFN-2	8.4190	8.1031	0.3159	3.75	No change

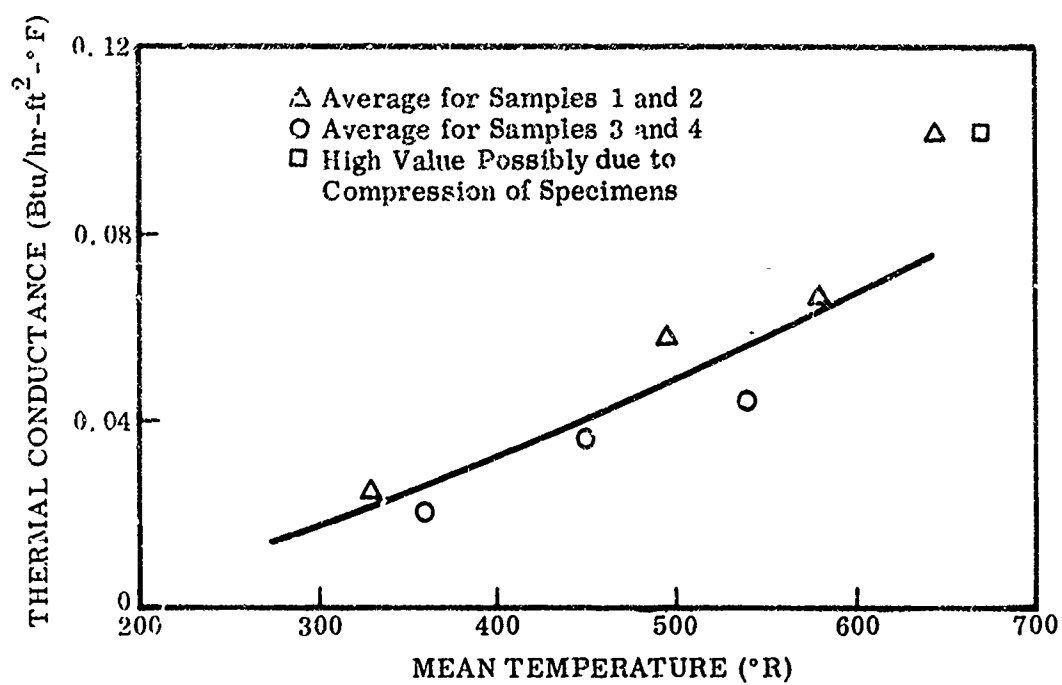


Figure 149 Thermal Conductance of Foam Structure (With Hard Facing)

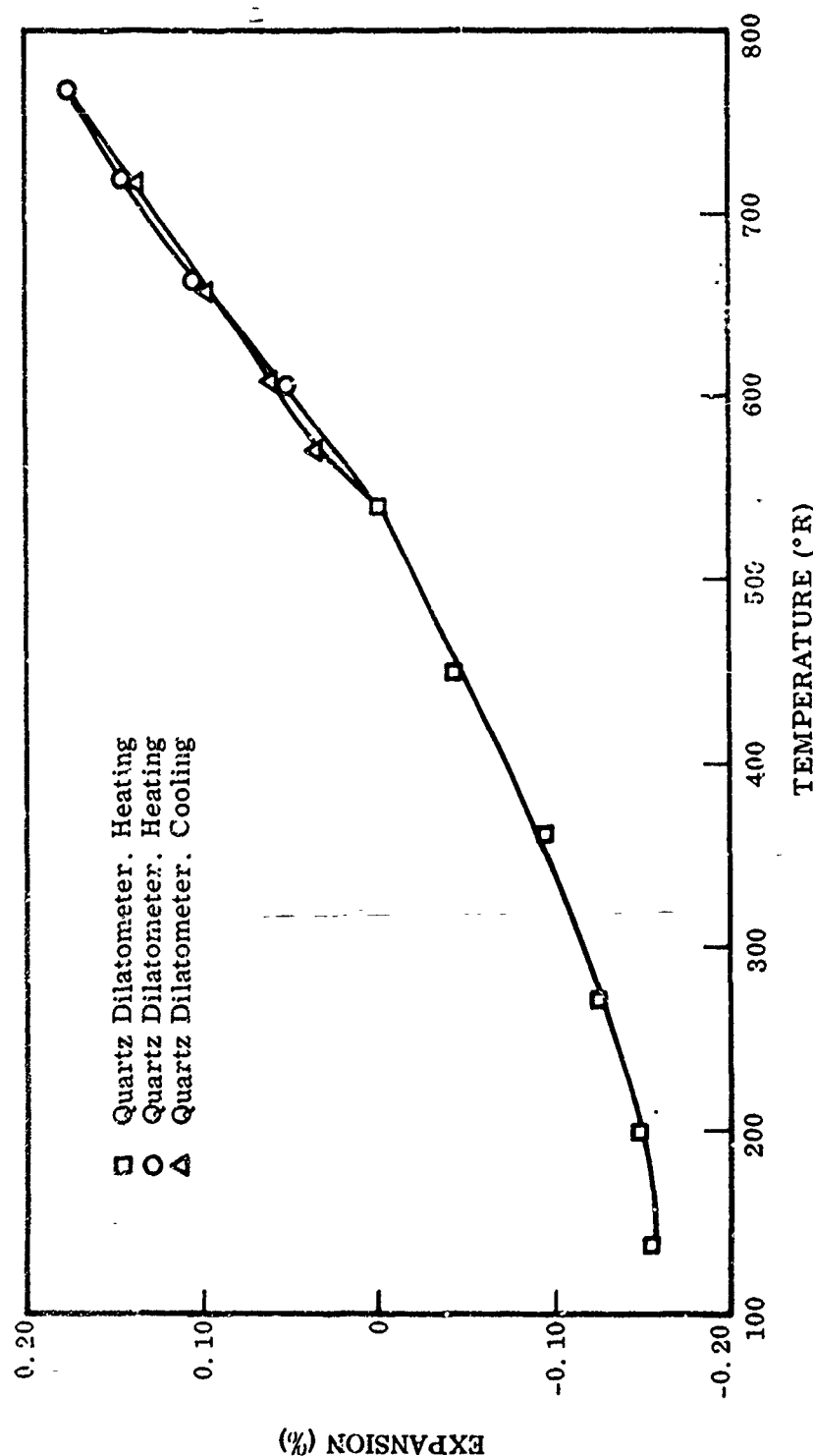


Figure 150 Linear Thermal Expansion of Reflective Surface

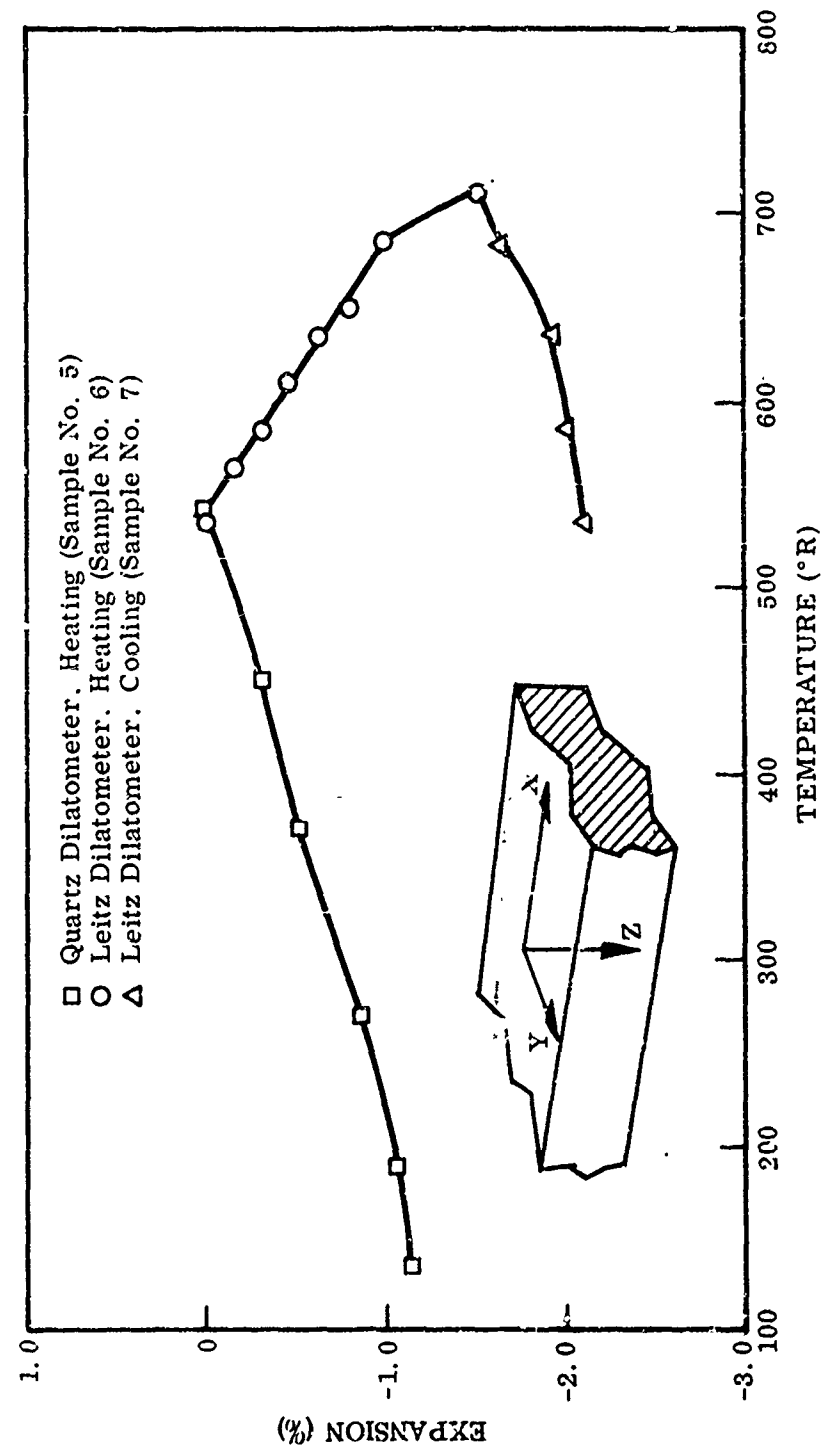


Figure 151 Linear Thermal Expansion of Foam Structure in X-X Direction

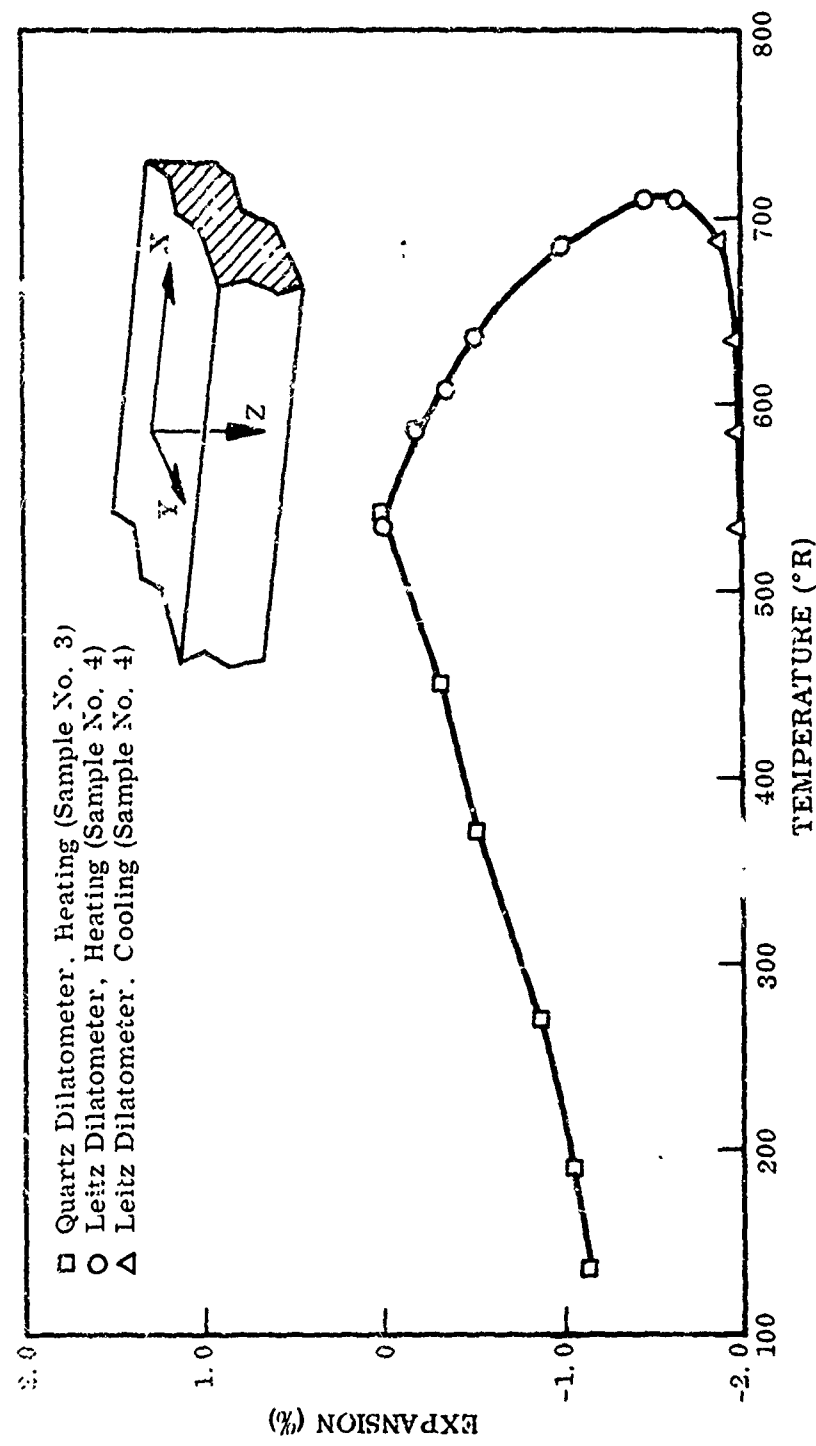


Figure 152 Linear Thermal Expansion of Foam Structure in Y-Y Direction

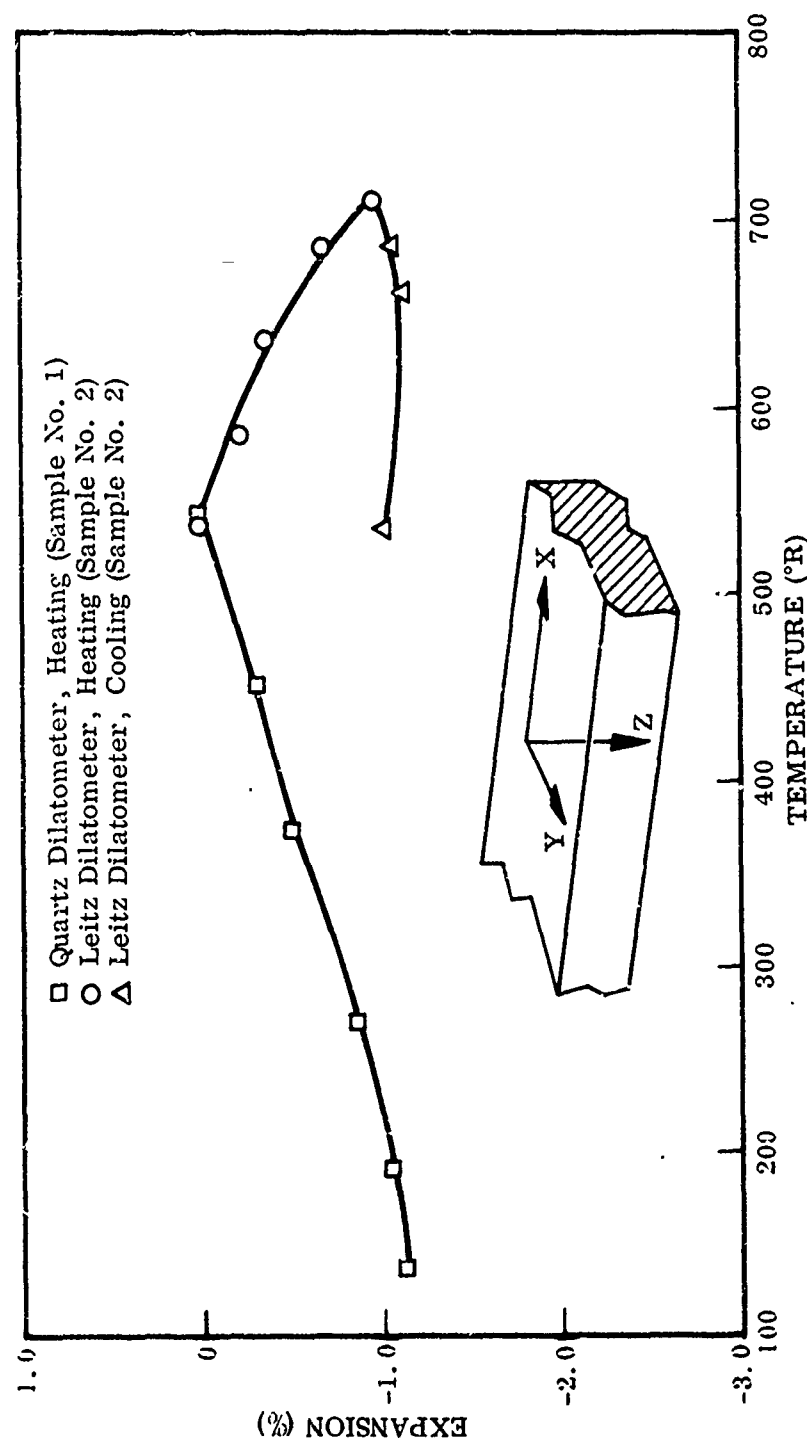


Figure 153 Linear Thermal Expansion of Foam Structure in Z-Z Direction

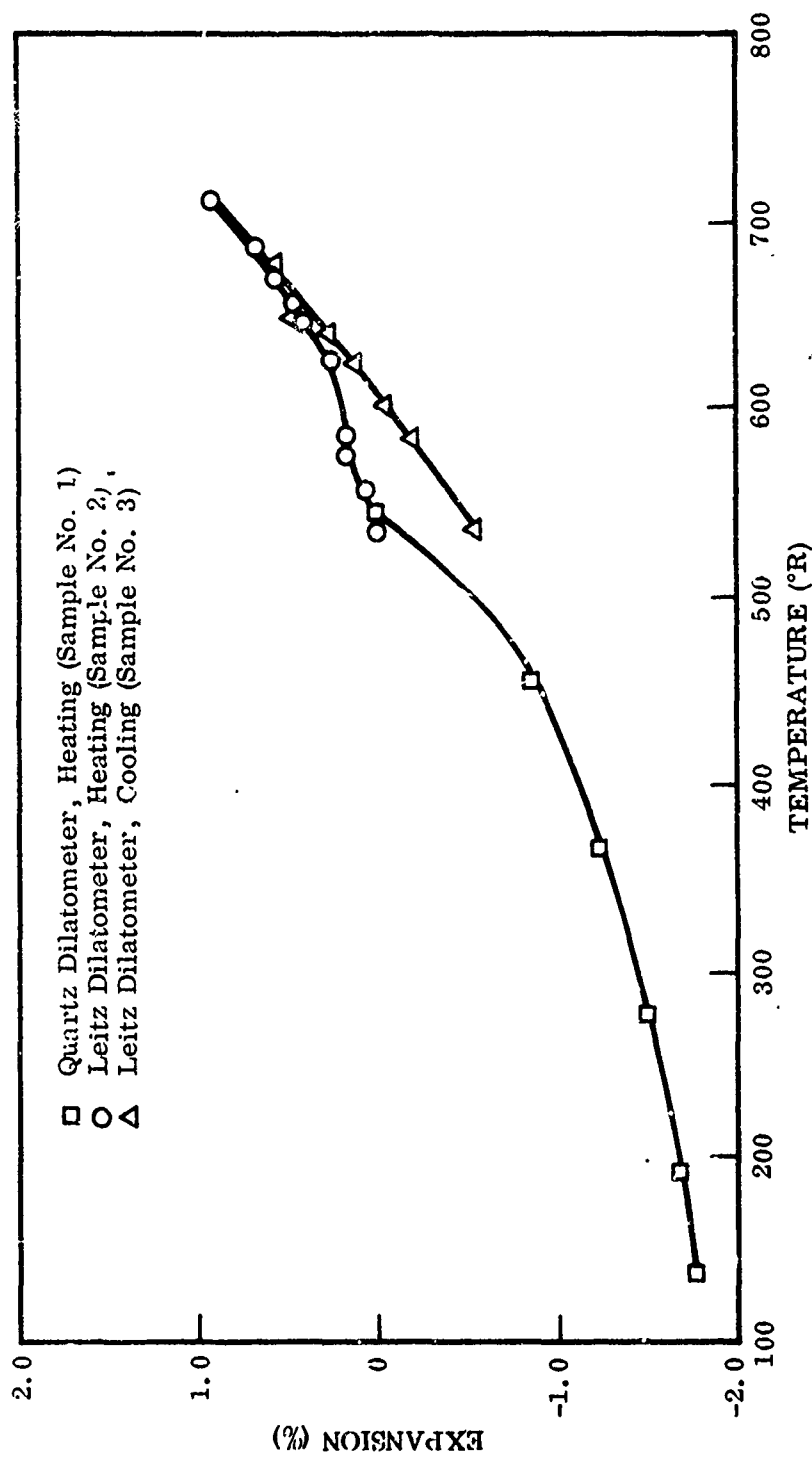


Figure 154 Linear Thermal Expansion of Epoxy Backing Surface

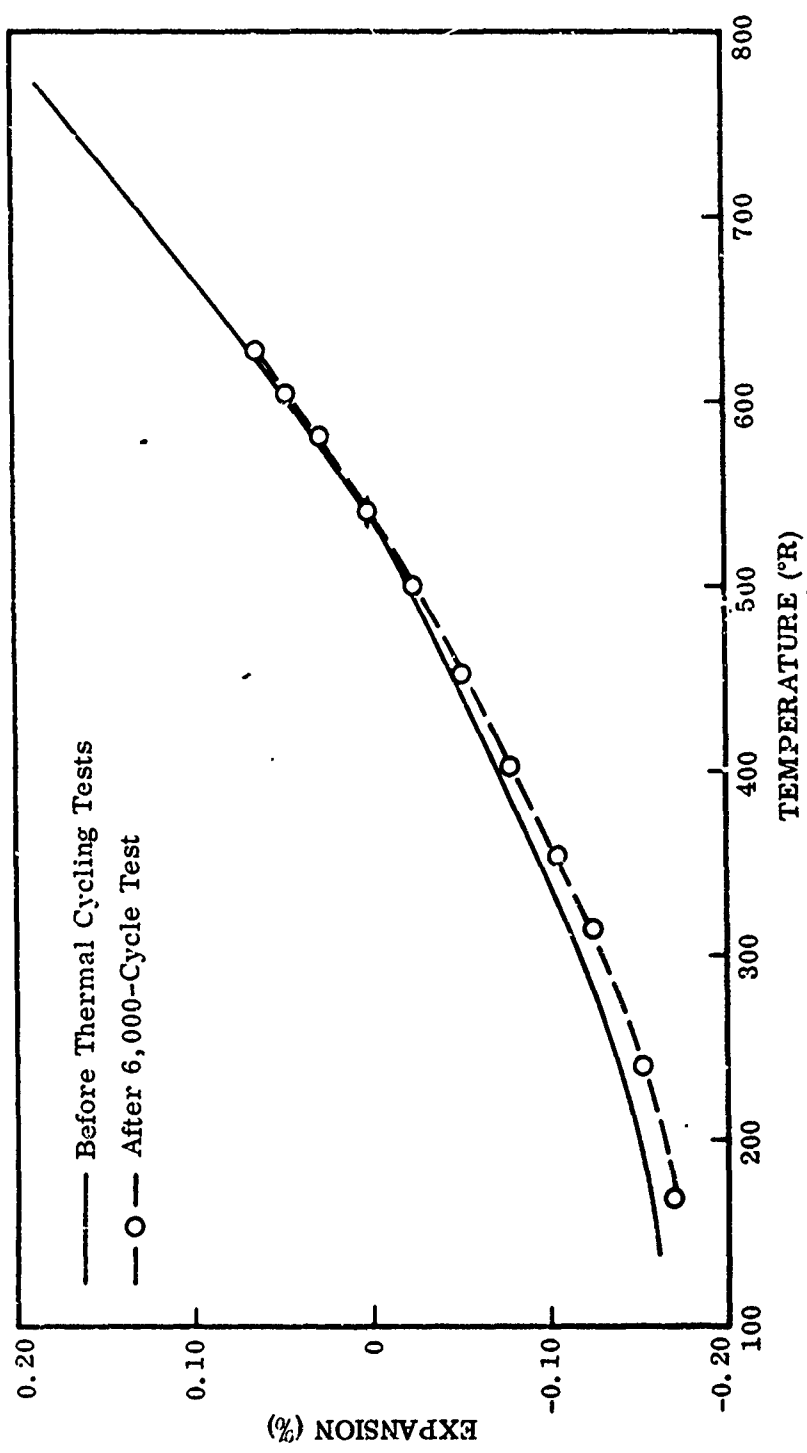


Figure 155 Comparison of Linear Thermal Expansion of Reflective Surface Before and After 6,000-Cycle Thermal Cycling Test

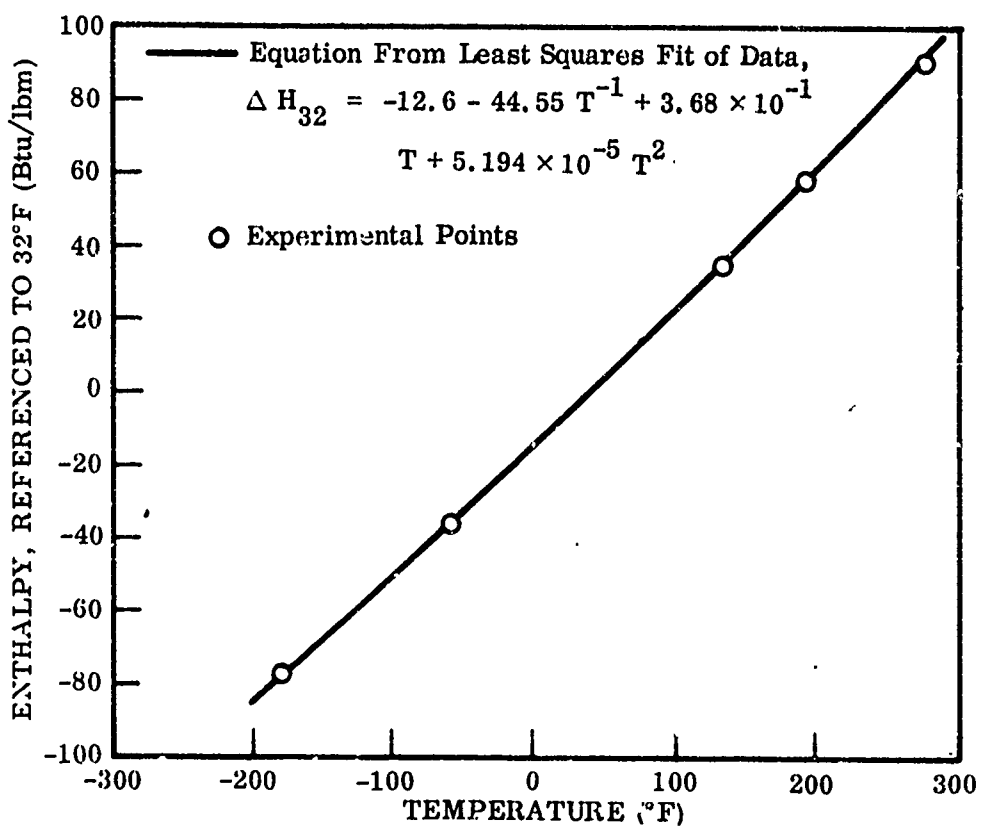


Figure 156 Enthalpy of Foam Structure Referenced to 32° F
(Bulb Density $\approx 1.4 \text{ lb/ft}^3$)

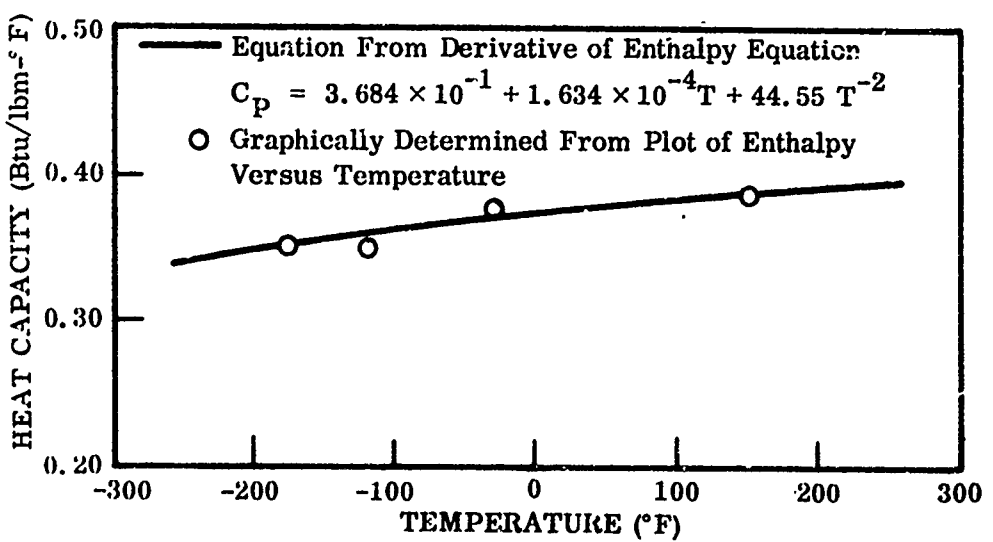


Figure 157 Heat Capacity of Foam Structure

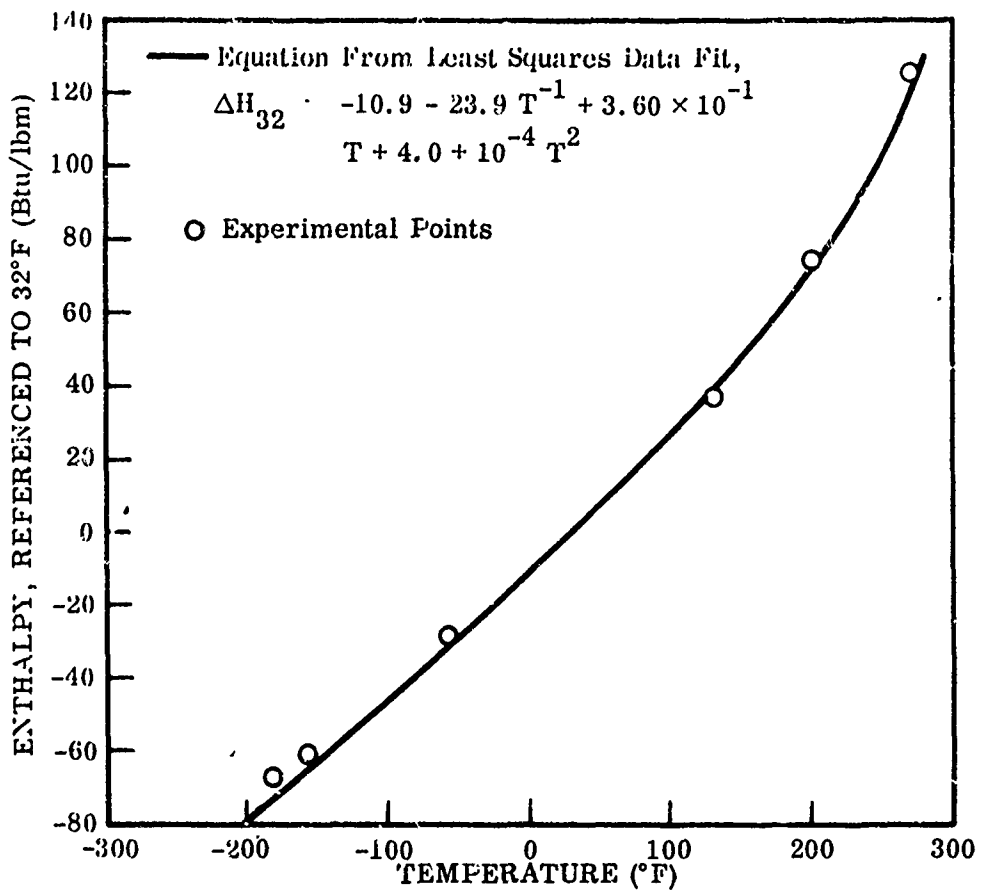


Figure 158 Enthalpy of Epoxy Backing Surface

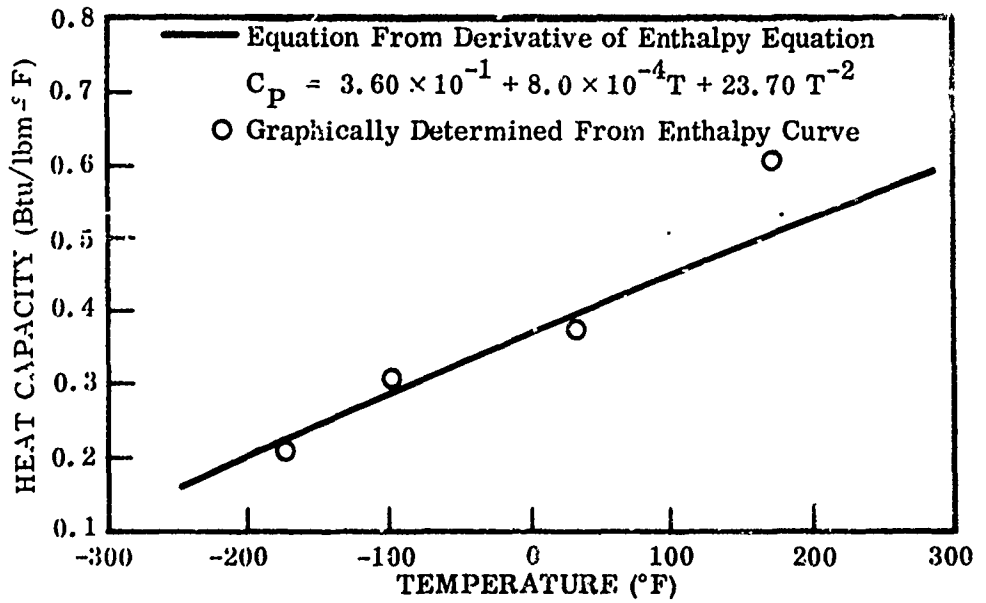


Figure 159 Heat Capacity of Epoxy Backing Surface

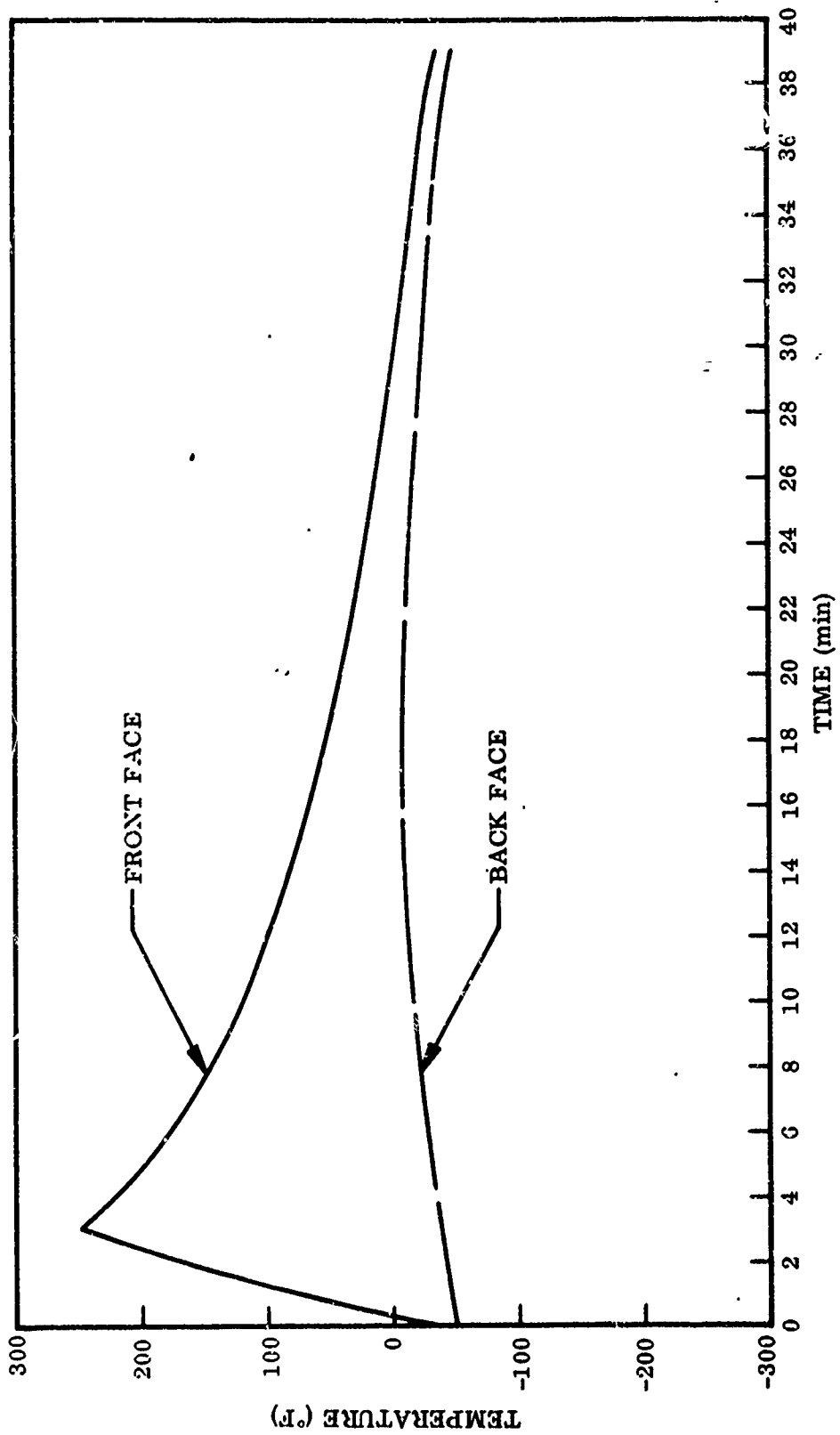


Figure 160 Temperature Histories of Front and Back Faces During Thermal Cycling

Table LXIX. Behavior Under Thermal Cycling, Composite Structure

Specimen	Duration of test (cycles)	Pre-test condition	In situ condition		Post-test condition	Reflectance after exposure
			Cycle	Condition		
BGM-1	100	Sample flat and smooth (see Figure 63a)	1	Large blisters appeared on cooling cycle at 30° F and below (see Figure 63b)	Blister remained on surface of sample	Judged not suitable for testing
			2-35	Blister increased in size		
			36-106	No further changes noted (see Figures 63c and 63d)		
BGM-2	1,900	Sample flat and smooth	1	Large blister appeared upon cooling (see Figure 63e)	After test, two large and one small blister were noted on back surface; front surfaced warped in many places.	Judged not suitable for testing
			2-327	No further changes, except sample appears to be more distorted		
			328-1,042	No further changes noted (see Figure 63f)		
BGM-3	6,000	Sample flat and smooth	0-6,004	Surface extremely wavy in appearance when cold, relatively flat when hot (see Figures 63g and 63h)	Front surface very wavy	Judged not suitable for testing

Table LXX. Summary of Optical-Properties Test Results

Exposure	Solar reflectance
Pre-test condition	0.85
Ultraviolet radiation (1-yr equivalent)	
RT	0.82
250° F	0.82
5 keV electrons (1-yr equivalent)	
RT	0.82
250° F	0.81
Combined environment (6-mo equivalent)	
RT	0.83
250° F	0.82

Table LXXI. Panel-Shear Test, Composite Structure

Temperature	Specimen designation	Modulus G (psi)	Elastic limit (psi)	Maximum stress (psi)	Final strain (%)
-200° F	BJ-6	222	2.82	4.32	2.40
	BJ-9	462	1.15	2.13	1.04
	BJ-10	216	2.24	3.23	1.66
	Average	300	2.07	3.23	1.70
	Deviation	(28.0%)	(44.4%)	(34.1%)	(38.8)
Room temperature	BJ-1	753	1.32	6.01	2.68
	BJ-2	251	7.67	7.67	3.19
	BJ-3	216	7.70	7.70	3.58
	Average	407	5.56	7.13	3.15
	Deviation	(47.0%)	(78.9%)	(15.7%)	(14.9)
+250° F	BJ-4	152	1.17	7.55	6.37
	BJ-5	148	2.86	6.87	5.44
	BJ-11	290	—	12.14	5.04
	Average	197	2.02	8.85	5.62
	Deviation	(24.9%)	(42.1%)	(22.4%)	(10.3)

Table LXXII. Panel-Bend Test, Composite Structure

Specimen designation	Beam width, b (in.)	Beam span, L (in.)	$\frac{EI/b}{in.^2-lb}$ in.	M_e/b (lb)	M_u/b (lb)	Tension face	Thickness (~ in.)
BK-2	1.97	9	1,062	12.9	20.1	Nonreflecting	1.0
BK-3	2.00	9	932	11.6	16.7	Nonreflecting	
BK-4	2.00	9	1,360	14.2	18.5	Reflecting	
BK-4	2.02	9	1,450	9.8	16.7	Reflecting	
Average ^(a)	-	-	1,405	12.0	17.6		
BK-6	2.00	9	380	3.0	13.5	Nonreflecting	0.50
BK-8	2.02	9	440	5.9	13.2	Nonreflecting	
BK-5	2.00	9	528	7.5	13.4	Reflecting	
BK-7	2.02	9	399	8.6	11.6	Reflecting	
Average ^(a)	-	-	410	4.4	12.5		

(a) Average is for weakest bending mode of each parameter.

Table LXXIII. Facing-Tension Test, Facing and Backing Materials

Temperature	Specimen designation	Modulus E (psi)	Elastic limit (nsi)	Maximum stress (psi)	Final strain (%)
-200° F(a)	BL-8	39.3×10^6	—	139×10^3	—
	BL-9	31.6×10^6	62.2×10^3	135×10^3	—
	BL-11	—	—	155×10^3	2.95
	BL-12	38.9×10^6	50.0×10^3	166×10^3	2.55
	Average	36.6×10^6	56.1×10^3	149×10^3	2.75
Room temperature(a)	Deviation	(1.4%)	(10.9%)	(9.4%)	(7.3)
	BL-1	25.3×10^6	50.0×10^3	107×10^3	1.20
	BL-2	—	—	100×10^3	5.30
	BL-4	42.3×10^6	—	102×10^3	3.40
	Average	33.8×10^6	50.0×10^3	103×10^3	3.30
+250° F(a)	Deviation	(25.1%)	—	(2.9%)	(63.6)
	BL-5	31.4×10^6	28.6×10^3	100×10^3	1.05
	BL-6	24.9×10^6	41.3×10^3	110×10^3	2.05
	BL-7	24.7×10^6	41.4×10^3	115×10^3	1.86
	Average	27.0×10^6	37.1×10^3	108×10^3	1.70
-200° F(b)	Deviation	(8.5%)	(22.9%)	(7.4%)	(38.2)
	BL-24	0.85×10^6	9.33×10^3	24.5×10^3	3.42
	BL-25	1.14×10^6	9.33×10^3	22.8×10^3	2.80
	BL-26	1.09×10^6	13.30×10^3	26.9×10^3	3.30
	Average	1.03×10^6	10.69×10^3	24.7×10^3	3.17
Room temperature(b)	Deviation	(17.5%)	(12.7%)	(7.7%)	(11.7)
	BL-13	0.476×10^6	3.66×10^3	7.20×10^3	4.50
	BL-14	0.430×10^6	1.73×10^3	8.73×10^3	5.90
	BL-15	0.480×10^6	2.10×10^3	7.53×10^3	5.30
	Average	0.462×10^6	2.50×10^3	7.82×10^3	5.23
+250° F(b)	Deviation	(6.9%)	(30.8%)	(7.9%)	(14.0)
	BL-20	46.3×10^3	3.5×10^3	6.20×10^3	18.2
	BL-21	47.0×10^3	4.0×10^3	5.90×10^3	17.5
	BL-23	60.0×10^3	5.0×10^3	7.47×10^3	16.0
	Average	51.1×10^3	4.2×10^3	6.52×10^3	17.2
	Deviation	(7.4%)	(16.7%)	(9.5%)	(7.0)

(a) Facing material.

(b) Backing material.

Table LXXIV. Facing-Separation Test, Composite Structure

Unexposed Specimens

Temperature	Specimen designation	Modulus E (psi)	Elastic limit (psi)	Maximum stress (psi)	Final strain (%)
-200° F	BM-10(a) BM-8(a) (b)	179 —	2.97 —	2.97 —	1.45 —
Room temperature	BM-1(a)	660	4.88	5.81	1.04
	BM-2(a)	526	2.20	2.61	0.96
	BM-3(a)	583	8.94	8.94	1.52
	Average	590	5.34	5.79	1.17
-250° F	Deviation	(10.8%)	(58.8%)	(55.0%)	(18.0)
	BM-4(c)	426	8.69	8.69	2.04
	BM-5(c)	177	3.55	4.33	2.73
	BM-6(c)	194	3.92	4.66	2.56
	Average	266	5.39	5.89	2.44
	Deviation	(33.5%)	(34.2%)	(26.5%)	(16.4)

Exposed Specimens

Specimen	Previous exposure	Modulus E (psi)	Elastic limit (psi)	Maximum stress (psi)	Final strain (%)
BFM-1	Thermal/vacuum environment (100 hr.)	—	—	0.705	—
BFB-3	Thermal/vacuum environment (1,000 hr.)	593	5.68	5.68	0.99
BFM-3	Thermal/vacuum environment (1,000 hr.)	417	4.52	4.52	1.08
BFM-2	Thermal/vacuum environment (6,000 hr)	331	4.23	4.23	1.28
BGM-1	Thermal cycling (100 cycles)	487	7.75	7.75	1.59
BGM-2	Thermal cycling (1,000 cycles)	522	5.83	6.42	1.29

(a) Glue-line failure.

(b) Specimen failed while cooling and is listed for report reference only.

(c) Foam fracture failure.

Table LXXV. Core-Compression Test, Composite Structure
Unexposed Specimens

Temperature	Specimen designation	Modulus E (psi)	Elastic limit (psi)	Maximum stress (psi)	Final strain (%)
-200° F(a)	BN-8	102	2.87	2.87	2.90
	BN-9	132	2.83	2.83	2.10
	BN-10	143	2.68	2.68	1.82
	Average	126	2.79	2.79	2.27
Room temperature(a)	BN-1	540	9.20	11.70	3.10
	BN-2	506	8.85	8.85	1.76
	BN-3	378	6.45	7.34	2.00
	BN-4	590	6.55	7.65	1.42
+250° F(a)	Average	593	7.76	8.88	2.07
	Deviation	(24.8%)	(16.9%)	(17.3%)	(31.4)
-200° F(b)	BN-5	683	6.57	7.04	1.45
	BN-6	309	4.37	4.37	1.40
	BN-7	285	4.42	—	—
	Average	426	5.12	5.70	1.42
Room temperature(b)	Deviation	(33.1%)	(14.7%)	(23.4%)	(1.4)
	BN-21	573	5.76	5.76	1.02
	BN-22	327	8.17	8.17	2.50
	BN-23	298	3.34	3.34	1.15
+250° F(b)	Average	399	5.76	5.76	1.56
	Deviation	(25.3%)	(42.0%)	(42.0%)	(34.3)
Room temperature(b)	BN-13	493	8.72	9.87	1.85
	BN-14	440	8.16	10.60	2.83
	BN-15	410	10.20	11.40	2.90
	BN-16	513	8.01	8.01	1.55
+250° F(b)	Average	464	8.77	9.97	2.28
	Deviation	(11.6%)	(8.7%)	(19.7%)	(32.0)
	BN-17	249	5.95	—	—
	BN-18	257	6.12	7.60	3.20
	BN-19	379	5.27	9.00	3.20
	BN-20	378	7.65	—	—
	Average	316	6.25	8.30	3.20
	Deviation	(21.2%)	(15.7%)	(8.4%)	(0)

(a) Approximately 0.5-in. thick.

(b) Approximately 1.0-in. thick.

Table LXXV --- Continued
Exposed Specimens

Specimen	Previous exposure	Modulus E (psi)	Elastic limit (psi)	Maximum stress (psi)	Final strain (%)
BFN-1	Thermal/vacuum environment (100 hr)	271	5.33	6.49	2.64
BFN-3	Thermal/vacuum environment (1,000 hr)	331	5.02	5.42	1.67
BFN-2	Thermal/vacuum environment (6,000 hr)	209	4.60	5.94	2.00

Note: Specimens were approximately 0.5-in. thick. Data should be compared with results of tests on unexposed specimens of same thickness.

Appendix III

TEST RESULTS - CANDIDATE MATERIAL C

Presented in this appendix are the results of all laboratory tests performed on Material C. Discussions of the tests, descriptions of test apparatus, test procedures and conditions, and interpretations of test results, covered elsewhere in this report, are not repeated here.

Material C is an aluminum honeycomb structure, with epoxy-bonded aluminum front and back sheets. Its reflective surface consists of successive layers of epoxy, silicon oxide, vacuum-deposited aluminum, and silicon oxide.

Results of the following tests are given in this appendix:

- Weight loss in vacuum (epoxy adhesive and leveling layer)
- Long-term thermal/vacuum exposure (composite structure)
- Thermal conductance of composite structure
- Behavior under thermal cycling
- Ultraviolet irradiation at room temperature and +250°F
- Exposure to low-energy electrons at room temperature and +250°F
- Exposure to combined environment (uv + e⁻) at room temperature and +250°F
- Panel shear (-200°F, room temperature, and +250°F)
- Panel bend
- Facing tension (-200°F, room temperature, and +250°F)
- Facing separation (-200°F, room temperature, and +250°F)
- Core compression (-200°F, room temperature, and +250°F)

See Figures 161 through 164 and Tables LXXVI through LXXXIV.

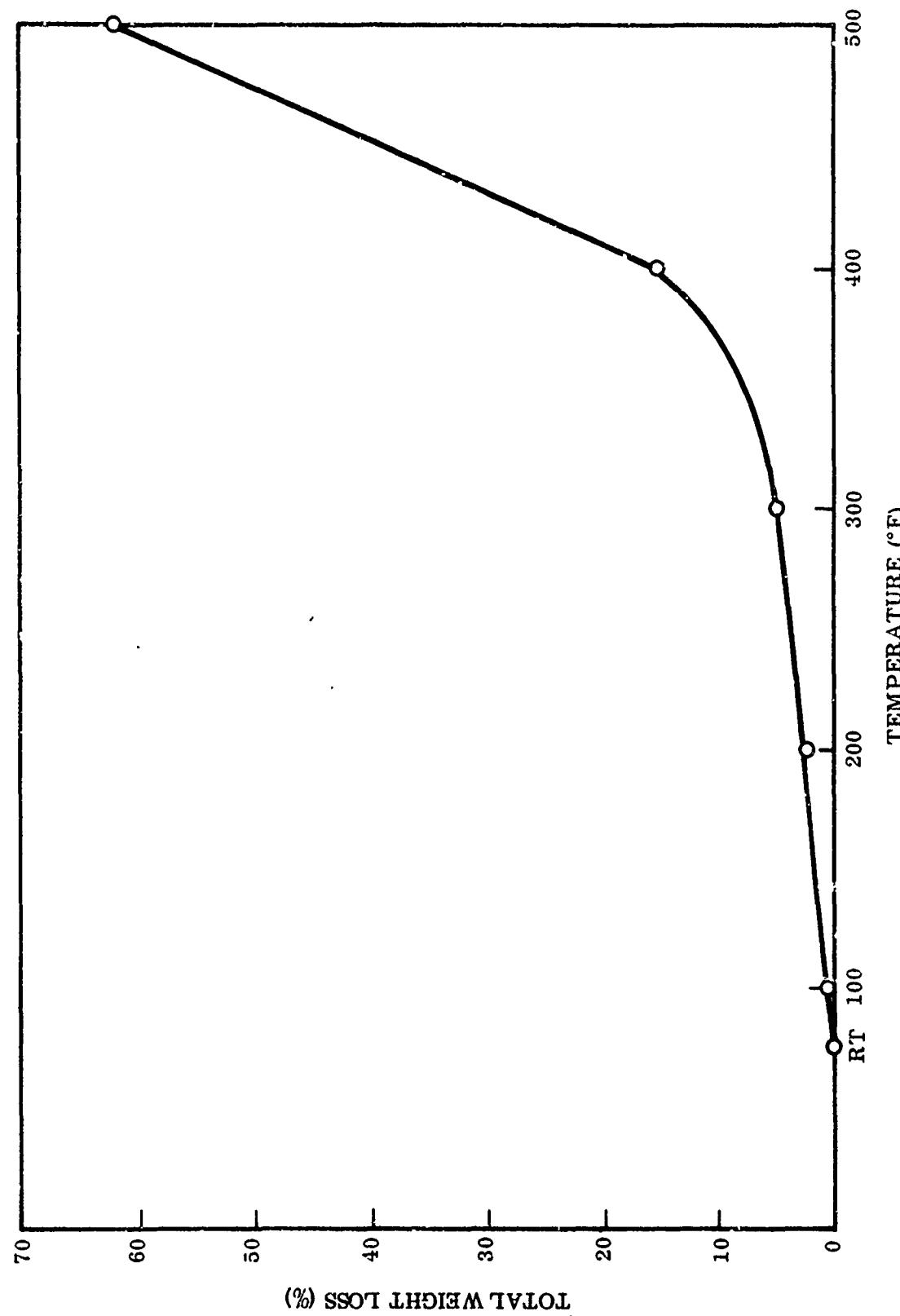


Figure 161 Equilibrium Weight Loss Versus Temperature, Epoxy Adhesive

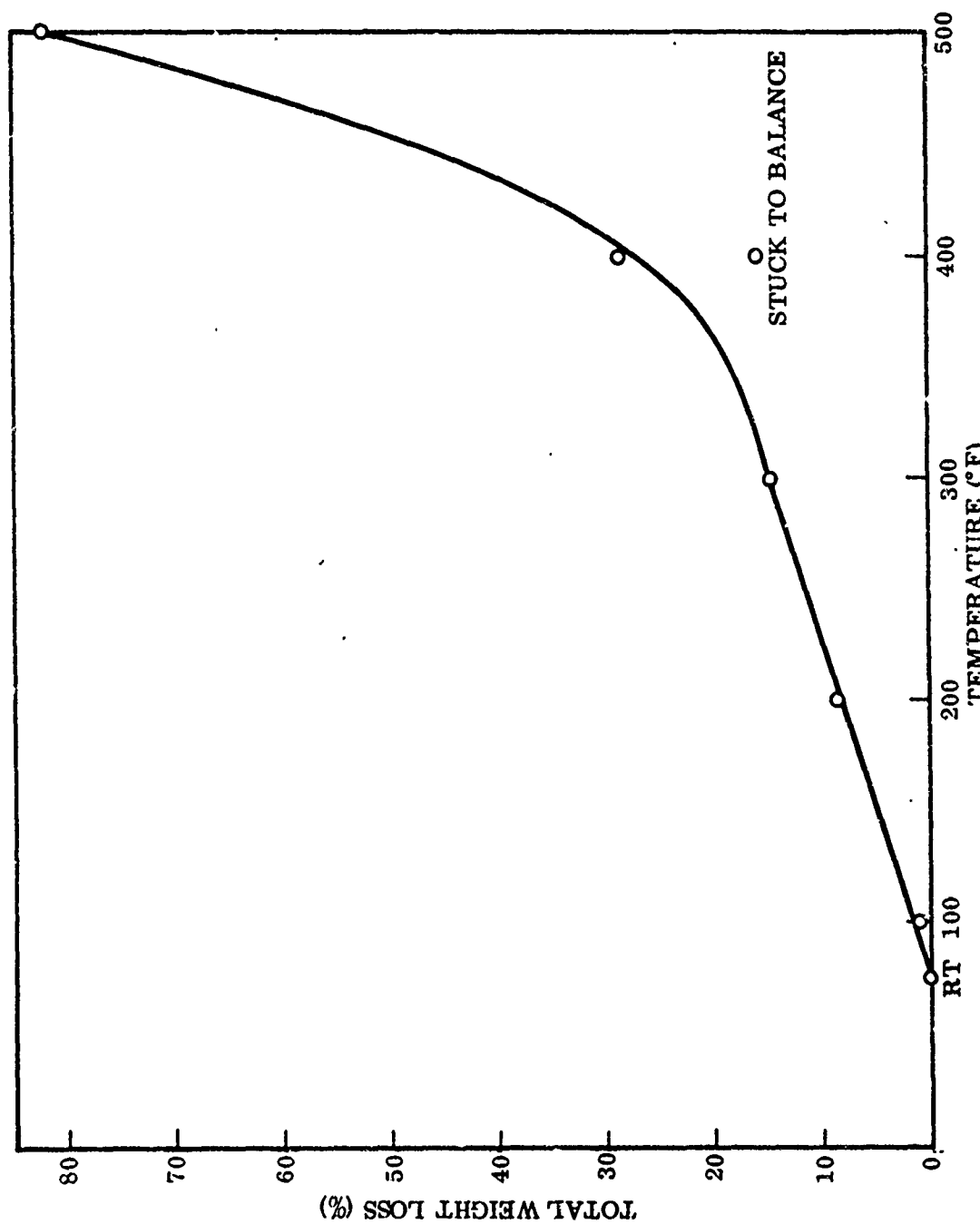


Figure 162 Equilibrium Weight Loss Versus Temperature, Epoxy Sublayer

Table LXXVI. Short-Term Weight Loss in Vacuum

Test conditions		Cumulative weight loss (%)	Maximum short-term temperature stability	Comments
Temperature (°F)	Total time (min)			
Epoxy adhesive				
100	48	0.34	Good to 350°F	Bloated, porous black residue at 500°F
200	96	2.47		
300	152	4.59		
400	212	14.93		
500	362	62.0		
Epoxy sublayer				
100	48	1.0	Marginal at 300°F; weight loss = 14.5%	Porous glassy black carbon formed at 500°F
200	96	8.15		
300	152	14.5		
400	212	27.5		
500	362	82.0		

Table LXXVII. Long-Term Thermal/Vacuum Exposure, Composite Structure

Specimen	Weight before (g)	Weight after (g)	Weight loss (g)	Change (%)	Post-test appearance
100-hour test					
CF-1	4.5874	4.5173	0.0701	1.53	One face turned brown
CFM-1	4.5562	4.4876	0.0686	1.51	Same as CF-1
CFN-1	4.5704	4.5005	0.0699	1.53	Same as CF-1
1,000-hour test					
CF-3	4.4452	4.3825	0.0627	1.41	Honeycomb impression visible on one face
CFM-3	4.4872	4.4154	0.0718	1.60	Same as CF-3
CFN-3	4.5307	4.4551	0.0756	1.67	Same as CF-3
6,000-hour test					
CF-2	4.6602	4.5835	0.0767	1.65	No change
CFM-2	4.5631	4.4926	0.0705	1.55	No change
CFN-2	4.6365	4.5540	0.0825	1.78	No change

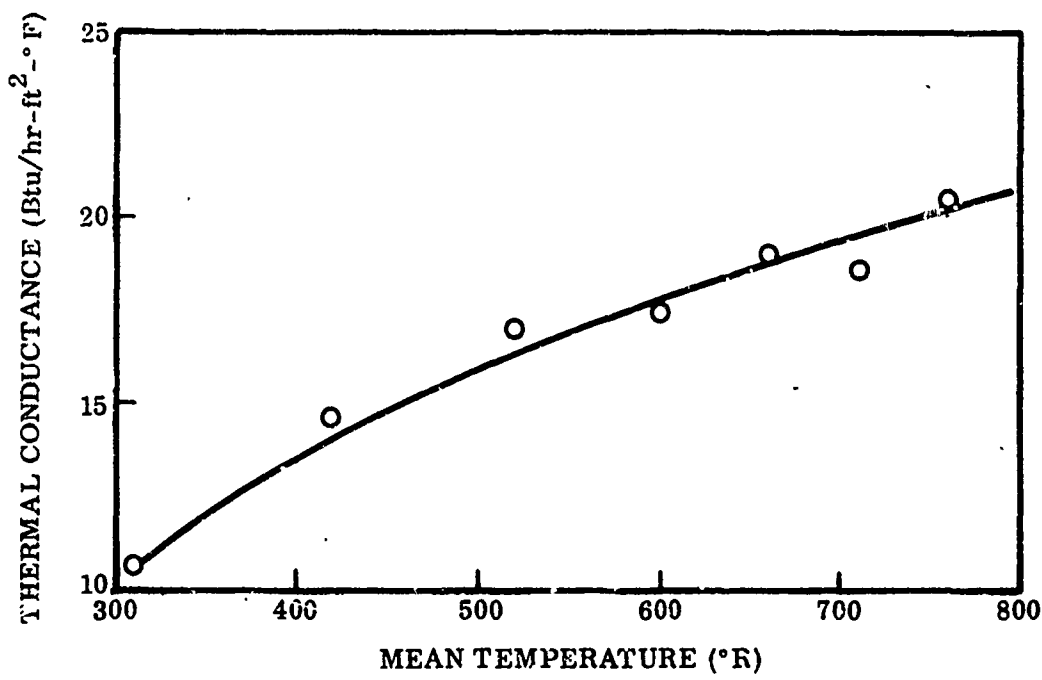


Figure 163 Thermal Conductance of Composite Structure

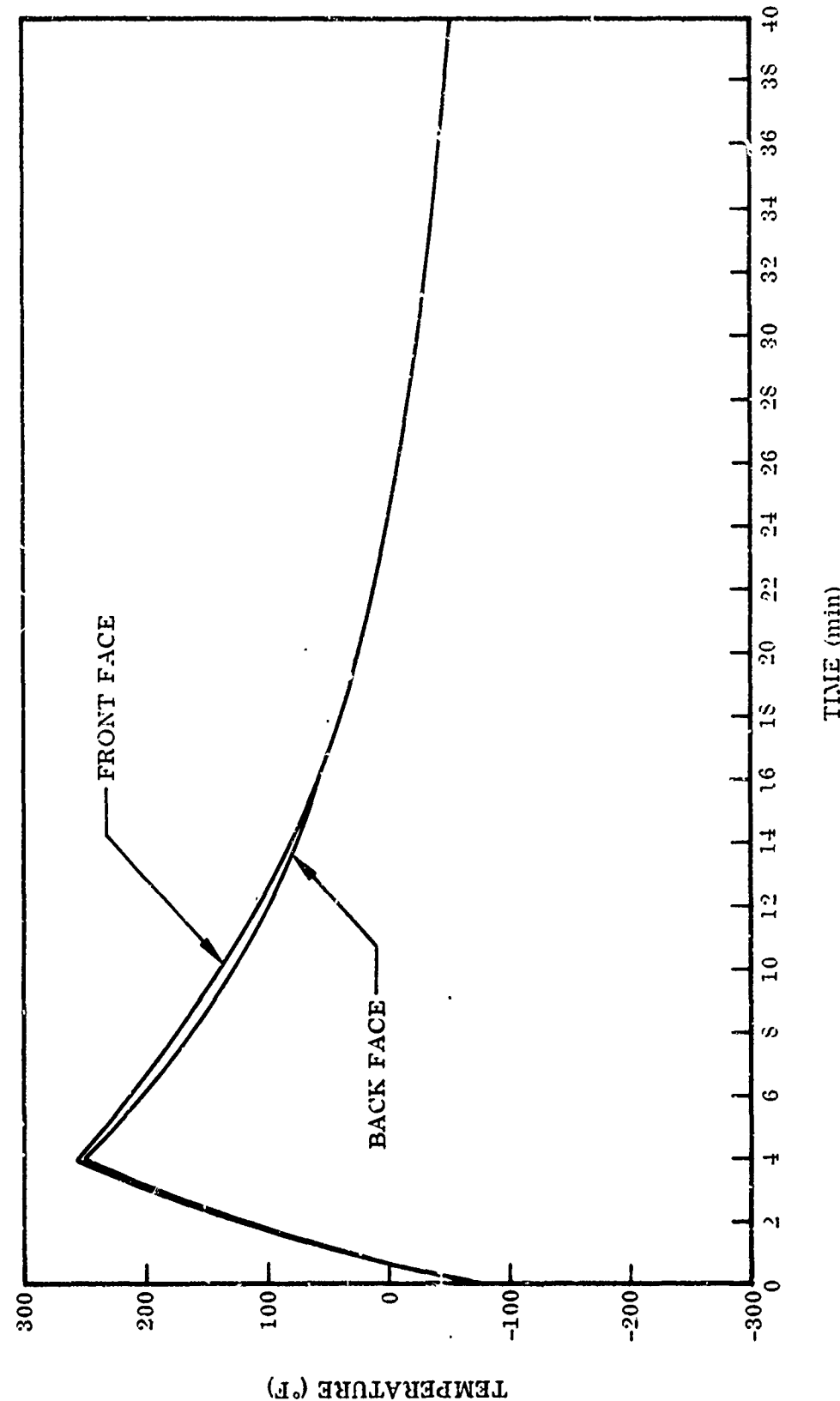


Figure 164 Temperature Histories of Front and Back Faces During Thermal Cycling

Table LXXVIII. Behavior Under Thermal Cycling, Composite Structure

Specimen	Duration of test (cycles)	Pre-test condition	In situ condition		Post-test condition	Reflectance after exposure
			Cycle	Condition		
CG-2	100	See Figure 65a	0-104	No change noted (see Figures 65b and 65c)	No change noted	No change
CGN-1	1,000	Front surface somewhat wavy; reflecting surface has striations & tiny blisters over about 50% of the surface	0-1,008	No change noted (see Figure 65d)	Visible blisters (3/16-in. diam.) on front surface	No change
CGM-3	6,000	Front surface somewhat wavy with many tiny dimples	0-6,000	No change noted (see Figures 65e and 65f)	No change noted	No change

Table LXXIX. Summary of Optical-Properties Test Results

Exposure	Solar Reflectance
Pre-test condition	0.90
Ultraviolet radiation (1-yr equivalent)	
RT	0.85
250° F	0.84
5 keV electrons (1-yr equivalent)	
RT	0.90
250° F	0.87
Combined environment (6-mo equivalent)	
RT	0.83
250° F	0.82

Table LXXX. Panel-Shear Test, Composite Structure

Temperature	Specimen designation	Modulus G (psi)	Elastic limit (psi)	Maximum stress (psi)	Final strain (%)
-200° F	CJ-7	6.08×10^3	147	248	5.73
	CJ-8	7.66×10^3	121	246	5.26
	CJ-9	7.58×10^3	56.8	245	6.96
	Average	7.11×10^3	108	246	5.98
	Deviation	(14.5%)	(47.2%)	(0.4%)	(13.7)
Room temperature	CJ-1	6.78×10^3	26.6	205	9.49
	CJ-2	7.12×10^3	38.7	212	6.18
	CJ-3	5.66×10^3	19.3	206	5.94
	Average	6.52×10^3	28.2	208	7.20
	Deviation	(13.2%)	(31.6%)	(1.4%)	(17.5)
+250° F	CJ-4	2.49×10^3	21.40	53.5	8.16
	CJ-6	—	—	54.5	1.56
	CJ-13	3.26×10^3	22.60	71.3	6.22
	CJ-14	2.59×10^3	16.75	76.0	4.90
	Average	2.78×10^3	20.25	63.8	5.25
	Deviation	(11.6%)	(20.9%)	(16.2%)	(70.3)

Table LXXXI. Panel-Bend Test, Composite Structure

Specimen designation	Beam width, b (in.)	Beam span, L (in.)	$\frac{EI/b}{\text{in.} \cdot 2\text{-lb}} \text{ in.}$	M_e/b (lb)	M_u/b (lb)	Tension face
CK-1	2.00	9	1,230	23.2	35.2	Back
CK-2	1.95	9	1,200	19.2	20.5	Front
CK-3	1.95	9	1,120	18.5	20.2	Front
CK-4	2.00	9	1,150	15.0	19.1	Front
Average	—	—	1,175	19.0	23.7	
CK-5	1.25	6	1,420	19.2	28.0	(a)
CK-6	1.28	6	1,210	10.5	11.9	(b)
CK-7	1.36	6	1,300	22.0	27.8	(c)
CK-8	1.28	6	1,290	16.8	18.1	(d)

(a) Specimen with discontinuity in compression.
 (b) Specimen with discontinuity in tension.
 (c) Specimen with lap joint; reflecting surface in compression.
 (d) Specimen with lap joint; reflecting surface in tension.

Table LXXXII. Facing-Tension Test, Facing Material

Temperature	Specimen designation	Modulus E (psi)	Elastic limit (psi)	Maximum stress (psi)	Final Strain (%)
-200°F	CL-9	11.65×10^6	21.7×10^3	53.1×10^3	7.50
	CL-10	10.30×10^6	39.4×10^3	54.9×10^3	5.12
	CL-11	12.10×10^6	22.8×10^3	54.9×10^3	7.07
	Average	11.35×10^6	28.0×10^3	54.3×10^3	6.56
	Deviation	(9.2%)	(26.0%)	(2.2%)	(21.9)
Room temperature (a)	CL-1	10.20×10^6	43.2×10^3	47.0×10^3	4.70
	CL-2	8.35×10^6	42.0×10^3	47.0×10^3	6.00
	CL-3	9.37×10^6	42.9×10^3	45.8×10^3	3.60
	CL-4	9.38×10^6	41.9×10^3	45.9×10^3	3.90
	Average	9.32×10^6	42.5×10^3	46.4×10^3	4.55
+250°F	Deviation	(10.4%)	(1.4%)	(1.3%)	(18.7)
	CL-5	11.00×10^6	—	42.0×10^3	1.19
	CL-6	10.80×10^6	17.2×10^3	43.2×10^3	4.48
	CL-7	9.35×10^6	20.6×10^3	44.0×10^3	3.90
	CL-8	9.12×10^6	25.4×10^3	44.2×10^3	3.50
Deviation	Average	10.07×10^6	21.1×10^3	43.3×10^3	3.27
	Deviation	(9.4%)	(18.5%)	(3.0%)	(63.7)

(a) The 0.2 percent offset yield strength at room temperature is given instead of the elastic limit.

Table LXXXIII. Facing-Separation Test, Composite Structure

Unexposed Specimens

Temperature	Specimen designation	Modulus E (psi)	Elastic limit (psi)	Maximum stress (psi)	Final strain (%)
-200°F	CM-7(a)	4.46×10^3	---	---	---
	CM-8(a)	4.08×10^3	512	550	16.8
	CM-9(a)	3.80×10^3	564	573	14.5
	Average	4.11×10^3	538	561	15.6
Room temperature	Deviation	(7.6%)	(4.8%)	(2.0%)	(7.1%)
	CM-1(a)	11.5×10^3	237	322	3.30
	CM-2(b)	12.2×10^3	139	---	---
	CM-3(a)	15.8×10^3	167	230	1.90
+250°F	Average	13.2×10^3	181	271	2.60
	Deviation	(12.9%)	(23.2%)	(16.7%)	(29.6%)
	CM-4(c)	9.25×10^3	102	125	2.08
	CM-10(c)	9.41×10^3	120	145	2.33
	CM-11(c)	10.55×10^3	128	140	2.48
	Average	9.74×10^3	117	137	2.30
	Deviation	(5.0%)	(12.8%)	(8.7%)	(9.6%)

Exposed Specimens

Specimen	Previous exposure	Modulus E (psi)	Elastic limit (psi)	Maximum stress (psi)	Final strain (%)
CFM-1	Thermal/vacuum environment (100 hr)	3.08×10^3	155	349	14.4
CF-3	Thermal/vacuum environment (1,000 hr)	5.01×10^3	301	364	8.3
CFM-3	Thermal/vacuum environment (1,000 hr)	2.47×10^3	326	360	15.0
CF-2	Thermal/vacuum environment (6,000 hr)	5.75×10^3	297	332	5.75
CFM-2	Thermal/vacuum environment (6,000 hr)	6.65×10^3	291	351	5.62
CG-2	Thermal cycling (100 cycles)	3.95×10^3	360	396	10.5
CGN-1	Thermal cycling (1,000 cycles)	6.93×10^3	362	390	9.53
CGM-3	Thermal cycling (6,000 cycles)	6.27×10^3	295	346	5.75

(a) Core-material tensile failure.

(b) Test-equipment failure; maximums not recorded.

(c) Glue-line failure.

Table LXXXIV. Core-Compression Test, Composite Structure

Unexposed Specimens

Temperature	Specimen designation	Modulus E (psi)	Elastic limit (psi)	Maximum stress (psi)	Final strain (%)
-200° F	CN-9	2.41×10^3	83	98	4.92
	CN-10	4.73×10^3	124	162	3.74
	CN-11	2.55×10^3	108	152	9.13
	Average	3.23×10^3	105	137	5.93
Room temperature	Deviation	(25.4%)	(20.9%)	(28.5%)	(37.0)
	CN-1	5.43×10^3	198	272	3.14
	CN-2	13.5×10^3	276	305	2.54
	CN-14	5.27×10^3	208	238	6.00
+250° F	Average	8.07×10^3	227	272	3.93
	Deviation	(22.3%)	(12.8%)	(12.5%)	(35.4)
	CN-6	5.30×10^3	213	213	9.58
	CN-7	5.83×10^3	200	200	7.78
	CN-8	—	—	203	—
	Average	5.56×10^3	206	205	8.68
	Deviation	(4.7%)	206	(4.1%)	(10.3)

Exposed Specimens

Specimen	Previous exposure	Modulus E (psi)	Elastic limit (psi)	Maximum stress (psi)	Final strain (%)
CF-1	Thermal/vacuum environment (100 hr)	10.65×10^3	257	257	2.36
CFN-3	Thermal/vacuum environment (1,000 hr)	11.05×10^3	246	282	2.98
CFN-2	Thermal/vacuum environment (6,000 hr)	9.50×10^3	196	227	2.61

Appendix IV

TEST RESULTS - CANDIDATE MATERIALS D-F

Presented in this appendix are the results of all laboratory tests performed on materials D, E, and F. Discussions of the tests, descriptions of test apparatus, test procedures and conditions, and interpretations of test results, covered elsewhere in this report, are not repeated here.

Materials D, E, and F are aluminum honeycomb structures, with epoxy-bonded aluminum front and back sheets. Their reflective surfaces consist of successive layers of epoxy, silicon oxide, and vacuum-deposited aluminum. Material F also has a silicon oxide overcoating. Material D differs from materials E and F, in that a different epoxy is used for the leveling layer.

Results of the following tests are given in this appendix:

- Weight loss in vacuum (epoxy adhesives and sublayers)
- Thermal conductance of composite structure
- Long-term thermal/vacuum exposure (composite structure)
- Behavior under thermal cycling
- Ultraviolet irradiation at room temperature and +250° F
- Exposure to low-energy electrons at room temperature and +250° F
- Exposure to combined environment (uv + e⁻) at room temperature and +250° F
- Panel shear (-200° F, room temperature, and +250° F)
- Panel bend
- Facing tension (-200° F, room temperature, and +250° F)
- Facing separation (-200° F, room temperature, and +250° F)
- Core compression (-200° F, room temperature, and +250° F)

See Figures 165 through 172 and Tables LXXXV through XCV.

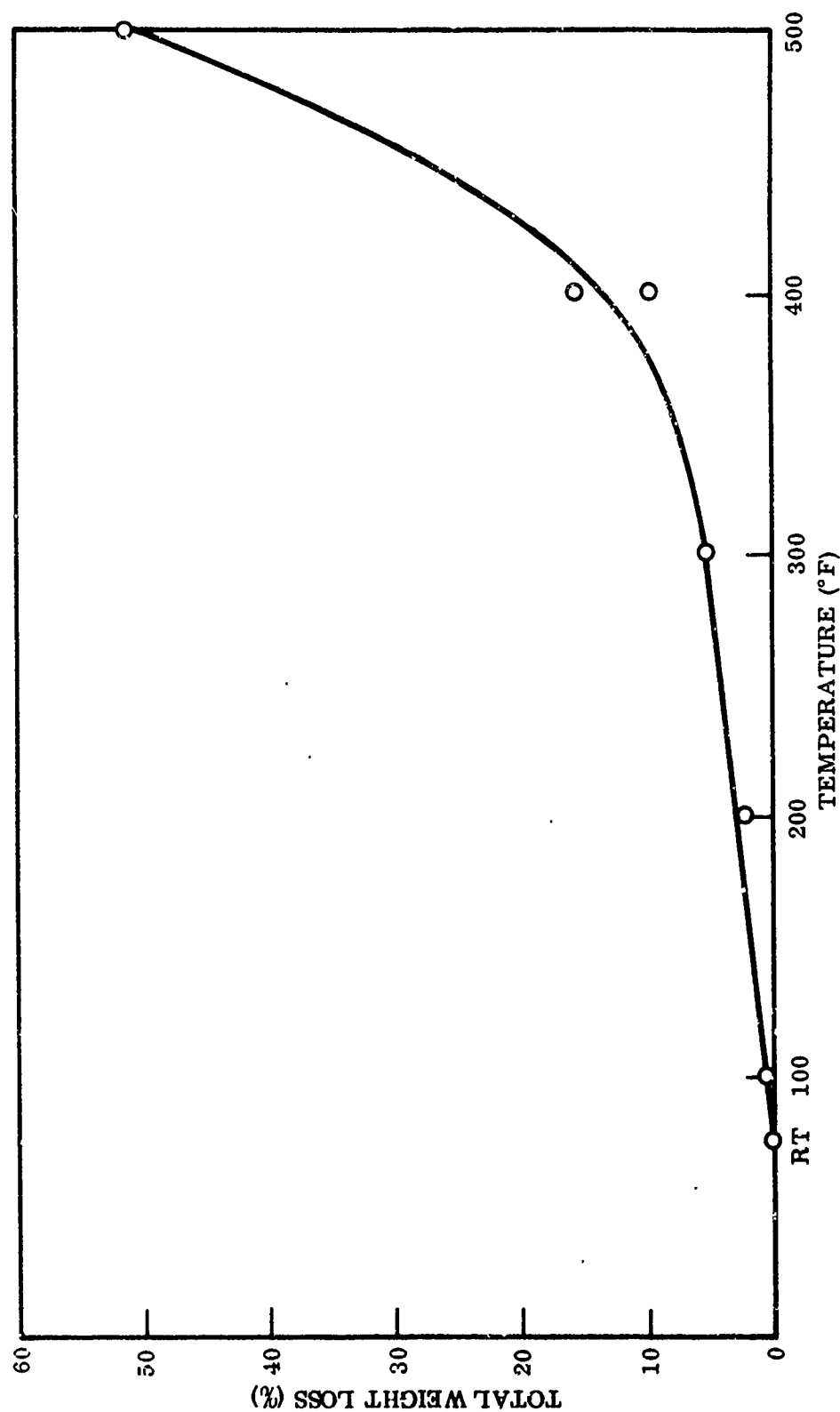


Figure 165 Equilibrium Weight Loss Versus Temperature, Epoxy Facing Adhesive

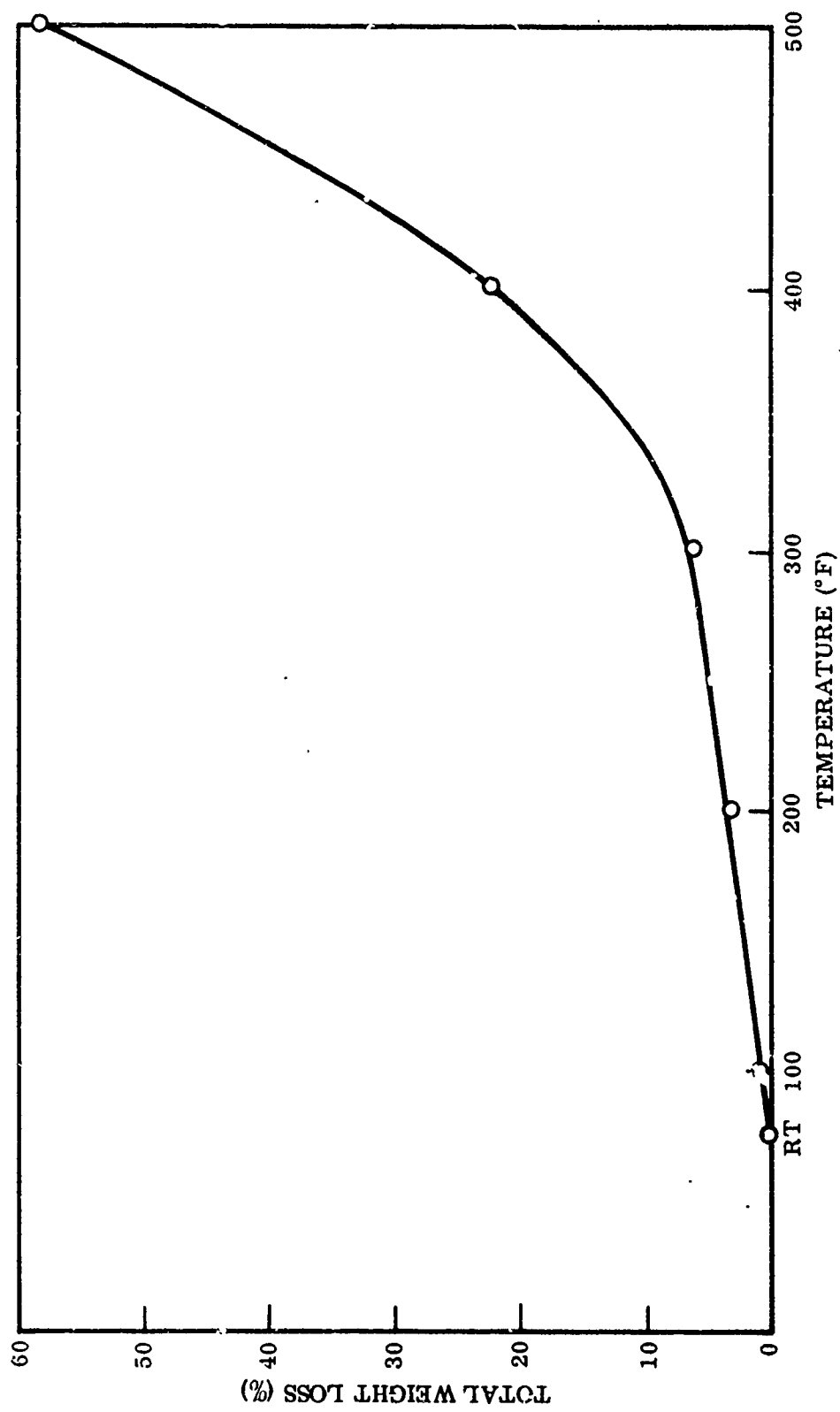


Figure 166 Equilibrium Weight Loss Versus Temperature, Epoxy Backing Adhesive

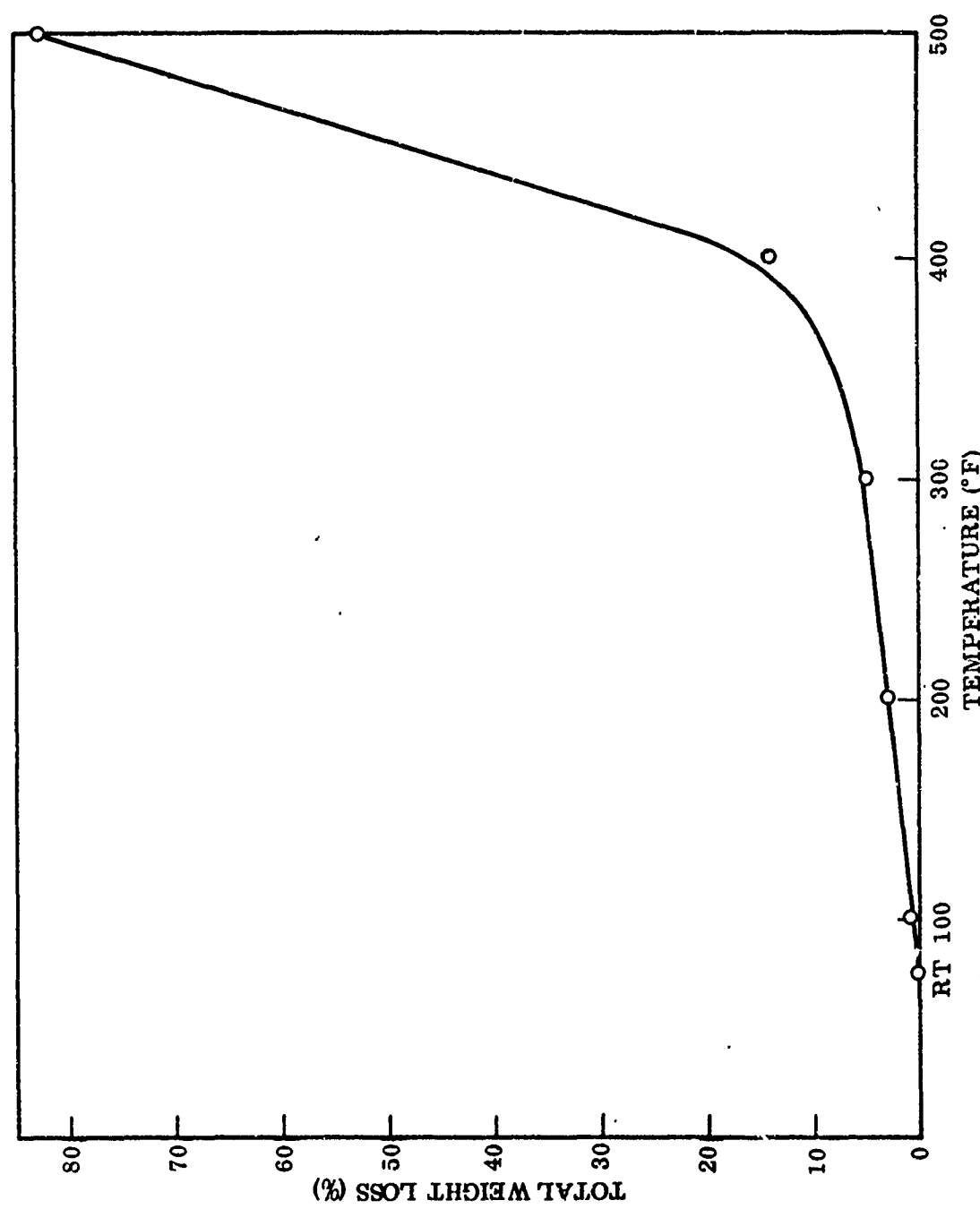


Figure 167 Equilibrium Weight Loss Versus Temperature, Epoxy Sublayer, Material D

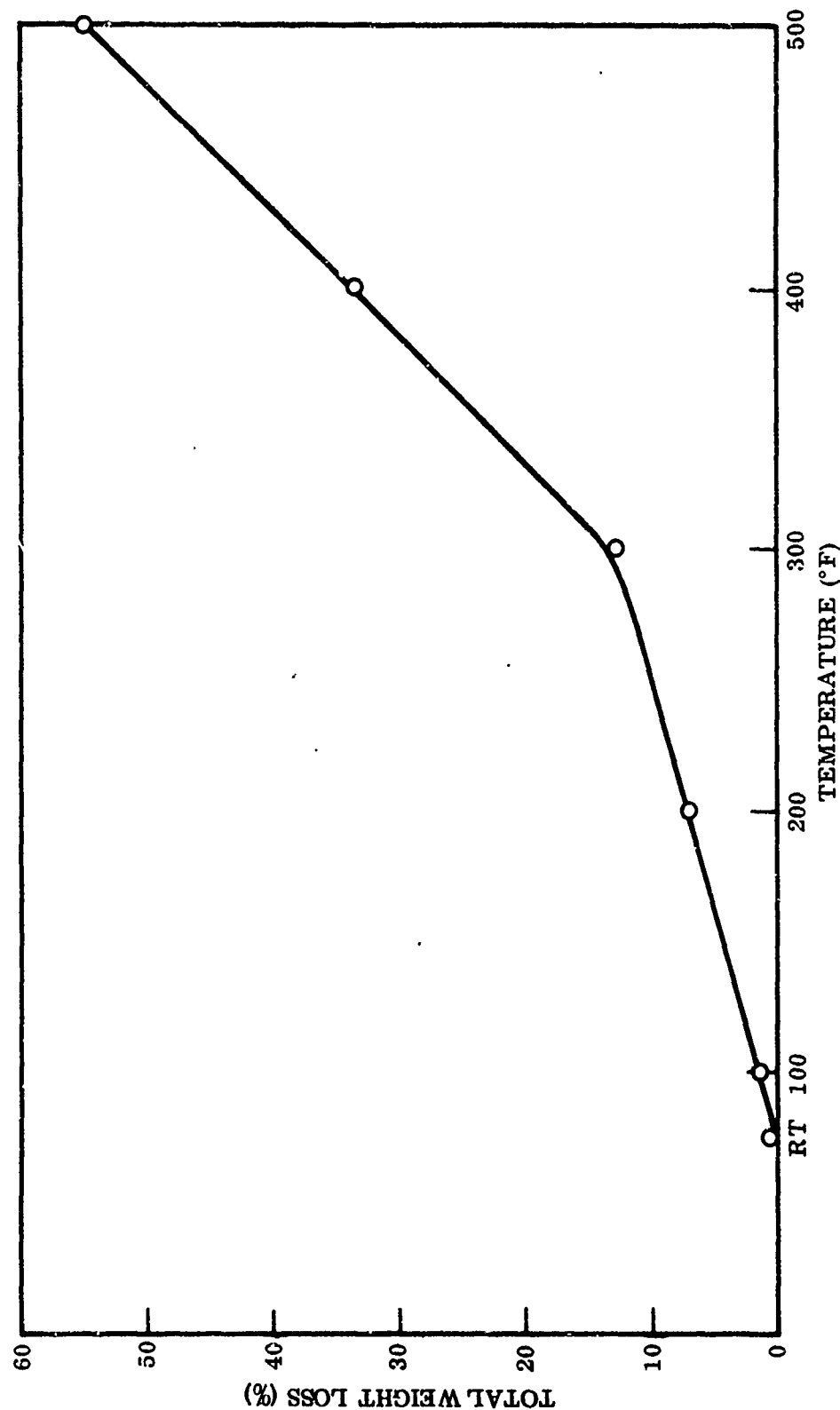


Figure 168 Equilibrium Weight Loss Versus Temperature, Epoxy Sublayer, Materials E-F

Table LXXXV. Short-Term Weight Loss in Vacuum

Test conditions		Cumulative weight loss (%)	Maximum short-term temperature stability	Comments
Temperature (°F)	Total time (min)			
Epoxy facing adhesive				
100	48	0.4	Good to 300°F; marginal at 400°F	Bloated, porous black residue at 500°F
200	94	2.23		
300	150	4.92		
400	185	9.9		
500	297	51.0		
Epoxy backing adhesive				
100	27	0.875	Good to 300°F	Bloated, porous black residue at 500°F
200	75	2.63		
300	128	6.05		
400	188	22.3		
500	308	58.0		
Epoxy sublayer, Material D				
100	48	0.53	Good to 300°F	Black glassy residue at 500°F
200	100	2.83		
300	156	4.6		
400	212	13.8		
500	362	82.7		
Epoxy sublayer, Materials E - F				
100	48	1.39	Probably to 300°F	Glossy brown film at 500°F
200	96	7.45		
300	152	12.8		
400	208	33.35		
500	358	54.5		

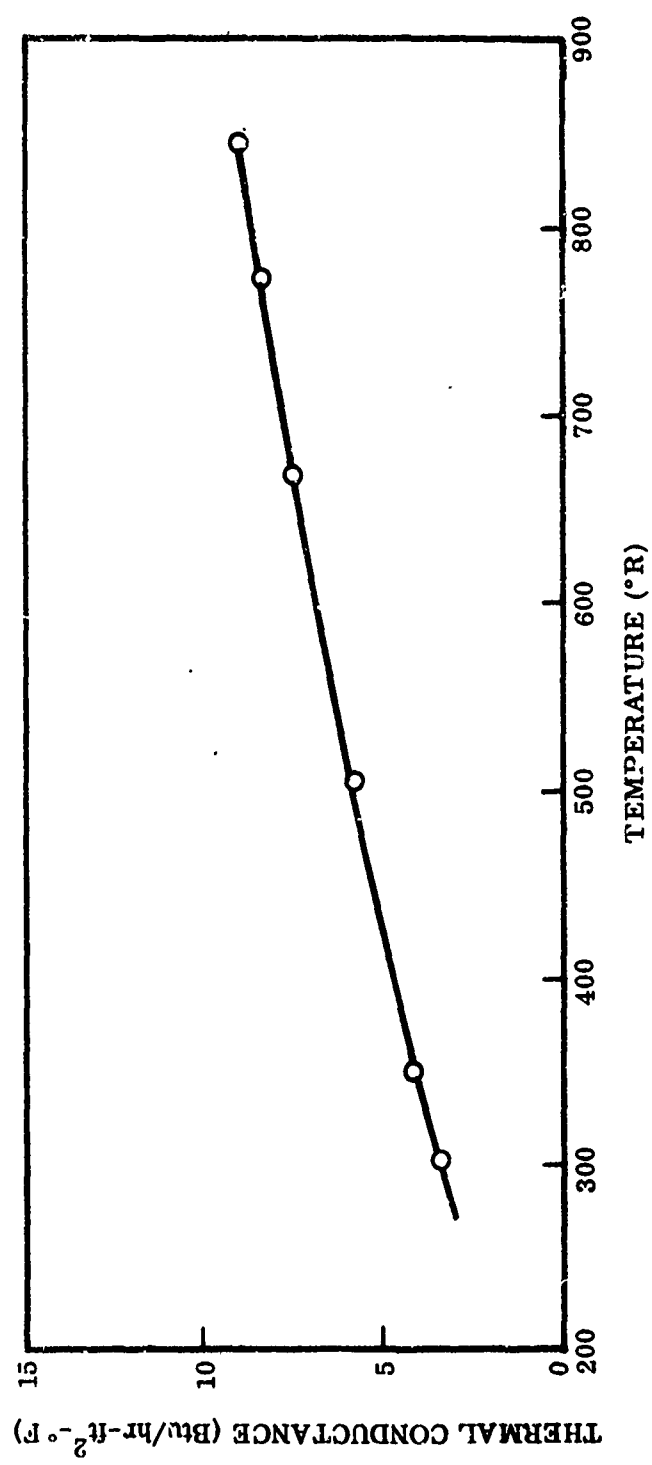


Figure 169 Thermal Conductance of Composite Structure

Table LXXXVI. Long-Term Thermal/Vacuum Exposure, Composite Structure

Specimen	Weight before (g)	Weight after (g)	Weight loss (g)	Change (%)	Post-test appearance
100-hour test					
EF-1	8.6000	8.5450	0.0550	0.64	White spots on one face
EFM-1	8.6462	8.5914	0.0548	0.635	No change
EFN-1	8.9963	8.9388	0.0575	0.64	No change
1,000-hour test					
EF-3	8.7416	8.6651	0.0765	0.875	Small dents on one face; hair-line cracks and minor discoloration on other face; slight flow and evaporation of bonding agent, causing discolored deposits on interior of honeycomb
EFM-3	9.7300	9.5966	0.1334	1.37	
EFN-3	8.9018	8.8244	0.0774	0.87	
6,000-hour test					
EF-2	8.8536	8.7724	0.0812	0.91	No change
EFM-2	9.0063	8.9008	0.1055	1.17	No change
EFN-2	8.7538	8.6678	0.0960	1.10	No change

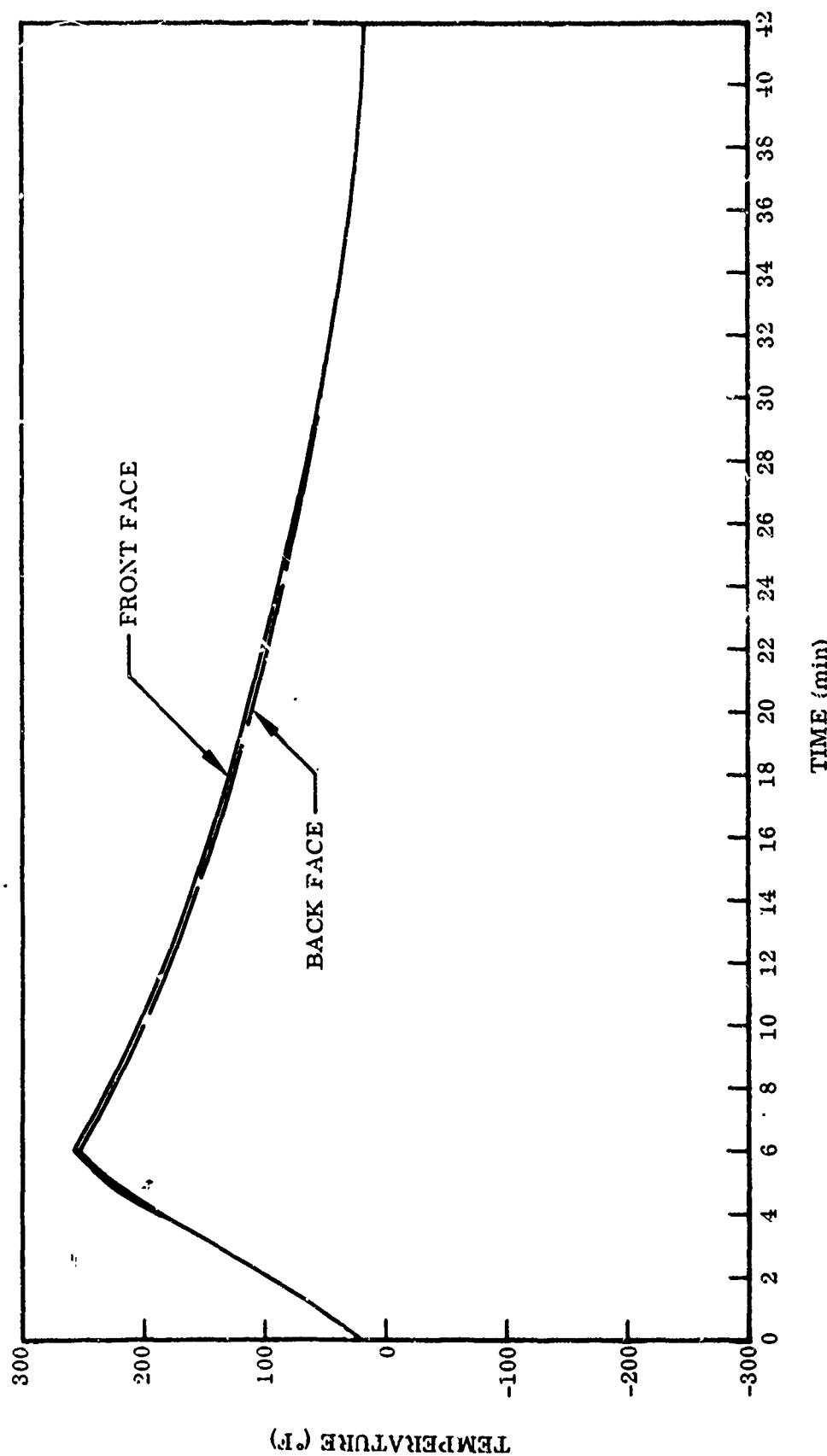


Figure 170 Temperature Histories of Front and Back Faces During Thermal Cycling, Material D

Table LXXXVII. Behavior Under Thermal Cycling,
Composite Structure, Material D

Specimen	Duration of test (cycles)	Pre-test condition	In situ condition		Post-test condition	Reflectance after exposure
			Cycle	Condition		
DGM-1	100	Very good reflecting surface on front face; no apparent imperfections on either face	0-100	No change noted (see Figure 67b)	Very fine cracks noted over entire front face of sample	No change
DGN-1	1,000	Very good surface	0-138 166 1,000	Craze marks noted over entire surface Peeling at several points on front surface, max. 1/4-in. dia. No further change noted	Very fine cracks noted over entire surface; aluminum reflective coating peeled at several points	No change (where surface intact)
DGN-3	6,000	Surface smooth	0-6,000	Craze marks noted over entire surface (not evident in Figures 65c and 67d)	Very fine cracks noted over entire surface	No change

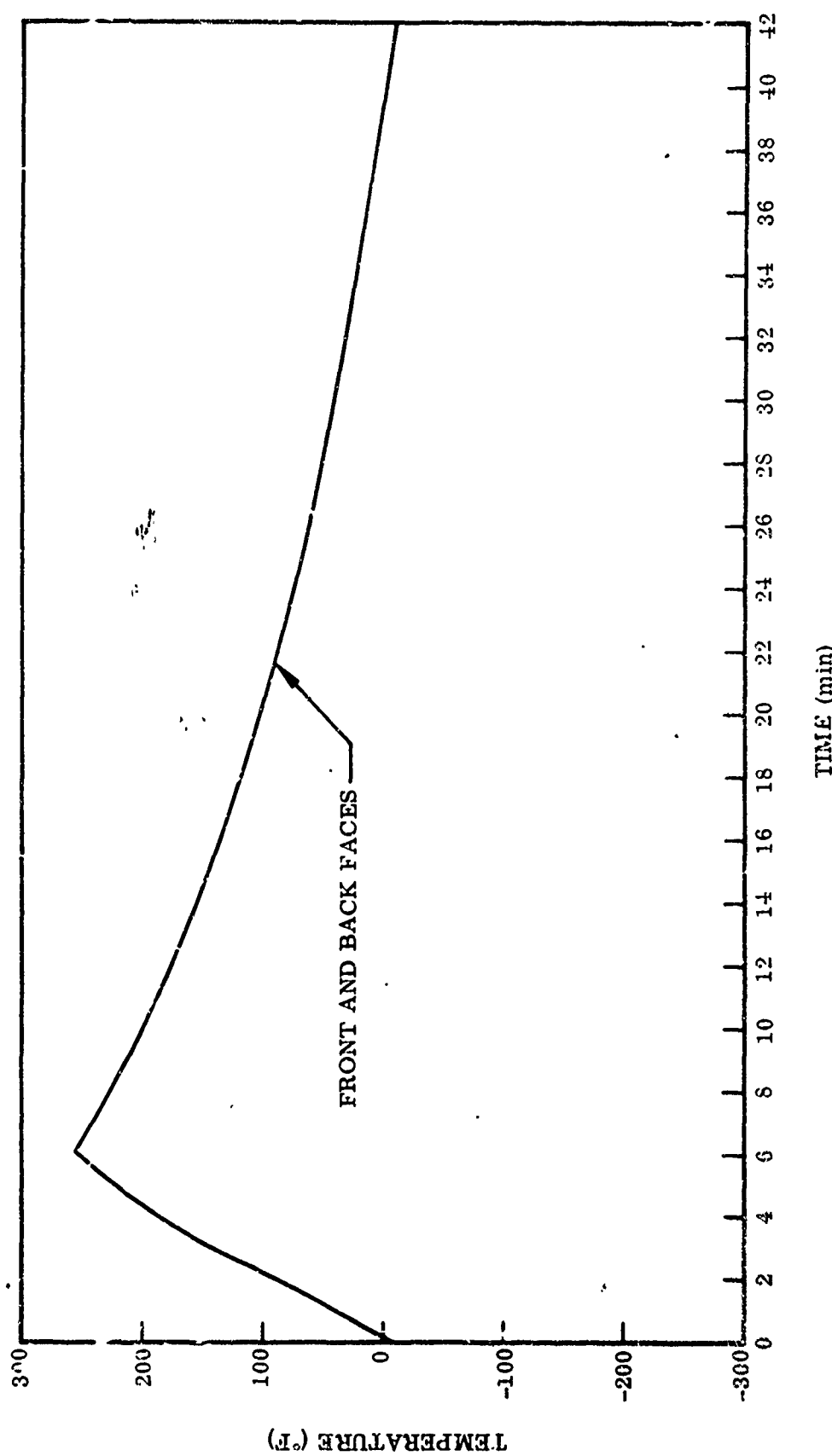


Figure 171. Temperature Histories of Front and Back Faces During Thermal Cycling, Material E

Table LXXXVIII. Behavior Under Thermal Cycling,
Composite Structure, Material E

Specimen	Duration of test (cycles)	Pre-test condition	In situ condition		Post-test condition	Reflectance after exposure
			Cycle	Condition		
EGM-1	100	Front sur- face smooth except for slight con- vexity at edges (see Figure 69a)	^ - 100	No changes noted (see Figure 69b)	Front surface unchanged	No change
EGN-1	1,000	Front sur- face smooth	0 - 885 895	No change noted Test failure - sample overheated	-	Not tested
EGN-3	1,000	Front sur- face smooth	0 - 1,000	Hairline defects covered front surface	Hairline cracks in coating; larger but less frequent than those in Material D	No change
EGM-2	6,000	Front sur- face smooth except for 1/8-in. dim- ple near center of surface and 1/16-in. dimple off center	0 - 111 147 148 - 356 357 - 4,292 4,292	No change noted Three small- hairline defects appeared on front surface Hairline de- fектs cov- ered entire front surface No change noted (see Figure 69c) Test failure - sample overheated	(Test not rerun)	Not tested

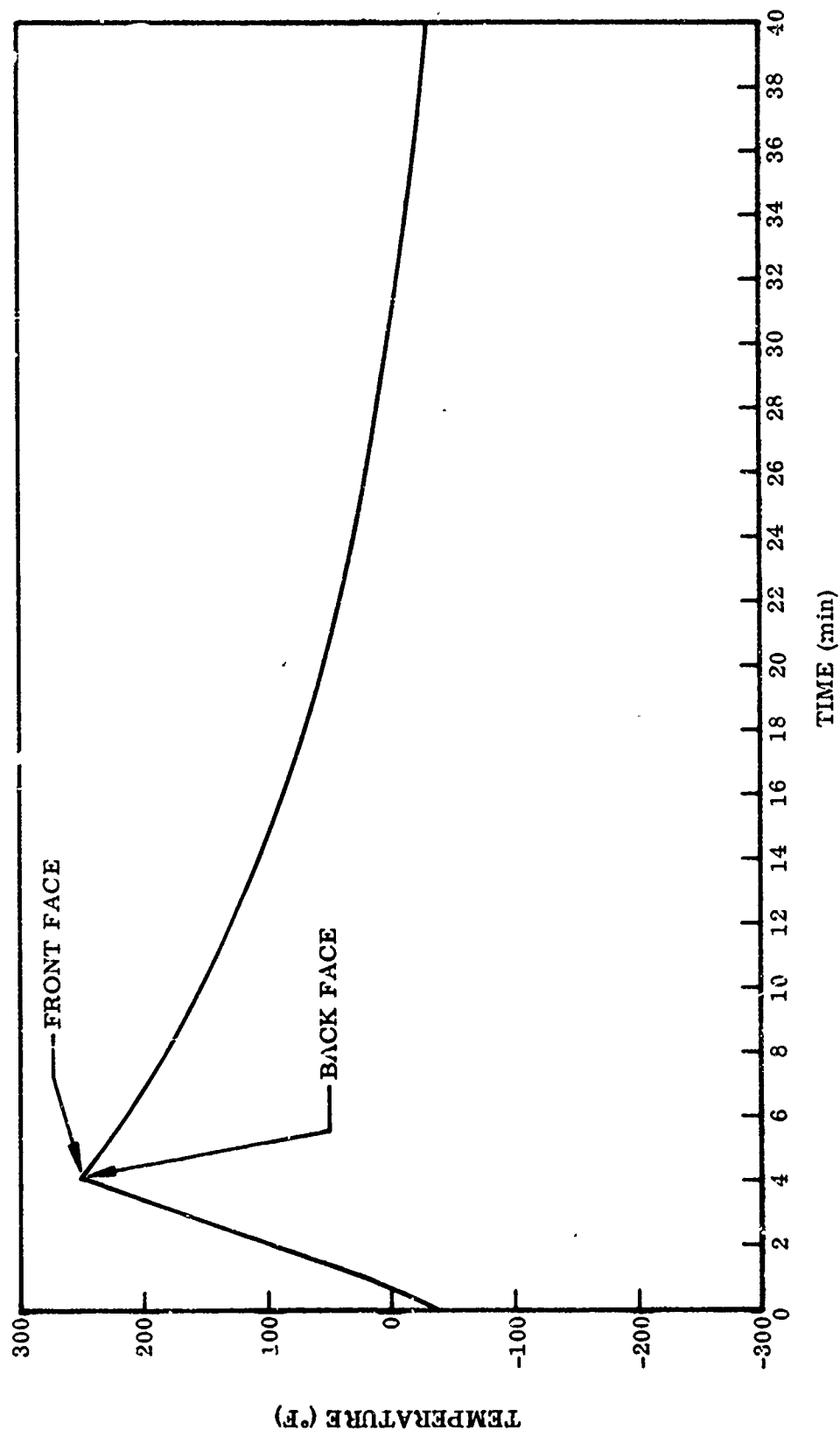


Figure 172 Temperature Histories of Front and Back Faces During Thermal Cycling, Material F

Table LXXXIX. Behavior Under Thermal Cycling,
Composite Structure, Material F

Specimen	Duration of test (cycles)	Pre-test condition	In situ condition		Post-test Condition	Reflectance after exposure
			Cycle	Condition		
FGM-1	100	Front face slightly con- cave on one side; sur- face has frosty appearance (see Figure 71a)	0-8	No change noted	Frosty appearance of front sur- face more pronounced. Craze marks clearly visi- ble. Honey- comb pattern clearly shows through on reverse side.	No change
			43	Network of craze marks noted on front sur- face (see Figure 71b)		
			96-150	Craze marks more distinct		
FGN-2	6,000	Front sur- face has frosty appearance (see Figure 71c)	22	Hairline craze de- fects show on front surface; surface appears frosty	See Figure 71e	Not tested
			23-882	No further change noted (see Figure 71d)		
			883	Edge raised slightly at three spots		
			1,137	Noticeable blue tinge to front sur- face noted; hairline craze de- fects appear green		
			1,246	Test failure (vacuum lost)		

Table LXXXIX --- Continued

Specimen	Scheduled duration of test (cycles)	Pre-test condition	In situ condition		Post-test condition	Reflectance after exposure
			Cycle	Condition		
FG-1	1,000	Front surface frosty blue in appearance	0-64 65-1,000	Hairline craze marks noted No further change noted	Hairline crazes in reflective coating	No change
FG-2	6,000	Front surface frosty blue in appearance; one small dimple noted in upper left corner of surface	0-27 28-63 64-2,086 2,087	Sample appears badly clouded Several hairline craze marks appeared on sample No further change noted Test failure -sample remained at test temperature for 9 hr as result of controller malfunction	-	Not tested
FGN-1	6,000 (test terminated at 3,000 cycles)	Front surface frosty blue in appearance	0-76 77-3,000	Craze marks noted No further change noted (see Figure 7if)	Hairline crazes in reflective coating	No change

Table XC. Summary of Optical-Properties Test Results

Exposure	Solar reflectance		
	Material D	Material E	Material F
Pre-test condition	0.92	0.92	0.89
Ultraviolet radiation (1-yr equivalent)			
RT	0.82	0.83	0.72
250° F	0.91	0.90	0.68
5 keV electrons (1-yr equivalent)			
RT	0.92	0.92	0.86
250° F	0.92	0.92	0.81
Combined environment (6-mo equivalent)			
RT	0.84	0.87	0.75
250° F	0.91	0.90	0.64

Table XCI. Panel-Shear Test, Composite Structure

Temperature	Specimen designation	Modulus G (psi)	Elastic limit (psi)	Maximum stress (psi)	Final strain (%)
-200° F	DJ-7	5.83×10^3	22.3	86.1	2.43
	DJ-8	5.69×10^3	25.0	92.8	2.31
	DJ-9	4.71×10^3	26.6	91.3	2.85
	Average	5.41×10^3	24.6	90.1	2.53
	Deviation	(12.9%)	(9.4%)	(4.4%)	(8.7)
Room temperature	DJ-1	2.52×10^3	13.40	46.8	8.17
	DJ-2	2.29×10^3	12.25	44.3	9.40
	DJ-3	2.21×10^3	14.40	38.6	7.18
	Average	2.34×10^3	13.35	43.2	8.58
	Deviation	(5.5%)	(7.9%)	(10.7%)	(16.3)
+250° F	DJ-4	830	2.82	6.15	1.06
	DJ-5	2,300	2.18	5.58	0.55
	DJ-6	1,530	1.71	5.22	0.52
	Average	1,553	2.24	5.65	0.71
	Deviation	(46.6%)	(23.6%)	(7.6%)	(26.8)

Table XCII. Panel-Bend Test, Composite Structure

Specimen designation	Beam width, b (in.)	Beam span, L (in.)	$\frac{EI/b}{\text{in.}^2 \cdot \text{lb}} / \text{in.}$	M_e/b (lb)	M_u/b (lb)	Tension face
DK-1	1.98	9	3,580	6.1	11.8	(a)
DK-2	1.98	9	2,920	9.1	10.8	(a)
DK-3	1.98	9	2,900	9.1	10.2	(a)
DK-4	1.98	9	3,290	6.8	9.9	(a)
Average	--	--	3,172	7.8	10.7	

(a) Symmetrical specimens.

Table XCIII. Facing-Tension Test, Facing and Backing Materials

Temperature	Specimen designation	Modulus E (psi)	Elastic limit (psi)	Maximum stress (psi)	Final strain (%)
-200° F(a)	DL-9	3.99×10^6	9.88×10^3	21.9×10^3	>13.0
	DL-10	4.56×10^6	6.66×10^3	22.3×10^3	17.0
	DL-11	7.13×10^6	6.42×10^3	21.6×10^3	13.9
	Average	5.23×10^6	7.65×10^3	21.9×10^3	—
	Deviation	(23.7%)	(16.2%)	(1.4%)	—
Room temperature(a)	DL-1	7.80×10^6	4.94×10^3	19.0×10^3	19.3
	DL-2	8.50×10^6	8.40×10^3	15.0×10^3	>14
	DL-3	7.76×10^6	5.83×10^3	15.4×10^3	12.8
	DL-4	8.05×10^6	6.42×10^3	15.8×10^3	>14
	Average	8.03×10^6	6.40×10^3	16.3×10^3	—
+250° F(a)	DL-5	4.42×10^6	5.00×10^3	13.9×10^3	20.2
	DL-6	2.29×10^6	5.19×10^3	13.3×10^3	13.2
	DL-7	4.18×10^6	4.94×10^3	14.2×10^3	20.6
	DL-8	5.32×10^6	3.21×10^3	13.7×10^3	13.7
	Average	4.05×10^6	4.58×10^3	13.8×10^3	16.9
-200° F(b)	DL-19	11.35×10^6	5.81×10^3	21.4×10^3	16.3
	DL-20	11.40×10^6	6.20×10^3	22.4×10^3	15.6
	DL-21	7.14×10^6	7.75×10^3	22.2×10^3	10.2
	Average	9.96×10^6	6.59×10^3	22.0×10^3	14.0
	Deviation	(28.3%)	(11.8%)	(2.7%)	(27.1)
Room temperature(b)	DL-13	7.96×10^6	3.02×10^3	15.1×10^3	>14
	DL-14	8.01×10^6	5.22×10^3	15.3×10^3	12.9
	DL-15	9.70×10^6	4.88×10^3	15.5×10^3	14.9
	Average	8.56×10^6	4.37×10^3	15.3×10^3	—
	Deviation	(7.0%)	(30.9%)	(0.7%)	—
+250° F(b)	DL-16	3.94×10^6	3.72×10^3	13.0×10^3	6.1
	DL-17	2.45×10^6	4.65×10^3	13.2×10^3	13.0
	DL-18	4.70×10^6	4.57×10^3	13.3×10^3	10.5
	Average	3.70×10^6	4.31×10^3	13.2×10^3	9.9
	Deviation	(33.8%)	(13.7%)	(1.5%)	(38.4)

(a) Facing material \approx 0.008 in. thick.(b) Backing material \approx 0.004 in. thick.

Table XCIV. Facing-Separation Test, Composite Structure

Unexposed Specimens

Temperature	Specimen designation	Modulus E (psi)	Elastic limit (psi)	Maximum stress (psi)	Final strain (%)
-200°F	EM-7 ^(a)	13.4×10^3	100.0	100.0	0.78
	EM-8 ^(a)	15.9×10^3	76.4	76.4	0.48
	EM-9 ^(a)	10.2×10^3	147.5	147.5	1.48
	Average	13.2×10^3	108.0	108.0	0.91
Room temperature	Deviation	(22.7%)	(30.2%)	(30.2%)	(47.3)
	EM-3 ^(a)	6.38×10^3	23.5	23.5	0.38
	EM-4 ^(a)	9.94×10^3	16.2	21.9	0.32
	EM-5 ^(b)	5.47×10^3	11.3	47.3	---
+250°F	Average	7.26×10^3	17.0	30.9	0.35
	Deviation	(24.6%)	(33.5%)	(29.1%)	(8.6)
	EM-1 ^(b)	1.11×10^3	4.50	5.49	0.85
	EM-2 ^(b)	1.16×10^3	7.45	8.02	0.84
	EM-3 ^(b)	1.58×10^3	5.45	9.88	0.87
	Average	1.28×10^3	5.80	7.80	0.85
	Deviation	(13.3%)	(22.4%)	(29.0%)	(1.2)

Exposed Specimens

Specimen	Previous exposure	Modulus E (psi)	Elastic limit (psi)	Maximum stress (psi)	Final strain (%)
DGM-1	Thermal cycling (100 cycles)	6.05×10^3	58.7	90.0	1.95
EFM-1	Thermal/vacuum environment (100 hr)	5.60×10^3	81.0	160	4.02
EFM-3	Thermal/vacuum environment (1,000 hr)	7.26×10^3	210	292	4.53
EF-2	Thermal/vacuum environment (6,000 hr)	8.16×10^3	158	181	2.46
EFM-2	Thermal/vacuum environment (6,000 hr)	8.97×10^3	162	204	2.63
EGM-1	Thermal cycling (100 cycles)	4.05×10^3	60.2	82.3	3.27
FGM-1	Thermal cycling (100 cycles)	3.85×10^3	64.0	76.7	2.41
FG-1	Thermal cycling (1,000 cycles)	4.44×10^3	57.8	84.5	2.70
FGN-2(c)	Thermal cycling (1,246 cycles)	5.58×10^3	72.5	99.8	3.04

(a) Plating failure.

(b) Glue-line failure.

(c) Initially scheduled to undergo 6,000 cycles. Testing was terminated after 1,246 cycles when vacuum was lost as result of frozen seal.

Table XCV. Core-Compression Test, Composite Structure

Unexposed Specimens

Temperature	Specimen designation	Modulus E (psi)	Elastic limit (psi)	Maximum stress (psi)	Final strain (%)
-200° F	DN-7	1.55×10^3	44.6	47.8	4.92
	DN-8	5.00×10^3	43.4	57.8	1.37
	DN-9	---	63.5	67.6	---
	Average	3.28×10^3	50.5	57.7	3.15
Room temperature	Deviation	(52.7%)	(14.1%)	(17.2%)	(56.5)
	DN-1	4.22×10^3	53.5	83.1	3.84
	DN-2	4.53×10^3	43.9	89.3	5.30
	DN-3	3.35×10^3	44.8	84.8	4.32
	Average	4.03×10^3	47.4	85.7	4.49
+250° F	Deviation	(16.8%)	(7.4%)	(3.0%)	(14.5)
	DN-4	6.20×10^3	32.5	51.8	11.88
	DN-5	8.30×10^3	67.3	66.3	9.64
	DN-6	8.64×10^3	51.3	54.7	6.96
	Average	7.71×10^3	47.0	57.6	9.49
	Deviation	(19.6%)	(30.8%)	(11.8%)	(26.7)

Exposed Specimens

Specimen	Previous exposure	Modulus E (psi)	Elastic limit (psi)	Maximum stress (psi)	Final strain (%)
DGN-1	Thermal cycling (1,000 cycles)	4.72×10^3	69.5	71.5	1.62
DGN-3	Thermal cycling (6,000 cycles)	8.93×10^3	76.8	82.8	1.04
EF-1	Thermal/vacuum environment (100 hr)	3.85×10^3	---	82.5	0.92
EFN-1	Thermal/vacuum environment (100 hr)			Test equipment failure - no data	
EF-3	Thermal/vacuum environment (1,000 hr)	13.8×10^3	91.8	95.6	0.71
EFN-3	Thermal/vacuum environment (1,000 hr)	9.88×10^3	76.5	87.1	0.94
EFN-2	Thermal/vacuum environment (6,000 hr)	6.52×10^3	76.7	83.9	1.45
EGN-3	Thermal cycling (1,000 cycles)	7.09×10^3	80.5	88.4	1.41
FGN-1	Thermal cycling (3,000 cycles)	0.91×10^3	11.5	18.4	2.40

Appendix V TEST RESULTS - CANDIDATE MATERIALS G-K

Presented in this appendix are the results of all laboratory tests performed on materials G, H, J, and K. Discussions of the tests, descriptions of test apparatus, test procedures and conditions, and interpretations of test results, covered elsewhere in this report, are not repeated here.

Materials G, H, J, and K consist of electroformed nickel front and back sheets, joined with epoxy to 1-1/2-in. diameter nickel cylinders. The reflective surfaces of materials G and H are vacuum-deposited silver, and material H also has a silicon-oxide overcoating. The reflective surfaces of materials J and K consist of successive layers of chrome, silicon oxide, and aluminum, and material K also has a silicon-oxide overcoating.

Results of the following tests are given in this appendix:

- Weight loss in vacuum (epoxy adhesive)
- Long-term thermal/vacuum exposure (composite structure)
- Thermal conductance of composite structure
- Thermal expansion (reflective and back surfaces)
- Behavior under thermal cycling
- Ultraviolet irradiation at room temperature and +250° F
- Exposure to low-energy electrons at room temperature and +250° F
- Exposure to combined environment at room temperature and +250° F
- Panel shear (-200° F, room temperature, and +250° F)
- Panel bend
- Facing tension (-200° F, room temperature, and +250° F)
- Facing separation (-200° F, room temperature, and +250° F)
- Core compression (-200° F, room temperature, and +250° F)

See Figures 173 through 180 and Tables XCVI through CIV.

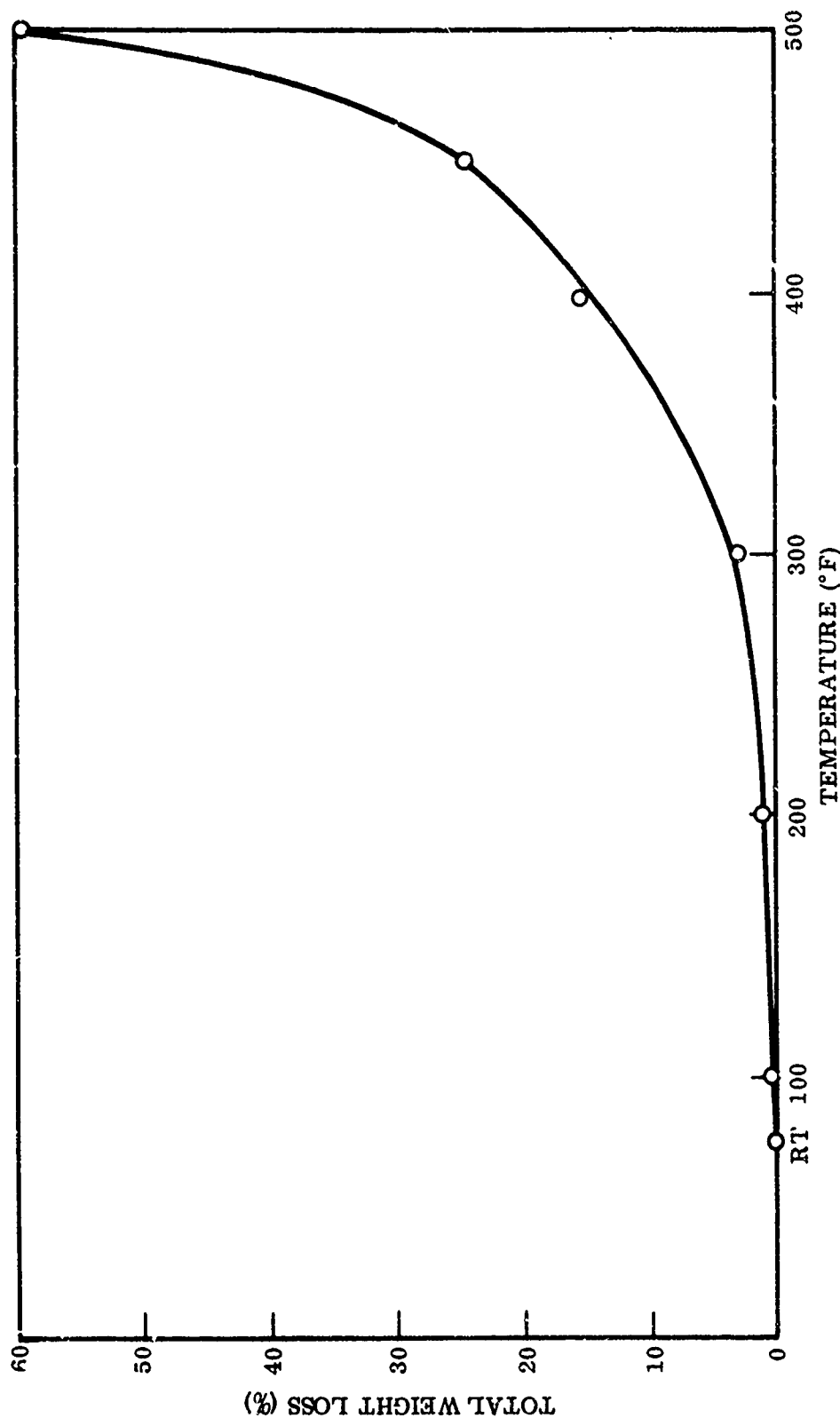


Figure 173 Equilibrium Weight Loss Versus Temperature, Epoxy Adhesive

Table XCVI. Short-Term Weight Loss in Vacuum, Epoxy Adhesive

Test Conditions		Cumulative weight loss (%)	Maximum short-term temperature stability	Comments
Temperature (° F)	Total time (min)			
100	48	0.27	Good to 300° F	
200	96	1.1		
300	152	2.8		
400	212	15.6		
500	362	59.62		

Table XCVII. Long-Term Thermal/Vacuum Exposure, Composite Structure

Specimen	Weight before (g)	Weight after (g)	Weight loss (g)	Change (%)	Post-test appearance
100-hour test					
GF-1	4.3653	4.3638	0.0015	0.03	Bonding between sheet and top of conical section separated before start of test; specimen fell apart from handling after test
GF-1-i	4.8585	4.8565	0.0020	0.04	Same as GF-1 before test; no change after test
GFN-1	4.2269	4.2250	0.0019	0.045	Bonding between sheet and top of conical section 100% separated before test; no change after test
1,000-hour test					
GF-3	4.4500	4.4472	0.0028	0.06	Bonding between sheet and top of conical section completely separated before test; polished face shows minor discoloration
GFM-3	4.7736	4.7750	0.0036	0.07	Same as GF-3 except 25% separation before test
GFN-3	4.0036	3.9993	0.0043	0.107	Same as GF-3 except 50% separation before test
6,000-hour test					
GF-2	4.1453	4.1395	0.0058	0.14	Bonding between sheet and top of conical section 50% separated before test; no change during test
GFM-2	4.3648	4.3592	0.0056	0.13	No change
GFN-2	4.2477	4.2435	0.0042	0.10	Same as GF-2

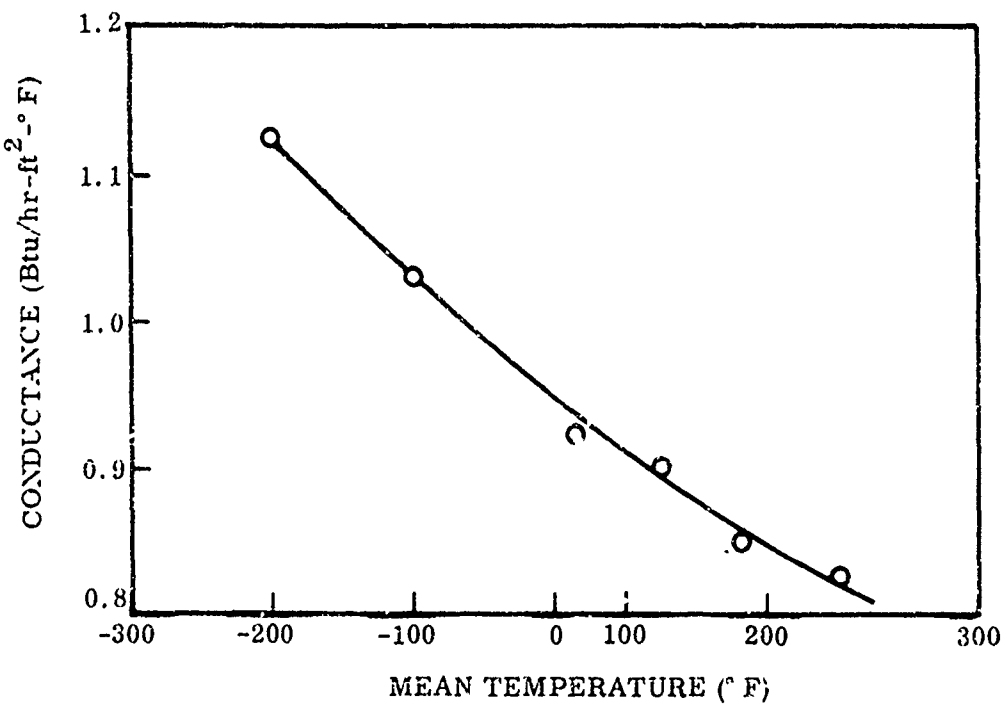


Figure 174 Thermal Conductance of Composite Structure, 1-in.-Thick Specimen

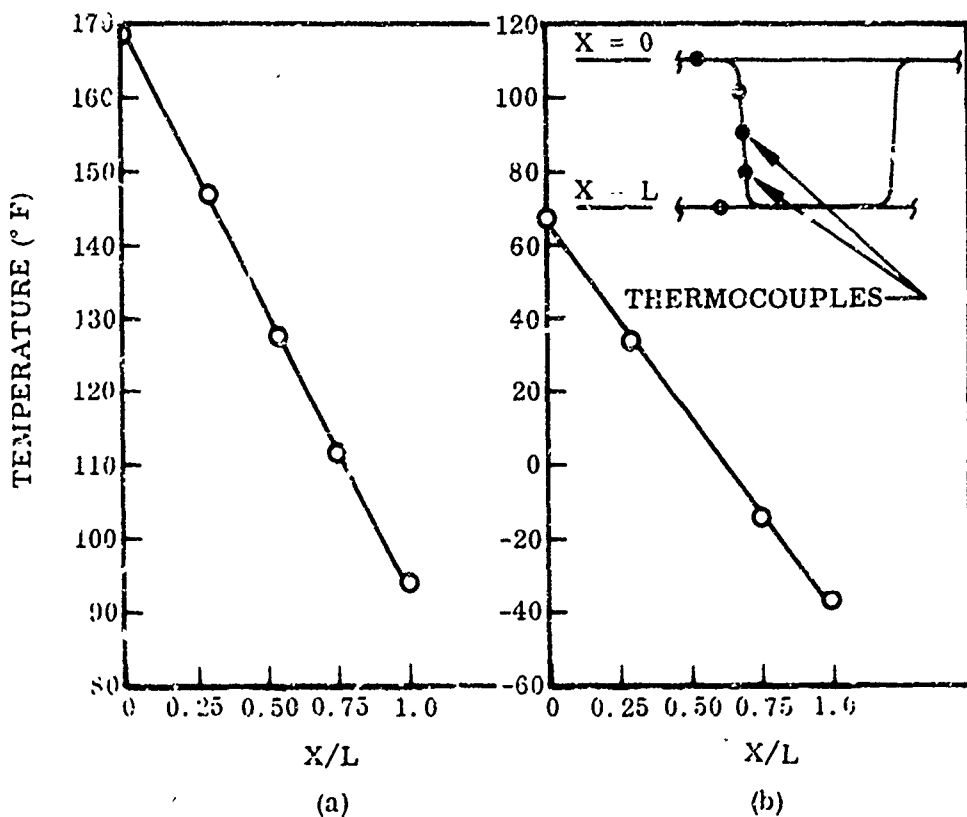


Figure 175 Temperature Distribution Along Wall of One Cylinder of Composite Structure ($X/L = 0$ and 1.0 Are on Faces of Structure)

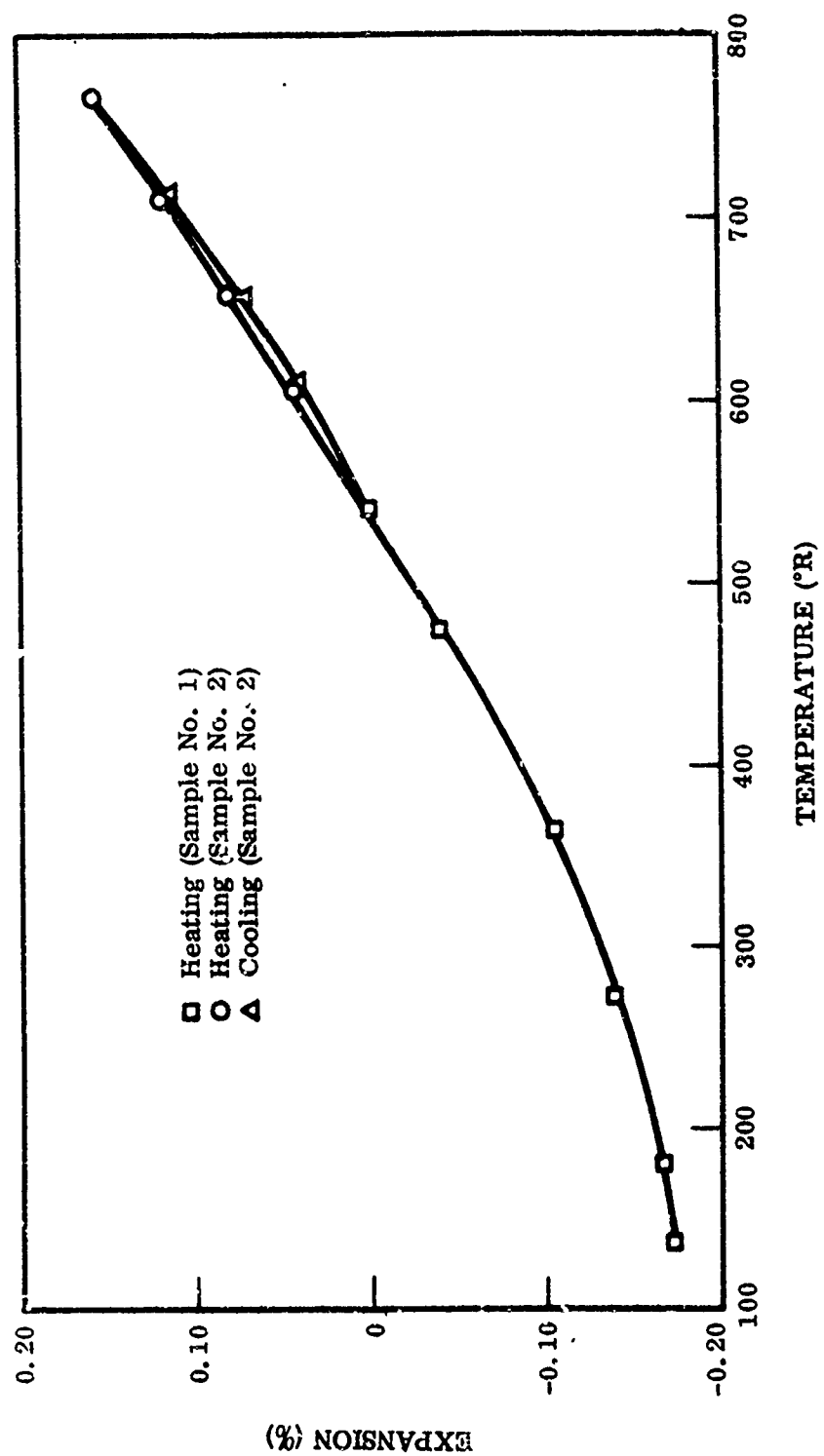


Figure 176 Linear Thermal Expansion of Reflective Surface

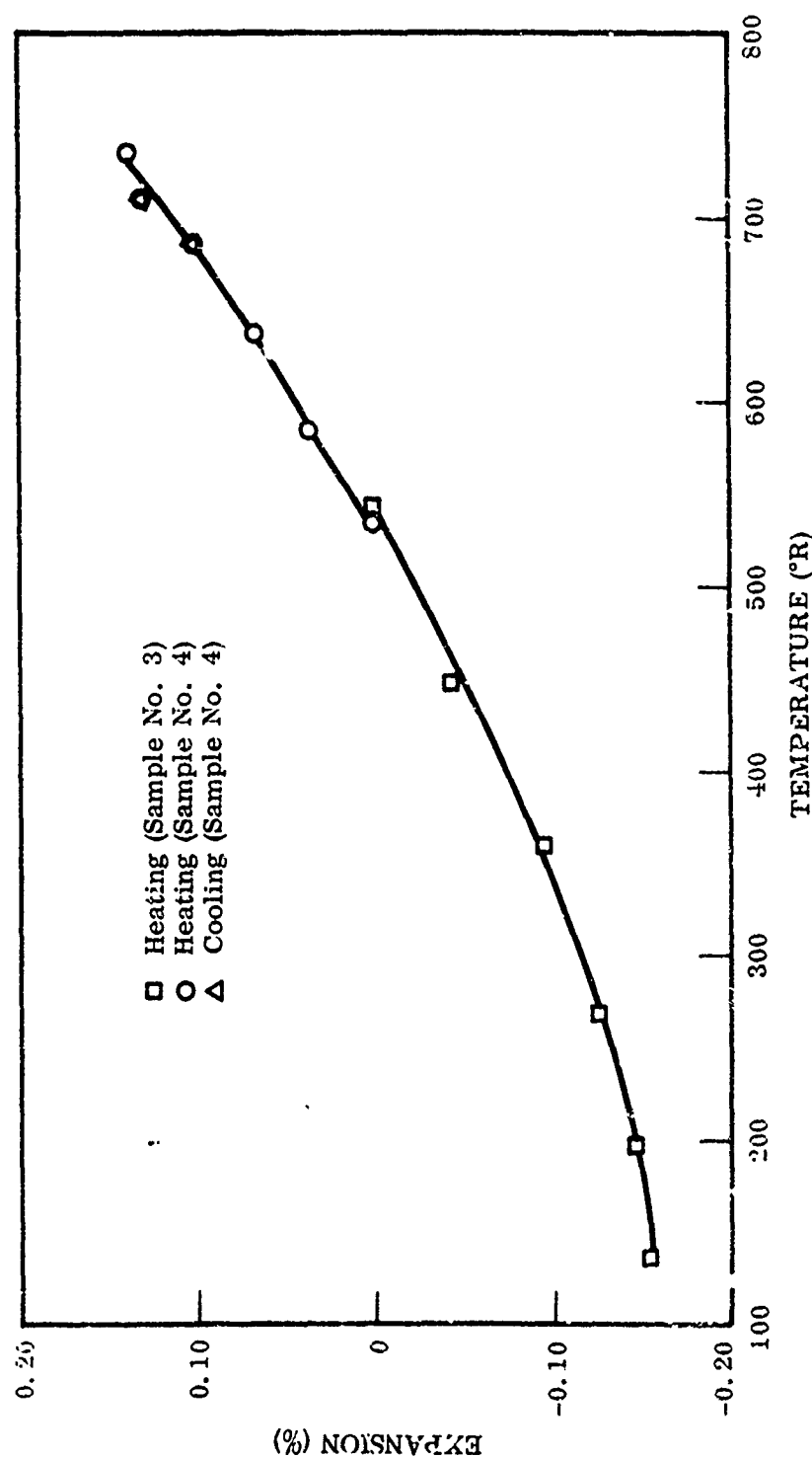


Figure 177 Linear Thermal Expansion of Back Surface

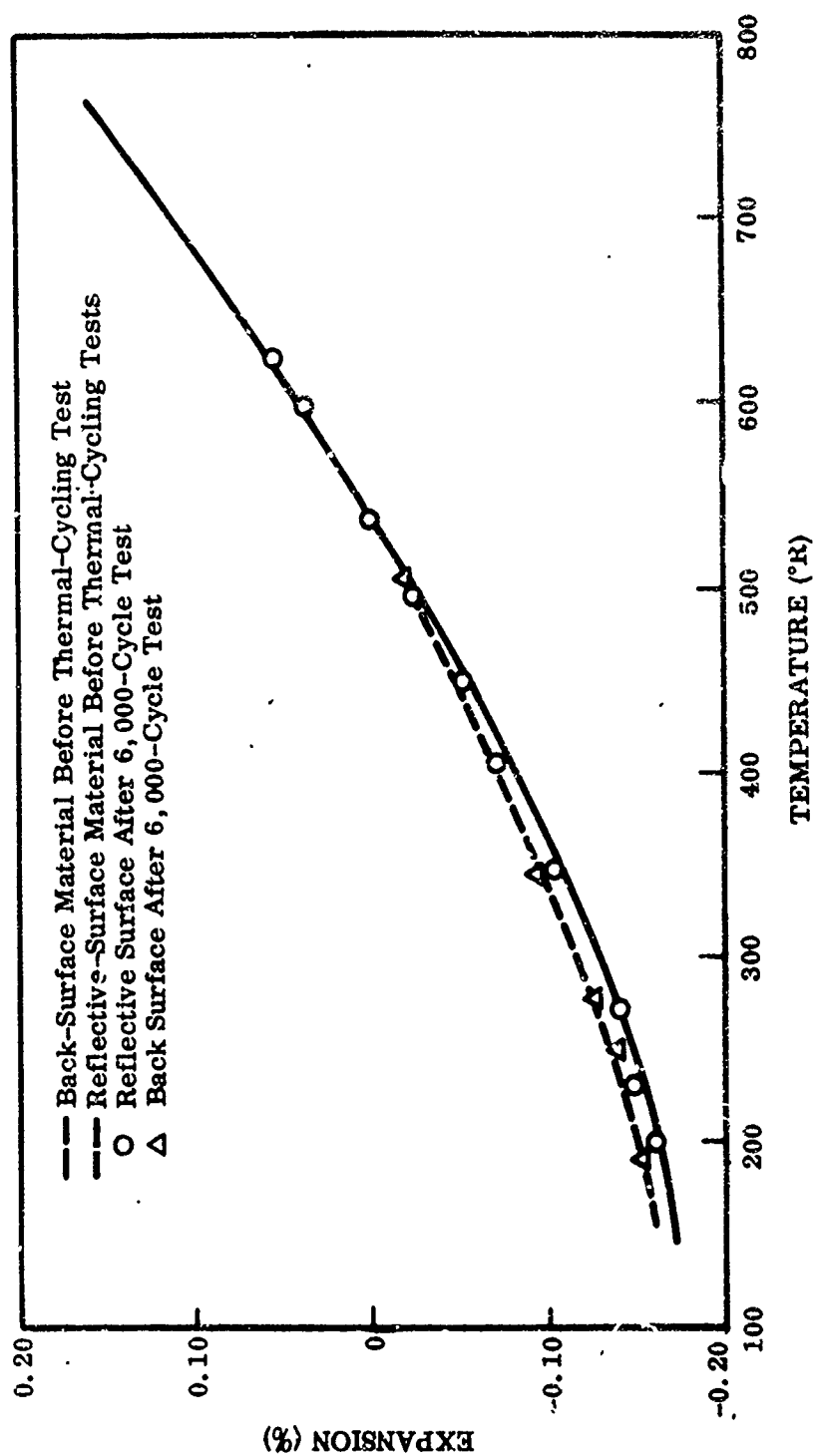


Figure 178 Comparison of Linear Thermal Expansion Before and After 6,000-Cycle Thermal Cycling Test

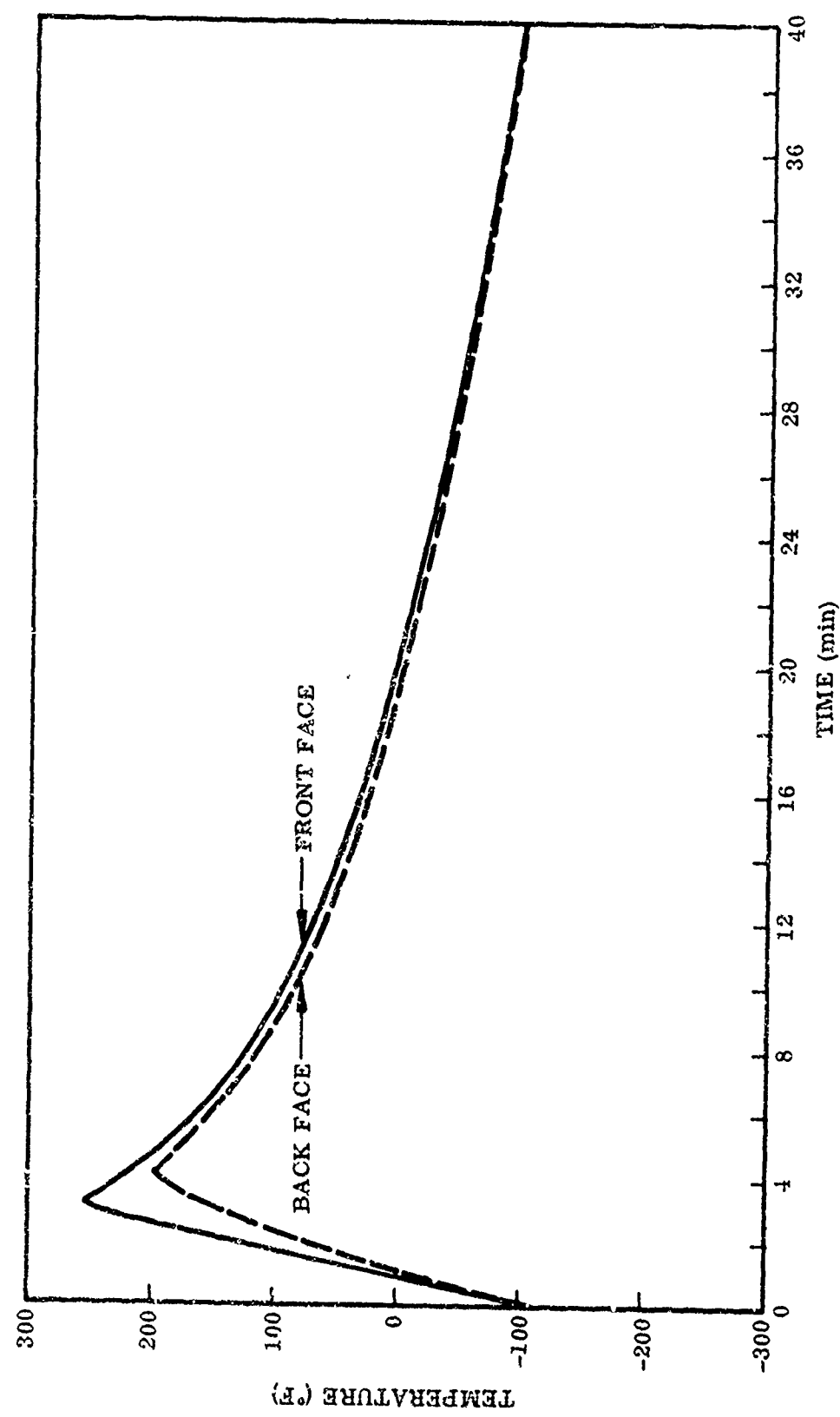
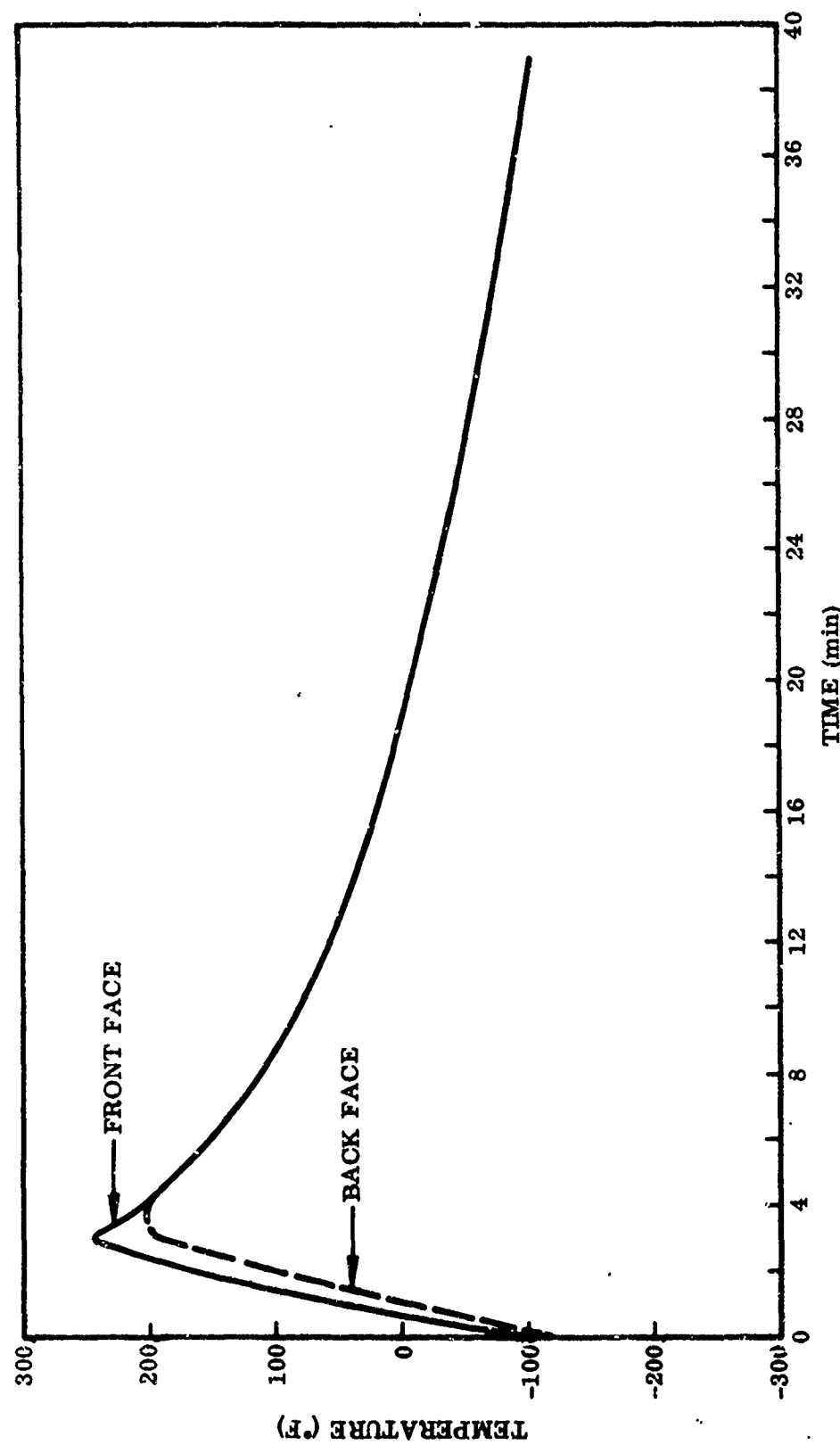


Figure 179 Temperature Histories of Front and Back Faces During Thermal Cycling, Material J



312

Figure 180 Temperature Histories of Front and Back Faces During Thermal Cycling, Material K

Table XCVIII. Behavior Under Thermal Cycling, Composite Structure

Material J

Specimen	Duration of test (cycles)	Pre-test condition	In situ condition		Post-test condition	Reflectance after exposure
			Cycle	Condition		
JGM-1	100	Sample surfaces flat (see Figure 73a)	0-118	No change noted (see Figures 73b and 73c)	No change noted	No change
JGN-2	1,000	Some dirt flecks and patches on reflective surface	0-1,031	No change noted	No change noted	No change
JG-1	6,000	Sample surfaces flat	0-6,000	No change noted (see Figure 73d)	No change noted	No change

Material K

Specimen	Duration of test (cycles)	Pre-test condition	In situ condition		Post-test condition	Reflectance after exposure
			Cycle	Condition		
KG-1	100	Sample surfaces flat (see Figure 75a)	0-100	No change noted (see Figures 75c and 75d)	No change noted	No change
KGM-2	1,000	Sample surfaces flat (see Figure 75e)	0-998	No change noted (see Figure 75f)	Epoxy bonding green in some places, mainly on back surface bonding. No other change noted	No change
KGM-1	6,000	Sample surfaces flat	0-6,002	No change noted (see Figure 75b)	No change noted	No change

Table XCIX. Summary of Optical-Properties Test Results

Exposure	Solar reflectance			
	Material G	Material H	Material J	Material K
Pre-test condition	0.93	0.91	0.92	0.88
Ultraviolet radiation (1-yr equivalent)				
RT	0.86	0.70	0.83	0.82
250° F	0.91	0.74	0.91	0.75
5 keV electrons (1-yr equivalent)				
RT	0.92	0.91	0.92	0.82
250° F	0.93	0.90	0.92	0.75
Combined environment (6-mo equivalent)				
RT	0.91	0.78	0.87	0.80
250° F	0.90	0.78	0.92	0.77

Table C. Panel-Shear Test, Composite Structure

Temperature	Specimen designation	Modulus G (psi)	Elastic limit (psi)	Maximum stress (psi)	Final strain (%)	Thickness (in.)
-200° F	GJ-14	588	1.00	1.00	0.17	1.0
Room temperature	GJ-1	555	3.08	5.10	1.72	0.5
	GJ-2	—	—	5.50	1.41	0.5
	GJ-18	349	1.21	2.50	0.96	1.0
	GJ-19	330	—	2.77	1.15	1.0
+250° F	GJ-3	—	—	(a)	—	0.5
	GJ-12	—	—	(a)	—	1.0

(a) Failure occurred with approximately 3-lb fixture weight.

Table CI. Panel-Bend Test, Composite Structure

Specimen designation	Beam width, b (in.)	Beam span, L (in.)	EI/b (in. ² -lb/in.)	M_c/b (lb)	M_u/b (lb)	Tension face	Thickness (~ in.)
GK-1 ^(a)	16.0	12.0	15.9	0.137	0.331	Nonreflecting	1
GK-3 ^(b)	16.0	12.0	28.4	0.181	0.390	Nonreflecting	
GK-2 ^(a)	16.0	12.0	17.3	0.140	0.264	Reflecting	
Average ^(c)	—	—	20.5	0.153	0.328		
GK-5 ^(d)	16.0	12.0	24.4	0.112	0.150	Nonreflecting	0.5
GK-7 ^(d)	16.0	12.0	37.2	0.050	0.425	Nonreflecting	
GK-6 ^(d)	16.0	12.0	23.2	0.138	0.134	Reflecting	
Average ^(c)	—	—	28.3	0.100	0.236		

(a) No specimen failure. Test was stopped when equipment limits of approximately 0.5-in. deflection were reached.

(b) Four cups of 24 unbonded at time of failure.

(c) All specimens used for averages.

(d) One cup unbonded at time of failure.

Table CII. Facing-Tension Test, Facing Material

Temperature	Specimen designation	Modulus E (psi)	Elastic limit (psi)	Maximum stress (psi)	Final strain (%)
-200° F	GL-8	—	—	152×10^3	4.40
	GL-9	47.8×10^6	31.4×10^3	152×10^3	4.20
	GL-10	—	—	154×10^3	3.60
	Average	47.8×10^6	—	153×10^3	4.07
	Deviation	—	—	(0.6%)	(11.6)
Room temperature	GL-2	18.2×10^6	22.7×10^3	111×10^3	2.30
	GL-3	—	—	123×10^3	3.98
	GL-4	—	—	121×10^3	3.70
	Average	18.2×10^6	—	118×10^3	3.33
	Deviation	—	—	(5.9%)	(31.0)
+250° F	GL-5	16.4×10^6	20.0×10^3	100×10^3	2.85
	GL-6	18.9×10^6	20.0×10^3	—	—
	GL-7	18.4×10^6	23.6×10^3	108×10^3	2.75
	Average	17.9×10^6	21.2×10^3	104×10^3	2.80
	Deviation	(8.4%)	(6.0%)	(3.8%)	(1.8)

Table CIII. Facing-Separation Test, Composite Structure

Unexposed Specimens

Temperature	Specimen designation	Modulus E (psi)	Elastic limit (psi)	Maximum stress (psi)	Final strain (%)
-200° F	GM-11	1.05×10^3	3.25	3.25	0.29
Room temperature	GM-1	672	3.34	3.34	0.57
	GM-2	24.2	0.475	0.600	3.09
	Average	348.1	1.92	1.97	1.83
	Deviation	(93%)	(75.5%)	(69.5%)	(68.8)
1250° F	GM-4	292	1.00	1.00	0.57

Exposed Specimens

Specimen	Previous exposure	Modulus E (psi)	Elastic limit (psi)	Maximum stress (psi)	Final strain (%)
GFM-3	Thermal/vacuum environment (1,000 hr)	74.6	2.87	2.87	3.78
GFM-2	Thermal/vacuum environment (6,000 hr)	603	5.00	7.60	1.46
JGM-1	Thermal cycling (100 cycles)	306	4.05	4.05	1.32
JGN-2	Thermal cycling (1,000 cycles)	174	1.53	2.11	1.34
KG-1	Thermal cycling	457	4.25	4.25	0.93

Table CIV. Core-Compression Test, Composite Structure

Unexposed Specimens

Temperature	Specimen designation	Modulus E (psi)	Elastic limit (psi)	Maximum stress (psi)	Final strain (%)
-200° F ^(a)	GN-7	530	2.74	2.74	0.52
	GN-8	295	3.22	3.60	1.37
	GN-9	518	4.45	4.78	0.97
	Average	448	3.47	3.71	0.95
Room temperature ^(a)	Deviation	(34.1%)	(21.1%)	(26.1%)	(45.3)
	GN-1	577	3.99	4.53	0.83
	GN-2	553	1.62	2.05	0.44
	GN-3	381	1.39	2.19	0.85
+250° F ^(a)	Average	504	2.33	2.92	0.71
	Deviation	(24.6%)	(40.3%)	(29.8%)	(38.0)
	GN-4	226	1.62	2.25	1.15
	GN-5	488	2.62	3.46	0.83
-200° F ^(b)	GN-6	280	2.09	2.92	1.16
	Average	331	2.08	2.88	1.05
	Deviation	(31.7%)	(22.1%)	(19.8%)	(20.9)
	GN-18	136	3.30	3.30	2.45
Room temperature ^(b)	GN-19	97	2.06	2.06	2.21
	GN-20	100	2.19	2.19	2.21
	Average	111	2.52	2.52	2.29
	Deviation	(11.7%)	(18.3%)	(18.3%)	(3.5)
+250° F ^(b)	GN-13	138	1.38	2.21	1.81
	GN-16	308	1.84	2.50	1.00
	GN-21	103	1.51	1.67	1.72
	Average	183	1.58	2.13	1.51
+250° F ^(b)	Deviation	(43.7%)	(12.7%)	(21.6%)	(33.8)
	GN-14	173	1.06	1.44	0.89
	GN-15	113	0.94	1.47	2.32
	GN-17	172	0.91	0.91	0.55
+250° F ^(b)	Average	156	0.97	1.27	1.25
	Deviation	(27.6%)	(6.2%)	(28.4%)	(56.0)

(a) Approximately 1.0-in. thick.

(b) Approximately 0.5-in. thick

Table CIV --- Continued

Exposed Specimens

Specimen	Previous exposure	Modulus E (psi)	Elastic limit (psi)	Maximum stress (psi)	Final strain (%)
GF-1	Thermal/vacuum environment (100 hr)	138	2.32	2.94	2.62
GFN-1	Thermal/vacuum environment (100 hr)	115	2.50	2.75	2.55
GF-3	Thermal/vacuum environment (1,000 hr)	127	2.19	2.50	2.10
GFN-3	Thermal/vacuum environment (1,000 hr)	163	1.94	1.94	1.26
GFN-2	Thermal/vacuum environment (6,000 hr)	127	0.71	0.71	0.52

Note: Specimens were approximately 0.5-in. thick. Data should be compared with results of tests on unexposed specimens of same thickness.

UNCLASSIFIED

Security Classification

DOCUMENT CONTROL DATA - R&D

(Security classification of title, body of abstract and indexing annotation must be entered when the overall report is classified)

1. ORIGINATING ACTIVITY (Corporate author)		2a. REPORT SECURITY CLASSIFICATION	
Lockheed Missiles & Space Company Sunnyvale, California		Unclassified 2b. GROUP N/A	
3. REPORT TITLE			
(U) Program ASTEC (Advanced Solar Turbo Electric Concept) Part I - Candidate Materials Laboratory Tests			
4. DESCRIPTIVE NOTES (Type of report and inclusive dates)			
Final Report, March 1966			
5. AUTHOR(S) (Last name, first name, initial)			
Hurtt, W. W., Program Manager Blakney, T. L. Cunningham, G. R. Rittenhouse, J. B. Vance D. A. Bradshaw, W. G. Pollard, H. E. Schmidt, W. F.			
6. REPORT DATE		7a. TOTAL NO. OF PAGES	7b. NO. OF REPS
March 1966		318 text pages	10
9a. CONTRACT OR GRANT NO.		9a. ORIGINATOR'S REPORT NUMBER(S)	
AF 33(615)-1577		AFAPL-TR-65-53	
b. PROJECT NO.		Part I	
678A c. d.		b. OTHER REPORT NO(S) (Any other numbers that may be assigned to this report) LMSC-D-03-65-4	
10. AVAILABILITY/LIMITATION NOTICES			
See notices page			
11. SUPPLEMENTARY NOTES		12. SPONSORING MILITARY ACTIVITY	
		A. F. Aero Propulsion Laboratory Wright-Patterson AFB, Ohio	
13. ABSTRACT			
<p>A space power system of the type envisioned by the ASTEC program requires the development of a lightweight solar collector of high reflectance which is capable of withstanding the space environment for an extended period of time. A survey of the environment of interest for ASTEC purposes revealed four potential sources of damage to collector materials: solar ultraviolet radiation, low-energy electrons encountered in the auroral zones, vacuum, and combined temperature levels and thermal cycling. A laboratory test program was conducted to determine the basic thermophysical, optical, and mechanical properties of materials developed by the solar-collector industry for use in the ASTEC program, and to test the degrading effects of various segregated and combined elements of the space environment on these materials. Of six material systems selected by AFAPL for testing, four were epoxy-bonded metal systems, one was phenolic foam with a metal surface, and one was polyurethane-rigidized nylon with an aluminized mylar surface. Three of the four metal systems were honeycomb configurations; these proved to be far superior from a structural standpoint to the nonhoneycomb types. All the reflective surfaces degraded to some extent in the simulated ASTEC environment, but material systems with bare metal surfaces were significantly more stable than systems with silicon oxide overcoatings. In addition, these systems had a higher initial reflectance. No material proved to be ideally suited in all respects for use in the ASTEC solar collector. Recommendations are made for additional testing to determine more exactly the mechanical properties of the most promising material or materials and to establish with greater certainty the degree of optical stability of these materials in the ASTEC environment.</p>			

DD FORM 1 JAN 64 1473

UNCLASSIFIED

Security Classification

UNCLASSIFIED
Security Classification

14. KEY WORDS	LINK A		LINK B		LINK C	
	ROLE	WT	ROLE	WT	ROLE	WT
INSTRUCTIONS						
<p>1. ORIGINATING ACTIVITY: Enter the name and address of the contractor, subcontractor, grantee, Department of Defense activity or other organization (corporate author) issuing the report.</p> <p>2a. REPORT SECURITY CLASSIFICATION: Enter the overall security classification of the report. Indicate whether "Restricted Data" is included. Marking is to be in accordance with appropriate security regulation.</p> <p>2b. GROUP: Automatic downgrading is specified in DoD Directive 5200.10 and Armed Forces Industrial Manual. Enter the group number. Also, when applicable, show that optional markings have been used for Group 3 and Group 4 as authorized.</p> <p>3. REPORT TITLE: Enter the complete report title in all capital letters. Titles in all cases should be unclassified. If a meaningful title cannot be selected without classification, show title classification in all capitals in parenthesis immediately following the title.</p> <p>4. DESCRIPTIVE NOTES: If appropriate, enter the type of report, e.g., interim, progress, summary, annual, or final. Give the inclusive dates when a specific reporting period is covered.</p> <p>5. AUTHOR(S): Enter the name(s) of author(s) as shown on or in the report. Enter last name, first name, middle initial. If military, show rank and branch of service. The name of the principal author is an absolute minimum requirement.</p> <p>6. REPORT DATE: Enter the date of the report as day, month, year; or month, year. If more than one date appears on the report, use date of publication.</p> <p>7a. TOTAL NUMBER OF PAGES: The total page count should follow normal pagination procedures, i.e., enter the number of pages containing information.</p> <p>7b. NUMBER OF REFERENCES: Enter the total number of references cited in the report.</p> <p>8a. CONTRACT OR GRANT NUMBER: If appropriate, enter the applicable number of the contract or grant under which the report was written.</p> <p>8b, 8c, & 8d. PROJECT NUMBER: Enter the appropriate military department identification, such as project number, subproject number, system numbers, task number, etc.</p> <p>9a. ORIGINATOR'S REPORT NUMBER(S): Enter the official report number by which the document will be identified and controlled by the originating activity. This number must be unique to this report.</p> <p>9b. OTHER REPORT NUMBER(S): If the report has been assigned any other report numbers (either by the originator or by the sponsor), also enter this number(s).</p> <p>10. AVAILABILITY/LIMITATION NOTICES: Enter any limitations on further dissemination of the report, other than those imposed by security classification, using standard statements such as:</p> <ul style="list-style-type: none"> (1) "Qualified requesters may obtain copies of this report from DDC." (2) "Foreign announcement and dissemination of this report by DDC is not authorized." (3) "U. S. Government agencies may obtain copies of this report directly from DDC. Other qualified DDC users shall request through _____." (4) "U. S. military agencies may obtain copies of this report directly from DDC. Other qualified users shall request through _____." (5) "All distribution of this report is controlled. Qualified DDC users shall request through _____." <p>If the report has been furnished to the Office of Technical Services, Department of Commerce, for sale to the public, indicate this fact and enter the price, if known.</p> <p>11. SUPPLEMENTARY NOTES: Use for additional explanatory notes.</p> <p>12. SPONSORING MILITARY ACTIVITY: Enter the name of the departmental project office or laboratory sponsoring (paying for) the research and development. Include address.</p> <p>13. ABSTRACT: Enter an abstract giving a brief and factual summary of the document indicative of the report, even though it may also appear elsewhere in the body of the technical report. If additional space is required, a continuation sheet shall be attached.</p> <p>It is highly desirable that the abstract of classified reports be unclassified. Each paragraph of the abstract shall end with an indication of the military security classification of the information in the paragraph, represented as (TS), (S), (C), or (U).</p> <p>There is no limitation on the length of the abstract. However, the suggested length is from 150 to 225 words.</p> <p>14. KEY WORDS: Key words are technically meaningful terms or short phrases that characterize a report and may be used as index entries for cataloging the report. Key words must be selected so that no security classification is required. Identifiers, such as equipment model designation, trade name, military project code name, geographic location, may be used as key words but will be followed by an indication of technical context. The assignment of links, rules, and weights is optional.</p>						